Morphodynamic behaviour of coastal hard-soft transitions

A case study of Maasvlakte 2

A. Lako

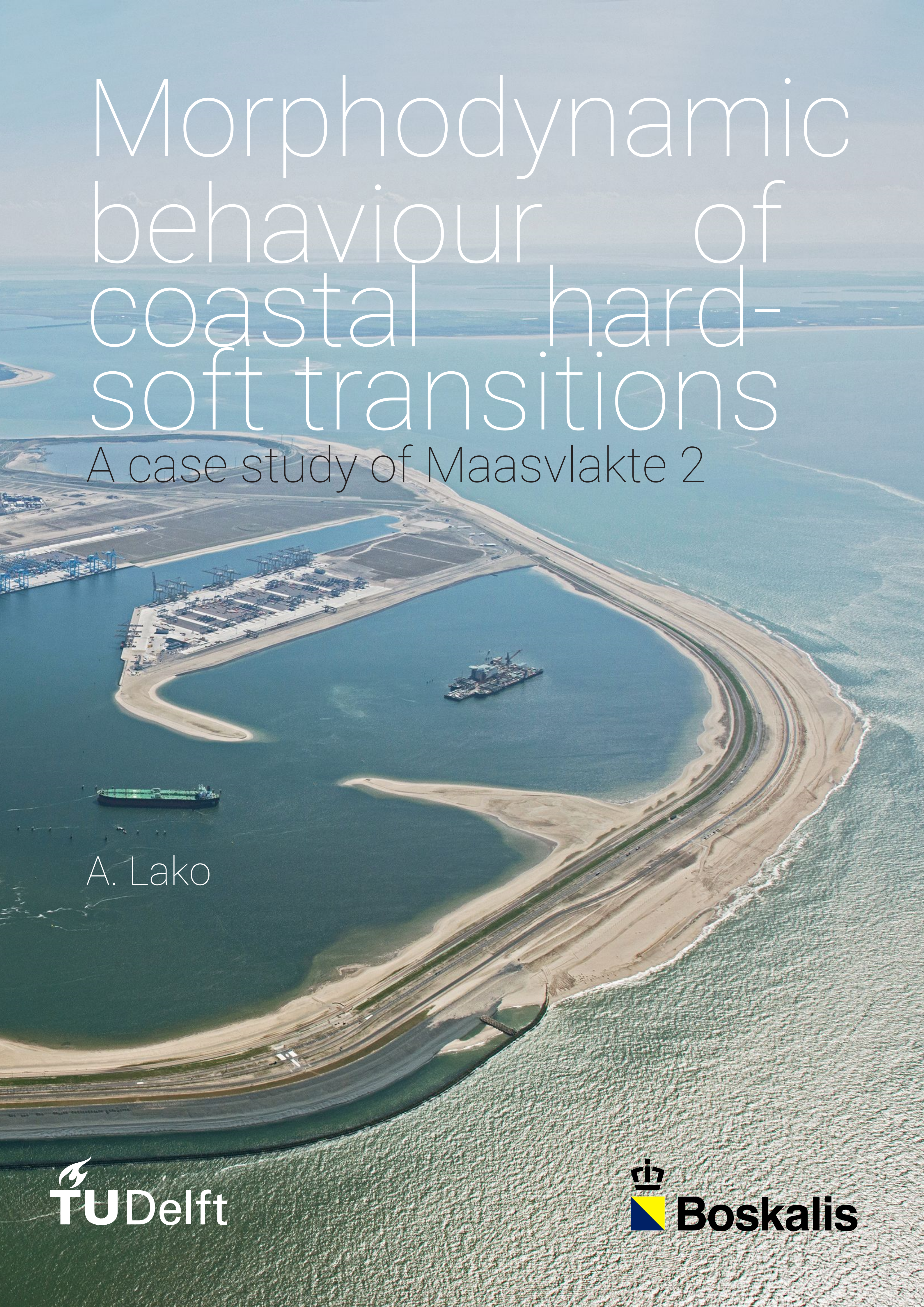

TU Delft

Boskalis

Morphodynamic behaviour of coastal hard-soft transitions

A case study of Maasvlakte 2

by

A. Lako

in partial fulfilment of the requirements for the degree of

Master of Science
in Civil Engineering

at the Delft University of Technology,
to be defended publicly on Tuesday 22 January 2019 at 13:00

Student number:	4239245	
Thesis committee:	Prof. Dr. Ir. S. G. J. Aarninkhof,	TU Delft, chair
	Ir. T. Vijverberg	Boskalis, daily supervisor
	Ir. A. P. Luijendijk,	TU Delft, Deltares
	Ir. P. Brandenburg,	van Oord
	Dr. Ir. M. Zijlema,	TU Delft

Cover image: Aeroview b.v.

Summary

All over the world, coastal protection measures are taken, which can be soft (e.g. sand nourishments on sandy beaches) or hard (e.g. seadikes or seawalls). Special care has to be taken to design the transition between these hard and soft flood defences, as they are often vulnerable components of a coastal defence system. This study therefore aims to give more insight into the morphological processes around hard-soft transitions, in order to make recommendations on design and nourishment plans for hard-soft transitions in the future.

To this end, the hard-soft transition of Maasvlakte 2 (MV2) was studied. For the case of Maasvlakte 2 the limited knowledge of hard-soft transitions resulted in a conflict of the assessment method of the flood defence and the nourishment strategy according to the client requirements. Monitoring of the soft flood defence revealed that the northernmost transects of the soft flood defence showed a higher dynamic variability than was allowed, so that the safety requirements were not met during several assessment moments.

The most important factors governing the morphological behaviour were studied using different numerical models (UNIBEST-LT/CL , SWAN (Booij et al., 1999) and XBeach (Roelvink et al., 2009)).

From the results of the case study of Maasvlakte 2, it was found that the most severe erosion at the hard-soft transition is found during periods with strong southward longshore transports, which causes positive longshore transport gradients at the transition. Cross-shore processes such as storm erosion also indirectly contribute to this by transporting sediment from higher in the profile to lower in the profile.

Regarding the influence of wave reflection, some preliminary results were found. This was because of the limitations in the models to capture the wave reflection well. Using SWAN and UNIBEST, the effect of short waves was investigated, which showed that reflection of short waves is larger at the deeper located part of the hard flood defence. However, the reflected waves in SWAN were signficiantly smaller than expected with the imposed reflection coefficient, for which several causes are given. The preliminary results from XBeach (substantiated with results found in literature) showed that bound long wave reflection is larger closer to the hard soft-transition, and that these reflected waves also reach quite far offshore.

As regards to the role of the tide, it was found that the dominant northward directed flood tidal current along the soft flood defence strengthens the supply of sediment from south during northward transport. On the other hand, the dominant southward directed ebb current along the hard flood defence hardly picks up any sediment and therefore it does not contribute to the morphological changes at the hard-soft transition.

Morphological behaviour of hard-soft transitions in general
Some generic observations in the morphological behaviour of MV2 are likely to be found at other hard-soft transitions:

- A strong dynamic variability is usually present at the hard-soft transition, in the form of coastline retreat which gives a rotated coastline shape. The timescale of this dynamic variability, and the degree of erosion and ability to recover itself are dependent on the prevailing wave climate.
- The reflection of short waves will likely be larger at the deeper part of the hard flood defence. Closer to the transition zone, where sediment from the soft flood defence is deposited, short wave reflection will be smaller, but long wave reflection will be larger. The reflection further depends on the wave climate, slope and roughness of the material and degree of transmission through the hard flood defence.
- In general the highest erosion will be observed in periods with oblique wave incidence where sediment is lost due to longshore sediment transport gradients. However, storm erosion (a cross-shore sediment transport process) also indirectly contributes to this loss of sediment.

Based on these findings, several recommendations are proposed to design a hard-soft transition. For example, the transition should be made as gradual as possible, and the reflection at the hard structure should be kept as low as possible, e.g. by making a gentle slope, and if possible, by allowing transmission of waves through the (partly) hard structure. Moreover this study presents some other design examples to minimise the nourishment frequency. Finally, recommendations are presented for further research.

Preface

This thesis is the result of work executed at Boskalis and concludes the degree Master of Science Civil Engineering (Hydraulic Engineering) at Delft University of Technology.

My sincere appreciation goes out to my graduation committee. First of all, I would to thank my daily supervisor from Boskalis, Thomas Vijverberg, for the time and effort he invested in me. Despite your busy agenda, we met on a regular basis and even if you already had eight other meetings that day, you were still actively involved in our meetings. After our meetings I usually came out with a more positive attitude towards my research, as you reminded me to be positive about my results and pick out the useful things, while still being critical.

Secondly, I would like to thank the chairman of the committee, Stefan Aarninkhof. Also you were always very enthusiastic and involved about the subject during meetings and during smaller chats, even though having such a busy agenda (*kudo's* for that). Moreover, you helped in keeping the broader view and objective of the research in mind, and reminding me to generalize my results. Arjen Luijendijk, thanks for your help with the UNIBEST model, and for being optimistic about my results – I think this 'glass is half full' attitude is very admirable. Marcel Zijlema, thanks for being part of my committee, and for pointing out some important processes which can play a role and which should be included. And Peter Brandenburg, thanks for being critical and also reminding me to be critical with my results. This definitely improved my thesis.

Besides my committee, I want to the Hydronamici from Boskalis, for being always open for questions and brainstorms, even if they were busy. Thanks to the workability guys for at times allowing me to take over their remote computer with my model runs and helping me out when these models were not doing what they should do. Specifically I would like to thank Guido van der Salm, Jordi Hoek, Antoon Hendriks and Mark Klein for helping me out with questions related to the different models I used.

Apart from the thesis-related support I got at Boskalis, I also want to thank the Hydronamici for being such a nice group of people and therefore making my time at Hydronamic a lot more fun. I enjoyed the legendary 'hydronamic drinks' and the refreshing running sessions after work. And of course I want to thank all of my fellow graduate students at Boskalis – you also made my time at Boskalis worthwile.

Finally, I need to thank my housemates who were always there to listen to my thesis-related issues and stories (and sometimes frustrations) and reassuring me that everything would eventually fall into place. Also, I would like to thank my friends and former housemates from Delft for making my student and unforgettable and fun time!

Last but not least I want to thank my parents and sister for supporting me throughout my entire study in Delft, for always being interested in what I do and for always being proud, no matter the result.

A. Lako
Delft, January 2019

Contents

List of Figures

List of Tables

List of Symbols

Symbol	Unit	Description
C	$m^{1/2}s^{-1}$	Chézy coefficient
D	m	Grain size
D_{50}	m	Median grain size
D_{90}	m	Grain size at which 10% of the sample's mass is smaller than this value
$E_{\omega,\theta}$	m^2Hz^{-1}	Absolute radian frequency
H_b	m	Significant wave height at breaking
H_{m0}	m	Significant wave height
H_s	m	Significant wave height
H_{rms}	m	Root-mean-square wave height
I_m	kgs^{-1}	Immersed mass of transported sediment
K	–	Coefficient in CERC-formula
K_r	–	Reflection coefficient
S	m^3s^{-1}	Sediment transport
S_{in}	m^3s^{-1}	Incoming flux of sediment transport
S_{out}	m^3s^{-1}	Outgoing flux of sediment transport
T	s	Wave period
T_p	s	Peak wave period
U_{10}	ms^{-1}	Wind speed at 10 m height
U_{Dir}	$°N$	Wind direction
V	ms^{-1}	Longshore current velocity
a	m	Thickness of bed load layer
c	ms^{-1}	Wave celerity
c_g	ms^{-1}	Wave group velocity
d	m	Active profile height
f	Hz	Frequency
f_p	Hz	Peak frequency
g	ms^{-2}	Gravitational acceleration
h	m	Water depth
h_0	m	Water level
n	–	Ratio of wave group velocity over phase speed
p	–	Porosity
s	–	Relative density of sediment
u	ms^{-1}	Flow velocity
α_b	°	Beach slope angle
γ	-	Breaker parameter
η	m	Wave amplitude
η_b	m	Long wave amplitude
θ	$°N$	Wave direction
ρ	kgm^1	Density
ρ_s	kgm^1	Density of sediment
ρ_w	kgm^1	Density of water
ϕ	°	Wave angle of incidence

Symbol	Unit	Description
ϕ_b	$^{\circ}$	Wave angle of incidence at breaking
ω	$rads^{-1}$	Radian frequency
ΔY	m	Coastal change in y-direction

Abbreviations and acronyms

Abbreviation	Description
BKL	Basis Kust Lijn
HPZ	Hondsbossche- and Pettemer Zeewering
MHW	Mean High Water
MLW	Mean Low Water
MV2	Maasvlakte 2
MWD	Mean Wave Direction
NAP	Normaal Amsterdams Peil
PUMA	Projectorganisatie Uitbreiding Maasvlakte

1
Introduction

Of all the sandy coasts around the world, 24% are eroding at rates exceeding 0.5 m/yr (Luijendijk et al., 2018). Along a large part of the (sandy) North sea coast, dunes and sandy beaches can be found, which form a natural protection against flooding. However, a large part of the coast suffers from structural (permanent) erosion, and sometimes storm impacts of these coasts reach an unacceptable level. Therefore, extra measures for coastal protection have to be taken, and hence numerous protection measures can be found along the Dutch Coast. These flood defences can be either 'soft' or 'hard' (or a mixture of both). Soft coastal protection measures are often in the form of sand nourishments on the shoreface or beach. Hard flood defences include series of groynes, offshore breakwaters, submerged breakwaters, revetments, seawalls or seadikes (Bosboom and Stive, 2015). Soft measures have become increasingly popular in the Netherlands over the last decades, because they are more 'natural' and interference in the sediment transport patterns is limited. Hard measures often have negative side-effects, such as erosion downstream of the structure and increased wave attack due to reflection of the waves and due to the development of a scour hole in front of the structure (Bosboom and Stive, 2015). However, hard measures are still being applied in some situations, for example when a heavily attacked port has to be protected or when the area required for a soft measure is not available. Therefore, we often see hard structures around ports and densely populated areas.

Special care has to be taken to design the transition between these hard and soft flood defences, as they are often vulnerable and unpredictable components of a coastal defence system. Many examples of hard-soft transitions can be found along the Dutch Coast, especially along the Zeeland coast and on the Wadden Islands. As a standard method for designing these transitions does not exist, many of these transition structures have been designed based on 'expert judgement' (Steetzel, 1995). This also explains why all transition structures are designed differently. Also for the safety assessment of these structures, a standard procedure is not available, so that a customized safety assessment has to be composed for such transitions (Boers, 2012).

The sandy part of the transition area is likely to be influenced by the adjacent hard structure. In general we can expect more erosion and a dynamic profile, because the presence of a hard structure obstructs the supply of sediment from upstream. But because of the limited studies conducted on this subject and the many different factors contributing to the morphological development, it is hard to predict how the sandy part of the flood defence will behave exactly. This study aims to give more insight into the cross-shore and longshore processes that occur on a sandy beach and dune system adjacent to a hard-soft transition, in order to optimise nourishment plans in the future, and possibly to improve guidelines for design and safety assessment of hard-soft transitions.

To this end, the hard-soft transition of the Maasvlakte 2 was studied as a case study. The Maasvlakte 2 was built between 2008 and 2013, after the construction of the Maasvlakte in the 1960s. For the construction of the Maasvlakte 2, a new port and infrastructure was build by reclaiming land adjoining the Maasvlakte, thereby further extending the Port of Rotterdam into the sea. The seaward side of the Maasvlakte 2 consists of an 11 km long flood defence - a soft coastal protection over 7.5 km along the southwestern part, and a hard flood defence along the nothernmost 3.5 km. The soft protection consists of a sandy beach with one dunerow behind, and the hard part is made up of a stoney dune, with an offshore breakwater in front (see Figure 1.1).

Figure 1.1: Location of study area: flood defence of the Maasvlakte 2

For the case study of the Maasvlakte 2, the limited knowledge of hard-soft transitions resulted in a conflict of the **assessment method** of the flood defence, and the **nourishment strategy** according to the client requirements, as it turned out they could not be met at the same time with the occurring morphological developments. The assessment method entailed that a minimum amount of sand volume (in m^3 sand) had to be contained per layer and per transect. This should be achieved by nourishing once every two years at the most, i.e. the nourishments should have a lifetime of two years. After observing the measured bathymetry over the last years, it turned out that it was not feasible to meet the required volumes per cross-section, by nourishing once every two years. The problems were mainly found in the beach and shoreface volumes of the northernmost transects (1) and the cone (2).

Based on several preliminary morphological studies conducted by Onderwater (2016, 2018a and 2018b) and Onderwater and van der Baan (2017), it was therefore decided to change the assessment method over a certain length of the flood defence. Additionally, the nourishment strategy was adjusted over the same length, namely to place the sand on a different (less active) part of the coastal profile to increase the lifetime. This new way of nourishing will be applied for the first time in the last months of 2018, and its effectiveness still has to be proven. Whereas the studies by Onderwater (2016, 2018a and 2018b) and Onderwater and van der Baan (2017) have already given some insight into the morphological situation of the system, this research will help in increasing our scientific knowledge of the morphological processes **behind** these observations. Additionally, this research will also extrapolate the morphological behaviour of MV2 to the morpholohical behaviour of hard-soft transitions in general. Moreover, this study is carried out based on additional survey data, that was not available in previous studies.

Not only the hard-soft transition, but also the curved coastline and tidal currents in front of the coast make this area especially complex. The bathymetry of the underwater profile and the configuration of the 'dry' beach and dune profile have been measured as part of the monitoring program. These data were firstly used for analysis of the morphology, as and later for validation of numerical models.

1.1. Context and relevance

The morphological processes around the hard-soft transition of Maasvlakte 2 are not fully understood yet, and thorough understanding of the system requires extra research. This can be traced back to the bigger problem of hard-soft transitions in general, which is that we do not know enough about these transitions yet, a standard design method for these structures is lacking, and a standard procedure for safety assessment is lacking as well. More research on this subject is therefore necessary to increase our broader understanding of hard-soft transitions. It can be used for future designs, assessment methods and nourishment strategies for hard-soft transitions, and hence reduce maintenance costs and efforts.

1.2. Research objective

The research objective is therefore *to contribute to a broader understanding of coastal hard-soft transitions and make recommendations on design- and nourishment strategies, by analysing the morphological behaviour of the hard-soft transition of Maasvlakte 2 as a case study*.

1.3. Research questions

The research objective should be achieved by answering central research question(s). Three central questions are formulated, of which some are subdivided into subquestions:

"1. What is the morphological behaviour around the hard-soft transition of Maasvlakte 2?"

1.1 Under which wave conditions and in which seasons do we observe most erosion and how often does this occur?

1.2 How does the evolved coastal shape (cross-shore and longshore) influence its own morphological changes?

1.3 What is the relative contribution of reflection and turbulence at the breakwater to the observed erosion around the hard-soft transition?

1.4 Are tide and wave-tide interactions an important factor contributing to the morphological changes around the hard-soft transition?

"2. What is the morphological behaviour around hard-soft transitions in general?"

"3. How can the design and nourishment strategy of hard-soft transitions be improved?"

3.1 How can the design and nourishment strategy of the hard-soft transition of MV2 be optimised?

3.2 What recommendations can be done for potential other hard-soft transitions?

1.4. Scope

To structure the research and 'design' the research project, the research object (hard soft-transitions) has been unraveled into key concepts, which can be visualized in a tree diagram. These key concepts have also been used to formulate the subquestions. The concepts with an asterix (*) will be studied within this research:

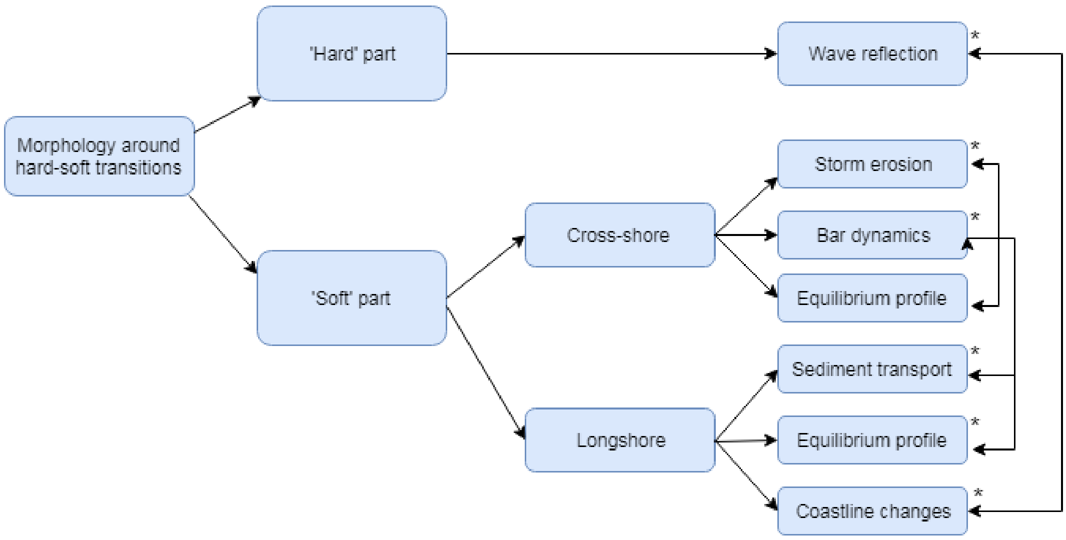

Figure 1.2: Tree diagram, unraveling key concepts from the research object

.

As can be seen from the tree diagram and the components indicated with (*), the scope also partly follows from the tree diagram. The scope of the research is narrowed down as follows:

Spatial domain
The study focuses only on the soft/sandy part of the transition. The effect of the hard structure on the sandy part is taken into account, but the hard flood defence itself is not studied. Moreover, the study will be focused on the lower part of the coastal profile, i.e. the beach, foreshore and shoreface (see Figure 2.1). The interaction with the dune higher in the profile will also be taken into account, but the process of dune erosion will not be the focus of this research.

Temporal domain
This study is focused on the 'natural' behaviour of the morphological system. Therefore, the measurements obtained during the last two years (2017 and 2018) will be used for this research, as there has not been any interference in the form of nourishments during these years. Within these years, the interested is focused both on the average behaviour (e.g. equilibrium profile), but also the cyclic behaviour, seasonal behaviour and post-storm response (so on smaller timescales). These smaller timescales have not been studied before, as measurements were not done on such a regular basis in the years before 2017.

Dimensions
Quite often a distinction is made between cross-shore processes and development (perpendicular to the coast) and longshore transport and coastlines changes (shore-parallel). Due to the relatively small spatial scale of this study area and the complex processes occurring here, these processes cannot really be seen separately from each other, and it is chosen to look at both directions.

Wave conditions
For the design and safety assessment of the flood defence (and of flood defences in general), design conditions were used, e.g. wave and water level conditions that belong to a 1/10,000 storm. The morphological studies conducted by Onderwater (2016, 2018a and 2018b) and Onderwater and van der Baan (2017) were also focused on these design conditions. For this case study, however, we are interested in the actual behaviour of the coastal profile, and therefore the wave conditions used will be actual measured conditions.

1.5. Research framework

A research framework is constructed, which is a schematic representation of the research objective and includes the appropriate steps that need to be taken in order to achieve it. The research framework is formulated as follows: A study of existing literature on coastal dynamics around hard-soft transitions (Chapter 2), and a data analysis of the case study (Chapter 3), will lead to a set of hypotheses (Chapter 3). These hypotheses will be investigated with suitable tools in Chapter 4. The results of these tests will be presented (Chapter 5) and discussed(Chapter 6), and this will lead to a conclusion (Chapter 7) and a set of recommendations (Chapter 8).

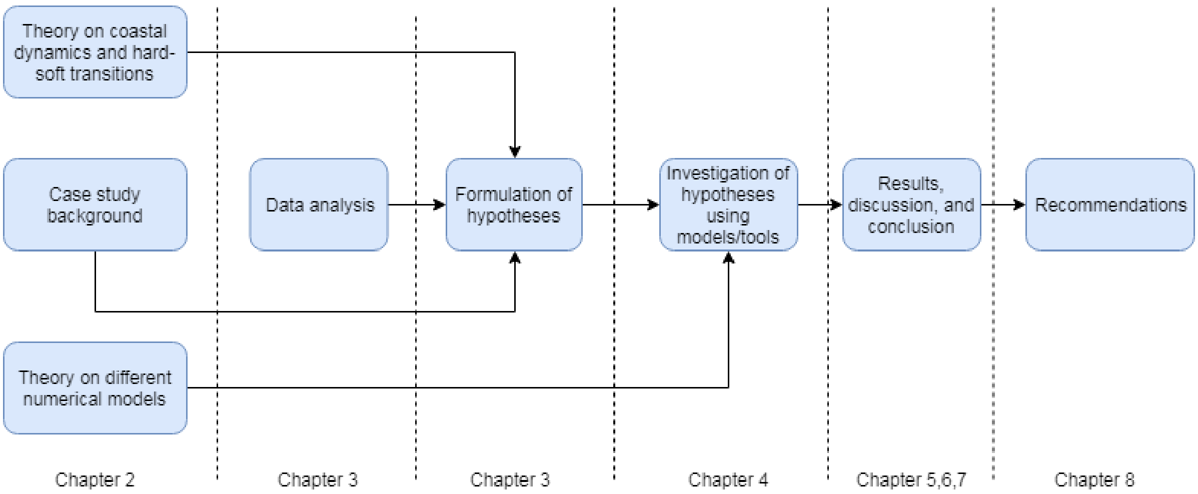

Figure 1.3: Visualisation of the research framework

.

1.6. Thesis Outline

This report contains the following chapters:

Chapter 2: Gives an overview of literature on coastal protection measures, existing hard-soft transition and background information on the case study.

Chapter 3: Presents the reader with a first analysis of the system. The system analysis consists of a data analysis (bathymetric and waves) and a theoretical approximation of potential sediment transport. Based on these observations, a number of hypotheses are formulated for effective investigation with numerical tools, which follows after.

Chapter 4: This chapter contains the methodology and the validation of the used tools.

Chapter 5: Presents the results of the model tests, accompanied with a discussion of each hypothesis.

Chapter 6: Contains the discussion of results in relation to the research questions

Chapter 7: Provides the conclusions following from chapter 5 and 6.

Chapter 8: Provides recommendations for future research.

2

Literature Study

The Literature study is built op as follows: First, the reader will be introduced to some basic concepts of coastal dynamics in Section 2.1. This section will be followed by a section on coastal protection measures, both hard and soft, in section 2.2. This section will also give an overview of existing literature (state-of-the-art) on hard-soft transitions. After that, the case study of the MV2 and some other examples of hard-soft transitions will be presented (sections 2.2.4 and 2.3).

2.1. Coastal dynamics

Coasts exists in many different types of coastal landforms, such as barrier islands, sea cliffs, tidal flats, river deltas, and sandy beaches (Luijendijk et al., 2018). The latter type, sandy beaches, are very dynamic, and will be the focus of this research. A recent study by Luijendijk et al. (2018) revealed that 31% of the world's ice-free shoreline are sandy, of which 24% are eroding at rates exceeding 0.5 m/yr, 28% is accreting and 48% is stable (Luijendijk et al., 2018). First of all, these numbers substantiate that sandy coasts are indeed very dynamic, as only 48% is stable. As 24% is eroding, it shows that a large number of sandy coasts around the world is eroding. Different measures to combat this erosion are discussed in section 2.2.

Along a large part of the sandy North sea coast, dunes and sandy beaches can be found. Dunes form a natural flood defence system to protect the coast from flooding. Characteristic for dunes is that a certain amount of dune erosion is accepted: the coast is **dynamic**. The shape of the cross-shore profile will vary on the timescales of storms and seasons. During and after storm conditions, the dune profile will look different, and during calm conditions the dune profile will restore itself.

When explaining the basic concepts of coastal dynamics, a distinction is made between cross-shore profile development (perpendicular to the shore) in section 2.1.1 and longshore transport and profile changes (shore-parallel) in section 2.1.2. To provide a better understanding of the processes, each of them will be treated separately first. Later on, these processes will be combined because *in this case study*, these processes mutually influence each other and therefore cannot be seen separately from each other.

2.1.1. Cross-shore profile development

Before explaining the cross-shore dynamics of (sandy) coasts, the different features of the cross-shore profile are distinguished, see Figure 2.1

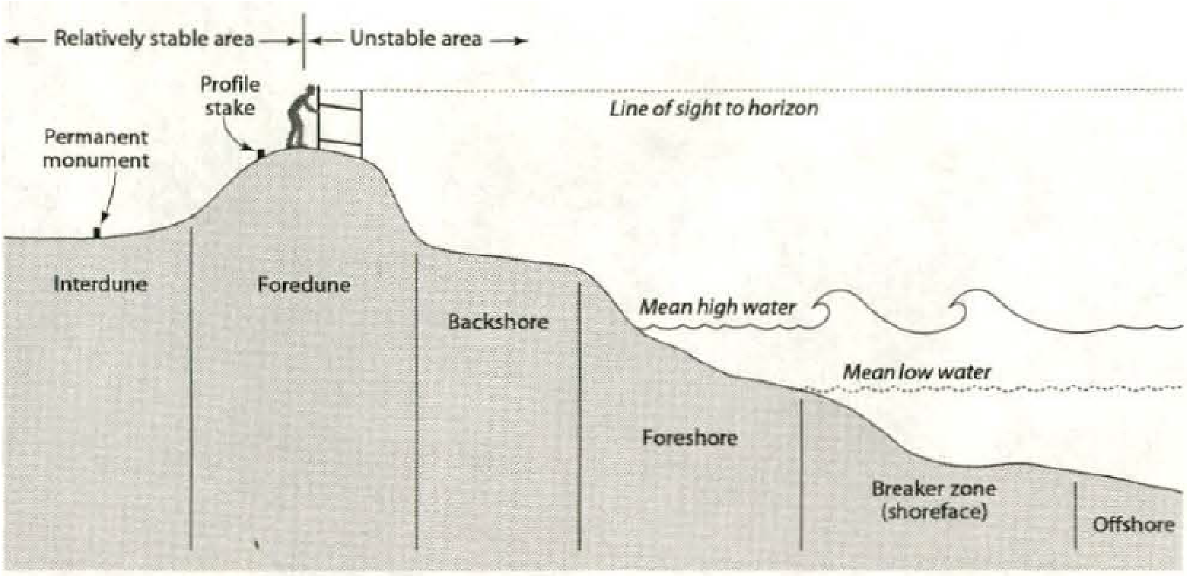

Figure 2.1: Cross-shore profile of a dune system. Source: Woods Hole Oceanographic Institute (Institute, 2001)

.

The foreshore, or intertidal area, covers the area between Mean High Water level (MHW) and Mean Low Water level (MLW). The shoreface, or breaker zone, is the zone over which waves break, and over which a lot of sediment transport takes place.

Dune erosion

When large waves (high and long waves) hit the dune front (foredune), the sand is eroded due to the combination of high turbulence and a strong undertow. The sediment is transported offshore by an undertow, and further offshore, where the offshore transport capacity decreases, the sediment is deposited in the breaker zone, also called the surf zone (see Figure 2.2a). Due to the smaller water depth created by this deposition, wave attack on the dune behind is decreased and further dune erosion is decreased as well. The new cross-shore profile is more efficient in dissipating the wave energy and therefore it will naturally decrease the dune erosion during the rest of the storm. (Bosboom and Stive, 2015).

A coastal engineering assumption often used when describing cross-shore phenomena, and also used for coastal profile modelling, is that a sediment balance is contained. Therefore, although the profile changes over time due to storm and seasonal changes, it is assumed that a **dynamic equilibrium profile** exists (Bosboom and Stive, 2015).

Dynamic equilibrium profile and post-storm profile

In theory a stable equilibrium profile could exist, if a constant wave forcing is present. In reality, however, wave forcing and water levels are constantly varying and the beach responds to this much slower than the forcing mechanisms. Therefore a stable equilibrium is never reached. However, the variations in the cross-shore profile are confined to an envelope. The mean position of this envelope is called the **dynamic equilibrium profile**. (Bosboom and Stive, 2015).

Several empirical formulations for the dynamic equilibrium profile exist, amongst others the ones by Bruun (1954) and Dean (1977). Later, Vellinga (1986) developed a formulation for an 'erosion' or post-storm profile, which is particularly suitable for the Dutch dunes and uses a different time scale than Bruun (1954) and Dean (1977). Note that this is different from the dynamic equilibrium profiles defined by Bruun and Dean, as it describes the cross-shore profile after a storm, rather than a profile that is the mean of all dynamic oscillations. The formulations of the Bruun (1954), Dean (1977), and Vellinga (1986) profiles can be found in Appendix B.1. A visualization of the dynamic equilibrium profile and the post-storm profile is presented in Figure 2.2

The dynamic equilibrium profiles described by Bruun (1954) and Dean (1977) can be used as tools to predict the expected dynamic equilibrium profile, e.g. to design the slope of a new land reclamation or artificial beach. Therefore, for the design of the soft flood defence of the Maasvlakte 2, the design profile of the beach was also a Dean (1977) profile.

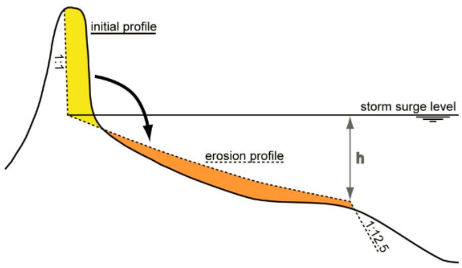

(a) 'Erosion profile' or post-storm profile. From Bosboom and Stive (2015). After Vellinga (1986)

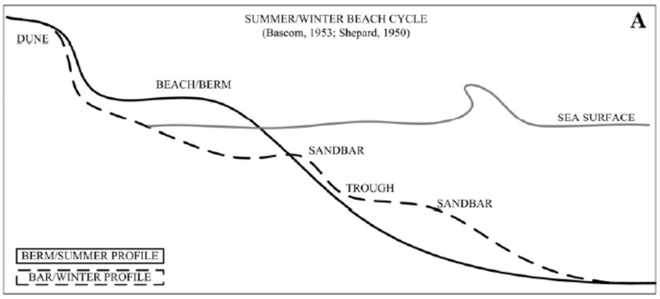

(b) Typical winter- and summer beach profile, showing seasonal variablity. From: Caccioppoli (2013).The mean of these oscillations is the **dynamic equilibrium profile**

Figure 2.2: Dynamics of sandy beaches: post-storm profile (a) and winter-and summer profile (b).

The **post-storm profile** predictions suggested by Vellinga (1986) can be used for basic safety checks for the Dutch dunes. Empirical 1D dune erosion prediction models, such as DUROS+, are therefore also based on the erosion profile proposed by Vellinga (1986). Also the safety assessment of the soft flood defence of the MV2 is done with the use of DUROS+ and therefore also follows a Vellinga (1986) profile.

Bar Dynamics

The deposition of the eroded dune sediment during winter or storm conditions, as described in the foregoing sections, can also give rise to development of sand bars [1] in the shoreface. During winter, when energetic waves occur, these sand bars typically move offshore. During calmer summer conditions, when waves are less energetic but more skewed, the sand bars gradually move onshore and eventually attach to the shore. This results in a seasonal variability of the beach profile, see Figure 2.2b. Furthermore, these bars also show cyclic behaviour over longer time scales, in the order of years. The sand bars are formed in the intertidal zone (foreshore), after which they move offshore while growing in size, and disappear at the end of the breaker zone (Bosboom and Stive, 2015). In the Netherlands, this cycle takes about 4 to 5 years in South Holland. When the shoreface slope is milder and the bars are larger, this cycle will take longer (order of 12 years) because more energy is needed to move the bars. Literature shows that shoreface nourishments often give rise to double barred systems and a net onshore bar migration several years following the nourishment operation (Radermacher et al., 2018, Kroon et al., 1994; van Duin et al., 2004; Lodder and Sorensen,2015). On the contrary, sandbars in unnourished systems are found to exhibit a net offshore migration (NOM; Ruessink and Kroon, 1994; Plant et al., 1999; Shand and Bailey, 1999; Ruessink et al., 2003; Tatui et al., 2016; Walstra et al., 2016) and beach nourishments tend to strengthen this migration.

Due to the time scale of the available measurements of MV2, this will be interesting to look at as well. The generation, propagation and decay of sand bars is rather complex, depending on many counteracting processes, none of which are modelled very accurately (Roelvink and Reniers (2009). Therefore, according to Roelvink and Reniers (2009), obtaining the right bar behaviour in a numerical model is a tight act. Therefore it will be interesting to do a short analysis of bar dynamics based on measured data, but a thorough analysis using a model might not be effective.

The formulations of the dynamic equilibrium profile by Bruun (1954) and Dean (1977) and the storm-profile by Vellinga (1986) are all based on the assumption that the amount of sediment in the active zone remains constant. This is true for uniform coast without sources and sinks. There are, however, numerous causes which make this assumption invalid, resulting in structural gains or losses of sediment. Some of these causes are:

- gradients in alongshore sediment transport (e.g. due to curved coastlines, sediment sinks, and hard-soft structures)

[1] Sandbars are shallow submerged ridges parallel to the shoreline

- aeolian transport (transport by wind)
- sea level rise
- tide effects

The first item will be discussed below.

2.1.2. Longshore transport and coastline changes

Next to the cross-shore processes discussed in the foregoing section, sediment transport can also occur in longshore direction (parallel to the shore). These longshore processes are also very important, as they are responsible for changes in coastline shape and orientation. These changes are caused by *gradients* in transport rates along the coast.

The net longshore sediment transport can generally be expressed as (Bosboom and Stive, 2015):

$$\langle S_y \rangle = \int_h^a V(z) \cdot C(z) dz \qquad (2.1)$$

In which:
S_y = net longshore sediment transport excl. pores [m^3/m/s]
V(z) = longshore current velocity at height z above the bottom [ms/s]
C(z) = time-mean sediment concentration at height z [m^3/m^3]
a = thickness of bed load layer [m]
h = local (still) water depth [m]

The longshore current velocity V(z) can have several different driving forces, but it is often found to be driven predominantly by breaking waves which approach the coast at an angle (Bosboom and Stive, 2015).

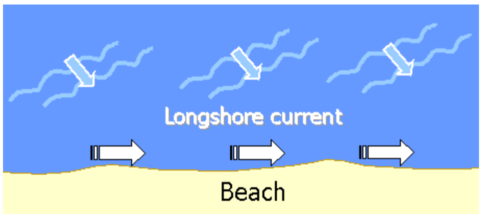

Figure 2.3: Schematization of the wave-driven longshore current. Source: Texas A&M University – Corpus Christi

.

The **longshore transport** can be schematized and calculated with an **(S,ϕ) curve**, and the associated **changes in coastline position** can be calculated with the **single line theory**.

The (S,ϕ) curve is a general concept in coastal morphology, which gives the transport as a function of the wave angle for given set of wave conditions (Bosboom and Stive, 2015). It is based on the CERC [2] formula (Komar and Inman, 1970), a formula that describes bulk longshore sediment transport, which can be expressed as follows:

$$S = \frac{K}{16(s-1)(1-p)} \sqrt{\frac{g}{\gamma}} sin2\phi_b H_b^{2.5} \qquad (2.2)$$

With:
S = deposited volume of sediment transported [m^3/s]
K = coefficient [-]
s = relative density of the sediment ρ_s/ρ_w [-]
p = porosity [-]
g = gravitational acceleration [m/s^2]
γ = breaker index [-]

[2]The CERC formula was developed by the Coastal Engineering Research Center (CERC) of the American Society of Civil Engineerings (ASCE)

ϕ_b = wave angle of incidence at the outer edge of the breaker zone [-]
H_b = wave height at breaking [m]

Assuming that K, s, p, g and γ are constant over the coastal stretch, the sediment transport S over the breaker zone is dependent on the wave height at breaking (H_b) and the wave angle of incidence at the outer edge of the breaker zone (ϕ_b).

The formula of Kamphuis (1991) is slightly different as it also includes the effects of beach slope and wave steepness. He formulated an expression for the immersed transported sediment $I_m = \rho(s-1)(1-p)S$:

$$I_m = 2.27 H_{s,b}^2 T_p^{1.5} (\tan\alpha_b)^{0.75} D^{-0.25} (sin2\phi_b)^{0.6} \tag{2.3}$$

Which can be rewritten to the sediment transport to derive at the same format as the CERC formula:

$$S = \frac{I_m}{\rho(s-1)(1-p)} = \frac{2.27 H_{s,b}^2 T_p^{1.5} (\tan\alpha_b)^{0.75} D^{-0.25} (sin2\phi_b)^{0.6}}{\rho(s-1)(1-p)} \tag{2.4}$$

With:
I_m = immersed mass of transported sediment [kg/s]
T_p = peak period [s]
D = median grain size diameter [m]
$tan\alpha_b$ = beach slope [-]
and $H_{s,b}$ and ϕ_b as defined below equation 2.2.

The CERC formula has some limitations, namely that only the wave-induced longshore current is taken into account; that sand properties such as grain size are not taken into account, and that only the total sediment transport in the breaker zone is given (Bosboom and Stive, 2015). Still, it is a very useful tool to estimate sediment transport due to oblique wave incidence. The (S,ϕ) curve can be drawn precisely when a set of wave conditions and sediment characteristics (H_0, K, p and s) is given, but it can also be drawn qualitatively based on the fact that the longshore sediment transport is propotional to S $\propto$ ${H_{s,b}}^{2.5} \sin 2\phi_b$ (Bosboom and Stive, 2015). The curve shows a maximum longshore transport for an angle somewhat smaller than 45°. An example of an (S-ϕ) curve for a given set of wave conditions is given in Figure 2.4 below.

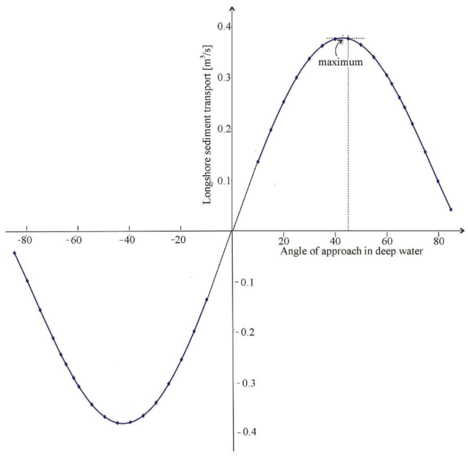

Figure 2.4: (S,ϕ) curve for wave conditions: $H_{rms,0}$ = 2 m, T = 7 s, p = 0.4 and s = 2.65. Source: Bosboom and Stive (2015)

.

The single line theory is a 1D schematization which relates the sediment transport to the associated coastline changes. It is assumed that the shape of the cross-shore profile does not change in time (as shown in Figure 2.5a). In the single line theory, a certain portion/stretch of a beach is considered. The coastline will be stable as long as $S_{in} = S_{out}$. Erosion will take place in the considered area if $S_{in} < S_{out}$, and accretion will take place when $S_{in} > S_{out}$ (Bosboom and Stive, 2015).

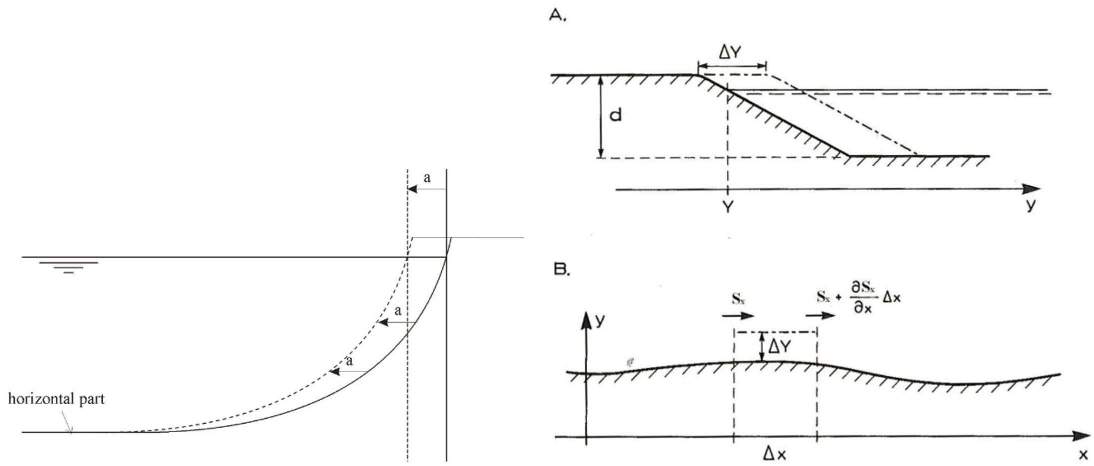

(a) Schematization of the beach profile in the single-line theory. From Bosboom and Stive (2015)

(b) Longshore transport S_x and coastal change ΔY in a coastline model. Upper figure (A): cross-section; Lower figure (B); top view. From Bosboom and Stive (2015), adjusted from Fredsoe and Deigaard (1992).

Figure 2.5: Single line theory schematization. Source: Bosboom and Stive, 2015

The single-line theory works as follows. Take a (changing) stretch of beach, like in Figure 2.5b. If the shoreline moves forward with ΔY during Δt, the volume gained over a distance δx is ΔxΔYd (upper figure). In along-shore direction (lower figure), the net volume of sediment entering the segment with length Δx during Δt is (Bosboom and Stive, 2015):

$$-\frac{\partial S_x}{\partial x}\Delta x \Delta t \tag{2.5}$$

Because of continuity, these two volumes should be equal to eachother (net inflow of sediment = accumulation of sediment) (Bosboom and Stive, 2015):

$$\Delta x \Delta Y d = -\frac{\partial S_x}{\partial x}\Delta x \Delta t \tag{2.6}$$

Which can be rewritten to:

$$\frac{\partial Y}{\partial t} + \frac{1}{d}\frac{\partial S_x}{\partial x} = 0 \tag{2.7}$$

And since the angle of wave attack relative to the coastline (ϕ) determines to a large degree the sediment transport S_x, the chain rule can be applied to write equation 2.7 as (Bosboom and Stive, 2015):

$$\frac{\partial Y}{\partial t} + \frac{1}{d}\frac{\partial S_x}{\partial \phi}\frac{\partial \phi}{\partial x} = 0 \tag{2.8}$$

Finally, the rotated coastline changes the relative angle of wave attack ϕ, since the wave angle is relative to the coastline: ϕ = ϕ'-∂Y/∂x and ∂ϕ = -∂Y/∂x. Therefore, the coastline position Y can finally be written as a parabolic partial differential equation:

$$\frac{\partial Y}{\partial t} + \frac{1}{d}\frac{\partial S_x}{\partial \phi}\frac{\partial^2 Y}{\partial x^2} = 0 \tag{2.9}$$

This is the equation that is also solved in 1D coastline models as UNIBEST-LT/CL or GENISIS (Bosboom and Stive, 2015).

2.2. Coastal protection

As discussed in section 2.1, sandy beaches are highly dynamic and 24% of these beaches are eroding (Luijendijk et al., 2018). In case of structural erosion, an important task of coastal engineers is to protect these coasts. For this reason, numerous flood defences and flood protection measures can be found along the

Dutch Coast. Soft protection measures are often in the form of sand nourishments on the foreshore, beach, or dune. Hard flood defences include series of groynes, offshore breakwaters, submerged breakwaters, revetments, seawalls or seadikes (Bosboom and Stive, 2015).

2.2.1. Soft coastal protection (nourishments)

When a stretch of coast suffers from structural erosion, the beach can be nourished with sand. As nourishing sand does not alter the sediment transport patterns in a significant way, erosion can go on and the nourishment has to be repeated on a regular basis. Along most of the Dutch coastline, a nourishment lifetime of 5 to 10 years is aimed for. This is different for man-made structures such as Maasvlakte 2, for which a nourishment of 2 years was aimed for.

Nourishments can be placed either higher in the profile (beach nourishment - between NAP +3 m to NAP -1 m) or lower in the profile (shoreface nourishments - around NAP -5 m). Shoreface nourishments provide beachface stability by protecting the beach from severe wave attack during storms. Beach nourishments, on the other hand, immediately disburden the beach, but are prone to severe beach erosion during storms (Roelvink and Reniers, 2009).

Because a large part of the Dutch coast is structurally eroding, a new national policy for coastal defence of the Netherlands was established in 1990: the "Dynamic Preservation" policy. To ensure the safety of the low-lying polders and meanwhile make sure the coastal dunes are sustainably preserved, it was decided to maintain the coastline at a position seaward of the reference coastline (BKL) of 1991 (Hillen and Roelse, 1994). Since 1991, between 5 and 15 million m^3 of sand has been added to the Dutch beaches annually. In the beginning, this was done with beach nourishments, and later on a trend towards shoreface nourishments took place, as can be observed in Figure 2.6. The figure also shows that the annual average nourishment volume has increased over time.

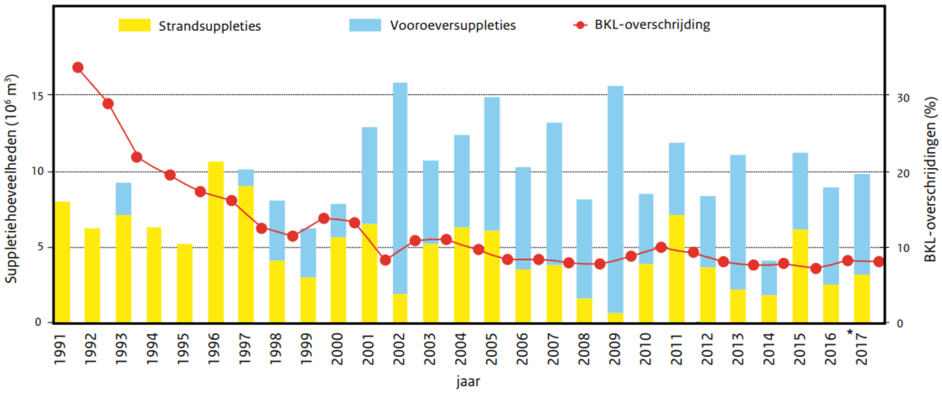

Figure 2.6: Average annual nourishment volume of the Dutch coast. Yellow = beach nourishments, blue = shoreface nourishments. Red = exceedance of BKL. A trend is observed from breach to shoreface nourishments, but both types are still applied. Source: Rijkswaterstaat (2017)

.

2.2.2. Hard coastal protection measures

To protect coasts suffering from structural erosion or erosion during storm events, hard structures are still widely used as well. When talking about hard protection measures, one has to make a distinction between two types, characterised by their function (Bosboom and Stive, 2015):
(1) Structures that aim to interfere/prevent structural erosion by influencing the longshore transport rate: e.g. groynes, dams, and detached and emerged breakwaters.
(2) Structures that aim to prevent storm erosion and flooding during extreme events: e.g. sea walls, revetments, sea dikes.

To give a clear impression of the beforementioned types of hard coastal protection measures, figures of the different structures are presented in Figure 2.7. As the hard-soft transitions that this research is about are all transitions with structures preventing storm erosion and flooding (2), we will not go further into detail on the structures mentioned in (1).

Below, the most commonly applied flood defences to protect the coast from storm erosion, are explained shortly.

Seawalls
A seawall is a (nearly) vertical, impermeable structure built parallel to the shore between a low-lying each and a higher mainland or dune. Seawalls are effective to counteract storm erosion, by cutting of the supply of material from the mainland or dune. Seawalls are *not* effective to prevent structural erosion. A risk of seawalls is that large scour holes in front of the seawall can develop: the vertical structure reflects the waves, which leads to increased turbulence, eroding the material at the toe of the sea wall.

Revetments
Revetments are rather similar to seawalls, but they are generally more gently sloped. They can be constructed out of different materials, varying from smooth to rough. Also in the case of revetments, a scour hole can be expected in front of the revetment structure. The scour hole will generally be smaller than in the case of a seawall, because the gentler slope is less reflective and therefore creates less turbulence.

Sea dikes
Just like river dikes, sea dikes are meant to prevent flooding. The design of the two types is however very different. The difference between sea dikes and revetments is that a beach in front of a sea dike is absent. An example of a sea dike is found in Figure 2.7d.

(a) Groynes at Den Helder. Source: Beeldbank RWS.

(b) Revetment.

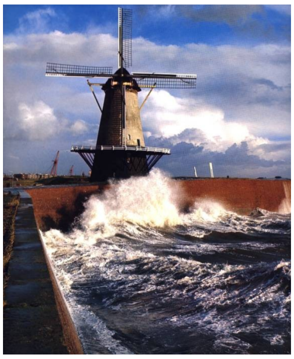

(c) Seawall at Vlissingen.

(d) Seadike at Westkapelle, Zeeland. Source: RWS

Figure 2.7: Examples of hard coastal protection structures

2.2.3. Transition structures

As there are different types of flood defences (soft and hard), it means that there are also transitions between these types. Special care has to be taken to design the transition between these hard and soft flood defences, as they are often vulnerable and unpredictable components of a coastal defence system. Many examples of hard-soft transitions can be found along the Dutch Coast, especially along the Zeeland coast and on the Wadden Islands. As a standard method for designing these transitions does not exist, many of these transition structures have been designed based on 'expert judgement' (Steetzel, 1995). Also for the safety assessment of these structures, a standard procedure is not available, so that a customized safety assessment has to be composed for such transitions (Boers, 2012).

There are, however, a number of reports that provide some guidelines with useful 'grips' to design a safe and durable transition structure. A first analysis of transition structures and some advice for guidelines can be found in Steetzel (1995). Based on this advice, more detailed guidelines were presented in (Boers, 2012) and (van Verkeer en Waterstaat, 2007). In his study, Steetzel (1995) gives an overview of existing hard-soft transition structures along the Dutch coast. He investigated these cases, and concluded that in most cases some information can be found on the final design, but documentation about the design method is lacking. His conclusion from the short assessment of existing hard-soft transitions is that most of them have been designed based on ad hoc 'engineering judgement'.

In the report (Boers 2012), technical guidelines for assessing the safety of flood defence dunes and hybrid flood defences are presented. For dunes, a detailed test/assessment is available. For hybrid flood defences or transition constructions, no such standard procedure is available, but a step-by-step approach is proposed.

For these constructions, a case-specific assessment needs to be developed, for which this report (Boers, 2012) can be used as support and guidance.

A standard procedure for the safety check of dunes is given in (Boers, 2012). According to the procedure, a so called critical profile (green area in Figure 2.9) should remain after dune retreat. The critical profile has the function of just preventing flooding of the dune at the moment the normative storm has finished. After the dune retreat process has reached the critical point of dune retreat, the critical profile prevents the system from flooding.

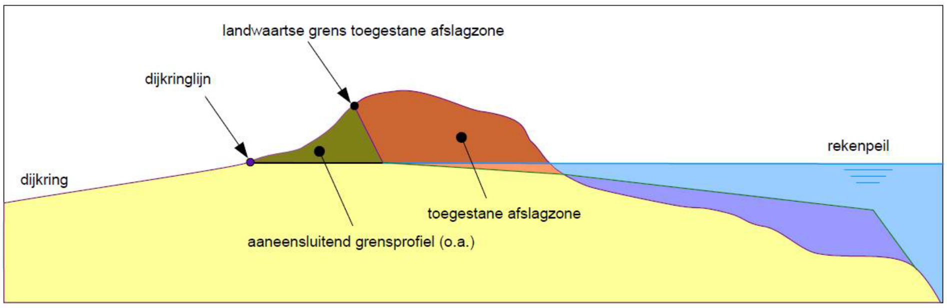

Figure 2.8: Critical profile for the design and safety assessment of dunes. Source: Boers (2012)

.

Prescribed formulas for calculating the minimum height, width and corresponding volume of the critical profile exist, which can be found in Appendix B.2.

The following processes can occur within a flood defence dune system during a storm:
1. Retreat of the foredune
2. Loss of sand from the system, e.g. due to a transition construction
3. Flooding or outflanking
4. Erosion due to hard flood defences.

For the case study of Maasvlakte 2, the first two processes are relevant, which will therefore be discussed below:

1. Foredune retreat
In the presence of a storm, waves can penetrate until the foredune. Due to the wave attack, dune erosion can occur. The dune volume will therefore decrease, but not disappear from the system, as it will be deposited at the shoreface. This will protect the foredune: due to the shallower foreshore, the waves will start to break sooner and therefore the wave attack on the foredune will decrease. And this will, in turn, slow down the dune erosion process further (Boers, 2012).

2. Loss of sand from the system
In a situation of a straight coast without loss of sediment from the dune profile, the volume of erosion is equal to the volume of deposition. In this case we speak of a closed sediment balance. There are, however, many situations in which a net loss of sediment in alongshore direction occurs during a storm. This leads to additional dune erosion. This net loss can have several causes:

- When eroded sand is deposited in deep tidal gullies that are present in the cross profile, they no longer have an effect on the breaking of waves, thus therefore not decreasing the wave attack.
- A gradient in alongshore transport. This can be the case when the coast is curved or when waves come in with an angle to the coast.
- In case of a transition construction, the eroded sand can be transported from one flood defence to another. For example, sediment from the deposition zone of a dune can be transported to the deeper scour hole formed near the toe of a dike.

For the design and assessment of transition structures, some guidelines are provided as well. As was mentioned, there are no strict guidelines for designing such a hard-soft transition, but it is advised to make the transition gradual, and a design example is given in (van de Graaff, 1984):

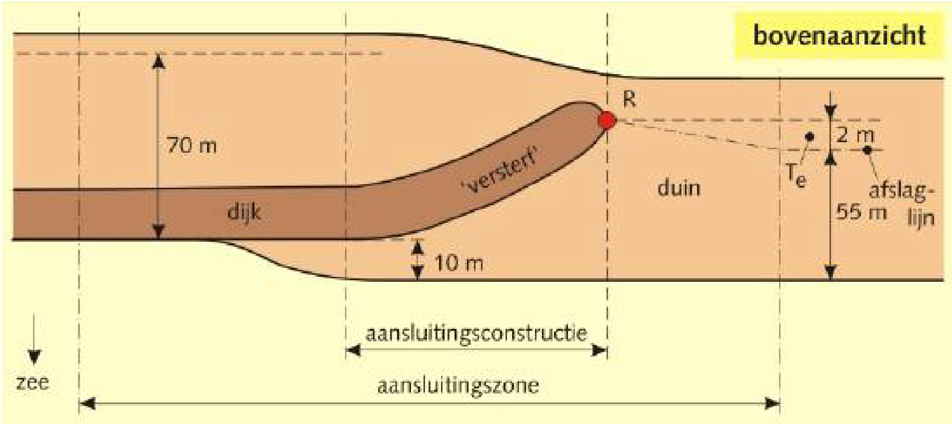

Figure 2.9: Design example for transition structures. Source: van de Graaff (1984)

.

When comparing this design example to the design of the hard-soft transition structure of the MV2, it can be noticed that the designs are quite similar in shape. However, the hard flood defence of the MV2 is not a dike (like in the design example), but a permeable breakwater, which allows for water and sand to go through. It is therefore quite unique and cannot be compared to any hard-soft transition.

As for the assessment (safety check) of transition structures, some guidelines are provided in Boers (2012). The guidelines are presented in a step-by-step guide. For three common types of hard-soft transitions (transition unprotected dune-dike, protected dune-dike and unprotected dune - protected dune), some calculation rules are given as well. The guidelines can be found in Appendix B.3.

2.2.4. Examples of hard-soft transitions in the Netherlands

In view of making the research generally applicable in a later stage, an inventory of other hard-soft transitions was made. To look for other examples, the North Sea coast (Belgium, the Netherlands, Germany and Denmark) was analysed for other hard-soft transition structures. This domain is focused on, because this coast has similar characteristics. Within the Netherlands, the central part of the Holland coast has relatively less coastal structures and therefore transitions. Most coastal structures are found in Zeeland in the south and along the Wadden Islands. In Appendix B.4, an overview of some similar transitions are listed, accompanied by aerial photographs from Google Earth.

One of the examples found in Appendix B.4 - the case of Westkapelle in Zeeland, the Netherlands - has also been analysed in a paper by van Santen et al. (2012). The objective here was to explore possibilities of assessing complex coastlines by a 2DH model in the future, instead of using a 1D model, which is common practice now (and which is often not sufficient, as these models are not able to capture important 2D processes that play a role in complex coastlines). The focus of this paper was on the difference in performance between 1D and 2DH models when modelling complex coastlines. This test case showed that for complex coasts, using a 2DH storm impact model like XBeach is a good alternative for 1D models like DurosTA. See Appendix B.5 for a summary of the results of this paper.

2.3. Case Study Maasvlakte 2

For this research, the hard-soft transition of the coastal protection of the Maasvlakte 2 was studied as a case study. In this study the focus is on the 11 km long flood defence and particularly the transition area between the hard and soft coastal protection, as presented in Figure 2.10.

Figure 2.10: Location of study area: flood defence of the Maasvlakte 2

To construct the flood defence, first, part of the hard flood defence was constructed and part of the soft flood defence. In July 2012, the last gap of the flood defence was closed. The Maasvlakte 2 was officially completed on May 22nd, 2013. After completion, there was a so-called adaptation period of five years that lasted from the day of completion until 17th April, 2018. During this adaptation period, knowledge was assembled about, amongst others, the morphological behaviour of the soft coastal protection. The knowledge gained during this period can then be used as input for the maintenance strategy during the maintenance period, which runs from 17 April 2018 until 17 April 2023. After that, the management and maintentance of the coastal protection will be assigned to Rijkswaterstaat.

2.3.1. Design

The southwestern part of the flood defence is designed as a soft coastal protection of 7.5 km, with a beach and one dunerow behind. This type of flood defence was chosen for several reasons: it is cheaper, more natural, and perturbation to the natural sediment patterns is minimal. A soft coastline as flood defence does require some space in order to create the design equilibrium slope. In this area, the available space was sufficient. Additional advantages of having a soft flood defence here, is that it allows for recreation and growth of vegetation. Along the most northern part of the flood defence, the available space and nautical safety were not sufficient for a soft flood defence, therefore a hard structure (a breakwater made out of blocks) has been constructed over a length of 3.5 km in the north. A top view of the design of the flood defence is given in Figure 2.11. Detailed cross sections of both the hard and the soft coastal protection of the Maasvlakte 2 can be found in Appendix B.6. The transition is relatively gradual. The hard flood defence is unique due to the permeability of the breakwater, the transverse dam on the north side of the transition, and the cobble beach behind it. The soft beach was designed as a equilibrium profile defined by Dean (1977).

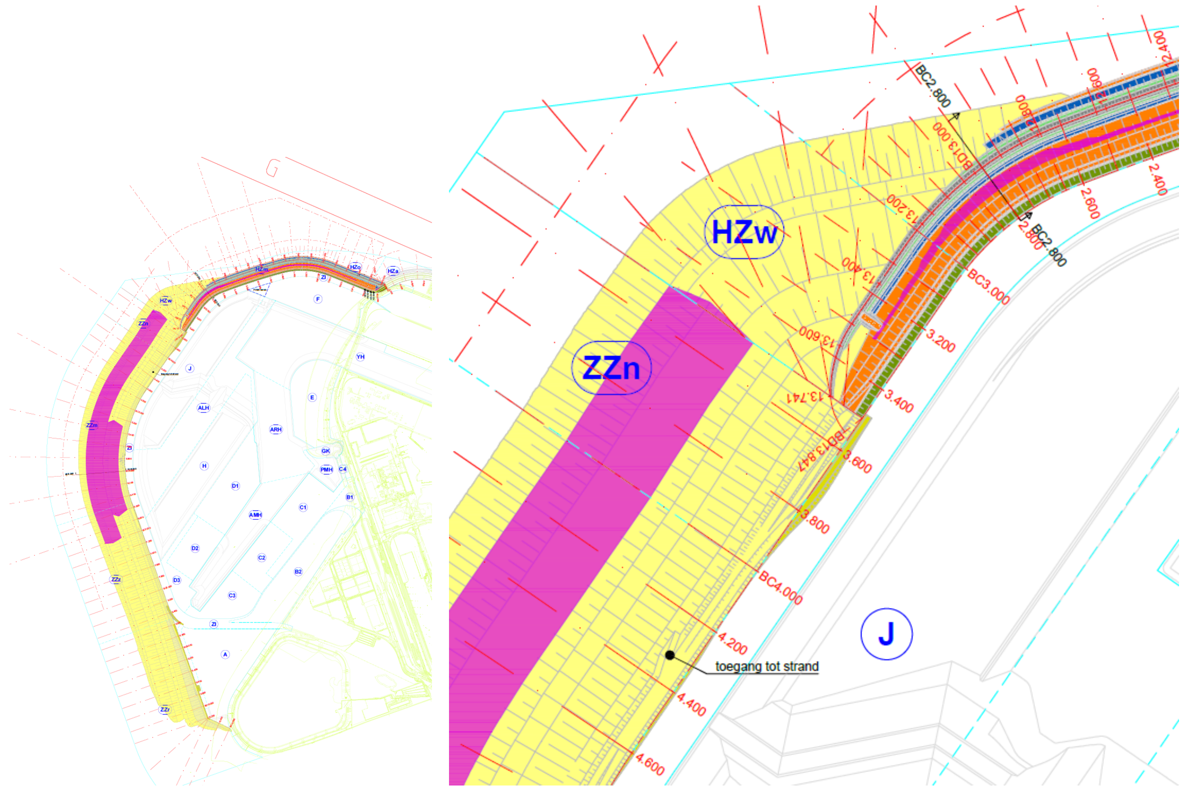

(a) Topview design entire flood defence MV2

(b) Topview design flood defence zoomed into transition hard-soft

Figure 2.11: Top view of the design of the flood defence

2.3.2. Maintenance

According to the initial planning, big nourishment operations were to be carried out every two years. During the adaptation period (2013-2018) three nourishments were planned: in April 2014, 2016 and 2018. In addition, some smaller nourishments were done with the drift sand that was transported behind the dune row (on the biking lane) by aeolian transport. This sand was relocated back to the beach on a yearly basis. An estimation of the planned nourishments was made, which can be seen in Table 2.1. The exact amount of volume of the nourishments was still to be determined on the basis of bathymetry measurements during the adaptation period, showing the amount of eroded sediment and therefore the required nourishment volumes.

Monitoring of the flood defence revealed that the northernmost transects (300 m south of the hard-soft transition) showed a higher dynamic variability than was allowed, so that the safety requirements were not met during several assessment moments. Therefore, with the requirement of a nourishment lifetime of two years, the minimum required volumes of sand per layer were not met. However, it was chosen not to carry out more frequent nourishments, so that the natural behaviour could be monitored without too much interference in the form of nourishments. Moreover, morphological studies showed that big nourishments were not efficient in this area as they eroded quickly. An overview of the planned and actually executed nourishments are given in Table 2.1 and 2.2 respectively. As can be seen from the tables, the total volume of executed nourishments (3.1 million m^3) is smaller than the volume of planned nourishments in the same period (2014-2016, so 1.55+2.38 = 3.93 million m^3). Moreover, no shoreface nourishments have taken place, because this layer constantly had sufficient sediment volume. Instead, sand was nourished more offshore, in order to meet the requirement for the minimum amount of volume in this layer (Vijverberg, 2018).

Table 2.1: Planned nourishment volumes (in million m^3) during the adaptation period. (Vijverberg, 2018)

year	dune	beach	shoreface	offshore	**total**
1 (2014)		0.57	0.99		**1.55**
3 (2016)		0.83	1.55		**2.38**
5 (2018)		0.83	1.55		**2.38**
total	**0**	**2.22**	**4.09**	**0**	**6.32**

Table 2.2: Executed nourishment volumes (in million m^3) during the adaptation period. (Vijverberg, 2018)

year	dune	beach	shoreface	offshore	**total**
1 (2014)		0.76		0.31	**1.7**
1 (2014)		0.35			
1 (2014)		0.3			
3 (2016)		0.35		0.58	**1.4**
3 (2016)		0.46			
total	**0**	**2.22**	**0**	**0.89**	**3.1**

Monitoring and assessment

The underwater profile and beach profile of the soft flood defence has been measured several times throughout the adaptation period, in order to gain more insight into the system, and for the aim of conducting safety assessments. Based on the measured bathymetry, the loss of sediment observed and the volume requirements, the required nourishment volumes were calculated. The bathymetry has been measured every year between 2013 and 2018, and more frequently in 2017 and 2018. An overview of the available measurements can be found in Chapter 3.

With the obtained measurements, assessments were made to check the safety of the flood defence. The assessments are done every year after the storm season (around April). The safety assessment comprised that each layer should contain a minimum amount of sediment volume per transect of 200 m, of which the exact values can be found in the "Beheer- and Instandhoudingsplan" (PUMA, 2013).

Within the design and assessment of MV2, the different **layers** ('schillen') are defined as follows (visible in Figure 2.12):

- Dune (Duinreep): Above +3.0 m NAP
- Beach (Strandoever): Between +3.0 m NAP and -4,0 m NAP
- Shoreface (Vooroever) : between -4.0 m NAP and -8.0 m NAP
- Offshore (Kustfundament): below -8.0 m NAP

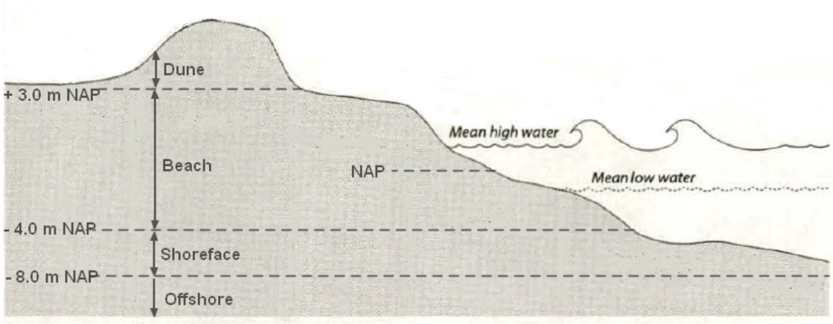

Figure 2.12: Definition of the layers used in the beach of Maasvlakte 2, which will be also referred to later in the study.

.

2.3.3. Morphological studies

To ensure safety of the soft flood defence and gain insight into the morphological behaviour around the hard-soft transition, several studies were conducted (Onderwater (2016), Onderwater and van der Baan (2017), Onderwater (2018a) and Onderwater (2018b)). These morphological studies were carried out with the main objective to find a practical solution for the excessive erosion in the area, and to reformulate the method for assessing the safety of the system, such that the requirements, set by the client, can be met after the adaptation period. This section gives an overview of the observations done in these studies.

After realising that the morphological processes around the hard-soft transition of the MV2 led to a conflict between the assessment method and the nourishment strategy, Onderwater (2016) conducted a first morphological study. The aim of this study was to identify the causes for this, so that suitable measures can be taken in order to be able to meet to the requirements of nourishing at most every two years while meeting the safety standards. The reason for this study was the assessment of the volumes of the morphological transects from 2015, from which it was visible that several transects (the five northernmost) did not have enough spares to be able to to withstand the expected erosion for the coming year. The following analyses were carried out: analysis of erosion- and sedimentation patterns, analysis of requirements, analysis of the wave climate, observations based on Google Earth, analysis of current patterns and tide-induced sediment transports, wave pattern around the Northern Termination, wave-induced sediment transports, and combination of wave- and tide-induced sediment transports.

From the analyses, three main aspects were observed from the morphological system around the northern termination:

- A rotation of the coastline: the northernmost 300 m coastline of the soft flood defence was rotated with an angle to the original orientation.
- A characteristic cross-shore profile, with a sand bar and a trough
- Natural dynamics: because of the Northern Termation being the end of a coastal profile, large gradients in sediment transport occur, so that a certain dynamic can be expected.

Furthermore, it was found that the nourishments on the beach in 2014 on the cone turned out to be rather ineffective and eroded again quite fast. The layer volume of the shoreface appeared to be rather stable and even bigger than the required volume. In the layer volumes of the beach for transects 'Cone 335' and 'Cone 350', a deficit of sediment was often observed. Based on these analyses, six solutions were proposed to solve the erosion problem, of which one was chosen. This solution consisted of adjusting the method for safety assessment, taking into account 2D effects around the cone, adjusting the required layer volumes, and redefining the location in the cross-shore profile for the nourishments.

After the Q2 2017 measurements, it appeared that also with the new assessment method, the assessment requirements were not met. Therefore, more knowledge on the morphological system was gained by conducting model simulations (Onderwater and van der Baan, 2017) with the 2DH process-based model Xbeach (Roelvink et al., 2009). The aim of this study was to analyse the 2D-effects around the hard-soft transition, as well as to investigate what the effect of the altered bottom configuration was on the erosion-sedimentation patterns, and on the amount of dune retreat. Based on these findings, a decision was made on whether and where the safety assessment can be adjusted, in order to have a safety assessment that is better suited for the morphological development of the soft flood defence and the cone. The main conclusions from this study were:

- When modelling the morphological development for the design bottom configuration, erosion can be seen higher in the profile and sedimentation can be seen lower in the beach profile. When modelling with the most recently measured bottom configuration, not one erosion-sedimentation pattern is visible, but two: a sand bar- and trough have developed in the profile.
- Three wave directions have been simulated: waves from 297 °N, 317 °N and from 341 °N. The 317 °and 341 °N directions cause the highest erosion rates, because of the larger gradients in alongshore sediment transport. See section 2.1.2.
- It was found that due to the relatively larger volume of sand on the shoreface as was the case with the profile in 2013, more wave damping took place on the shoreface and foreshore, which resulted in a decrease of dune retreat of about 7 to 8 meters.
- So indeed, the altered bottom configuration as it was in 2013 did have a (positive) effect on the dune retreat, which gives opportunities to adjust the safety assessment method.

In a subsequent report, Onderwater (2018a) builds on the knowledge gained in (Onderwater and van der Baan, 2017), and makes recommendations on new methods for the safety assessment of the flood defence, so that the requirements of nourishing once every two years can be met. An important conclusion from this report is that it appears from the 2017 measurements that the nourishment of 2016 eroded very quickly (just like was the case for the 2014 nourishment). From the 2016 measurements, after a year without big nourishment (2015), the system seemed to be more stable. Therefore, Onderwater (2018a) recommends the following:

- It is recommended not to make the assessment based on layer volumes, but based on position of the dune retreat point relative to a critical retreat point (similar to the standard safety assessment for uniform coasts from (Boers, 2012)).
- It is also concluded that the frequent nourishment brings about a negative trend in the sediment volumes. It is therefore recommend to interfere less in the system ('leave the system alone'), which can be done by: a) nourishing less frequently, and/or b) not nourishing in the active zone (shoreface and foreshore) anymore.

The latter solution - to nourish higher in the profile, not in the active zone - proposed in (Onderwater, 2018a) is then worked out further in (Onderwater, 2018b). The solution following from this report is to strengthen the dune profile by heightening and widening the dune. The goal of this measure is to shift the dune retreat point seawards, and to increase the lifetime of the nourishment so that the requirement of nourishing once every two years, can be met. From model simulations with Unibest-CL+ and DurosTA, it followed that with the strengthened dune profile, the nourishment lifetime requirement should be met.

The newly defined profile with the strengthened dune will be applied for the first time in the the last months of 2018 (so that beach grass or marramm grass can grow fast). Together with a smaller nourishment on the beach, this should be sufficient to assure safety of the dune for the next two years.

3

System Analysis

This chapter presents a sysem analysis of the hard-soft transition of MV2 based on available data. The system analysis consists of a data analysis (bathymetry and waves) and a theoretical approximation of potential sediment transports. Based on these observations, a number of hypotheses are formulated at the end of this chapter for effective investigation with numerical tools, which are carried out in the remaining part of the study.

3.1. Analysis of bathymetric survey data

To make an initial analysis of morphological trends and features, one can start by plotting the available bathymetric data in different ways. Bathymetric surveys were conducted at the following moments:

- 24/03/2013 (2013 Q2)
- 01/05/2014 (2014 Q2)
- 23/04/2015 (2015 Q2)
- 30/03/2016 (2016 Q2)
- 9/5/2017 (2017 Q2)
- 14/8/2017 (2017 Q3-1)
- 16/10/2017 (2017 Q3-2)
- 19/12/2017 (2017 Q4)
- 11/01/2018 (2018 Q1)
- 14/03/2018 (2018 Q2)
- 20/09/2018 (2018 Q3)

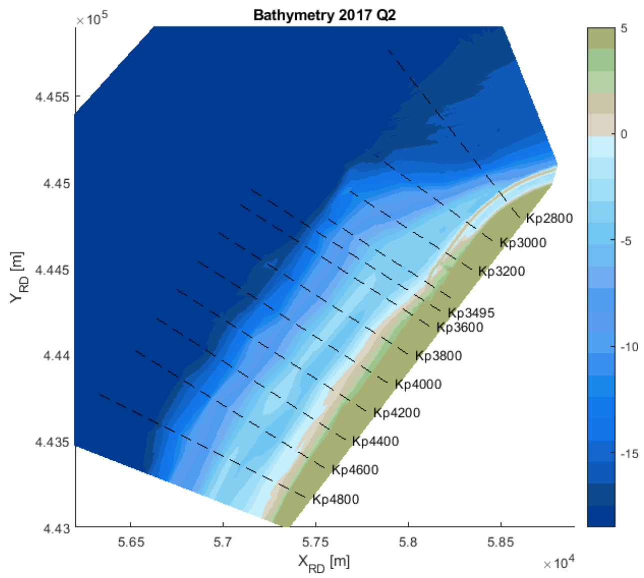

Figure 3.1: Bathymetry measured at 2017 Q2 (9/5/2017). This figure also shows the location of the different transects which were used in the design and assessment of the MV2, and which will also return frequently in this study. The transect that separates the soft flood defence from the hard flood defence is Kp3495.

The following plots and analyses were carried out: 1) 2D scatter and contour plots; 2) 1D cross-sections of transects; 3) sedimentation-erosion plots, showing the difference in volume between certain periods.

The results per period were compared with the wave conditions in that period, to see which wave conditions are responsible for certain observations in the morphological behaviour. The wave data were obtained from measurements at Europlatform, which is made publicly available by Rijkswaterstaat [1]. For the wave data, the following analyses were made:
1) Timeseries of significant wave heights; 2) Wave roses, per period and for the entire year, and 3) Potential

[1] The data can be download from http://waterberichtgeving.rws.nl/

longshore sediment transport, based on wave data; 4) Dominant wave direction per period, based on energy flux method

3.1.1. Analysis of 2D plots

Figure 3.2 and 3.3 show the depths in the area around the hard-soft transition for the survey moments 2017Q3 and 2017Q4, respectively. More figures of other survey moments can be found in Appendix C.1. From Figure 3.2 and the figures in Appendix C.1, the following observations were made:

- A subtidal sandbar (at approximately -2 m NAP) is clearly visible from the 2014 Q2 measurements onwards. During several surveys, also an emerged sandbar is present, at approximately +2 m NAP. This sandbar is especially visible during the 2017Q2 and 2018Q2 surveys.
- Moreover, the relatively homogeneous sandbar present in and before 2017Q3 has become 'disrupted' between the 2017Q3 and 2017Q4 surveys; a stronger longshore variability is present.
- The subtidal sandbar is slowly moving onshore, which could be the consequence of shoreface nourishments, as was found in literature (Radermacher et al., 2018, Kroon et al., 1994; van Duin et al., 2004; Lodder and Sorensen,2015). Especially between 2017Q3 and 2017Q4, the sandbar shows a big onshore 'jump' (better visible in the cross-sections presented in Figure 3.4). This can still be due to the combination of earlier shoreface nourishments and wave action pushing the bar onshore.

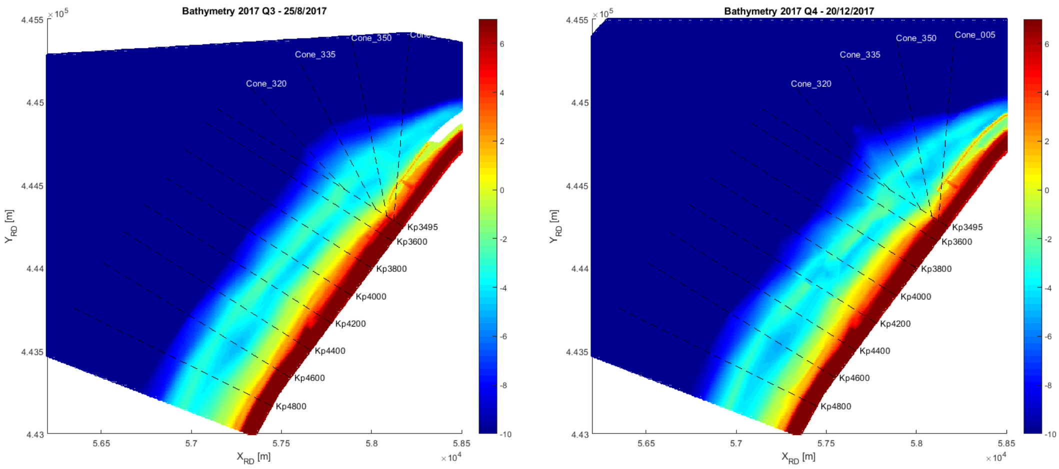

Figure 3.2: Depth plots for surveys 2017Q3 and 2017Q4

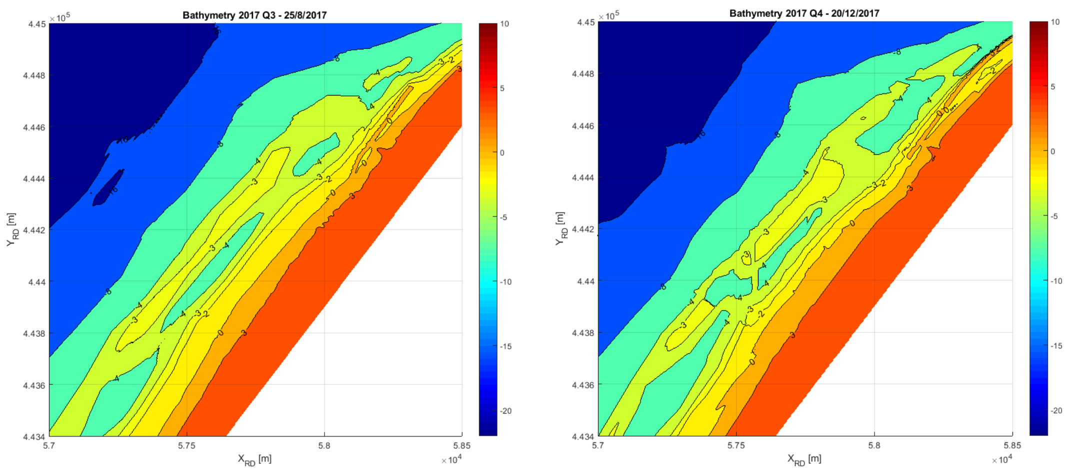

Figure 3.3: Contour plots for surveys 2017Q3 and 2017Q4

3.1.2. Cross-sections

The temporal variability of the profile can also be examined by comparing different cross sections. In appendix C.3, different cross-sections around the hard-soft transitions are compared over time. From Figure 3.4 it can be seen that the most northern transects (for example Kp3495, Kp3600 - figure 3.4a and 3.4b - show high dynamic variability of the cross-shore profile, whereas the transects more to the south (e.g. Kp4800, see Figure 3.4c) are much more stable. Moreover, from these plots again the erosion of the upper profile and simultaneous onshore migration of the subtidal sandbar between 2017Q3 and 2017Q4 is visible.

In order to investigate whether the barred system developed as a consequence of the breakwater of the hard flood defence or from nourishments, and what determines the position and migration of the bar system, one can also look at transects more to the south. This shows that also along the southern part of the soft flood defence (transect 7000), a subtidal bar is present (see Figure 3.4d). Apparently, the subtidal sandbars is present over the full length of the soft flood defence and is not just bound to the hard-soft transition. To find possible trends in the dynamic behaviour of the barred system in the northern transects, a closer look is taken at the northern transects (Kp3495, Kp3600 and Kp3800) in Figures 3.5.

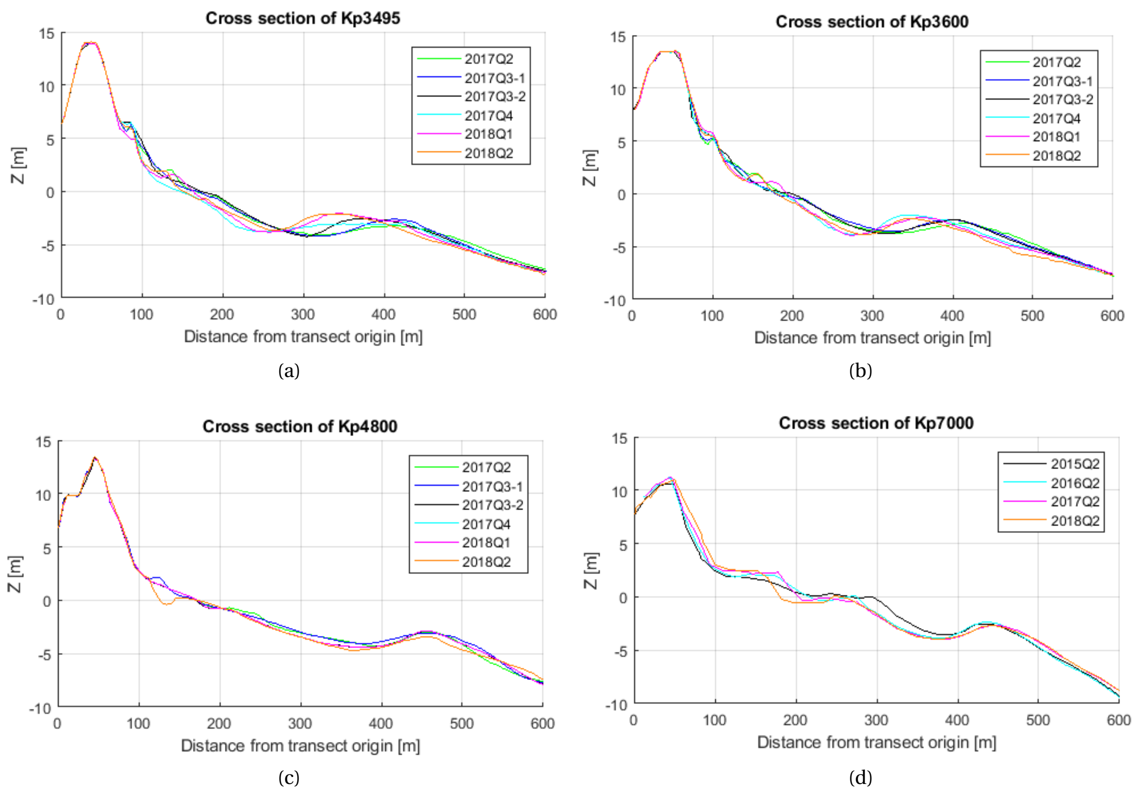

Figure 3.4: Cross sections of transect 3495, 3600, 4800 between 2017 and 2018; and cross section of transect 7000 between 2015 and 2018.

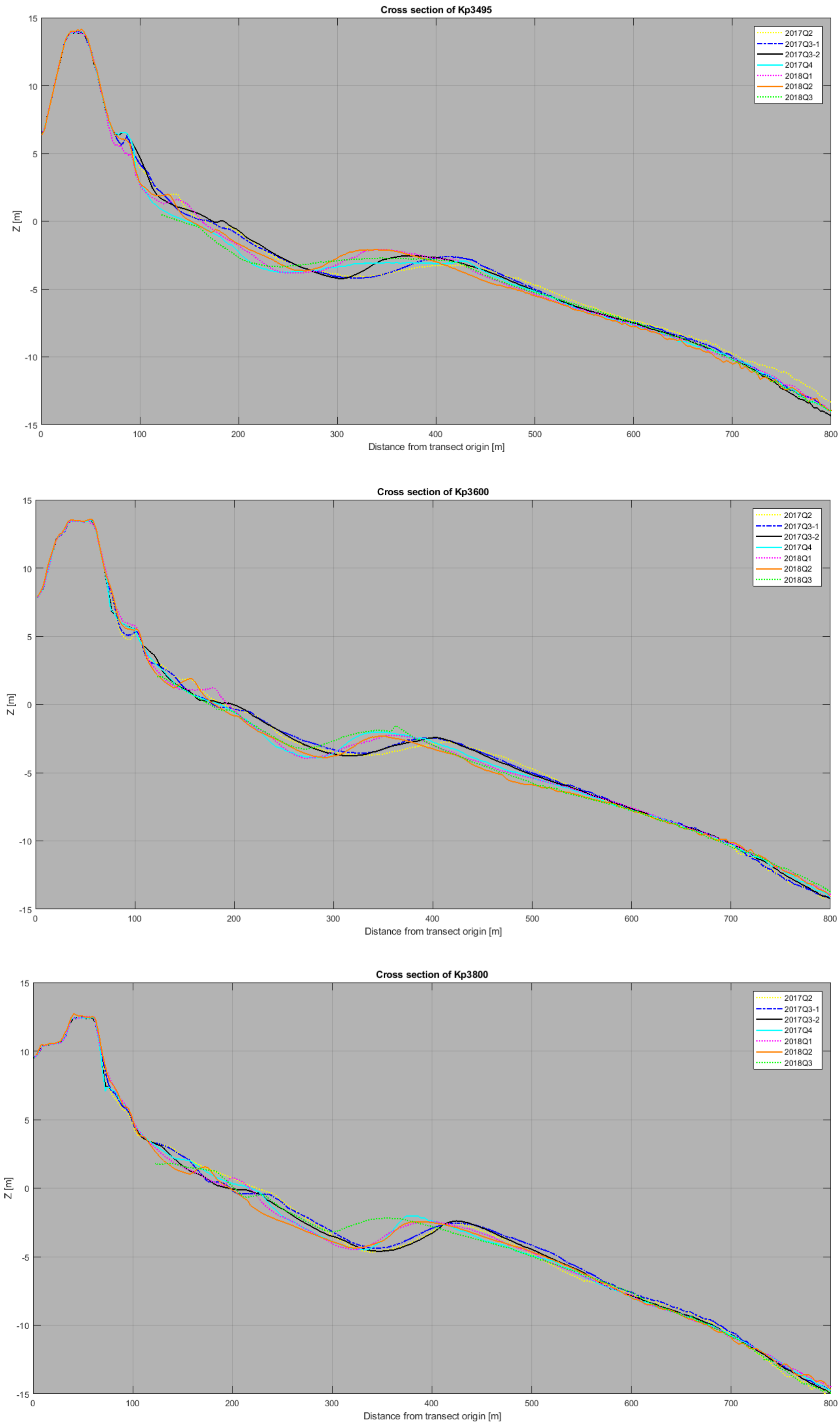

Figure 3.5: Cross-sections of different survey moments for the northernmost 3 transects: Kp3495, Kp3600 and Kp3800.

From Figure 3.5, some interesting trends can be found:

- Transect Kp3495: Between surveys 2017Q3-2 and 2017Q4 (black and lightblue lines, respectively), the subtidal bar is almost entirely flattened out/disappeared, together with severe erosion of the beach (between +3 and -4 m). In the subsequent two surveys, 2018Q1 and 2018Q2 (pink and orange lines), the bar has 'grown back' again, but shifted onshore. Between surveys 2018Q2 and 2018Q3 (green and orange lines, respectively), again, the bar has been flattened out together with erosion of the beach.
- Transect Kp3600: Between surveys 2017Q3-2 and 2017Q4, the bar shows a rapid onshore jump. In the subsequent two surveys, 2018Q1 and 2018Q2, the bar stays quite stable, but moves a bit offshore again. During survey 2018Q3 (green line) the bar again shows a rapid onshore jump.
- Transect Kp3800: This transect shows the same behaviour as transect Kp3600, but even bigger jumps are observed.

3.1.3. Sedimentation-erosion patterns

A clear way of visualizing the magnitude of sedimentation and erosion between two surveys is by making sedimentation-erosion plots. The results of this are presented in Appendix C.4 . It has to be noted that between 2017Q2 and 2018Q2, not all surveys cover the entire area of interest. For example, part of the surveys of 2017Q3 and 2018Q2 are not complete, and therefore the data of the previous survey is pasted into the empty part of these surveys. Therefore, it looks from the sedimentation-erosion plots of 2017Q2-Q3 and 2018Q1-Q2 like there is an area with no volumes changes in the most northern part. Two of the sedimentation-erosion are especially interesting to present here because they show very similar patterns around the hard-soft transition: the ones of 2017Q3-2-2017Q4 and 2018Q2-2018Q3: an area of severe erosion is found around the hard-soft transition (indicated with number 1) and on the cone for both cases, and further downstream, between transects Kp3600 and Kp4000, an area of sediment deposition is found nearshore (indicated with number 2) and another area of erosion is found further offshore (indicated with number 3).

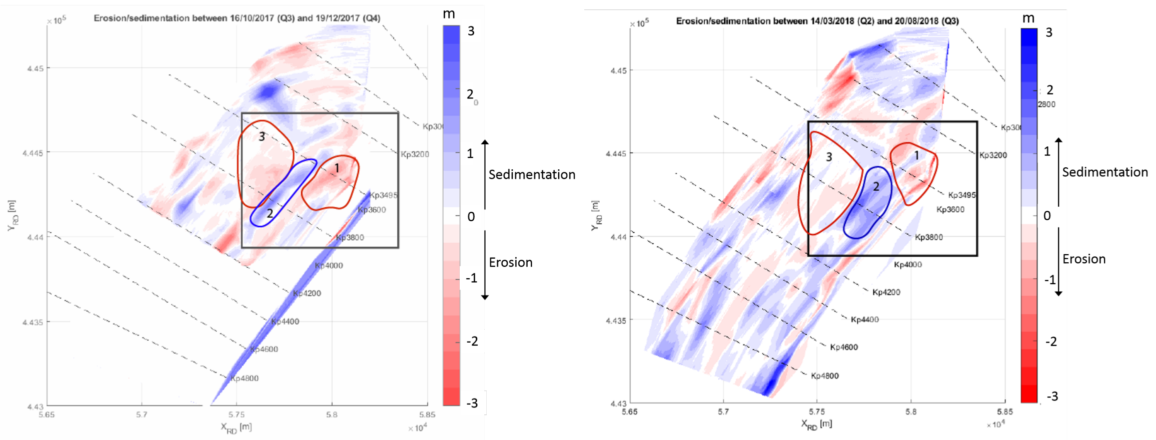

Figure 3.6: Sedimentation patterns for 2017Q3-2-2017Q4 (left) and 2018Q2-2018Q3 (right).

To make the results more quantitative, the area was divided into polygons, and the amount of volume change per polygon was calculated between each consecutive survey. Because each polygon has a different size and every period between two surveys differs in length as well, the output volumes were scaled by dividing by the polygon volume (in m) and by the number of days in the period. The sedimentation-erosion plots are presented in figure 3.8. What is striking from the figures is that we see again predominantly erosion in between the 2017Q3 and 2017Q4 surveys, whereas we see more sedimentation between 2017Q4 and 2018Q1 (except in polygon 2). Moreover, polygon 16 appears to be very dynamic, as it experiences high values of erosion as well as sedimentation.

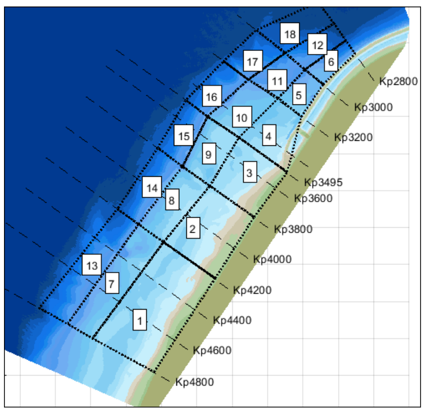

Figure 3.7: Subdivision of the study area into compartments for sedimentation-erosion calculations.

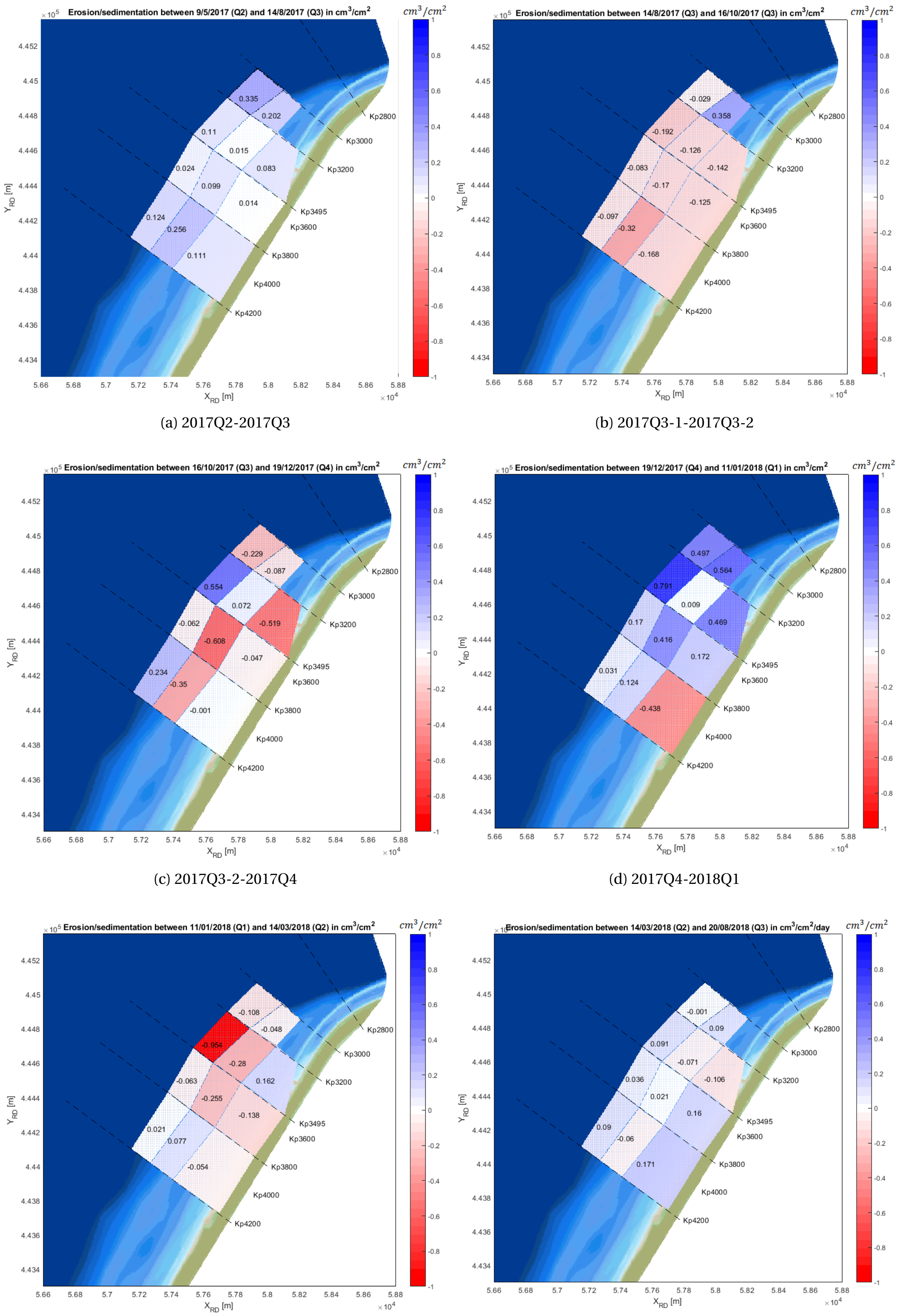

(a) 2017Q2-2017Q3

(b) 2017Q3-1-2017Q3-2

(c) 2017Q3-2-2017Q4

(d) 2017Q4-2018Q1

(e) 2018Q1-2018Q2

(f) 2018Q2-2018Q3

Figure 3.8: Sedimentation and erosion between 2017 and 2018.

3.2. Analysis of wave data

3.2.1. Timeseries and waveroses

The observed morphological changes can be related to the wave climate for each period. In this stadium, the offshore wave conditions measured at Europlatform were used as they were not converted to nearshore conditions yet. From the figures in the previous section, it was observed that especially between 2017Q3 and 2017Q4 significant erosion and onshore migration of the subtidal bar took place. When looking at timeseries of wave heights between 2017Q2 and 2018Q3 (Figure 3.9), we see that it is not just the wave height that is responsible for this erosion and bar migration, since high waves occur between 2017Q4 and 2018Q1 as well. Apparently, the direction plays a role as well.

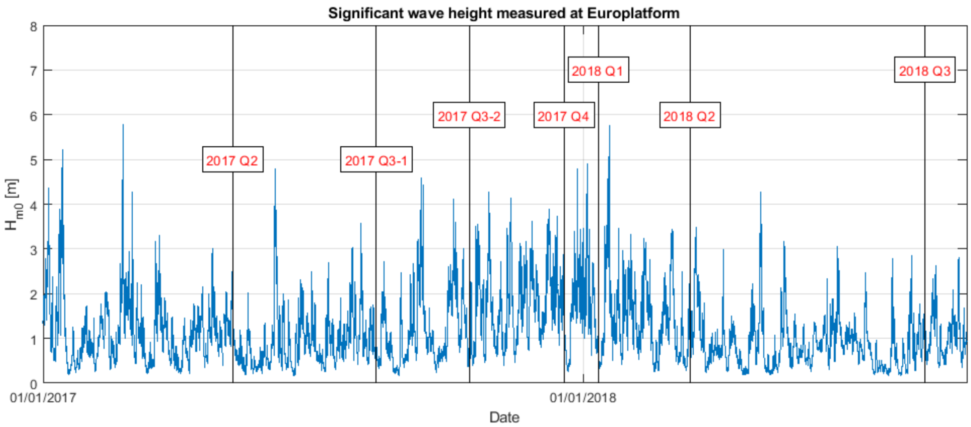

Figure 3.9: Significant wave height measured at Europlatform from january 2017 to may 2018.

A better approach is to look at the wave roses, which show the frequency of waves coming from particular directions. The wave roses for each period between two surveys are presented in Figure 3.10. The wave climates are clearly different from one another. First of all, the wave roses for the periods 2017Q2-2017Q3, 2017Q3-1-2017Q3-2 and 2018Q1-2018Q2 (wave rose a, b and e) are calmer than the other two (wave rose c and d) as they show smaller wave heights. Additionally, the wave roses for the periods 2017Q3-2017Q4 and for 2018Q2-2018Q3 (wave rose c and f) both show a large part of the waves are large waves coming from northern directions. Between 2017Q4 and 2018Q1 large waves occurred as well, but as can be seen from Figure 3.10d, these are coming from the southwest. The waves coming from NNE are expected to attack the coast more due to increasing sediment transport gradients at the hard-soft transition. In contrast, the waves from the southwest measured at Europlatform might allow the system to recover by supply from sediment downstream. This might explain why significantly more erosion was observed between 2017Q3-2017Q4 compared to 2017Q4-2018Q1. This will be investigated further during the model tests in Chapter 5 .

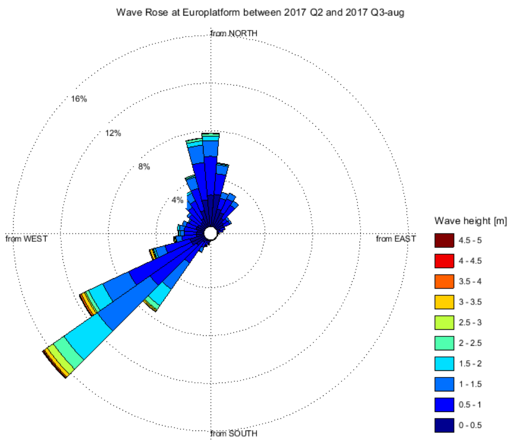

(a) Period 1: 2017Q2 - 2017Q3

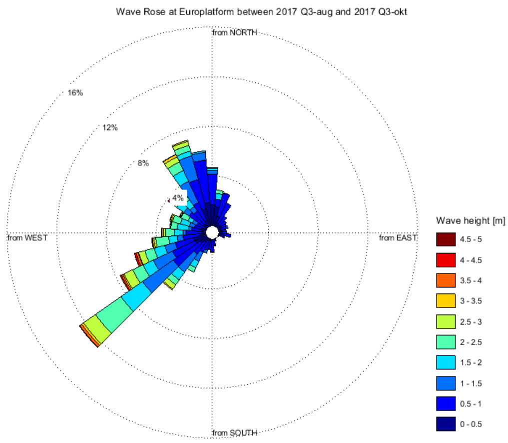

(b) Period 2: 2017Q3_1 - 2017Q3_2

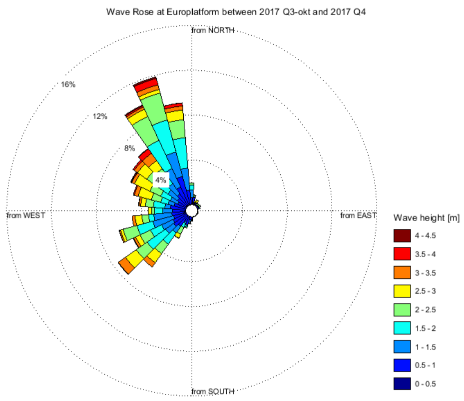

(c) Period 3: 2017Q3_2 - 2017Q4

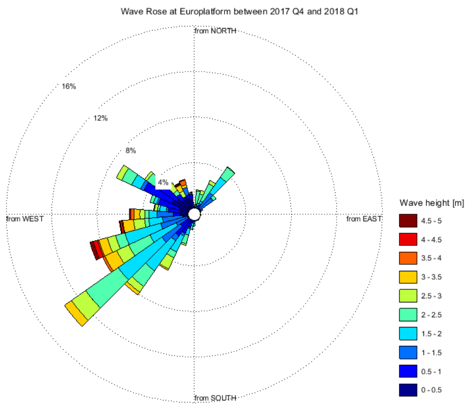

(d) Period 4: 2017Q4 - 2018Q1

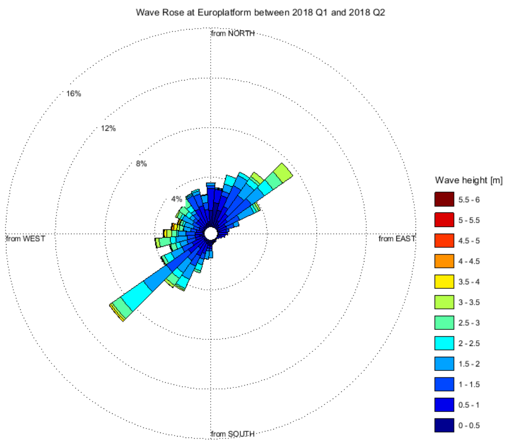

(e) Period 5: 2018Q1 - 2018Q2

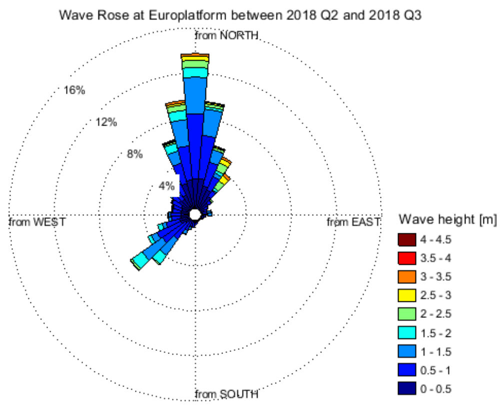

(f) Period 6: 2018Q2 - 2018Q3

Figure 3.10: Wave roses per period between two surveys. Each concentric circle represents a different frequency, starting at zero at the center to increasing frequencies at the outer circles. Each spoke is broken down into color-coded bands that show wave height ranges.

3.2.2. Wave energy flux

Another way of analysing the wave climate is by computing the magnitude and direction of the wave energy flux. Since the wave energy is proportional to $H_s^{2.5}$, the magnitude and resulting direction of the wave energy flux can be computed as is visualized in Figure 3.11 below. Each line segment represents the magnitude and direction of one directional class (divided into 9 classes, each representing 20°). For example, the blue line starting at (x=0, y=0) represents the waves coming from directions in between 220 °and 240 °N, and its length is equal to the sum of each wave height in this bandwidth to the power of 2.5. Visualisation of the same computation for other years can be found in Appendix C.5.

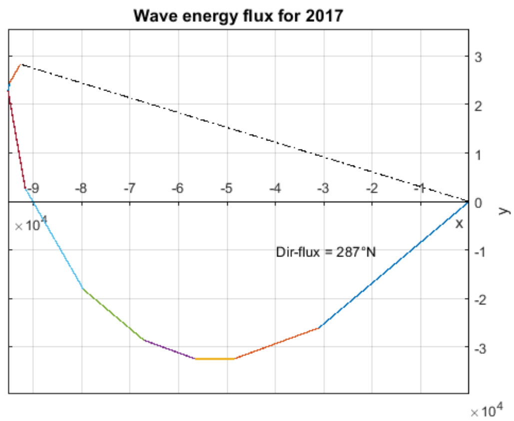

Figure 3.11: Visualisation of the computation of the wave energy flux, here showing the wave energy flux for 2017.

First of all, it was checked what the average resulting direction of the wave energy flux was for the years 2013 - 2018. In earlier studies (Onderwater, 2016), it was found that in the period 1979-2001 the resulting direction of the wave energy flux was 280 °N. For the period 2012-2015 it was 270 °N and for the period 1979 - 2015 it was 279 °N. The computed values for 2013 until 2018 are found in Table 3.1 below. As can be seen, the average direction of the resulting wave energy flux for the years 2013 - 2018 (280.7) is almost the same as the wave climate between 1979-2015 (279). This means that the wave climate did not deviate significantly from historical wave climates.

Table 3.1: Direction of wave energy flux for 2013 - 2018 based on wave data at Europlatform

Year	Resulting direction wave energy flux
2013	292
2014	267
2015	262
2016	284
2017	287
2018	292
Average	**280.7**

Secondly, it was checked what the magnitude and direction of the wave energy flux for every period within the time span 2017 Q2 - 2018 Q2 was. Since the waves from this period were also converted to nearshore data with SWAN (see Chapter 4 for an explanation of the SWAN model and its set-up), the wave energy flux can be computed both with offshore data from Europlatform, and with nearshore data from SWAN. The results are listed in Table 3.2 below. The following can be said about these results:

- The average of the resulting directions for periods 1 to 5 is 272 °N, but with nearshore data the average resulting direction is 299 °N. This is a difference of more than 25 °. Apparently, the wave energy flux direction with offshore data computed with offshore data does not represent the nearshore wave conditions very well (also when neglecting the wave conditions < 220 °N and > 40 °N. This means that when drawing conclusions from offshore wave data, the deviation between the offshore and nearshore wave data should be taken into account.

- When looking at the different periods, one can see that in period 1 and 4 (2017Q2 - 2017Q3 and 2017Q4 - 2018Q1) the wave energy flux is from the same direction (292 °N and 293 °N). In periods 2 and 5, the wave direction is also from nearly the same direction (299 °N and 300 °N). During period 3, the waves are relatively more from the North (311 °N).

Table 3.2: Direction of wave energy flux for 2017Q2-2018Q2 based on offshore data (Europlatform) and nearshore data (SWAN output).

	Period	Europlatform Bandwidth 220-40 (Coast orientation 310)	Nearshore Bandwidth 220-40 (Coast orientation 310)
1	2017Q2-2017Q3	250	292
2	2017Q3_1-2017Q3_2	270	299
3	2017Q3_2-2017Q4	301	311
4	2017Q4-2018Q1	266	293
5	2018Q1-2018Q2	275	300
6	2018Q2-2018Q3	343	-
Average		**272.4**	**299**

3.3. Analysis of sediment transports

Now that the observed erosion/sedimentation patterns and corresponding wave climates have been analysed, one can look at potential longshore sediment transports to see if these hold a connection to one another. A first approximation can be done by means of theoretical formulations.

One way to visualise the longshore sediment transport rates at the coast is by computing the cumulative sediment transports based on the complete timeseries of wave heights, wave directions and peak periods from 2017-2018 as measured at Europlatform. This can be done by calculating the sediment transport using the nearshore CERC (Komar and Inman, 1970) formulation (eq. 2.4 in Chapter 2) or the Kamphuis (1991) formula (eq. 2.3 in Chapter 2), taking the cumulative sum at every timestep, starting at t=0 in January 2017. This results in Figure 3.12.

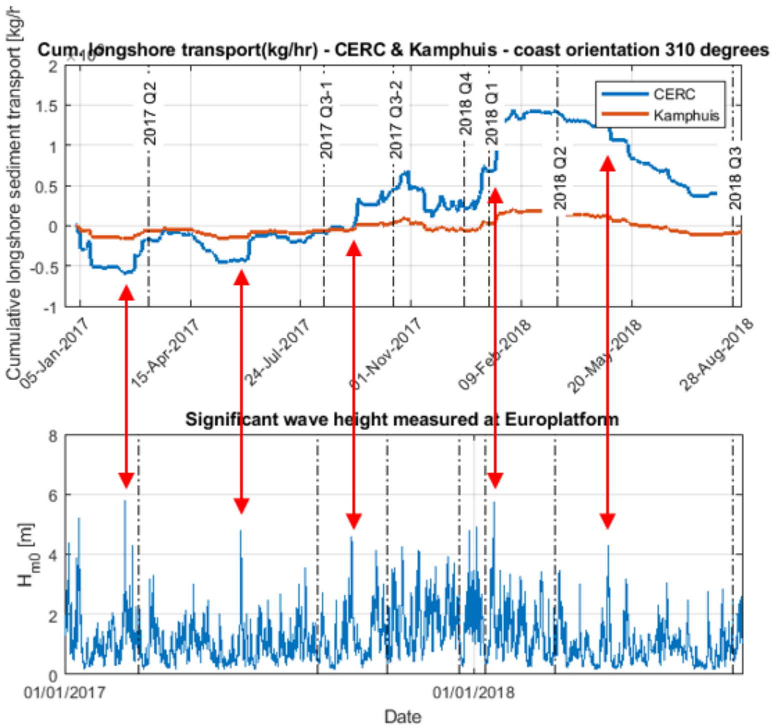

Figure 3.12: Upper figure: Cumulative longshore transport in kg/hr for CERC formula (blue line) and Kamphuis formula (red line). Positive sediment transport rates indicate transport in northeast direction; negative sediment transport rates indicate transport in southwest direction. Lower figure: Significant wave height in m for same period.

Although the difference between the two formulations is quite significant, the general trend is similar. The graph should only be used for qualitative purposes, as the sediment transports were calculated by substituting deep water wave parameters in the CERC (Komar and Inman, 1970)- and Kamphuis (1991) formulations that actually require wave parameters at the breaker line. Therefore the exact outcome should not be used for any quantitative calculation. Moreover, the difference in outcomes between the two formulations can be explained by the fact that in the CERC (Komar and Inman, 1970) formulation the sediment transport is proportional to $H_s^{2.5}$ whereas in the Kamphuis (1991) formula the sediment transport is proportional to H_s^2. When using nearshore conditions the outcomes should be relatively similar, but when filling in deep water wave heights which are significantly larger, both formulations will overestimate the sediment transport, but the CERC (Komar and Inman, 1970) formulation will overestimate the sediment transport even more than the Kamphuis (1991) formula.

What can be seen from Figure 3.12 is that there is relatively little sediment transport between 2017Q2 and 2017Q3, increasingly northeast-directed transport between 2017Q3-1 and 2017Q3-2, southward transport between 2017Q3-2-2017Q4, and a lot of northward directed transport between 2017Q4 and 2018Q1. From then on, mostly southwest-directed transport can be seen. Form the CERC (Komar and Inman, 1970) formula the net cumulative sediment transport in the period 2017Q2-2018Q2 is clearly northeast-directed, as well as for the Kamphuis formula.

When the longshore transports are compared to the measured significant wave heights during the same period as shown in Figure 3.12, we see indeed that high wave events are linked with large jumps in the longshore sediment plot. Downward jumps are the consequence of waves coming from the north-northwest direction, whereas upward jumps are the consquence of waves coming from south-southwest direction. The same computation and visualization was done for the other five years, resulting in Figure 3.13.

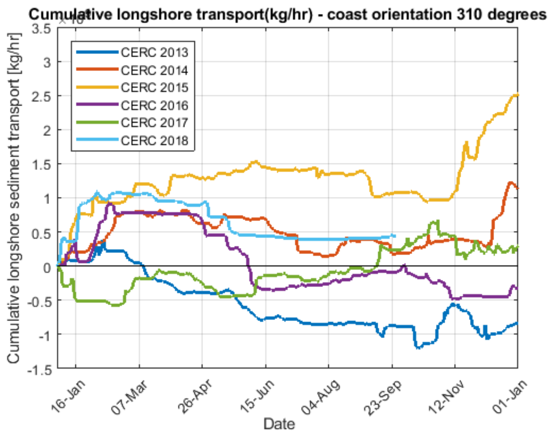

Figure 3.13: Cumulative longshore transport in kg/hr for CERC formula. Positive sediment transport rates indicate transport in northeast direction; negative sediment transport rates indicate transport in southwest direction.

The sediment transports visualized in Figures 3.12 and 3.13 were computed for a coastline orientation of 310 °N. This holds for the northenmost 350 meters coast, where the coastline has rotated on average 10 °with respect to the original coastline, obtaining a coastline orientation of 310 °.

The sediment transports show quite some differences between the six years, however some similar trends can be recognized. Almost all years start with a period of northeast-directed transport (except 2017), followed by a period of southwest-directed transport from March/April. In the summer months there is relatively little sediment transport and then from October/November high wave events are inducing sediment transport in both northeast and southwest direction again. In chapter 6, the wave climate is discussed more thoroughly.

3.4. Discussion

The main findings from the system analysis are as follows:

- A distinct bar and trough are present in the coastal profile over the last years. In the northernmost transects, the bar is very dynamic whereas at the southern transects it is more stable. The periods 2017Q3-2017Q4 and 2018Q2-2018Q3 show similar trends in the bar dynamics.
- An onshore migration of the subtidal bar can be observed, and most significantly between surveys 2017Q3 and 2017Q4 and between surveys 2018Q2-2018Q3 around the hard-soft transition.
- The rotated coastline over the northenmost 300 m that was observed in earlier measurements and satellite images in 2013 (Onderwater, 2016), is still present in the latest measurements.
- The most severe erosion around the hard-soft transition occurs between the 2017Q3 and 2017Q4 surveys, as well as between 2018Q2 and 2018Q3, during which relatively more waves are coming from N-NW direction. During these periods, especially the transects around the hard/soft transition experience severe erosion.
- Between the 2017Q4 and 2018Q1 survey, there is surprisingly much sedimentation.
- Potential longshore sediment transport is predominantly directed northwards.
- Years 2014, 2015, 2016 and 2018 started with a period of northeast-directed sediment transport, followed by a period of southwest-directed sediment transport from March/April. In the summer months there is relatively little sediment transport and then from October/November it seems that high wave events are inducing sediment transport in both northeast and southwest direction again.

3.5. Formulation of hypotheses

After the system was analysed based on measurements, hypotheses were formulated in order to effectively use models for the actual investigation to answer the research questions. The four subquestions needed to answer the central question about MV2, concern the relative importance of wave direction, the coast's own shape, reflection and turbulence due to the breakwater, and wave-tide interaction. Sections 3.1.3, 3.2 and 3.3 suggest that waves from north/northwest cause more erosion whereas waves from south/southwest may allow the coast to recover by supplying sediment. The first hypothesis therefore reads:

Hypothesis 1: "Wave Direction"
Waves from northwest cause more erosion than waves from southwest, which is due to positive gradients in longshore sediment transport and increased wave attack.

Moreover, we have seen that the most northern part of the soft flood defence, just south of the transition, is much more dynamic and experiences higher erosion rates than further south. This can have several causes, such as the rotated coastline in the northern part, and reflection and turbulence caused by the breakwater. It is expected that both contribute in some way, so the next two hypotheses read:

Hypothesis 2: "Effect of coastal shape"
The evolved coastal profile as observed in 2017, with a distinct bar and trough in cross-shore direction and a rotated coastline in the northern part, influences the morphological changes of the coast.

Hypothesis 3: "Reflection at the breakwater"
Reflection of waves at the breakwater is an important cause for the observed erosion close to the hard-soft transition.

Another interesting finding of the system analysis was the dynamic spot observed at some distance offshore of the hard-soft transition (polygon 16 in Figure 3.7). As earlier studies showed that under average wave conditions tide plays a role at depths <-10 m, and there is a net offshore tidal current at the hard-soft transition, it is well possible that this dynamics spot is the result of the tide. However, in earlier studies (Onderwater, 2016) it was found that tide does not play an important role in the morphological behaviour of the shoreface and beach. Though, this was not checked with measurements. The last hypothesis is therefore:

Hypothesis 4: "Tide"
Tide and wave-tide interactions do not play an important role in the morphological behaviour around the hard-soft transition.

4

Methods and Tools

Since all hypotheses formulated in Chapter 3 concern different processes and different directions, different tools - each one suitable for its purpose - will be used to investigate them. This will be explained in the following chapter.

4.1. Tool 1: UNIBEST

UNIBEST (Deltares, 2018) is a coastline model that is suitable for modeling longshore sediment transport and coastline changes. It also includes a wave propagation module that transforms waves from the model boundary to the surf zone. The model is based on a relationship between the orientation of the coast and the longshore transport for each cross-shore ray, which is presented in an S-ϕ curve. UNIBEST-LT/CL is the most commonly used model, which is well suitable for modeling longshore transports (LT) on curvilinear coastlines (CL). As UNIBEST is a coastline model suitable for modeling longshore sediment transport and coastline changes, one can expect that the output generated by this model will be mainly caused by wave (and, if specified, tide-) induced longshore sediment transport (and not by other processes such as storm erosion and reflection of the breakwater).

4.1.1. Model set-up

The UNIBEST-LT/CL+ model requires boundary conditions at the model boundary. As only the wave measurements at Europlatform were available, these wave measurements had to be transformed to nearshore boundary conditions suitable for the UNIBEST model. This was done with SWAN [1](Booij et al., 1999) using a special SWAN-user interface available at Boskalis (DIONE [2]). In Figure 4.1 the location of Europlatform and the location of the Output points are indicated (23 points, indicated in Figure 4.1 together as one point: 'Output points'). The bathymetric data used as input for the model was downloaded from EMODnet (European Marine Observation and Data Network) and has a spatial resolution of about 230 m. More about the set-up of the SWAN model can be found in section 4.2.

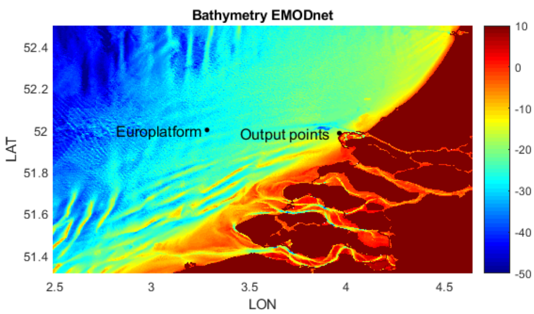

Figure 4.1: Location of Europlatform and the output points projected on EMODnet bathymetry

[1]Simulating WAves Nearshore; a third-generation wave model developed at TU Delft

[2]DIONE is graphical userface for SWAN, developed by Aktis Hydraulics for Boskalis and van Oord, which uses the SWAN (Booij et al., 1999) model for wave transformation

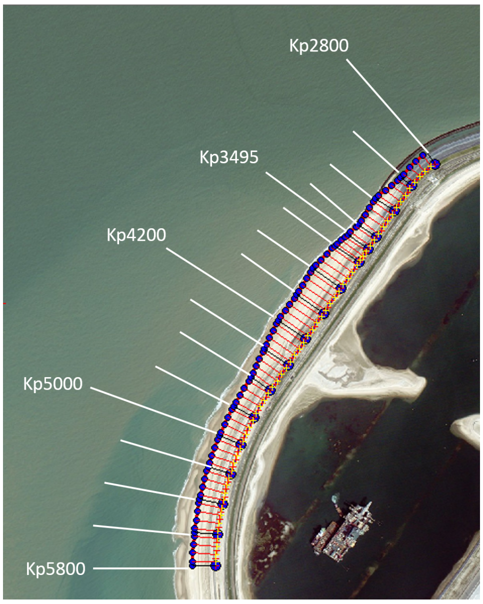

Figure 4.2: Visualisation of the UNIBEST-CL model set-up. The lines represent the different cross-shore transects.

The CL-model comprises of 17 locations, representing transects Kp2800 up to and including Kp5800 (see Figure 4.2. The cross-shore profiles were obtained by extracting depth data along lines from the bathymetric data of the 2017 survey measurements. At the end of every transect, the boundary conditions from SWAN (Booij et al., 1999) is imposed. As transport formula the formula of Bijker (1976, 1971) was chosen (the same as used in design calculations such as Onderwater (2018a)), because this empirical formula based on experience with the Dutch coast gives realistic outcomes for typical wave-driven longshore transport. The breaker parameter γ was set to 0.8. A median grain size, D_{50} of 330 μm is used and a D_{90} of 500 μm. For the first simulations, the wave scenario was specified as a timeseries for each period separately. Later on the timeseries were reduced to wave climates that induced the same morphological changes (this is verified in section 4.4.4), so that tide could be added as well. The tide was initially neglected for testing the first two hypotheses, but later it was included to test the last hypothesis about the tide.

The final model input parameters, imposed wave climate, imposed schematized tide, and tables and visualisations of the cross-shore profiles can be found in Appendix D.1.

4.1.2. Model assumptions and limitations

In UNIBEST, the following assumptions were done:

- Im the model itself it is assumed that the cross-shore coastal profile does not change in shape, and the calculated volume changes are distributed evenly over the entire cross-shore profile. In reality this is not completely true, as we saw in Chapter 3 that the shape of the cross-shore profile changes significantly over time. However, for modelling the longshore changes the assumption is just.
- In the UNIBEST model, water level variations were not taken into account. This was done in order to only look at the effect of waves.

The model has the following limitations:

- Cross-shore sediment transports and processes are not taken into account
- Wave reflection is not taken into account
- Boundary conditions can only be imposed as timeseries at the model boundary (not as a spectrum)
- Furthermore, it has to be noted that the sediment transports UNIBEST calculates are **potential transports**. This means that when there is sediment available next to an area where there is no sediment available (e.g. the breakwater) it will immediately model sediment transport here, whereas in reality there is a certain inertia before the sediment transport will be set into motion.
- The tide can only be imposed at the model boundary as well, as a schematized tide. The tidal flow velocities are taken parallel to the coast. Therefore the offshore directed tidal current at the hard-soft transition cannot be modelled. However, the tide can be varied per transect, so the tidal velocities were set smaller at the hard-soft transition.

4.1.3. Calibration

The UNIBEST model was briefly calibrated by varying the active profile height to fit the measurements. This is the profile height that is active in the sediment transport computed by UNIBEST. After calibration an active profile height of 10 m was used. A comparison to the results acquired with an active profile height of 7.5 m can be found in Appendix D.1.5. Moreover, the model was further improved by adjusting the coastline orientation and cross-shore profiles for each run to the measured profiles and coastline orientations in that period. The transport formula (formula of Bijker (1976, 1971)) was not calibrated, because it was conciously chosen as this was used in the design calculations as well, and because this empirical formula based on experience with the Dutch coast gives realistic outcomes for typical wave-driven longshore transport. The median grain size (330 μm) was not calibrated either, because this is the median grain size that has been determined in measurements.

For a calibration and validaton of the model, the results need to be compared to measurements. Therefore one is interested in the cumulative effect of all wave conditions occuring in one period, the cumulative coastline changes (ΔY, as depicted in Figure 4.3b) at the end of each period were plotted in m/day. Volume changes of the measured survey data were calculated for the same control volumes and periods, and these volumes were divided by the estimated active profile height of the coastal profile (the same as used in UNIBEST) to get the 'coastline change' in the same way as is done in UNIBEST-CL.

The method for calculation of coastline changes from survey data is illustrated in Figure 4.3. First the total sedimentation-erosion pattern was calculated as before, by taking the difference between two surveys. Next, the area was divided into cells of about 50 m wide, and a length corresponding to the active profile height (approximately 1 km). Next, the volume change per cell was divided by the cell width 'x' and by the active profile height 'd' , to get the coastline change. Finally, the coastline change was divided by the number of days in the period to get the coastline change in meters per day.

Several options were tested to model the breakwater. At first, the breakwater was modelled as a revetment in the model that prevents erosion but does allow sedimentation in front of it. Because all erosion is prevented (only the accumulated sand in front of the breakwater can be eroded), the computed sediment in front of the breakwater will be overestimated and a large amount of sediment will accumulate in front of the breakwater. A second, alternative approach was tested and proved to give more realistic results. In this approach, the part of the cross-shore profile behind the breakwater was cut off in the LT-model, taking into account the smaller area contributing to sediment transport (see Appendix D.1.1). In the CL-model, the revetment was taken out, allowing for erosion and coastline retreat at the breakwater as well.

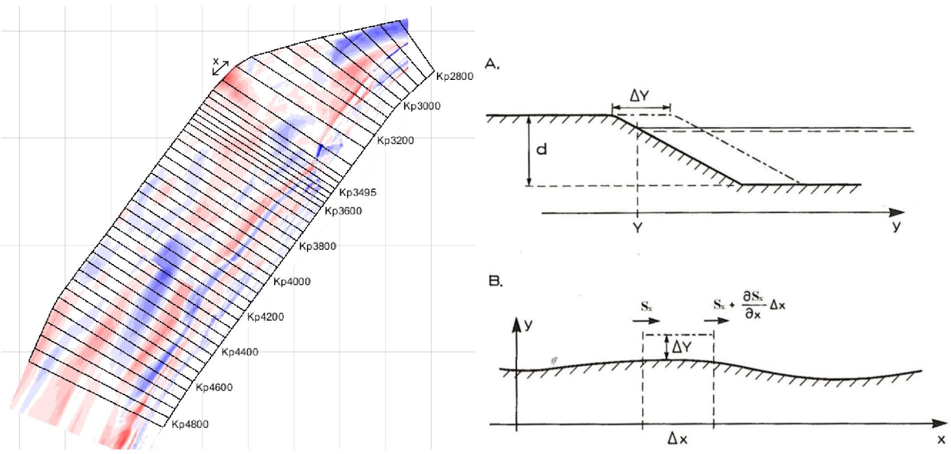

(a) Step 1: the are is divided into cells of width 'x' (approximately 50 m) for which the sedimentation/erosion volumes are calculated

(b) Step 2: The calculated sedimentation/erosion volume per cell is divided by 'x' and by 'd' (the Active Profile Height) as defined in UNIBEST

Figure 4.3: Visualisation of the method for calculating the coastline changes from measurements in the same way as UNIBEST

4.1.4. Validation

For a validation, the model was run for five periods separately, corresponding to the periods in between two surveys that were used for earlier analyses as well. In this way it can be seen for which conditions or periods the model performs well, so that we know under which conditions the model is usable to use for hypothesis testing. To recap, the five periods read:

- Period 1: 2017 Q2 – 2017 Q3: 9/5/2017 – 14/8/2017 (98 days)
- Period 2: 2017 Q3 – 2017 Q3: 14/8/2017 – 16/10/2017 (64 days)
- Period 3: 2017 Q3- 2017 Q4: 16/10/2017 – 19/12/2017 (65 days)

- Period 4: 2017 Q4 – 2018 Q1: 19/12/2017 – 11/01/2018 (24 days)
- Period 5: 2018 Q1 – 2018 Q2: 11/01/2018 – 14/03/2018 (63 days)

Note that period 6, 2018Q2-2018Q3, was not taken into account in the models, as these measurements were not yet available at the time the models were set up.

The results are depicted in Figure 4.4. When looking at the comparison of modelled and measured coastline changes rates in Figure 4.4, one can see that UNIBEST-CL cannot entirely reproduce the observed coastline changes, but similar trends can be recognized. Moreover, the order of magnitude of sedimentaton and erosion is the same. When the model results do not match with reality, this can have several reasons. Firstly, it could be due to cross-shore processes dominating in this period, which UNIBEST-CL cannot solve as it only considers longshore changes. However, it can also be because of other processes that are not captured in the model or because of errors in the measurements. From these figures we can conclude that UNIBEST-CL is a suitable tool to test Hypotheses 1 and 2, as some periods show good agreement with measurements.

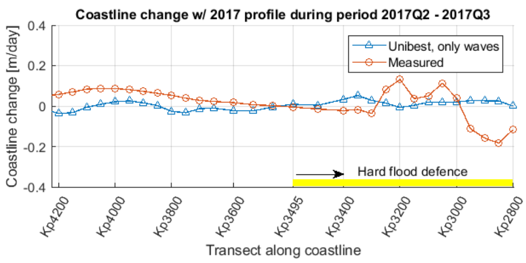

(a) Period 1: 2017Q2 - 2017Q3

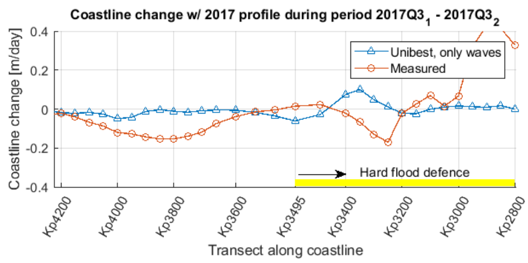

(b) Period 2: 2017Q3-1 - 2017Q3-2

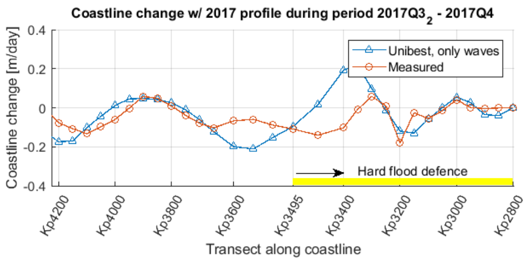

(c) Period 3: 2017Q3-2 - 2017Q4

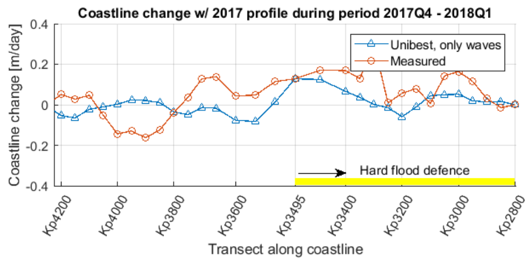

(d) Period 4: 2017Q4 - 2018Q1

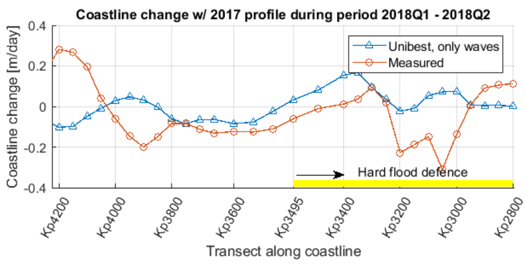

(e) Periode 5: 2018Q1 - 2018Q2

Figure 4.4: Coastline change per day for each period. Positive coastline change means coastline advance and negative coastline change means a retreat of the coastline. The blue line represents the model results and the red line represents the coastline retreat computed from measurements. The location of the hard flood defence is indicated with the yellow bar.

4.2. Tool 2: SWAN

SWAN is a third-generaton phase-averaged wave model for calculating wave parameters in coastal areas, estuaries and lakes. The inputs required are wind, bottom, and current conditions. A further description of the model can be found in (Booij et al., 1999). First of all, SWAN was used to transform wave data from Europlatform to the model boundaries for UNIBEST, as described earlier in section 4.1.1. But apart from using SWAN as a tool to get boundary conditions, it can also help in answering several hypotheses. To support hypotheses 2 and 3, a wave model can help in finding out how waves transform on their way to the hard-soft transition, how their refraction pattern is influenced by the coastal shape and how this influences the degree of wave attack. This can, in the end, influence sedimentation/erosion patterns and sediment transports. Moreover, a structure can be added to the model with which the reflection of waves can be turned on or off by specifying a reflection coefficient. This makes the model a useful tool to test Hypothesis 3, regarding the effect of reflection.

4.2.1. Model setup

Grid and bathymetry

For all runs, the grid dimensions were used as depicted in Table 4.1.

Table 4.1: Grid dimensions

Grid	delta x [°]	delta y [°]	delta x [m]	delta y [m]	cells in x direction [-]	cells in y direction [-]
A	0.005	0.0031	360	330	250	250
B	0.0012	0.00075	86	80	350	400
C	0.0003	0.00018	21	19	400	450
D	0.0001	0.00006	7	6	350	480

As can be seen from Table 4.1, the coarsest grid has grid cells of 360 x 330 m and the finest grid has grid cells of 7 x 6 m. For each of the three scenarios, a new depth file had to be composed. As mentioned earlier, the depfiles were created by nesting the different surveydata (resolution 2,5 m x 2,5 m) in the coarse bathymetry data from EMODnet (resolution 230 m x 230 m). Figure 4.5 a, b, c and d show the depfiles for grids A, B, C and D respectively, with the depfiles C and D represting the bathymetry as measured in 2013.

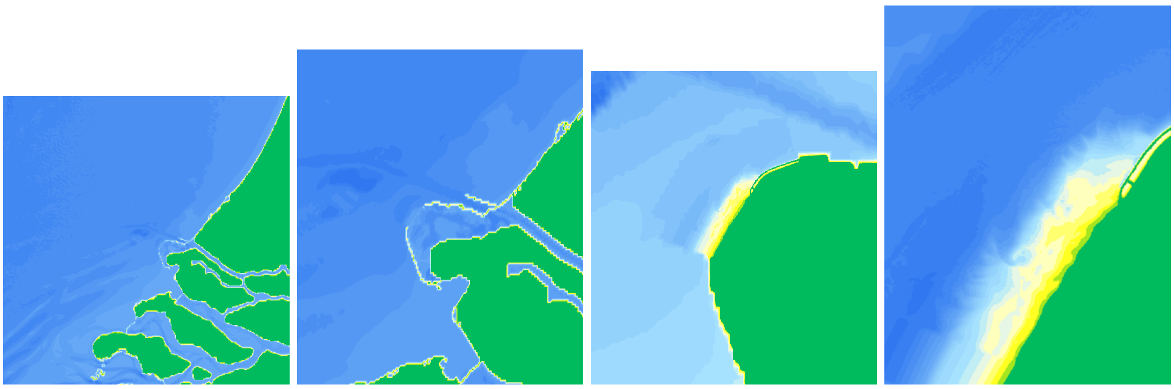

(a) (b) (c) (d)

Figure 4.5: Depfiles for the 2013 scenario, for grid A, B, C and D respectively.

Wave forcing

For the generation of the boundary conditions for UNIBEST, the SWAN model was run with timeseries of a full year (2017Q2 - 2018Q2). For the purpose of testing hypothesis 2, different scenarios were required, and the grid needed to be refined at the study area, both increasing the computational time. Therefore, a selection of 9 wave conditions was made to reduce the computational time. The wave scenarios were chosen such that they cover different directions, see Figure 4.6. From these directions, relatively high wave events were chosen as they will be more interesting when looking at morphological impacts. Table 4.2 shows the wave conditions used. The wave conditions are all conducted from the timeseries measured at Europlatform, so they represent yearly normal to high wave conditions.

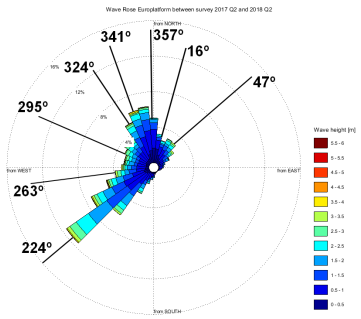

Figure 4.6: Wave directions chosen for SWAN runs

Table 4.2: The 9 selected wave conditions for the assessment of hypothesis 3 in SWAN. The wave parameters listed here are the wave parameters as measured at Europlatform.

θ [°N]	H_{m0} [m]	T_p [s]	Waterlevel [m]	U_{10} [m/s]	U_{Dir} [°N]	γ [-]	Spreading [°N]
227	4.51	8.333333	0.806495	2	220	3.3	30
263	5	9.090909	-0.7516	0	280	3.3	30
341	4.03	8.333333	-0.60901	1.5	320	3.3	30
295	5	8.333333	0.354607	1.4	280	3.3	30
341	3.14	10	0.283642	1.3	330	3.3	30
47	3.36	7.142857	-0.7217	1.6	70	3.3	30
324	4.6	9.090909	-0.69455	1.8	310	3.3	30
357	3.28	7.692308	-0.73214	1.3	10	3.3	30
16	2.61	7.142857	-0.40956	1.2	330	3.3	30

The master input files for the SWAN runs, as well as a visualisation of the nested grids, the output points and the wave conditions imposed can be found in Appendix D.2.

4.2.2. Model assumptions and limitations

SWAN is a phase-averaged model. Phase-averaged models are well suited for processes which have weak variations over the scale of a wavelength. Averaged properties are dealt with, using kinematic propagation equations and an energy balance equation (Battjes et al., 1994). Phase-averaged wave propagation models are based on conservation of action or energy density: energy is added/removed through source terms and propagated based on linear wave theory (Folley, 2016). With this information, the most important dynamic and probabilistic properties of the local wave field can be predicted. However, a phase-resolving mode is required to capture all instantaneous processes such as strong processes and rapidly changing bathymetry (Boshek, 2009). Because the waves are phase averaged, the individual waves, the wave groups and accompanying bound long waves are not taken into account. Therefore bound long waves are not included in the SWAN results. Thus, the reflection modelled by SWAN only concerns the short wave reflection. Another limitation of the SWAN model is that it becomes unstable when the resolution is too fine, because it is a phase-averaged model which accommodates only weak variations over the scale of a wavelength. Therefore the computational grid should not be made too small. This is why the grid cells were not made smaller than 6 x 7 as applied in the model.

4.2.3. Motivation of input parameters and validation

Since no wave buoys were available nearshore to validate the modelled nearshore wave parameters, site-specific model validation was not possible. However, the SWAN model has been used for a wide range of locations and applications which proves its general performance. The breaking index chosen is a default value, and the friction coefficient of 0.038 is a recommended value for sandy bottoms and therefore suitable for the North Sea. Moreover, validation tests with SWAN for the Haringvliet (just south of the Maasvlakte 2) conducted in 1982 (Booij et al., 1999) showed good agreement with buoy data. Finally, if UNIBEST gives realistic results with boundary conditions generated by SWAN, this is also an indirect validation of the SWAN model (at least for the offshore domain between Europlatform and the UNIBEST boundary).

4.3. Tool 3: XBeach

XBeach (Roelvink et al., 2009) is a (relatively new) 2D process-based model that can model hydrodynamic and morphodynamic processes for sandy beaches. Although it originally started as a special tool for modelling storm impact on sandy coasts, it has since been extended to many fields of application and to other time scales than its original storm time frame. XBeach consists of different modules, solving horizontal equations for wave propagation, flow, sediment transport and changes in bathymetry. It therefore has a wide range of applicability. The model has three different modes, with different applications (Roelvink et al., 2015):

- Surfbeat mode (instationary): the original application, which resolves short wave variations and associated long waves. The incident wave energy variation (short wave envelope in Figure 4.7) is solved with the wave action balance, while the infragravity water level elevation is solved with the nonlinear shallow water equations (long waves - red line in Figure 4.7). Individual incident waves (short waves - blue in Figure 4.7) and their phase are thus not solved.
- Hydrostatic mode (stationary): solves the short wave amplitude separately from the long waves, currents and morphological change. The wave-averaged equations are solved. The hydrostatic mode is computationally less demanding (than the non-hydrostatic mode), but has the disadvantage that short wave phases are not simulated (Roelvink et al., 2015).
- Non-hydrostatic mode (wave-resolving): this is a more complete, but therefore also more computationally demanding mode (Roelvink et al., 2015). XBeach non-hydrostatic is a phase-resolving model and therefore does solve the individual incident waves (short waves - blue in Figure 4.7). Both incident and infragravity waves are solved with the nonlinear shallow water equations including non-hydrostatic pressure (Roelvink et al., 2015).

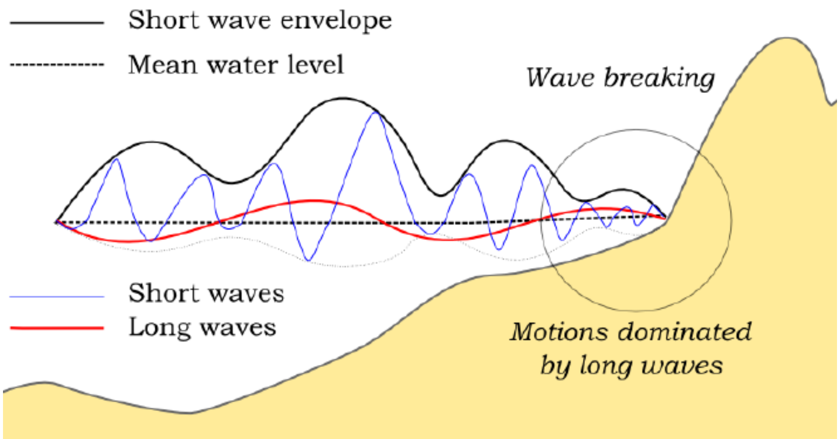

Figure 4.7: Principle sketch of the relevant wave processes

XBeach is in principle a 2DH model, but it can also be set up as a 1D cross-shore model, where longshore gradients are ignored. In this research, however, we are interested in 2D processes and therefore the 2DH model will be used.

The **hydrostatic mode** neglects all infragravity motions, and is therefore useful for calm conditions with small waves, where these motions would be really small anyway (Roelvink et al., 2015). This mode is therefore not considered very suitable, as the flood defence of the MV2 also encounters large waves, in which case these infragravity motions cannot be neglected. The **surfbeat mode** already includes a lot more processes. It also takes into account wave-driven current (longshore current, rip currents and undertow) and wind-driven currents, which are important processes in the MV2 case. The **non-hydrostatic mode** is even more complete. Especially (short wave) run-up, overwash and wave skewness and asymmetry are processes that are solved within this mode. The disadvantage is that this is a much more computationally expensive mode, as much higher spatial resolution and associated smaller time steps are needed.

4.3.1. Model set-up and motivation of input parameters

For earlier morphological studies, an XBeach was already set up by Onderwater and van der Baan (2017). This model was run in instationary mode (surfbeat), using the bottom configuration as measured in 2017Q2 as bathymetry. The computational grid is made up of 491 x 490 grid cells, with a refined grid cell resolution (10 x 10 m) around the hard-soft transition. This grid cell size was small enough to model the sedimentation-erosion patterns well. The modelling of wave reflection might require a higher model resolution, but this would increase the computational time significantly. Therefore the grid was kept as it was. The breakwater is implemented in the XBeach model as an impermeable, non-erodible layer. The input files of the model, as well as the implementation of the non-erodible layer can be found in Appendix D.6

4.3.2. Model assumptions and limitations

In XBeach the following assumptions are done:

- The water level variations due to the tide are included in the model, but not the tidal flow velicities.
- The breakwater is taken as an impermeable, non-erodible layer (so transmission of waves is not included in the model)

The following limitations are concerned with the model:

- The model is computationally demanding (especially the nonhydrostatic mode), so running the model for a whole year or whole period would take too long. Therefore the model was only run with one storm.
- Using the surfbeat mode, individual short waves are not solved.

4.3.3. Calibration and validation

The model, ran in surfbeat mode, was validated for one period, see Figure 4.8a. Moreover, the sedimentation-erosion patterns were compared to measurements as is shown in Figure 4.8b. It can be seen that also the XBeach model results resemble reasonably well with measurements. Therefore, concerning the time available, it was chosen not to calibrate the model further, as the results agree well enough with measurements to use it as a tool. The differences between the measured and modelled results can be explained by the fact that the tide is not included in the model, and because of gaps in the measurements.

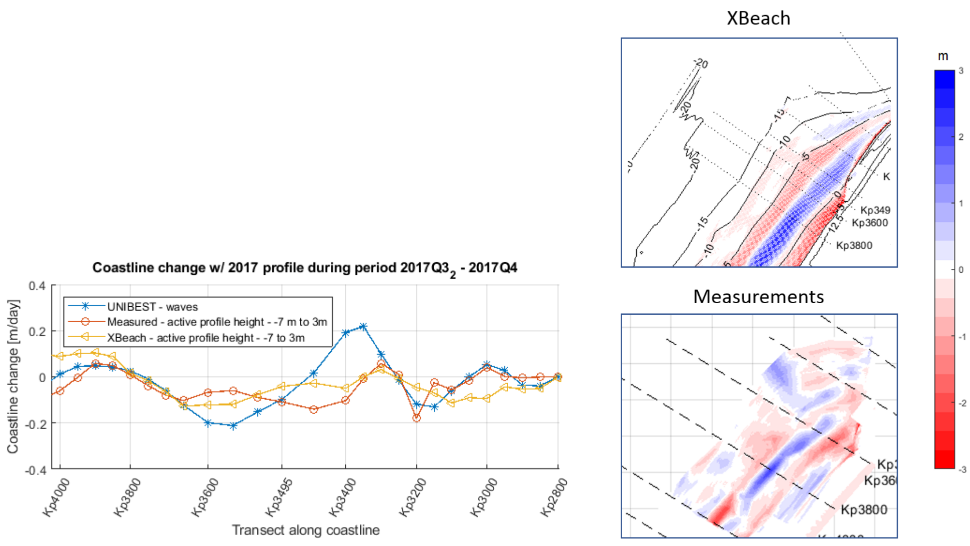

(a) XBeach validation for longshore changes (compared to measurements and UNIBEST)

(b) Comparison sedimentation-erosion patterns computed with XBeach versus measured

Figure 4.8: XBeach validation: 1D and 2D

4.4. Methodology for investigation of hypotheses

In the following section, the approach to test every hypothesis is clarified (for example, different scenarios to be tested, or specific settings that have been applied). In this section, only the method for the tests is explained - the results of the simulations are presented in the Chapter 5.

4.4.1. Hypothesis 1: Wave direction and longshore transports

Findings in the data analysis (sections 3.1.3, 3.2 and 3.3) suggest that waves from northwest cause more erosion whereas from southwest may allow the hard-soft transition to recover by supplying sediment. To investigate this hypothesis, UNIBEST was run for five periods (as was already done in the validation). From these periods, the period '2017Q3-2017Q4' is a period that represents the north/northwestern waves, and the period '2017Q4-2018Q1' is a period that represents the southwestern waves. If the model results resemble the measured coastline changes, this means the observed erosion or sedimentation is caused (mainly) by longshore sediment transport, as this is the underlying process calculated by UNIBEST. If the model results do not match with measured sedimentation or erosion, this might be because cross-shore processes are more dominant in this period, which are not captured well in the model. However, there are other reasons that could cause a mismatch between the modelled and measured results (for example other factors that are not included in the model such as tide or reflections, or gaps in the measurements).

4.4.2. Hypothesis 2: Effect of evolved coastal features

Cross-shore featues

In order to assess the effect of specific coastal features present in the bathymetry as measured in 2017, it was compared with other bottom configurations. Therefore not only the wave transformation with the 2017 bottom configuration was tested, but also with the 2013 bottom configuration and design bottom configuration. The 2013 bottom configuration was chosen because this is a situation where the subtidal bar did not develop yet. Therefor, by comparing the 2017 bathymetry to the 2013 bathymetry, the effect of the subtidal bar can be assessed. The following scenarios were tested:
1. Using the design bottom data nested in the EMODnet bathymetry. Characteristics:
- smooth bathymetry, no bars
- entire coastline until hard-soft transition orientation 305 °N.
2. Using the 2013Q2 survey data nested in the EMODnet bathymetry
- non-uniform bathymetry, no (distinct) bar
- relative large volume of sediment on shoreface
- northernmost 300 m of coast rotated. Coast orientation 320 °N.
3. Using the 2017Q2 survey data nested in the EMODnet bathymetry
- distinct bar and trough
- relative less sediment on shoreface
- northernmost 300 m of coast rotated. Coast orientation 320 °N.

Figure 4.9 a, b and c show the different depfiles for the D-grid used for the different scenarios.

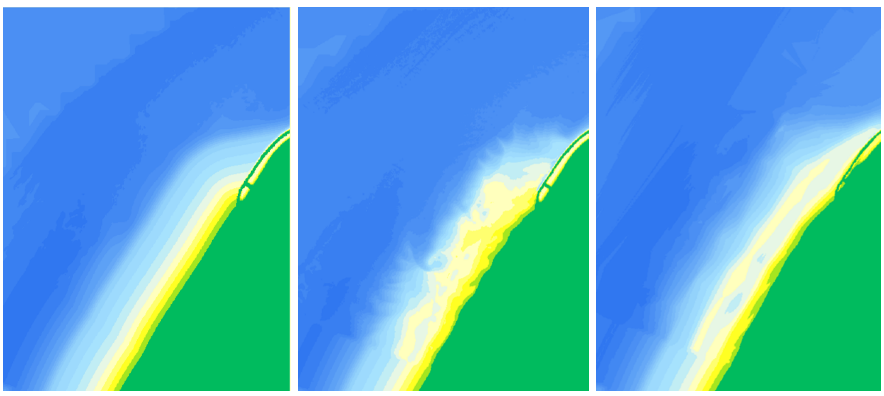

(a) Design (b) 2013 (c) 2017

Figure 4.9: Depfiles D-grids for design bottom, 2013 bottom and 2017 bottom, respectively.

The same was done for UNIBEST: To test the effect of the cross-shore shape (shore-normal) on the distribution of sediment transports, two UNIBEST models were set up, one with the bottom profile measured in 2013 and one with the 2017 bottom profile. For the UNIBEST model, the computational time was not a limiting factor, so here the wave climates as mentioned earlier, were used (from 2017Q2-2018Q2).

Longshore featues
To test the longshore feature of the coastal shape (a rotated coastline over the northernmost 300 m of the soft flood defence), two scenarios were compared in UNIBEST: one with a straight coastline and one with a rotated coastline.

4.4.3. Hypothesis 3: Wave reflection

The large amount of erosion observed close to the hard-soft transition, suggest that reflection of waves by the breakwater plays a role in this. In order to investigate the effect of reflection, it was aimed to model the morphological behaviour of the system with and without reflection. Before looking at the morphological effects of wave reflection, it is first important to understand the hydrodynamic processes occuring with wave reflection.

Intermezzo: theory on long wave reflection
Firstly, it is important to distinguish between roughly two types of waves that arrive at the coast (or at the breakwater): short waves and long waves. Short waves will break in the surf zone as a result of depth-induced breaking. Along the northern part of the breakwater the water is deeper so the waves will not break, and consequently more short waves will reach the breakwater and might reflect over there. Therefore, reflection of short waves is expected to play a larger role along the northern parts of the breakwater than around the hard-soft transition and the soft flood defence, where shallower water depths are present.

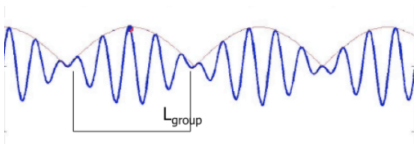

Figure 4.10: Visualisation of wave groups and the bound long waves travelling with them. Source: Lecturenotes Coastal Dynamics II.

Next to short waves, long waves also play a role. The short waves tend to travel in groups (see Figure 4.10). These wave groups travel with the wave group velocity, c_g=nc . The wave energy also travels with this wave group velocity, and this wave energy influences the surface elevation. The variations in surface elevation caused by the wave groups are called bound long waves. The bound long waves travel with the wave group velocity and are therefore dependent on the groupiness of short waves. According to Longuet-Higgins and Stewart (1962) the depth depency of the bound long waves is given by: $\eta = h^{-5/2}$. Note the negative exponent, so an inverse relationship between the parameters. This means that bound long waves become bigger in shallower depth near the shore (shoaling). As the wave groups enter the surf zone, the short waves break and their groupiness is reduced. The bound long waves become released of the wave groups and transform into free long waves. Now they don't travel with the short wave energy anymore, but with a speed given by $c = \sqrt{gh}$ (dispersion relation). According to Green's Law the reflected (free) long wave will be less dependent on depth than the incoming (bound) long waves, so that the reflected waves will dissipate less quickly than the incoming long waves would. The depth dependency of both type of waves are:

$$\text{Incoming bound long wave amplitude} : \eta = h^{-5/2} \tag{4.1}$$

$$\text{Reflected long wave amplitude} : \eta = h^{-1/4} \tag{4.2}$$

This means that at intermediate water the reflected long waves can even be larger than the incoming bound long waves. Therefore the reflection coefficient of long waves can theoretically be larger than 1 (see Figure 4.11).
Several test and experiments to verify these theoretical values are described in literature (Battjes et al., 2004; van Dongeren et al., 2007). In these tests it is found that for very steep slopes the shoaling parameter for the incoming bound long waves, which is theoretically expected to be 2.5, is in reality a lot smaller (order of magnitude 0.25).

In other words, the incoming wave amplification is very weak. This can be explained by the fact that the beach is too steep for the waves to adjust properly. For milder slopes, the shoaling parameter is somewhat larger, but never reaches the 2.5 limit that was proposed by Longuet-Higgins and Stewart (1962).

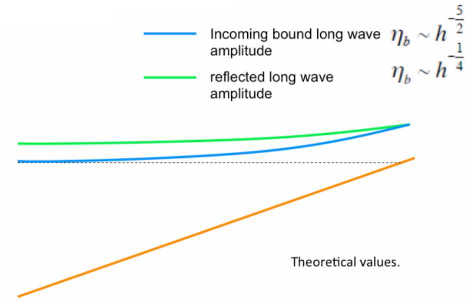

Figure 4.11: Visualisation ofshoaling and reflection of infragravity waves according to Green's law. Source: Lecture notes Coastal Dynamics II.

Physical model tests

First of all, reflection coefficients were already determined by measuring during physical scale model tests in the Deltagoot (van Gent and van der Werf, 2010) and Scheldegoot (Hofland and van Gent, 2010) during the design stage. The measured reflection coefficient is defined as:

$$K_r = \frac{H_{m0,r}}{H_{m0,i}} \tag{4.3}$$

Where K_r is the reflection coefficient (-), and $H_{m0,i}$ and $H_{m0,r}$ are the significant wave heights in m for the incoming and reflected waves respectively, measured at the toe of the structure. Studies describing the results of these scale model tests in the Scheldegoot (Hofland and van Gent, 2010) showed reflection coefficients of 0.14 – 0.18. These were relatively small compared to earlier model tests performed in the Deltagoot (van Gent and van der Werf, 2010), which showed reflection coefficients of 0.15 to 0.28. The tests performed in the Scheldegoot (Hofland and van Gent, 2010) were performed for the following conditions:
1. H_s= 2m, T_p = 6 s and h_0 = 0 m.
2. H_s = 2 m, T_p = 6.6 s and h_0 = 1 m
3. H_s = 5 m, T_p = 9.3 s and h_0= 1 m.

The tests were done with a characteristic cross-section from the middle section of the hard flood defence. The reflection coefficients found in the model tests are quite low compared to other hard structures, but this can be partly explained by the permeable character of the breakwater. In the model tests it was found that wave transmission was 0.2 - 0.3 (-) for water levels around NAP, and 0.6 - 0.7 (-) for the highest water levels (Hofland and van Gent, 2010). As this part of the wave energy is subtracted from the wave energy that would normally be reflected in the case of an impermeable structure, this reduces the reflection coefficient significantly and therefore explains the relatively low values found.

The values from these tests are relatively small and therefore suggest that wave reflection at the breakwater is not a dominating factor in the morphological behaviour of the hard-soft transition. However, the following has to be commented on the way the reflection coefficients were determined:

- The tests to determine the reflection coefficient were specifically carried out with conditions that are normative for reflection. This entails low water levels and low wave conditions. This makes the results more conservative and reliable.
- The reflection was measured and calculated for a cross-section that represents the middle section of the breakwater. This cross-section was chosen, because the aim of the reflection tests was to ensure that ships in the navigation channel close to the hard flood defence would not experience hindrance caused by wave reflection.
- The reflection coefficient was determined with the method of Mansard and Funke (1980). To determine the reflection coefficients from measurements, the wave signal has been analysed for the frequency domain of $0.5f_p$ < f < $2.2f_p$. This domain was chosen because it was stated that these frequencies contain the majority of the wave energy (order of magnitude 99%) and the method of Mansard and Funke (1980) works best for these frequencies (Hofland and van Gent, 2010).

- The frequency domain $0.5f_p < f < 2.2f_p$ contains short waves, but does not contain bound and free long waves, which have frequencies $f < 0.5f_p$. In other words, reflection of long waves (infragravity waves) is not included in the determined reflection coefficient of 0.14 – 0.28.
- For the middle section, for which the reflection coefficient was determined, the frequency domain is well chosen because here indeed it can be assumed that low waves are negligible. The energy in the low frequency domain ($f < 0.5f_p$) is caused mainly by infragravity waves, which are produced by the process of wave breaking (surfbeat). In the middle section, one is not looking at very shallow water (especially not for the tests with low wave heights), so it can be expected that the amount of wave energy within these frequencies is negligible (Hofland and van Gent, 2010).
- However, further south along the breakwater (close to the hard-soft transition – the area that is relevant for this study), the water is shallower. This means that:
  - The bound long waves have had more time to shoal with shallower depth
  - Some of the bound long waves have been transformed into free long waves due to wave breaking.
  - In other words, a larger part of the wave energy has been transferred from higher frequencies to low frequencies.
  - Therefore it is expected that also reflection of long (infragravity) waves will play a role here.

Modelling approach

From the theory described in Intermezzo 4.4.3, it follows that at the hard-soft transition, both long and short waves are expected to play a role and therefore both frequency bands should be investigated. As is described in section 4.2.2, SWAN is a phase-averaged model that does not solve short wave variations and therefore bound long waves are not included in the model. Therefore SWAN will only compute short wave reflection; long wave reflection will be neglected. As was described in section 4.3, XBeach surfbeat computes both long and short wave variations, but the individual short wave processes are not solved. Therefore, XBeach surfbeat will only model long wave reflection, but not short wave reflection. XBeach non-hydrostatic is a phase-resolving model and therefore does solve the individual incident waves (Roelvink et al., 2010). Therefore, in XBeach nonhydrostatic both short and long wave reflection will be resolved. In this research, the following modelling approach was followed:

- To start with, the effects of short wave reflection were investigated with a combination of SWAN (for the hydrodynamic part) and UNIBEST (for the morphological part). This was done because the UNIBEST and SWAN models were already being used, so it would be relatively easy to do this analysis using existing models.
- Secondly, the effects of long wave reflection were investigated with XBeach surfbeat.[3]

SWAN and UNIBEST

The assessment of the effect of short wave reflection using SWAN and UNIBEST comprises of two parts:
1. The hydrodynamic effect of short wave reflection on wave heights in front of the breakwater (in SWAN)
2. The morphological effect caused by these larger wave heights (in UNIBEST)

In SWAN, a structure was added, and a reflection coefficient was specified. A run was done with a reflection coefficient K_r=0, and one with the actual reflection coefficient. A reflection coefficient of K_r = 0.2 was chosen to use in SWAN, as this is in between the values measured in the Deltagoot and the Scheldegoot.

The structure that was added to the model to test hypothesis 3, was implemented as an obstacle in SWAN as depicted in Figure 4.12b. The location of the obstacle in the model is defined by a sequence of corner points of a line. The obstacle was defined with the least amount of points possible, because if too many points are defined, the reflected wave energy computed will be smaller. Also sharp edges were avoided since these also lead to incorrect reflection results. Lastly, obstacle lines are only effective when the obstacle line is bordered by wet points on both sides. Therefore the obstacle line was shifted slightly seaward of the original

[3] For a full analysis of both long and short wave reflection, the nonhydrostatic mode is more suitable as it resolved all wave frequencies correctly. Therefore XBeach was also run in nonhydrostatic mode. However, running the model in nonhydrostatic mode introduced large errors in the wave boundaries which could not repaired within this study. A possible cause of the error introduced is the fact that XBeach only uses one vertical layer. Therefore to fix this error, more layers should be defined in the vertical. This is not possible in XBeach, but another model should be used such as SWASH, which is also a phase resolving model but also allows defining more layers in the vertical.

breakwater, and the bathymetry behind the breakwater was lowered such that the land side of the obstacle also consists of wet points (see Figure 4.12b).

Several output points off the coast at the crossing of the transects and contour lines at depths -2.5m, -5m, -7.5m and -10m were identified, as depicted in Figure 4.13.

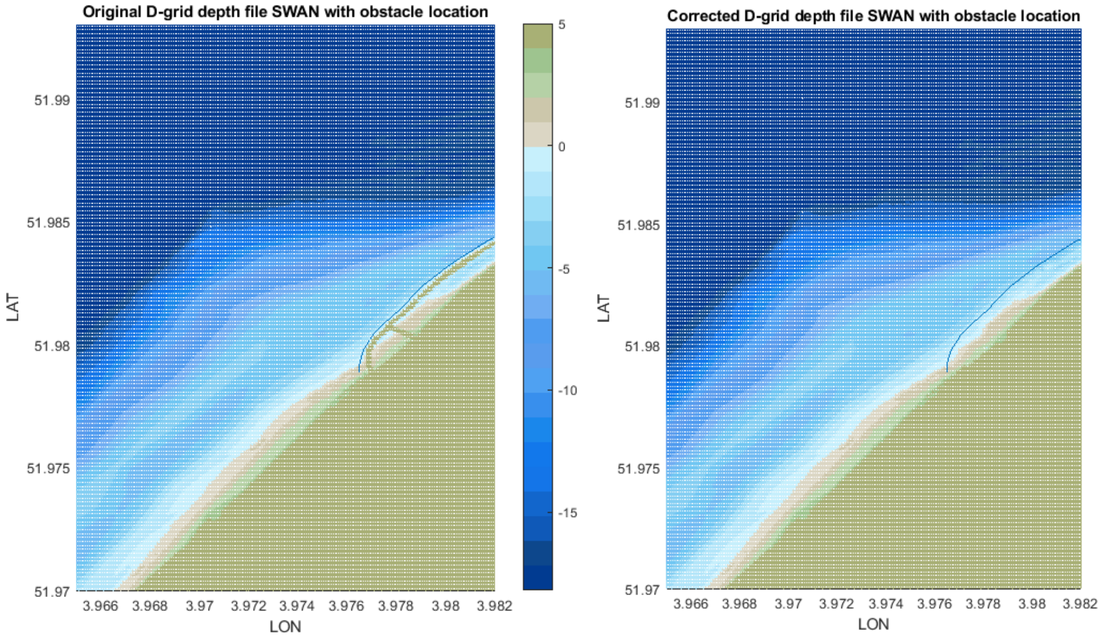

(a) Original depth file with the location of the obstacle. This file was not used, because the points behind the obstacle should be wet as well.

(b) Corrected depth file with the location of the obstacle, as it was implemented in SWAN. The grid points behind the obstacle were also made wet, to ensure a correct implementation of reflection.

Figure 4.12: A visualisation of the implementation of an obstacle in the SWAN model.

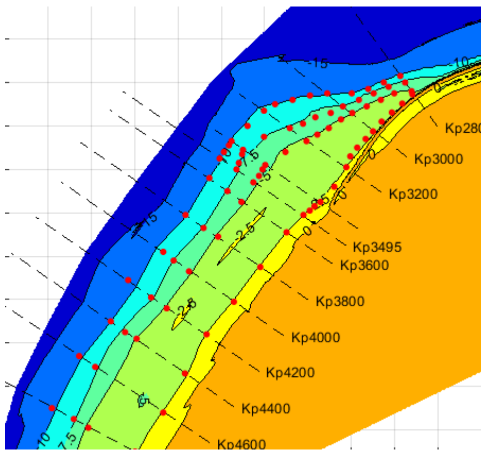

Figure 4.13: Output points used to review the wave height with and without wave reflection using SWAN.

The wave heights at these output can then be used as input for the UNIBEST model, and the effect on the morphological changes can be investigated. However, the UNIBEST has some limitations in taking into account wave reflection:

- First of all, it is not possible in UNIBEST to define a wave spectrum. Therefore the distribution of energy in the two-dimensional frequency-direction spectrum, which will be divided over two directional peaks (one belonging to the incoming wave, and one belonging to the reflected waves), cannot be captured in the UNIBEST model. Only one wave condition per time step can be given, for which the wave outputs were used as calculated by SWAN. This is the sum of incoming and reflected wave as wave height, and the weighted average of the wave directions as wave direction, calculated as follows:

$$H_s = 4\sqrt{\int\int E(\omega,\theta)d\omega d\theta} \tag{4.4}$$

  where H_s is the significant wave height in meters, $E(\omega,\theta)$ is the variance spectrum and ω is the absolute radian frequency determined by the Doppler shifted dispersion relation.

- Secondly, when the wave condition is specified at the model boundary (at, say, 5 m depth), in UNIBEST the wave will dissipate and decrease in energy as it propagates towards the coast, as it is modelled as a purely incoming wave. In reality, however, the wave consists of an incoming and a reflected wave signal. The reflected wave originates at the breakwater (with reflection coefficient K_r=0.2) and dissipates by bottom friction in the same way as the incoming wave (for short waves), but in the other direction. So actually the reflected wave is bigger at the breakwater than at a distance of e.g. 100 m from the coast. This effect is not taken into account, and therefore the effect of the reflection on the longshore sediment transports will likely be slightly underestimated in a model such as UNIBEST. The results can therefore be used as a lower limit.

XBeach

In XBeach, the two parts (hydrodynamic + morphological effects) that are assessed separately when using SWAN and UNIBEST, are combined in one model.

The drawback of using XBeach that the reflection cannot be simply turned off or on, so a different way has to be thought of to purely assess the effect of reflection. Several methods were considered. One way is to run the model in stationary rather than instationary form (because in stationary mode, both long and short wave reflections are not solved). This might, however, also influence other processes than only reflection. Another way is to 'eliminate' the reflection with a workaround. For example, the bed friction just in front of the breakwater (and on the breakwater itself) can be set artificially high. This can be done by locally changing the Chézy coefficient, which is a measure for the bed friction. Ideally, the Chézy coefficient is set to 5 or 10 so that the reflected wave is damped out immediately after reflection. This method has the limit that the Chézy coefficient can only be set to a minimum of 20 $m^{1/2}s^{-1}$, so the reflected wave will only be partly damped. An even better method would be to create an absorbing boundary at the breakwater, thus eliminating all wave reflections. However, this is not possible to specify in the params file of XBeach. To do this, the source code has to be adjusted. Considering the time and resources available within this research, it was therefore chosen to use the workaround with adjusted Chézy coefficients to assess the effect of long wave reflection. A visualisaton of how the locally varying Chézy coefficient was implemented can be found in Appendix D.6.6.

The XBeach model was first run for a storm of 45 hours, with the storm peak having a wave height of 3.5 m from 330 °N at the model boundary. This represents a strong north-northwestern storm, inducing southward transport along the breakwater and accompanying erosion around the hard-soft transition. See Appendix D.6 for all model inputs.

4.4.4. Hypothesis 4: Tide

In order to investigate the relative importance of tide in the morphological behaviour of the hard-soft transition, model runs were done in- and excluding the tide in UNIBEST. In UNIBEST, in total 1000 conditions can be specified per model, which equals the number of wave conditions * the number of tide conditions. Therefore it was chosen to schematize the tide with 10 conditions, and reduce the wave time series to a wave climate of (maximum) 100 conditions. To assure that the reduced wave climate is a correct representation of the actual waves, it was shown that in UNIBEST, a simulation with the full time series and a simulation with the reduced wave climate, give the same results. This shows that the reduced wave climate is a good representation of the actual waves as the morphological changes it induces resemble the ones caused by the actual waves very well. Figure 4.14 shows the validation for one period. For the other periods the wave climate was validated in the same way, as can be seen in Appendix D.1.6

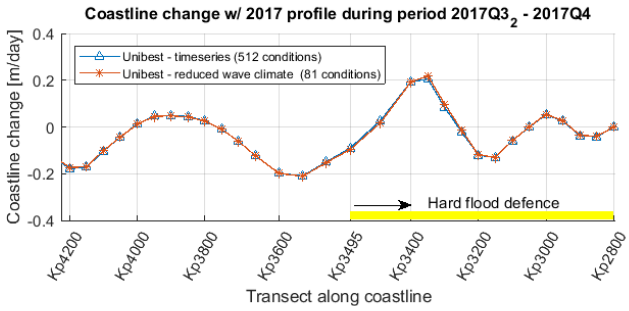

Figure 4.14: Validation of reduced wave climate for UNIBEST with only wave input.

Next, the tide was added. The tidal data was acquired based on measurements obtained at Maasmond Stroommeetpaal (Rijkswaterstaat), and earlier analyses on tidal current patterns carried out by Onderwater (2016) in Delft3D. These studies showed the following:

- Just south of the hard-soft transition, the flood tidal velocities are larger than the ebb tidal velocities, and therefore the tide-averaged tidal current has a net northward directed current and a residual sediment transport in the same direction.
- North of the hard-soft transition, the ebb tidal velocities are larger than the ebb tidal velocities, resulting in a net southward-directed tidal stream. However, the residual sediment transport is still in northward direction.

Therefore, a hypothetical tide was schematized that fulfills these conditions, as depicted in figure 4.15. It shows that the schematized vertical tide (blue line) follows the measured vertical tide. Moreover, it was found that the horizontal tide has a small lag (delay) compared to the vertical tide. The schematized tides imposed for other transects can also be found in Appendix D.1.4.

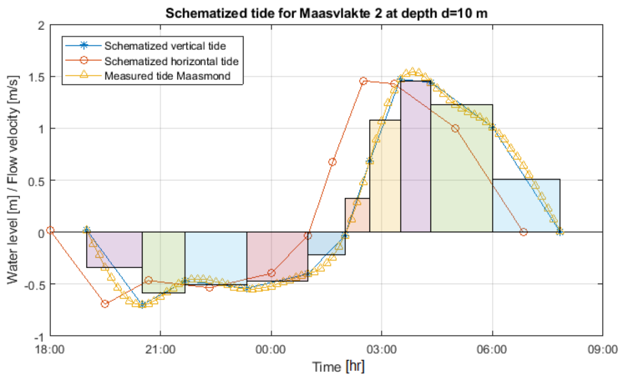

Figure 4.15: Schematized tide for transects Kp5800 to Kp4000.

4.5. Overview of simulations

An overview off all the used simulations can be found in Appendix D.8.

5

Results and discussion of hypotheses

In this chapter the results of the model runs are presented and discussed in relation to the hypotheses.

5.1. Hypothesis 1: Wave direction

In this hypothesis, the importance of wave direction for the observed erosion was assessed. As was explained in Section 4.4.1, model simulations were done with UNIBEST for different periods and were compared with survey data. From these periods, the period 2017Q3-2017Q4 mainly represents waves from north/northwest, and the period 2017Q4-2018Q1 represents mainly waves from south/southwest. The cumulative coastline changes (Y-Y0) at the end of each period were plotted in m/day, as shown in Figure 5.1. Volume changes of the measured survey data were calculated for the same control volumes and periods. These volumes were divided by the estimated active profile height of the coastal profile (the same as used in UNIBEST) to get the 'coastline change' in the same way as is done in UNIBEST-CL. It is thus assumed that the coastal profile does not change in shape and the calculated volume changes are distributed evenly over the entire cross-shore profile.

5.1.1. Results

The results of these two simulations are given in Figure 5.1. The blue points represent the coastline changes as computed by UNIBEST and the red line represents the coastline changes computed from the measurements. The results are plotted in alongshore direction, with the transects labelled on the x-axis. The hard flood defence runs between transects Kp3495 to Kp2800.

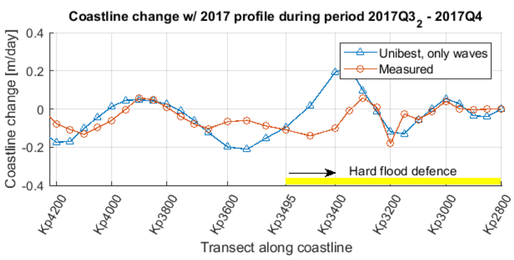

(a) Period 3: 2017Q3-2017Q4

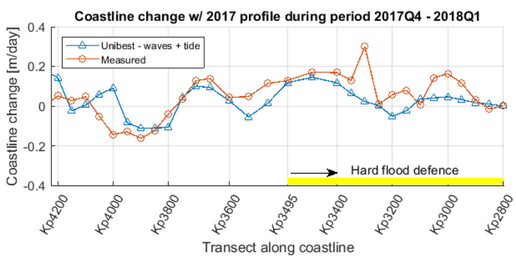

(b) Period 4: 2017Q4 - 2018Q1

Figure 5.1: UNIBEST results for two periods. Left: 2017Q3-2017Q4, only waves. Right: 2017Q4-2018Q1, waves and tide.

As can be seen from Figure 5.1, the model results resemble the measured sedimentation and erosion quite well during both periods. Especially during the period 2017Q4-2018Q1, the results match the measurements almost exactly. Note that the result of 2017Q4-2018Q1 is including the tide whereas the result of 2017Q3-2017Q4 is for waves only (why this is done will be elaborated further in section 5.4) . During this period we see that the profile is recovering (overall positive coastline change between transects Kp3800 and Kp3200), while waves are coming mainly from Western directions in this period and hardly any waves are coming from the North. This means that under the influence of these western waves, the profile recovers. This is almost entirely because of longshore sediment transport in combination with tide. The latter is also important for the last hypothesis, which will be discussed in Section 5.4.

During period 2017Q3_2-2017Q4 (left figure), the results also agree well with measurements. However, a slight shift in sedimentation-erosion pattern is observed around the hard-soft transition. This could be due to effects of reflection of northwestern waves, which will be investigated in hypothesis 3 (Section 5.3).

During other periods the model gives less realistic results (see Figure 5.2), as the modelled results deviate more from measurements. This can be explained by the fact that during these periods, there is less longshore transport and the system will be dominated more by cross-shore processes. As these are not calculated by UNIBEST, this explains the larger difference between modelled and measured results. Note that for period 1 (2017Q2 - 2017Q3_1), the results resemble the measurements also quite well, as both the modelled results and measurements show very little coastline changes. This is because this was a relatively calm period where apparently both cross-shore processes and longshore processes were not very significant.

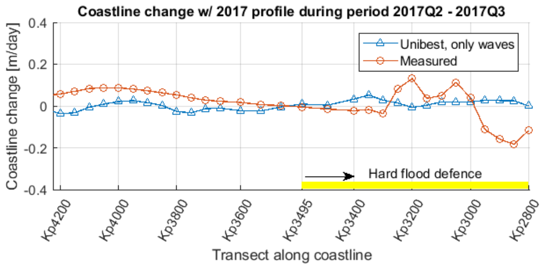

(a) Period 1: 2017Q2-2017Q3_1

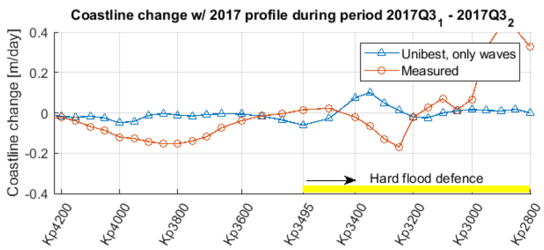

(b) Period 2: 2017Q3_2-2017Q3_2

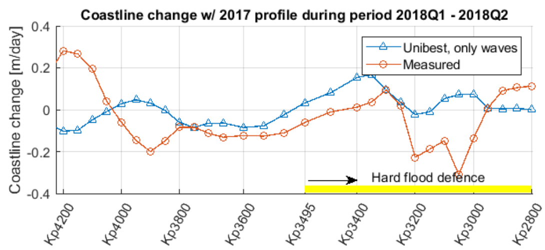

(c) Period 5: 2018Q1 - 2018Q2

Figure 5.2: UNIBEST results for remaining three periods.

Moreover, the cross-shore distribution of sediment transports caused by a typical wave from north/northwest (H_s = 1.56, MWD = 350.8 °N at the model boundary 1 km from the coast) was plotted in Figure 5.3a. Here, one can clearly see an increase in southward-directed sediment transport when moving south from Kp2800 to Kp3400.

- **Figure 5.3a**: At about 100 m from the transect origin, the magnitude of sediment transport increases from the dark colours to lighter colours, with its peak around Kp3600 after which it starts decreasing in size again. The hump on the right hand side of the figure is the sediment transport over the subtidal bar, which also increases with lighter red colours until a maximum at transect Kp3600, after which it decreases in size again for transects further south (lighter red colours). Note that the curves of transects Kp2800 until Kp3400 are 'cut off' at their peak. This is because the breakwater is located here, which interrupts the longshore sediment transport in cross-shore direction. The extra transects (e.g. Kp3000-2, Kp3000-3) were added to the model in order to increase the spatial resolution.
- **Figure 5.3b**: The total volume of sediment transport per transect is depicted in Figure 5.3b. This also shows how the **southward directed** sediment transport increases from transect Kp3000 to transect Kp3600, leading to erosion, after which it decreases again between transects Kp3800 and Kp4200, leading to sedimentation.

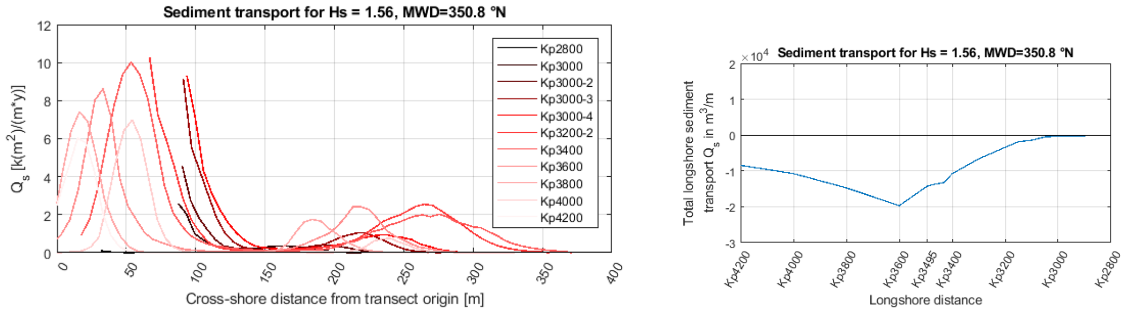

(a) Longshore transport distribution in southward direction per ray

(b) Total longshore transport per ray for Northen waves (350 °N)

Figure 5.3: Positive longshore transport gradient in southward direction for Northern waves (350 °N)

5.1.2. Discussion of hypothesis

"Waves from North/Northwest cause more erosion than waves from West, due to larger gradients in longshore sediment transport and increased wave attack."

From the results it can be concluded that indeed waves from north/northwest cause more erosion due to larger gradients in longshore sediment transport. Moreover, it has also shown that waves coming from west/southwest not only cause less erosion, but actually feed the transects just south of the hard-soft transition with sand and therefore enables the system to recover. On top of that, using a one-line model that only takes into account longshore transport has also given insights into whether the system is cross-shore- or longshore- dominated. Since the model could reproduce the morphological changes during periods with the highest erosion rate at the hard-soft transition (2017Q3-2017Q4) and the highest sedimentation rate (2017Q4-2018Q1), this has shown that the largest erosion- and sedimentation around the hard-soft transition are dominated by longshore processes, rather than cross-shore processes.

5.2. Hypothesis 2: Effect of coastal features

In this hypothesis, the effect of the evolved coastal shape as it was in 2017 was assessed. This evolved coastal shape consists of cross-shore features (bar and trough; less volume on shoreface in 2017) and longshore features (rotated coastline over northern 300 m of the soft flood defence for both 2013 and 2017 profiles).

5.2.1. Results: UNIBEST

Cross-shore features

To test the effect of the cross-shore shape (shore-normal) on the distribution of sediment transports, two LT-models were set up, one with the bottom profile measured in 2013 and one with the 2017 bottom profile. Both models were forced with the same wave conditions (from 2017-2018). One can then look at the distribution of the sediment transport over the cross-shore length. Figure 5.4 on the right shows again the difference in cross shore profiles between 2013 and 2017.

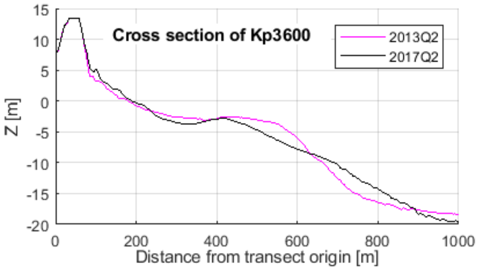

Figure 5.4: Typical cross-shore profile in 2013 (Q2) vs 2017 (Q2)

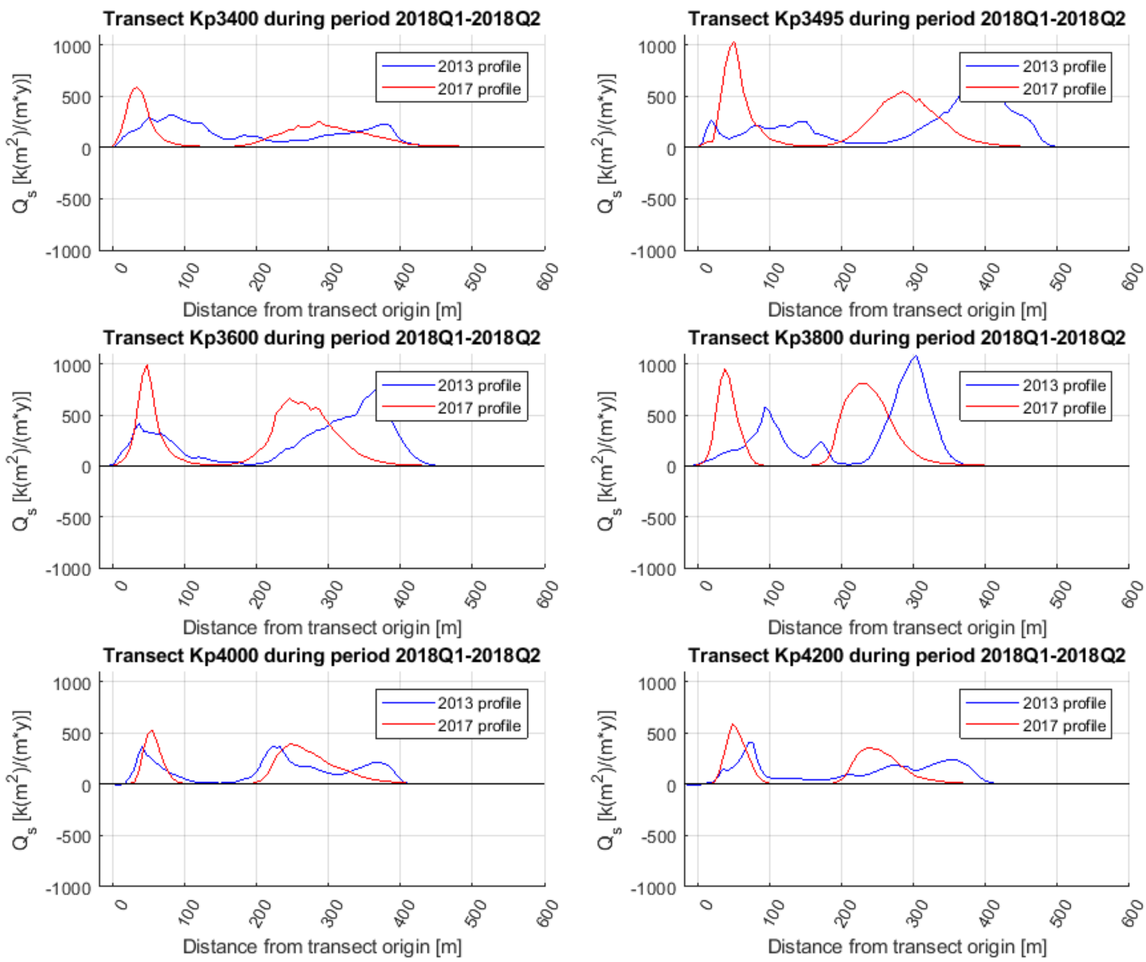

Figure 5.5: 2013 vs 2017

Figure 5.5 shows the distribution of longshore sediment transport for the different coastal profiles, for transects Kp3400 until Kp4200 from period 2018Q1-2018Q2. The hump on the left is the sediment transport induced by wave breaking on the beach and the hump on the right represents the sediment transport induced by wave breaking on the subtidal bar. It can clearly be seen that the distribution of sediment transports is quite different for the different cross-shore profiles. With the profile as it was in 2013, the highest sediment transport rates take place further offshore (around +/- 300- 400 m), whereas with the 2017 profile some sediment transport takes place at the subtidal bar (+/- 250 m offshore), but the largest portion of sediment transport takes places on the beach.

More interesting is to look at the gradients, because this is what changes the coast in longshore direction. Therefore one can again plot the coastline changes computed from UNIBEST, which are shown in Figure 5.6. One can see that apparently the differing distribution of sediment transport does not necessarily mean larger/smaller gradients in sediment transport over the entire profile, and therefore also not more erosion or sedimentation averaged over shoreface and beach. However, as could be seen in 5.5, the beach was exposed more to waves and this explains the fact that during the last years more erosion was observed on the beach compared to the shoreface. Also, just north of the hard-soft transition, there is a small difference due to the different bottom configuration: with the bottom configuration as in 2017, the transects just north of the hard-soft transition experience slightly less sedimentation for periods 1, 2, 4 and 5, and slightly less erosion for period 3. This is because there is more sediment present in front of the breakwater.

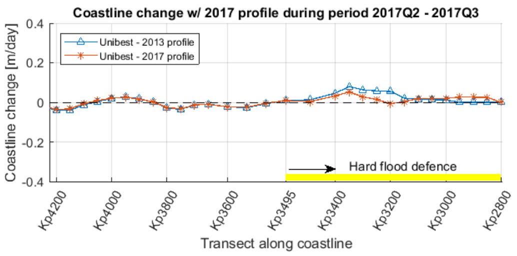

(a) Period 1: 2017Q2-2017Q3

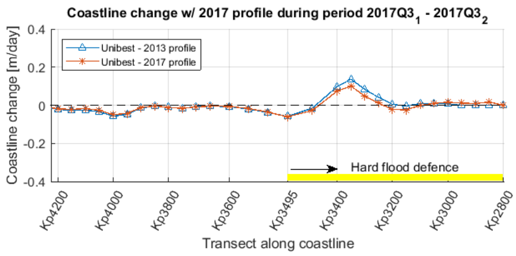

(b) Period 2: 2017Q3_1-2017Q3_2

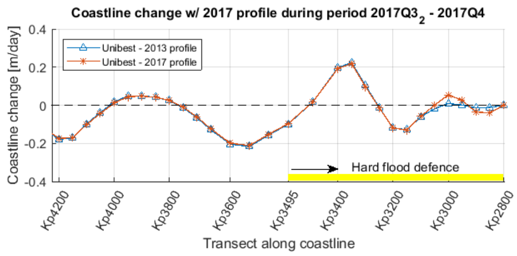

(c) Period 3: 2017Q3_2-2017Q4

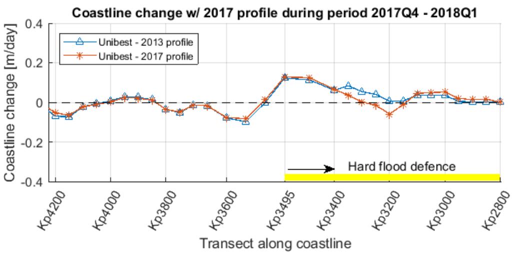

(d) Period 4: 2017Q4 - 2018Q1

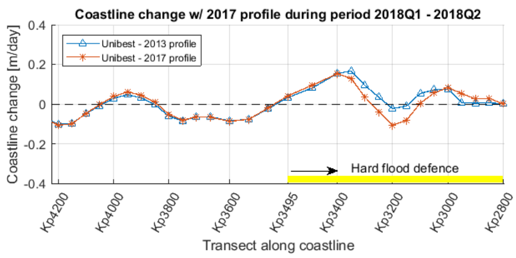

(e) Period 5: 2018Q1 - 2018Q2

Figure 5.6: UNIBEST results comparing the 2013 bottom configuration with the 2017 bottom configuration.

Alongshore features

The other feature of the evolved coastal shape is in alongshore direction (shore-parallel). The effect of the rotated northernmost 300 m of coastline (between Kp3800 and Kp3495) that is observed from 2013 quite constantly until now, was investigated with Unibest as well. For the non-rotated case, all transects in the model have a coast-orientation of 305 °N; for the rotated case, transect Kp3800, Kp3600 and Kp3495 have a coast-orientation of 320 °.

What can be seen from these figures, is that in the non-rotated case, the northernmost transects (Kp3600-Kp3400) erode more, resulting in the rotated profile. In other words, the rotated profile is indeed an equilibrium profile towards which the coast moves. The 'rotation' is also caused by the retreated coastline in the northernmost transects. This shape is maintained by frequent occurence of northern storms. Waves from the south make the northern transects rotate back slightly, until it is again reshaped by northern storms.

Another interesting observation can be done from Figure 5.7d. It shows that with the rotated profile (so with the northernmost transects retreated - as it is was in reality) there is clearly a lot of sedimentation around the hard soft transition (red line >0 between transects Kp3495 and Kp3400). Apparantly it fills up the 'gap' that was created by the retreated and rotated coastline. However, when the coast here would just be straight, the southwestern waves would not cause this accumulation of sediment, as can be seen from the blue line. In other words, southwestern storms cause a **recovery** of the hard-soft transition when it has been eroded, but if the coast is straight it will not cause extra accumulation of sediment.

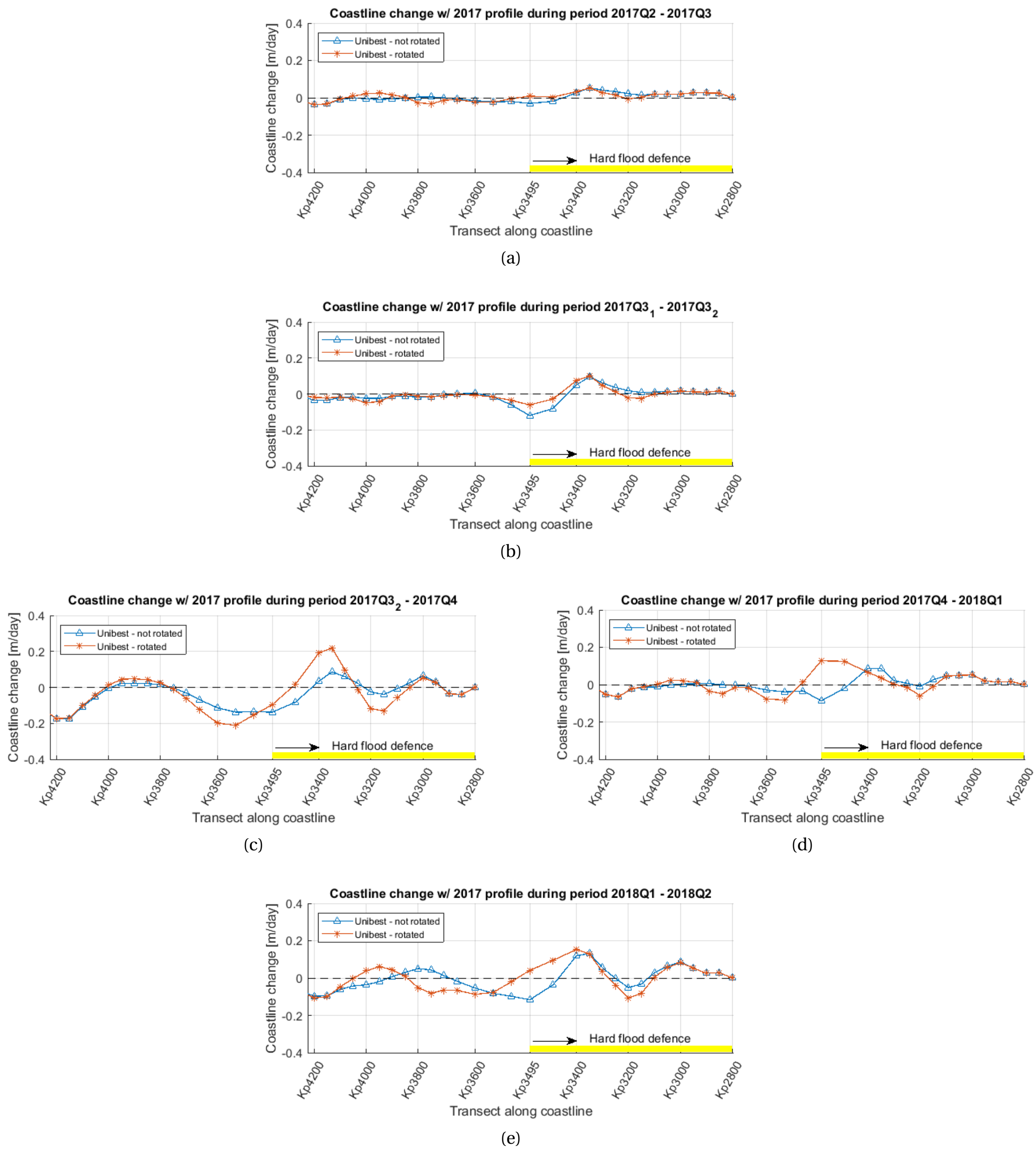

Figure 5.7: UNIBEST results comparing the a rotated vs a non-rotated coastline

5.2.2. Results: SWAN

Above, the effect of the cross-shore and longshore features on the longshore sediment transport and coastline changes was analysed, which appeared to be small. However, the cross-shore profile may influence (the location of) wave breaking, undertow and therefore influence cross-shore sediment transports and associated coastline changes. Figures 5.8a, b and c below show the transformation of waves for the design, 2013 and 2017 bottom configuration, respectively, for one wave condition with western waves. The results for all the other wave conditions can be found in Appendix E.1

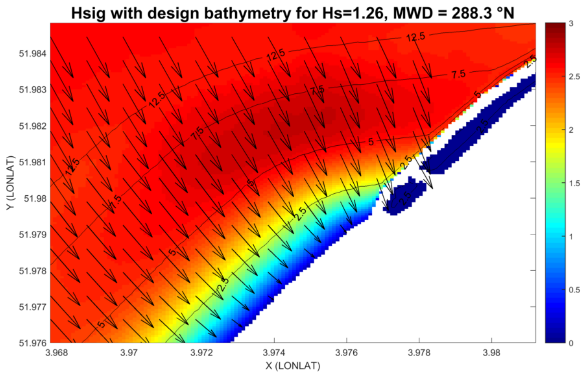

(a) Design

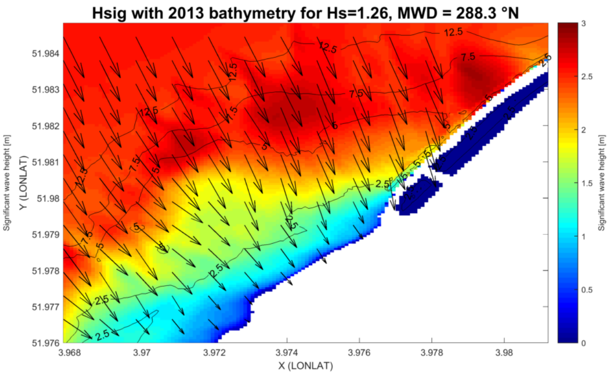

(b) 2013

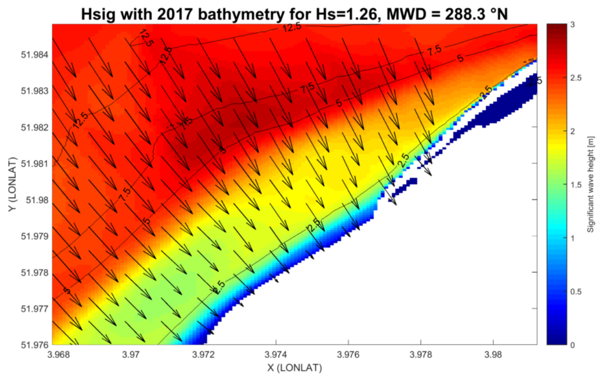

(c) 2017

Figure 5.8: Maps showing the development of the significant wave height for the design bottom, the bottom as measured in 2013, and the bottom as measured in 2017, respectively. The wave condition used here is Hs = 1.26, MWD = 288.3 °N (Hs = 4.03, MWD = 341 °N at Europlatform)

A few general remarks can be made based on these figures:

- The rotated coastline over the northenmost 300 m of the soft flood defence can be clearly recognized in both the situation in 2013, and in the situation of 2017.
- Both in 2013 and 2017, the offshore part of the coastal profile is a lot more extended than in the design, i.e. the waves start breaking earlier as would be the case with the design bottom configuration.
- From Figure 5.8c we see that in the situation with the 2017 bathymetry a lot of sediment has been transported to in front of the breakwater. Therefore this area is overall shallower as well and the southern part of the breakwater is sheltered more from waves than it was in 2013 or as it would be with the design bottom profile. Therefore, we also see larger wave heights in the northern part of the breakwater for the 2013 situation (darker red colours). This is also confirmed when looking at Figure 5.10b, where it can be seen that the underwater topography next to the breakwater is deeper for the 2013 situation than for the 2017 situation.
- From Figure 5.9c it can be recognized that with the 2017 bathymetry under northern waves, waves start decreasing in size further offshore, but they also remain that size until closer to the actual coast, so that the wave attack is larger, which could also be seen in Figure 5.5.

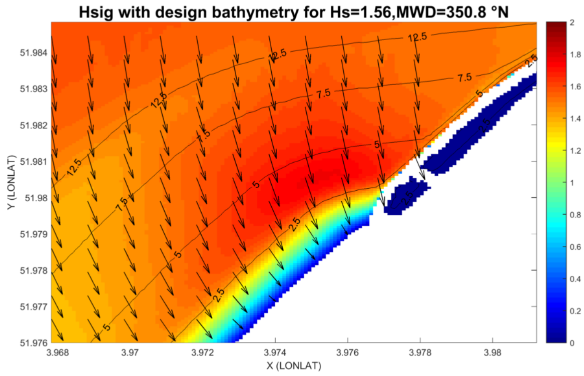

(a) Design

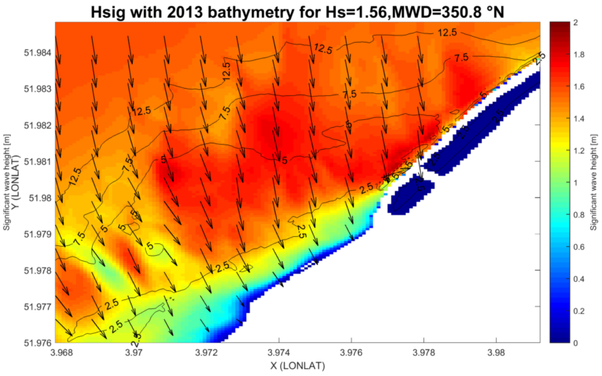

(b) 2013

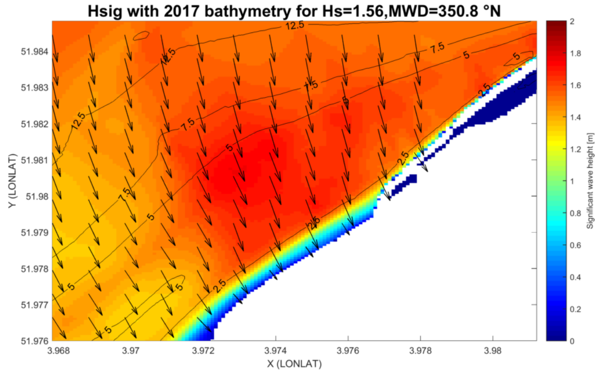

(c) 2017

Figure 5.9: Wave transformation for condition 9: Hs=1.56, MWD= 350.8 °N (H_s = 2.61, MWD = 16 °N at Europlatform)

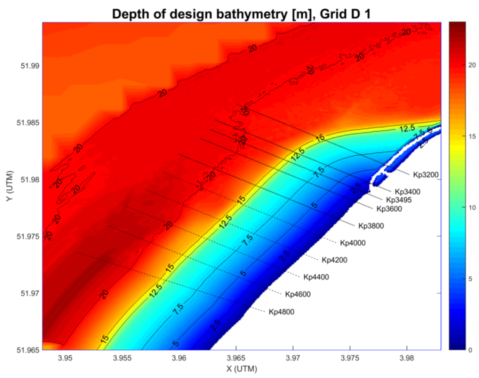

(a) Design

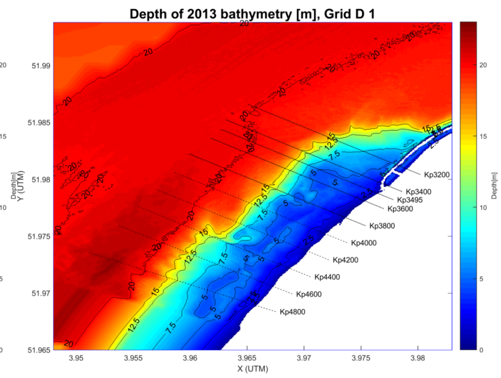

(b) 2013

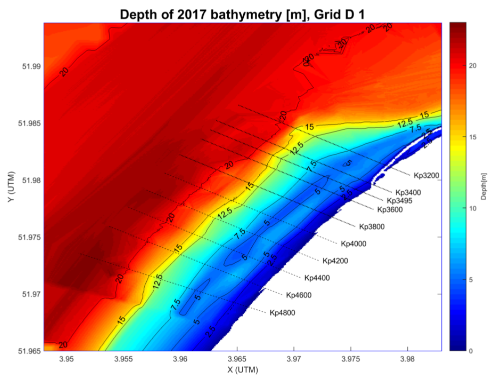

(c) 2017

Figure 5.10: Bathymetry from SWAN computations.

5.2.3. Discussion of hypothesis

"The evolved coastal profile as observed in 2017, with a distinct bar and trough in cross-shore direction and a rotated coastline in the northern part, has a significant effect on the morphological changes of the coast."

In cross-shore direction, the coastal profile as observed in 2017 contains less sediment on the shoreface and on the beach. Therefore, waves break higher in the profile. This leads to a higher vulnerability for cross-shore erosion, and it changes the cross-shore distribution of longshore sediment transport. This has relative little effect on longshore sediment transport gradients over the entire active zone, but it does give more beach erosion. From the transformation of waves from the SWAN model using different bottom configurations, it was also shown that with the latest bottom configuration (2017 Q2), waves break later/closer to the coast. This can produce stronger undertows and corresponding offshore-directed sediment transport.

In longshore direction, a typical characteristic of the evolved profile is the rotated section over the northenmost 350 m. The rotated profile is caused by southward sediment transports, during which the northernmost transects erode with increasing gradients, after which the eroded material is deposited further downstream when sediment transport gradients decrease. This shape is maintained by frequent occurence of northern storms. Waves from the south make the northern transects rotate back slightly, until it is again reshaped by northern storms. Moreover, the results show that the model is quite sensitive to small changes in the coastline orientation.

5.3. Hypothesis 3: Reflection

In this hypothesis, the relative effect of wave reflection on the observed erosion around the hard-soft transition was investigated. As was explained in section 4.4.3, short wave reflection was studied with SWAN and UNIBEST, and long wave reflection was investigated using XBeach surfbeat.

5.3.1. Results: SWAN

The assessment of the effect of wave reflection using SWAN and UNIBEST comprises of two parts:
1. The hydrodynamic effect of reflection on wave heights in front of the breakwater (in SWAN)
2. The morphological effect caused by these larger wave heights (in UNIBEST)

First, one can find the influence on the wave height at several distances from the coast by comparing the wave height at that point without reflection, to the wave height at the point with reflection (with K_r=0.2). Additionally, a run was done using reflection coefficient K_r=0.5. This was done for the 9 conditions that were also used for Hypothesis 2. For clarification, the wave conditions are listed again in Table 5.1. The 2D wave fields can be viewed in Figure 5.11. To see the relative effect more clearly, Figure 5.12a shows the wave heights for different wave conditions along depth contour = -2.5 m. Figure 5.12b shows the wave heights for different wave conditions at depth contour = -5 m.

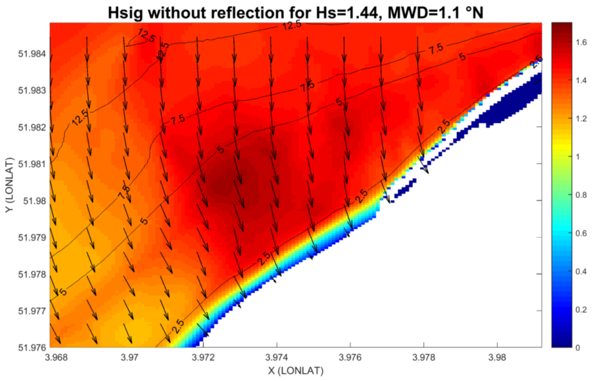

(a) H_s without reflection

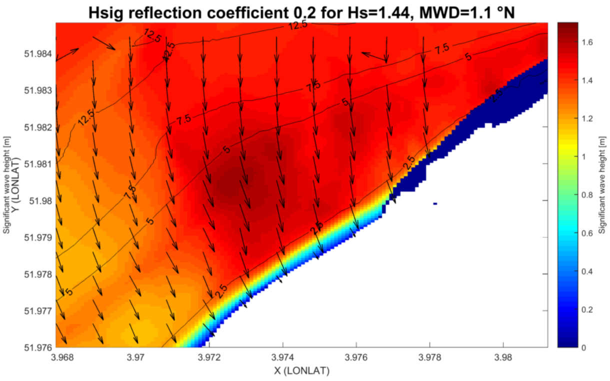

(b) H_s with K_r = 0.2

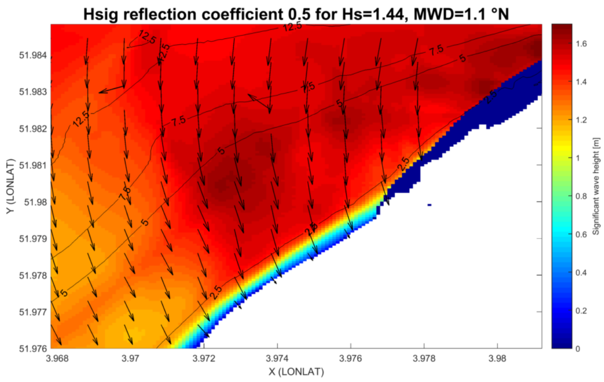

(c) H_s with K_r = 0.5

Figure 5.11: Wave transformation for condition 6: H_s = 3.36, MWD = 47 °N at Europlatform.

The relative increase in wave height by the reflected wave (in % from the incoming wave height) was also calculated along the depth contour lines -2.5 m and -5 m, of which the results are stored in Table 5.2 and 5.3. From these figures and tables, the following can be concluded:

- **Figure 5.11**: The effect of short wave reflection is noticeable in the northern part of the hard flood defence, but is relatively small at the southern part of the hard flood defence (see the darker red colours representing larger waves in the top right corner of the lower figure). This can be explained by the fact that the shore is shallower along the southern part of the hard flood defence. Therefore the majority of the short waves will have been dissipated by the time they reach the breakwater, and so the reflected waves will be smaller as well.

- **Figure 5.12**: When looking at the part of the coast south of the hard-soft transition (left of Kp3400 in the figures), one can see that the wave heights close to the coast (at depth contour -2.5m) are not affected by reflected waves, but further off the coast (at depth contour -5m) the wave heights are affected by the reflected waves. This can be explained when looking at Figure 5.13: when a wave approaches the breakwater with an angle of, for example, 350 °N, it reflectes with the same angle as it comes in, and therefore it reaches point 65, but does not reach point 90.

- **Tables 5.2 and 5.3**: From the tables, it can be seen that at the depth contours of -2.5 m and -5 m, the reflected wave has been damped out almost completely already. The reflection coefficient imposed at the breakwater was 0.2 (20 %), but the reflection coefficients found at point 76 (2.5 meter depth, 9 m from the coast) is only 0.015 (1.5%). This is remarkably low, because it means that within 9 m, 92.5% of the reflected wave has been damped out.

- Moreover, the increase in wave height at depth contour -5 m south of the hard-soft transition (at points 61 to 65) is only caused by wave conditions from north/northwestern directions, e.g. condition 9 with MWD = 17 °N and MWD = 341 °N(marked red in Table 5.3). This is visualised in Figure 5.13.

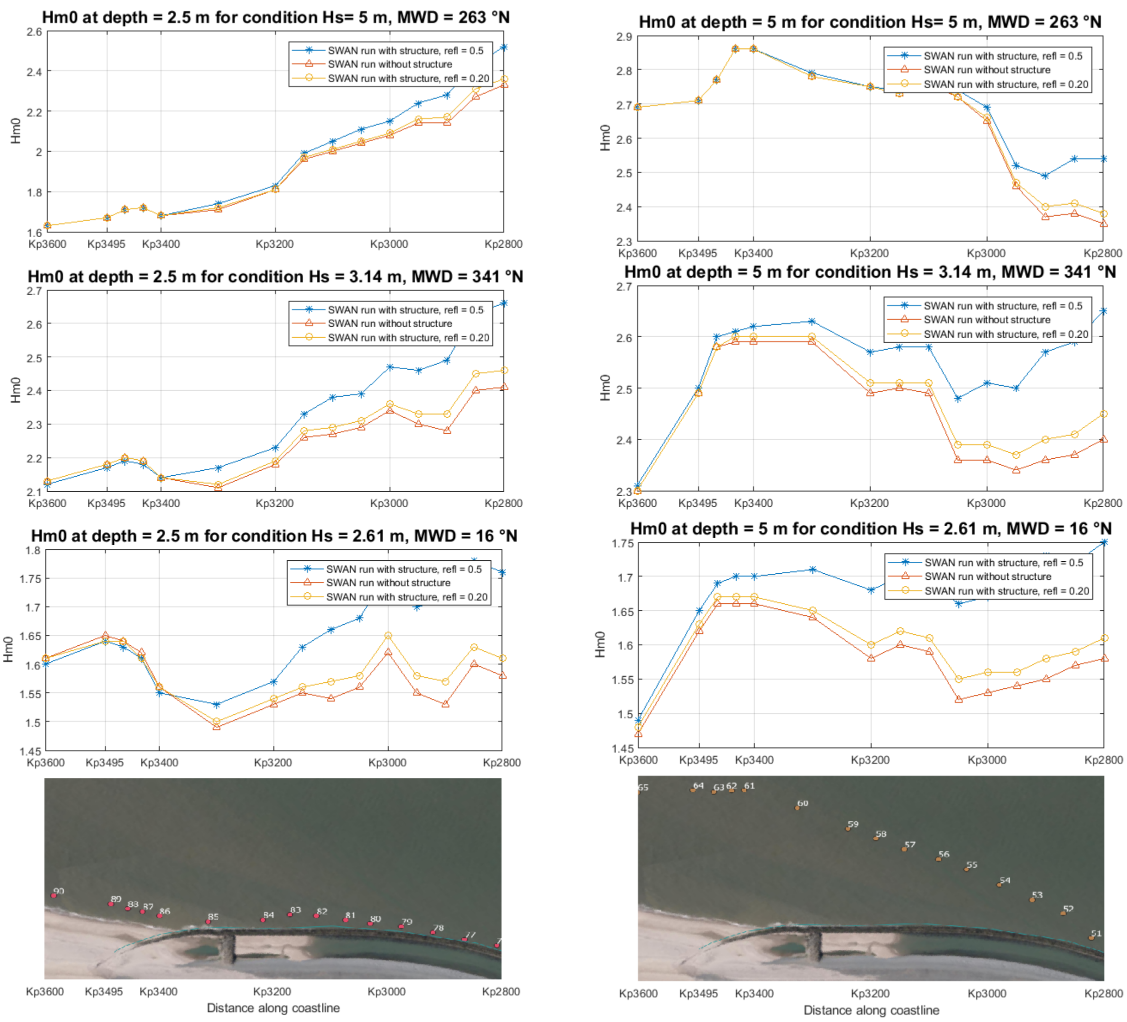

Figure 5.12: Hm0 with vs without reflection at depth contour -2.5 m (left) and at depth contour = -5 m (right).

Table 5.1: 9 conditions applied in SWAN for testing of reflection coefficient

Condition	Europlatform H_s (m)	Europlatform MWD (°N)	1 km from coast H_s	1 km from coast MWD (°N)
1	4.51	227	2.03	268
2	5	263	2.42	273.6
3	4.03	341	1.26	288.3
4	5	295	3.21	297.7
5	3.14	341	2.28	330.7
6	3.36	47	1.44	1.1
7	4.6	324	3.07	317
8	3.28	357	2.03	340.7
9	2.61	16	1.56	350.8

Table 5.2: % increase of Hm0 with reflection coefficient K_r = 0.2 at depth contour = -5 m. The column 'Distance' represents the distance measured from the output point to the breakwater or shore. The percentage is calculated with: $(Hm_{0,withreflection} - Hm_{0,basecase})/Hm_{0,basecase} * 100\%$

Point	Distance	% increase in waveheight per condition 1	2	3	4	5	6	7	8	9	Average
76	9	1.99	1.29	1.57	1.48	2.07	1.36	1.07	1.90	1.90	1.46
77	5	2.50	1.76	1.67	1.50	2.08	2.03	1.57	1.94	1.87	1.69
78	9	1.82	1.40	1.34	1.18	2.19	3.52	1.27	1.54	2.61	1.69
79	12	1.65	0.93	0.91	1.18	1.30	1.38	0.88	1.04	1.94	1.12
80	15	2.01	0.48	0.47	0.79	0.85	1.97	0.46	0.52	1.85	0.94
81	18	1.47	0.49	0.49	0.81	0.87	1.39	0.48	0.54	1.28	0.78
82	25	1.97	0.50	0.50	0.82	0.88	1.42	0.49	0.55	1.95	0.91
83	32	1.44	0.51	0.00	0.41	0.88	1.43	0.50	0.00	0.65	0.58
84	20	0.94	0.00	0.00	0.44	0.46	0.72	0.55	0.00	0.65	0.38
85	15	0.47	0.58	0.59	0.45	0.47	0.75	0.58	0.00	0.67	0.46
86	30	0.00	0.00	0.00	0.46	0.00	0.00	0.00	0.00	0.00	0.05
87	32	0.00	0.00	0.00	0.00	0.00	0.00	0.00	0.00	0.00	0.00
88	35	0.50	0.00	0.00	0.00	0.00	0.00	0.00	0.00	0.00	0.05
89	42	0.00	0.00	0.00	0.00	0.00	0.00	0.00	0.00	0.00	0.00
90	35	0.00	0.00	0.00	0.00	0.00	0.00	0.00	0.00	0.00	0.00

Table 5.3: % increase of Hm0 with reflection coefficient K_r = 0.2 at depth contour = -5 m. The column 'Distance' represents the distance measured from the output point to the breakwater or shore. The percentage is calculated with: $(Hm_{0,withreflection} - Hm_{0,basecase})/Hm_{0,basecase} * 100\%$

Point	Distance	% increase in waveheight per condition 1	2	3	4	5	6	7	8	9	Average
51	22	2.00	1.28	1.54	1.48	2.08	2.04	1.03	1.90	1.90	1.53
52	65	2.58	1.26	0.77	1.48	1.69	1.37	0.68	1.44	1.27	1.25
53	85	1.89	1.27	0.78	1.48	1.69	2.08	0.69	1.45	1.94	1.33
54	110	2.30	0.41	0.79	0.72	1.28	2.10	0.34	0.98	1.30	1.02
55	140	1.60	0.38	0.39	0.69	1.27	1.41	0.34	0.49	1.96	0.85
56	160	1.56	0.00	0.39	0.34	1.27	1.42	0.34	0.49	1.97	0.78
57	185	1.03	0.36	0.37	0.33	0.80	1.36	0.00	0.47	1.26	0.60
58	215	0.52	0.00	0.00	0.33	0.40	1.34	0.00	0.46	1.25	0.43
59	239	0.51	0.00	0.00	0.33	0.80	1.37	0.00	0.00	0.00	0.30
60	290	0.00	0.00	0.00	0.00	0.39	1.33	0.00	0.00	0.61	0.23
61	330	0.00	0.00	0.00	0.00	0.39	0.00	0.00	0.00	0.60	0.10
62	325	0.00	0.00	0.00	0.00	0.39	0.00	0.00	0.00	0.60	0.10
63	310	0.00	0.00	0.00	0.00	0.00	0.00	0.00	0.00	0.60	0.06
64	306	0.00	0.00	0.38	0.00	0.00	0.00	0.00	0.00	0.62	0.10
65	280	0.00	0.00	0.00	0.00	0.00	0.00	0.00	0.00	0.68	0.07

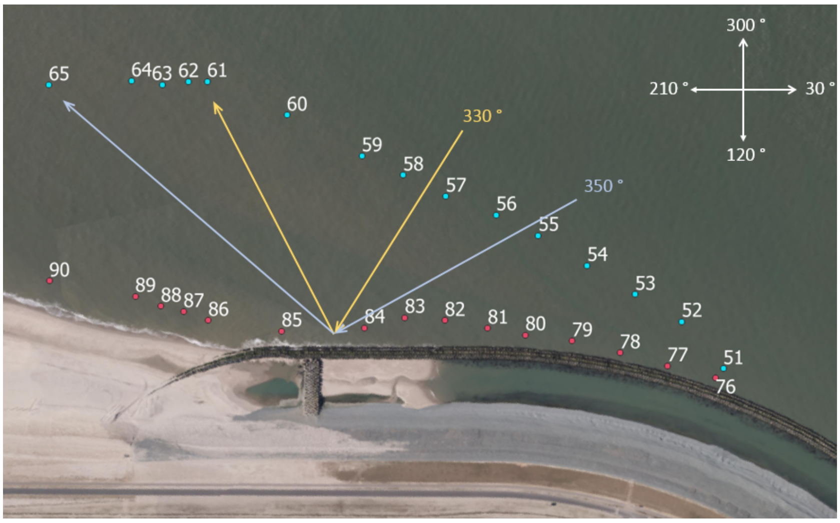

Figure 5.13: Viualisation of waves reflecting at the breakwater

From Figures 5.11 and 5.12 and Tables 5.2 and 5.3 it was shown that at a small distance from the breakwater, the effect of the imposed reflection in SWAN is already hardly noticable, especially with a reflection coefficient of 0.2. This suggests that the reflected waves have dissipated very quickly directly when it is reflected from the breakwater. To check this, one can look at the cross-shore transects of wave heights in SWAN. This is shown in Figure 5.14.

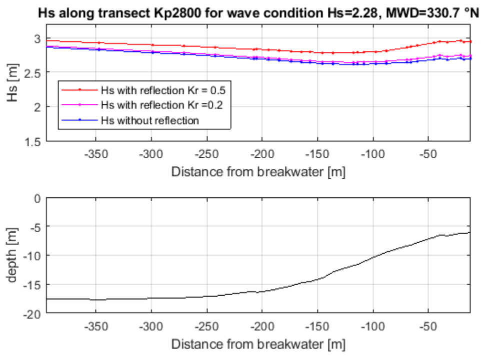

(a) Kp2800

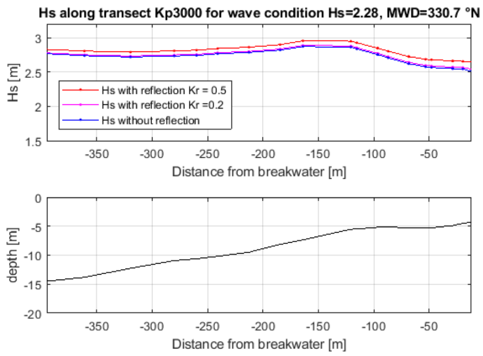

(b) Kp3000

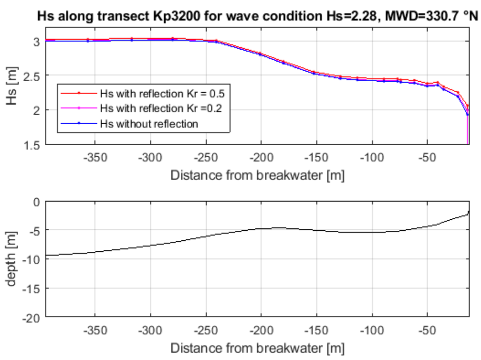

(c) Kp3200

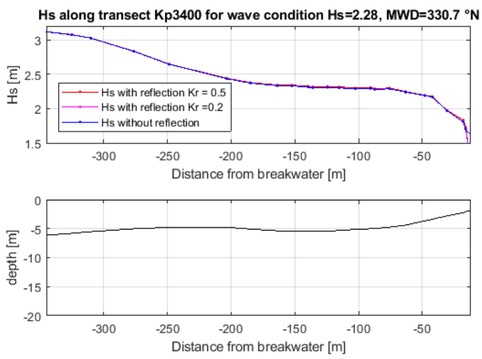

(d) Kp3400

Figure 5.14: Wave transformation for condition 5: Hs=2.28, MWD= 330.7 °N. The upper figures show the development of the wave height (both incoming and reflected) of four transects for three cases: with a reflection coefficient of 0.5, with a reflection coefficient of 0.2 and without reflection. The lower figures show the cross-shore bathymetry of the transects.

From Figures 5.14a-d it is again visible that the reflection is higher for the more northern transects (Kp2800 and Kp3000) than for the southern transects close to the hard-soft transition (Kp3200 and Kp3400). However, it is not visible from these figures that the reflected waves dissipate very quickly.

Concluding from the SWAN results, it was confirmed that short wave reflection indeed is very small near the hard-soft transition, because the water depth is shallow and therefore most short waves have been dissipated. However, also further north, where short wave reflection is expected to be larger (and should be about 20% because this is what is imposed at the breakwater), the modelled reflection is a lot smaller in SWAN. This can have several causes:

- It can be partly explained by the fact that the model resolution is still quite coarse for such small-scale shore processes. The minimum grid cell size is 6x7, so that ouput points can only be viewed at a distance of e.g. 5 m from the breakwater. This could mean that either the reflection is not visible with the current model resolution, or that the reflection is not even solved correctly with the current model resolution. To inspect the hydrodynamic processes in greater detail at the breakwater, the grid cell size could locally be reduced a bit further. However, as was described in Section 4.2.2, a limitation of the SWAN model is that it becomes unstable when the resolution is too fine. Therefore this has to be done with caution.
- Another explanation can be the way the obstacle is implemented in SWAN. As was described in Section 4.4.3, care was taken to use the least amount of point possible to define the obstacle, but possibly the amount of points was still too large and the results can be improved by reducing the amount of points.
- The reflection of the obstacle could also be incorrectly computed because of the way the grid is defined. The grid is a rectilinear grid, and therefore the grid lines and points are not perpendicular to the obstacle. This will possibly also influence the angle of inclusion of waves that are reflected in the model. Therefore an obstacle definition in SWAN might work better in combination with a curvilinear grid, where grid lines are perpendicular to the obstacle.
- Finally, it has to be noted that SWAN works well for water depths until the points of wave breaking, but does not model wave heights correctly beyond the point of wave breaking. Therefore it can be expected that at shallower depths (close to the hard-soft transition), the waves that reach the breakwater will not be modelled correctly. However, at these depths, short waves will have been broken so it can also be expected that short wave reflect is small (long wave reflection may be larger, but this is modelled in SWAN).

5.3.2. Results: UNIBEST

From the SWAN results showing the hydrodynamic effects of wave reflection, it was observed that with a reflection coefficient of 0.2, the wave heights at the depth contour of -5 m only increased with 1.5%. This suggests that when inspecting the morphological changes using UNIBEST, the effect of wave reflection will be very small as well. This was checked by imposing the new boundary conditions including the reflected waves in UNIBEST. In Figure 5.15 it is confirmed that indeed the underestimated wave reflections from SWAN have hardly any effect on the coastline changes UNIBEST.

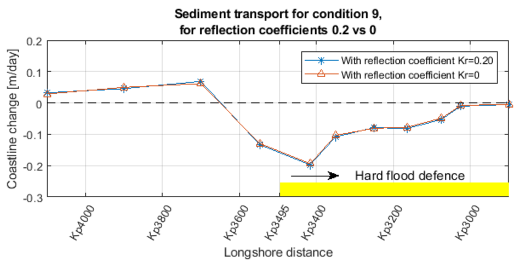

Figure 5.15: Computed coastline change for two cases: with reflection coefficient Kr=0 vs reflection coefficient Kr=0.2

Using SWAN and UNIBEST as tools to investigate the hydrodynamic and morphological aspects of wave reflection provided insufficient information on the actual morphololological system. This is because the reflected waves seem to be small at the model boundaries of UNIBEST and therefore the model cannot capture the wave reflection well. Moreover, it is doubtful whether the wave reflection is resolved well in SWAN, as the wave reflection seems a lot smaller than the 0.2 that is imposed as reflection coefficient on the breakwater. Therefore it was chosen to compare the results with results using XBeach, as described in Section 4.4.3.

5.3.3. Results: XBeach

The effect of **long wave reflection** was tested in XBeach. The hydrodynamic and morphological effects of reflection in XBeach (surfbeat) can be visualized by comparing waves and sedimentation-erosion patterns of both runs (a run representing a situation with reflection and a run representing a situation without reflection). The model was run with a 45-hour storm from north-northwest (≈ 320 - 330 °N) with a peak wave height of 3.49 m at the model boundary. All input files of the Xbeach simulations can be found in Appendix D.6. First of all, the wave heights were inspected over 6 typical transects. Furthermore, these wave heights were split into high frequency (HF) and low frequency (LF) waves. The low and high frequency waves are automatically split by the model, which means that there is no strict cutoff frequency but generally LF waves have frequencies f < $0.5 \cdot f_p$ and HF waves have frequencies f > $0.5 \cdot f_p$. The transects that were used for the XBeach visualisation differ slightly from the design transects because they are aligned with the XBeach grid, and are depicted in Figure 5.16. The wave height development over the 6 transects are depicted in Figure 5.17 and 5.18

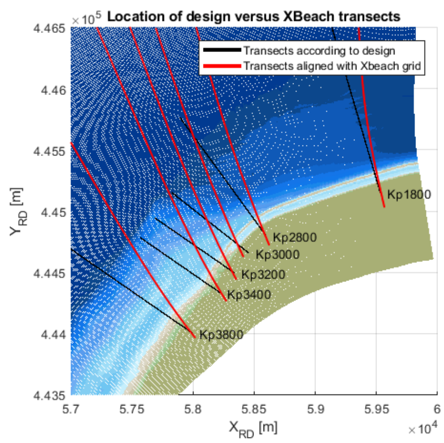

Figure 5.16: Location of transects aligned with the XBeach grid, versus transects that have been used in the design.

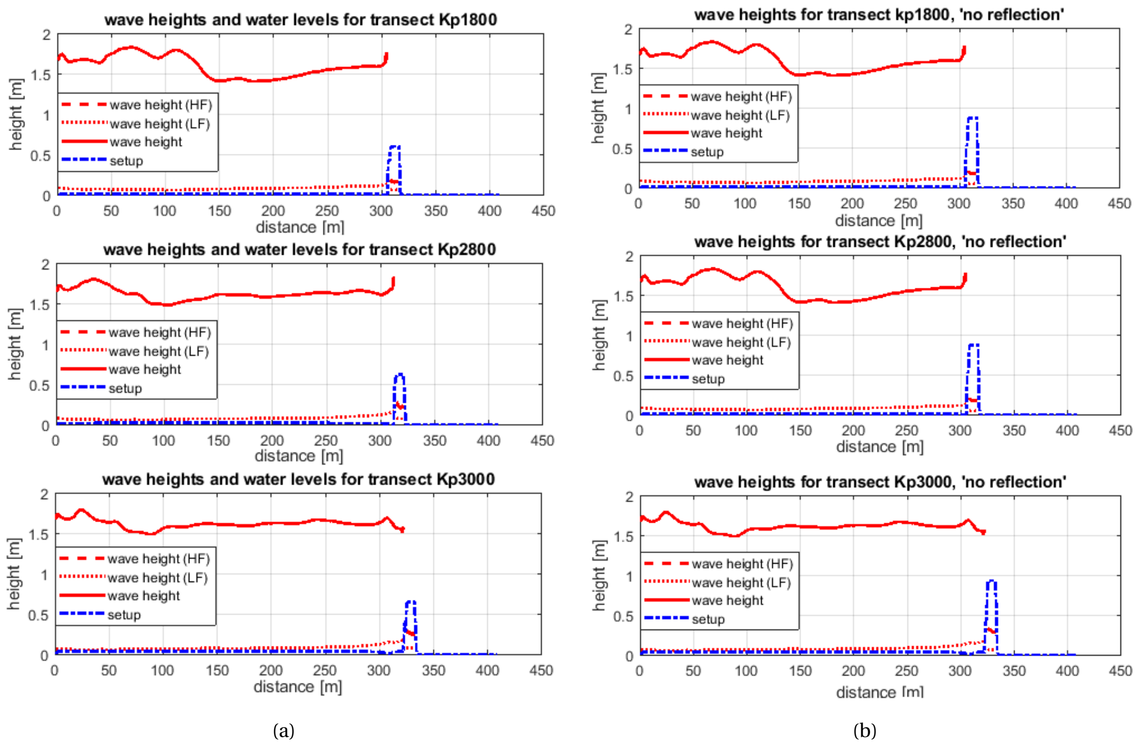

(a) (b)

Figure 5.17: Wave heights of LF waves (T < 25 s) and HF waves (T > 25 s) for transects Kp1800, Kp2800 and Kp3000 using XBeach surfbeat.

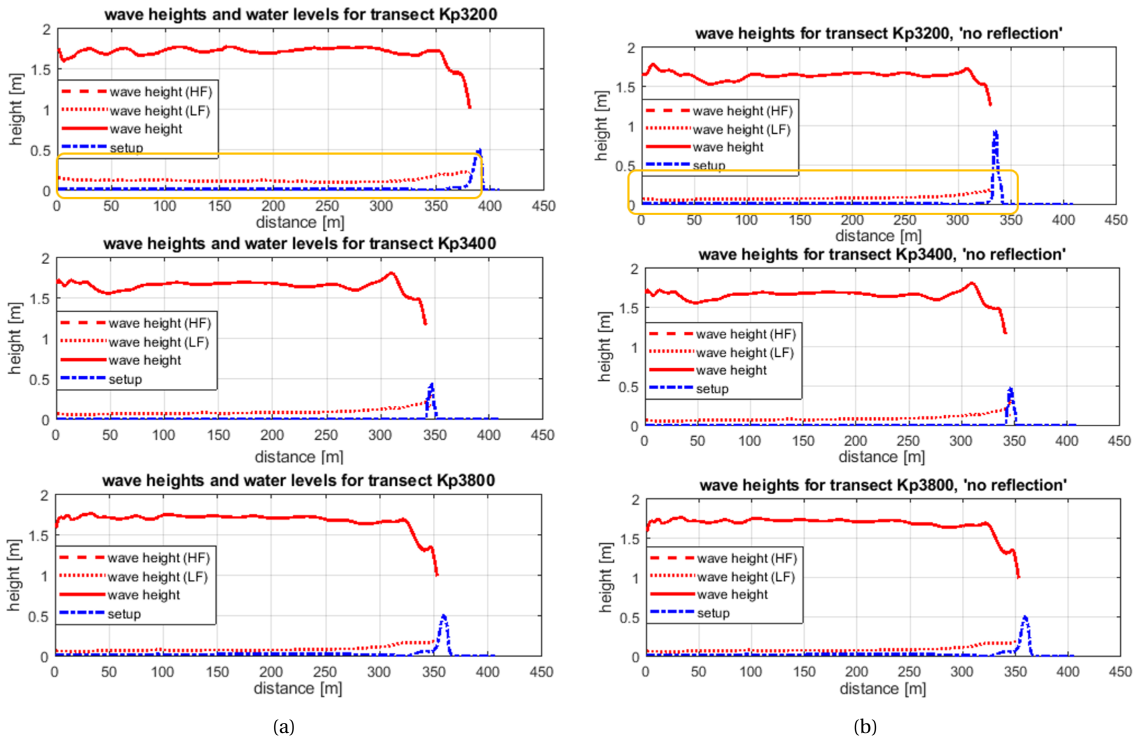

Figure 5.18: Wave heights of LF waves (T < 25 s) and HF waves (T > 25 s) for transects Kp3200, Kp3400 and Kp3800 using XBeach surfbeat.

From Figure 5.17 and Figure 5.18 the following can be observed:

- For transects Kp1800 and Kp2800 (along the northern part of the breakwater), relatively little differences are seen between the two different scenarios (with vs without reflection). This can be explained by the fact that surfbeat does not solve short wave processes such as short wave reflection. Therefore, both situations represent a case without reflection.
- At the most northern transects of the hard flood defence (transects Kp1800 and Kp2800) the Low Frequency waves are indeed negligible compared to the High Frequency waves. This confirms that the frequency domain for determining the reflection coefficients in the physical model tests is suitable for this location.
- However, at the transects closer to the hard-soft transition (Kp3200 to Kp3800) the Low Frequency waves are more prominently visible, especially close to the shore. Especially for transect Kp3200 the long (Low Frequency) waves are not negligible as they make up about 10% of the total wave height. As it was earlier stated that these long waves can reflect with reflection coefficients > 1, the reflection of these long waves has to be taken into account in the total reflection as well. Indeed, a difference can also be seen between the cases 'with' and 'without' reflection for Transect 3200: the Low Frequency waves are significantly smaller for the case 'without' reflection. This implies that the workaround method to increase the Chézy coefficient has at least some effect to the reflected waves.

Next, the reflection coefficient of the long waves (LF) was computed by splitting the waves into an incoming and outgoing signal. This was done using the method of Guza et al. (1984). Computing the reflection coefficients over the abovementioned five representative transects (from the 6 representative transects) yields the results as depicted in Figure 5.19a-e.

From Figure5.19a-e it can be seen that for all transects, the reflection coefficient of **long waves** is very high (+/- 0.9). However, if the long waves itself only make up a negligible part of the total waves (as is the case for transects Kp1800 and Kp2800), the contribution of this reflection to the total reflection will still be small. For transects Kp2800, Kp3200 (and Kp3400) it can be seen that the reflection coefficient rapidly increases with offshore distance and even reaches values higher than 1. This can be due to the phenomena explained in Section 4.4.3 and visualised in Figure 4.11. This means that for transects (or other wave conditions) where long waves play a role, reflection will also increase signficantly.

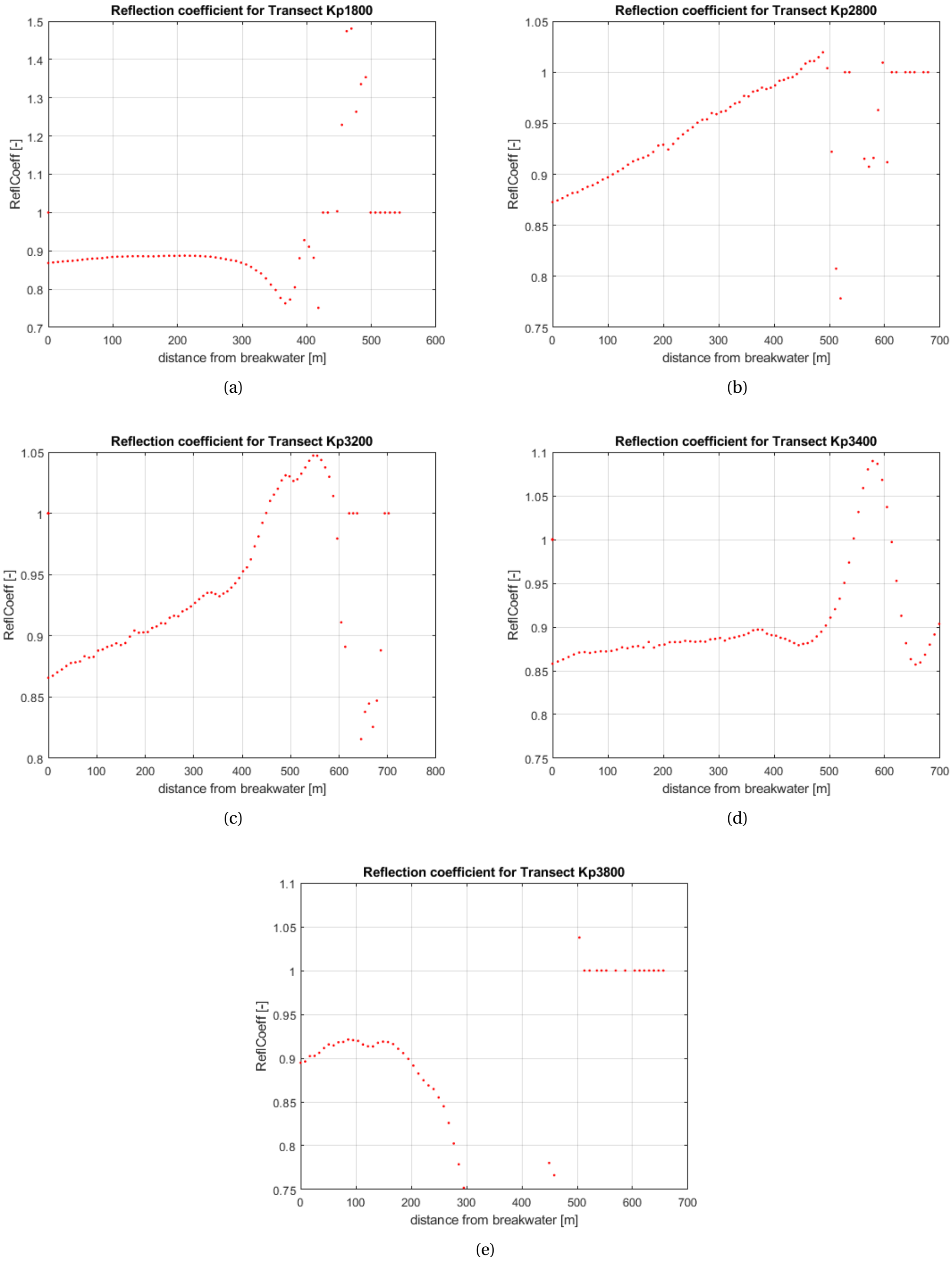

Figure 5.19: Reflection coefficients for Low Frequency waves along five transects.

Morphological effects
Next, the morphological effects of the reflection was assessed by comparing sedimentation-erosion patterns for cases with versus without reflection (using the workaround method of increased friction). The results are depicted in Figures 5.20a and 5.20b. Blueish colors indicate sedimentation, whereas reddish colours indicate erosion. From these Figures, it seems indeed that the sedimentation-erosion patterns are very similar for the two cases, which suggests that long wave reflection does not significantly influence the sedimentation-erosion patterns. However, to compare the two correctly one can subtract one sedimentation/erosion pattern from the other to see the relative difference between the two simulations. This is depicted in Figure 5.20c (in meters) and Figure 5.20d (in % of original erosion/sedimentation).

Here one can see that the reflection does have an effect. Along the breakwater the effect of reflection is increased erosion just seaward of the breakwater (red line along breakwater), which is deposited further seaward (blue line along breakwater). Also around the hard-soft transition the sedimentation-erosion patterns are influenced: there is slightly more erosion between transects Kp3000 and Kp3495 and more sedimentation between Kp3495 and Kp3800. Moreover, the following is observed:

- Along the northern part of the breakwater, reflected waves only have a limited ‘reach’: the bottom changes are only induced between 0 and 50 m from the breakwater. However, the reflected waves do not influence the sedimentation-erosion patterns far offshore, because the water depths increases quickly so the reflected long waves will not affect the bottom anymore. Furthermore it has to be noted that it is doubtful that the observed effect here is actually caused by reflection, or that the increased friction also induce other effects which cause te observed morphological changes.
- Further south, the reflected wave have a larger reach. This can be explained by the fact that bound long waves shoal here due to the shallower water depths, after which their energy is transferred to free long waves, which are far less depth dependent. Therefore the reflection coefficient increases with distance from the breakwater. Therefore we see a larger area of influence for transects Kp3200, Kp3000 and Kp2800. This explains the observed sedimentation-erosion pattern north of Kp3400.
- South of Kp3400, the sedimentation observed (indicated with ’3’) can be explained by the imposed wave conditions (note that it is not actually sedimentation, but it is just less erosion when compared to a case without reflection). The imposed storm is coming from a direction of 330 °N, which will induce a southward sediment transport. The increased (long) wave reflection at the breakwater causes extra erosion in the areas indicated with ’1’ and ’2’, and this sediment is likely to be transported southward by the southward longshore current. Apparenty some of this sediment will settle between transects Kp3495 and Kp3800, or at least, less sediment will be eroded there.
- According to these results, the extra erosion/sedimentation due to reflection is in some areas 5% to 10% of the initial sedimentation/erosion. However, this does not mean that there is 10 % more erosion overall, as it can be seen that there is also extra sedimentation. Only the patterns have changed.

The results in figure 5.20 should only be used for qualitative analysis of the effect of reflection, as the amount of reflection in XBeach for both scenarios is unknown:

- The reflection for the case ‘with reflection’ cannot be controlled (as is the case for SWAN). XBeach takes into account the slope of the breakwater, so the reflection might not be 100 percent. It does not, however, take into account transmission of waves or the roughness of the material, so it is expected that the reflection of waves at the breakwater will be overestimated with XBeach. Furthermore, XBeach surfbeat does not taken into account reflection of short waves.
- Also for the case ‘without reflection’ the reflection is not fully damped out, because the Chézy coefficient cannot be set lower than 20 $m^{1/2}s^{-1}$, which is probably not high enough for all long waves to damp out immediately.

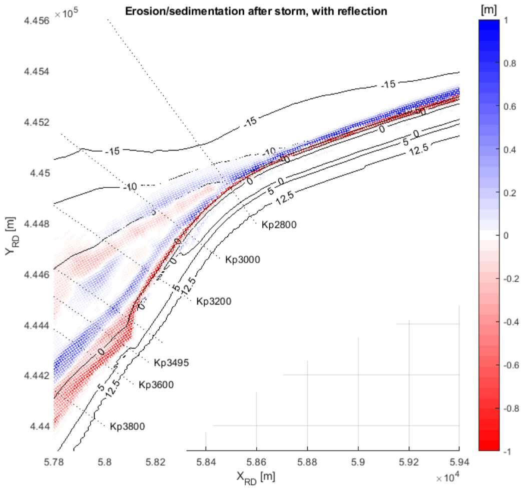

(a) Sedimentation/erosion pattern from XBeach, with reflection (base case)

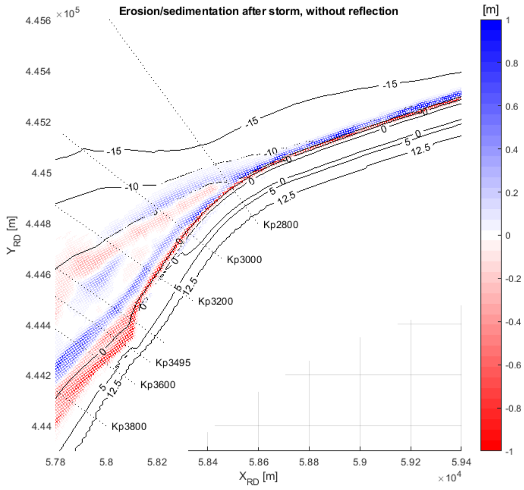

(b) Sedimentation/erosion pattern from XBeach, without reflection (increased friction coefficient on the breakwater)

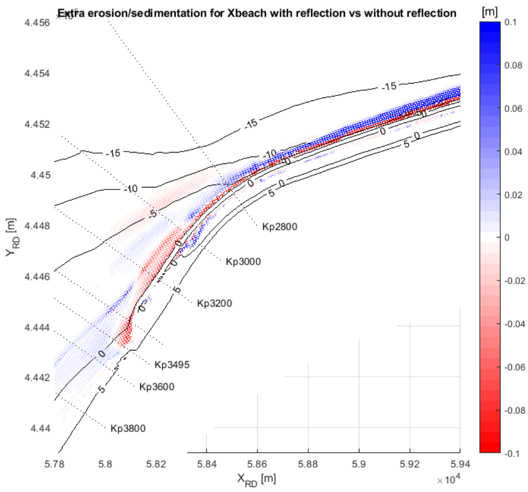

(c) Difference between sedimentation/erosion patterns with vs without reflection

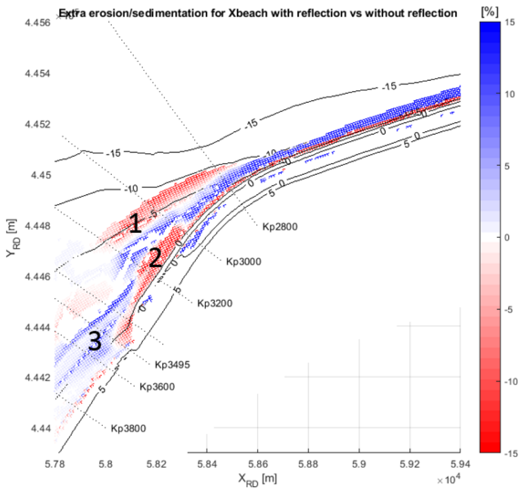

(d) Difference between sedimentation/erosion patterns with vs without reflection

Figure 5.20: Upper figures: sedimentation erosion pattern from XBeach for the case with (left) and without (right) reflection. Lower figure: relative difference between the two cases: extra erosion/sedimentation in meters (left) and in % of original erosion/sedimentation (right)

5.3.4. Discussion of hypothesis

> *"Reflection of waves at the breakwater is an important cause for the observed erosion close to the hard-soft transition."*

The current research presents results of a preliminary investigaton into the effect of wave reflection for the hard-soft transition of Maasvlakte 2. Regarding the role of reflection in the erosion close to the hard-soft transition, it can be concluded that the effect seems relatively small, especially in the case of waves from west/southwest. The main effect of reflection is a shift in the sedimentation-erosion pattern due to longshore transport gradients during southward transport under the influence of northern waves. This effect is also relatively smal but not negligible (order of magnitude 10%-15% of total erosion/sedimentation). Furthermore, the following remarks need to be made:

- The largest effect of reflection is directly next to the breakwater (as could be seen from the XBeach results), because there the effect of the reflected short waves is largest (see SWAN).
- Most likely, the reflection of short waves played a bigger role at the hard-soft transition just after construction, because at that time there was less sand deposited in front of the breakwater.

However, the following critical notes have to be added to the abovementioned findings:

- Wave reflection in a 2D field is a complex phenomenon, especially if long waves are concerned. The preliminary investigation has shown that around the hard-soft transition long wave reflection is large, and long waves make up 10-15% of the total wave height. Therefore the earlier found reflection coefficient of 0.2 that is representative for a cross-section along the middle part of the hard flood defence is not representative for the southern part.
- The method with which the morphological effects of wave reflection has now been assessed (in XBeach) gives an initial impression of the sedimentation-erosion patterns under the influence of wave reflection for certain wave conditions. However, this method will not eliminate all wave reflection and therefore a more suitable method should be chosen to compare the scenarios with and without reflection more correctly. Moreover, different wave conditions should be tested to see under which conditions wave reflection is highest (presumably low wave conditions with low water levels).
- Further research may help in finding more conclusive results concerning the total reflection coefficient at a southern section of the hard flood defence.
- Recommendations on how this should be done according to the author are presented in Chapter 8.

5.4. Hypothesis 4: Tide

In this hypothesis, the relative effect of tide and wave-tide interactions on the observed erosion around the hard-soft transition was assessed. To this end, two UNIBEST simulations were done: one with only wave input, and one with both tide and wave input. All other input parameters were kept the same.

5.4.1. Results

Comparing the coastline changes with and without the tide gives the following results:

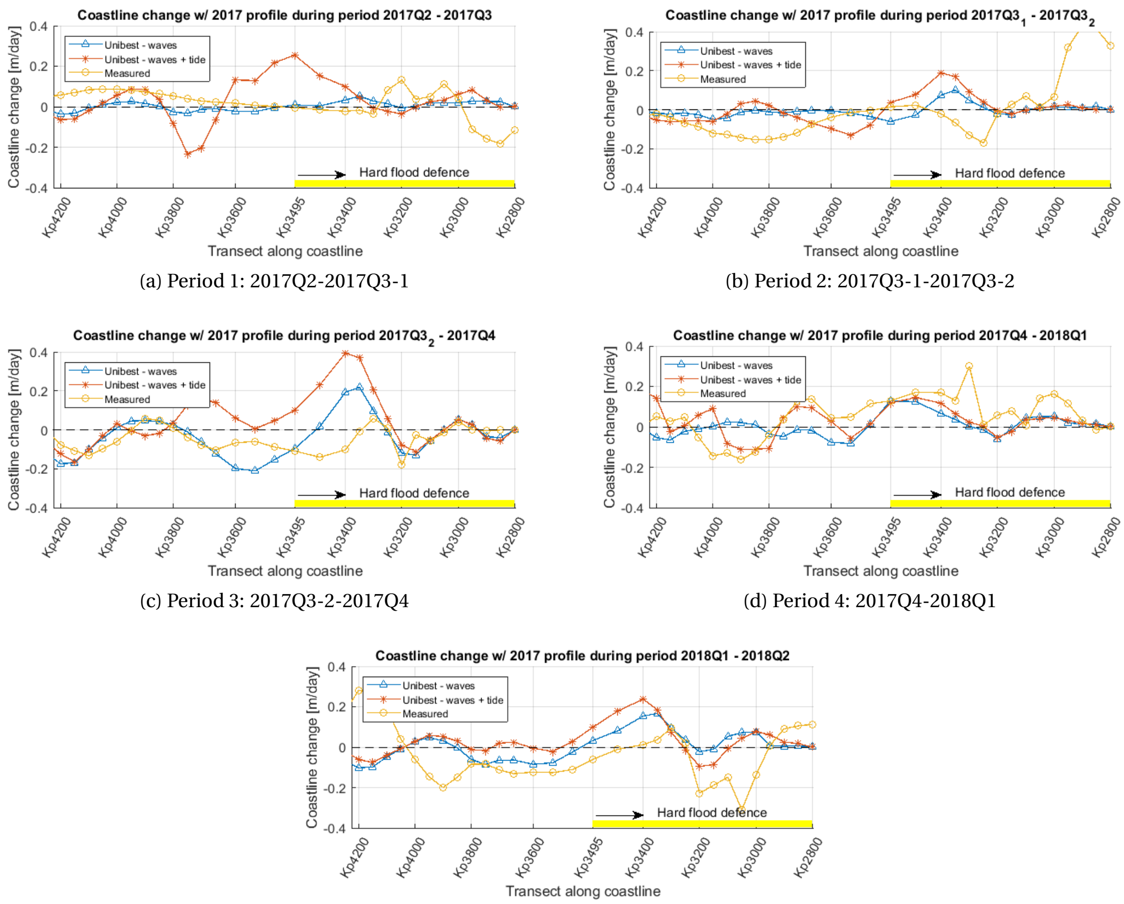

(a) Period 1: 2017Q2-2017Q3-1

(b) Period 2: 2017Q3-1-2017Q3-2

(c) Period 3: 2017Q3-2-2017Q4

(d) Period 4: 2017Q4-2018Q1

(e) Period 5: 2018Q1-2018Q2

Figure 5.21: Coastline change for different periods for only waves vs waves and tide

What is striking from these results is that for periods 1, 2, 3 and 5, the inclusion of the tide in the model does not make the results agree more with measurements. In contrast, in the period 2017Q4-2018Q1, the model results suddenly become a lot better when adding tide. This is also the period in which the largest portion of waves is coming from southwest and relatively little waves are coming from the north. This implies the following:

- During periods with predominantly western waves, the coastal system is dominated by (northward directed) longshore sediment transport in combination with tide. The combination of these two processes cause the northern transects to recover. In this period, UNIBEST can model the sediment transports by tide correctly, because sediment is available from the southern part of the soft flood defence. Therefore the tidal current is in the same direction as the tidal sediment transport.
- Earlier studies (Onderwater, 2016) claimed that wave-driven transports occurred mainly at depths > -4 m whereas tide-driven transports occurred mainly at depths < - 10 m. Moreover, it was claimed that tide-driven transports are not influenced by tide and wave-driven transports are not or barely influenced by tide-driven transports. These results show, however, that also above > -10 m depth, the tide has a significant influence on transports and associated coastline changes. This can be seen from

Figure 5.21 from period 2017Q4-2018Q1, which shows that without tide the coastline changes do not resemble the observed coastline changes, whereas when including the tide they do.

- However, when waves are coming from other (northern) directions, including the tide does not improve model results and actually makes the deviation between modelled and measured results larger. This means UNIBEST does not model the wave-tide interactions correctly for conditions with southward directed transport (period 1, 2, 3 and 5). This can be explained as follows: along the hard flood defence, the ebb-tidal current velocities are larger than the flood-tidal current velocities, resulting in a residual tidal current in southward direction. However, from earlier studies (Onderwater, 2016) it was already found that even though the **residual tidal current** is directed southward, the **residual sediment transport** by the tide is still directed northward. This is because the ebb-tidal current passes a relatively deep area in front of the breakwater where it hardly picks up any sediment, and consequently the southward tide-induced transport only starts to develop as it passes the soft flood defence. So, there is a southward directed ebb-tidal current along the hard flood defence, but it is not saturated with sediment. As was mentioned in Chapter 4 it is known that UNIBEST does not take into account this inertia in the development of sediment transport. This explains why the results deviate from the measurements.

When looking at the cross-shore distribution of longshore transport with and without tide (Figure 5.22 below), one can see that the maximum of the sediment transport occurs at a depth of -10 m (which is where the tide is imposed), and reduces towards the coastline. It can also be seen that sediment transports induced by tide and waves occur at the same locations and therefore do probably mutually influence eachother.

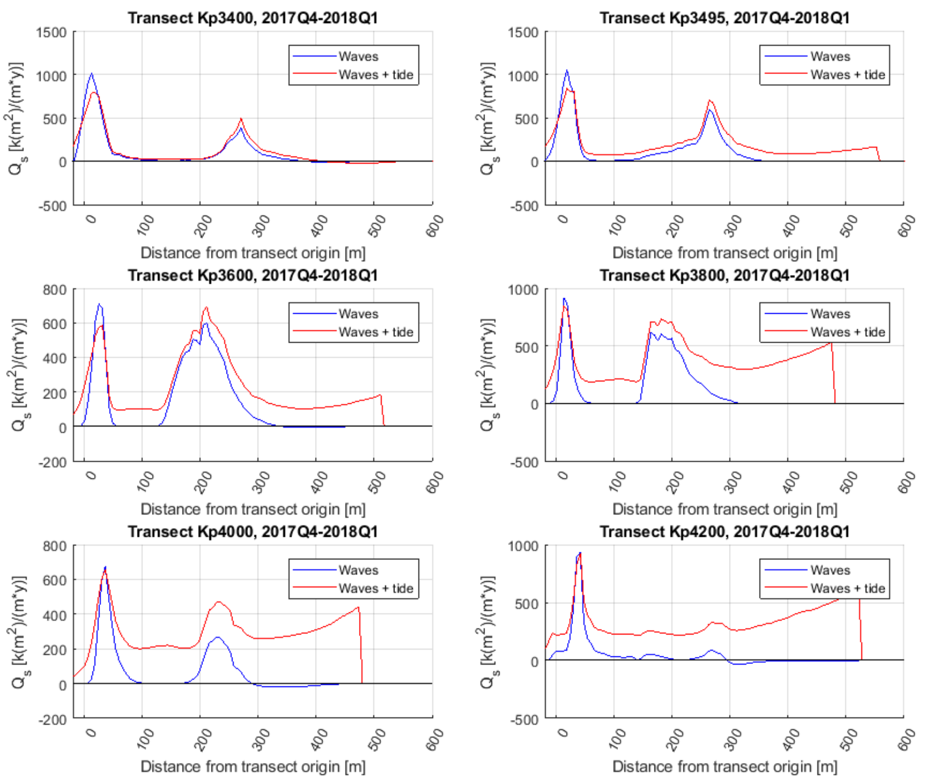

Figure 5.22: Cross-shore distribution of longshore sediment transport for the case with only waves vs the case with waves and tide.

5.4.2. Discussion of hypothesis

Tide and wave-tide interactions do not play an important role in the morphological behaviour around the hard-soft transition.

The first part of the hypothesis is refuted based on model results for UNIBEST including the tide. It has shown that also at depths smaller than 10 m, the tide has a significant effect on sediment transports, during northward direct transport. On the contrary, during periods with southward directed transport, the southward-direct ebb-tidal current may enforce the southward directed current, but does not carry any sediment. This is because the tidal current passes a deep area when travelling along the breakwater, where it picks up little sediment. Therefore, it can be concluded that the tide both stengthens the supply of sediment from south during northward transport, but also reinforces the erosion observed south of the hard-soft transition during southward transport because of the absence of sediment in this transport.

6

Discussion of research questions

In the previous chapter, the results of the model outcomes for the testing of the hypotheses were presented and briefly discussed. In this chapter, the results will be discussed in relation to the research questions.

6.1. Research question 1

"1. What is the morphological behaviour around the hard-soft transition of the Maasvlakte 2?"

1.1 Under which wave conditions and in which seasons do we observe most erosion and how often does this occur?

The highest erosion- and sedimentation rates around the hard-soft transition are caused by longshore processes, rather than cross-shore processes. Waves from north/northwest cause erosion of the hard-soft transition by increasing longshore transport gradients, whereas waves from west/ partly restore this erosion due to a negative longshore sediment transport gradient.

Predictability of the system based on wave climate
As was found in hypothesis 1, the system is strongly dominated by longshore processes during normal to yearly storm conditions. Thus, the system behaviour is strongly dependent on wave direction. As was observed, the strongest erosion at the transition occurs as a result of southward transport (caused by waves from the north), while the system can recover by supply of sediment from the south during northward transport (caused by waves from south/southwest). So, if one would know when these waves usually occur, it would be possible to predict the behaviour of the coastal system. However, the period during which these waves occur is not the same for every year, as can be seen in Figure 6.1 showing the potential sediment transport based on the CERC formulation for all years. The Figure below it, Figure 6.1, shows the position of the shoreline relative to the origin at the hard-soft transition (transect Kp3495), based on satellite imagery (Luijendijk et al., 2018). Indeed, similar patterns can be recognized between the two graphs: northward directed transport corresponding to coastline advance, and southward transport leading to coastline retreat. Figure 6.1 also shows that throughout the last five years, the net sediment transport has been in northward direction. Furthermore, the following remarks need to be made:

- As can be seen in Figure 6.1, the amount and direction of longshore transport does not show a recurring trend in each year. However, the big southwestern storms that cause large upward jumps in the sediment transport curve mainly occur from December to March, whereas the northern storms (corresponding to downward jumps in the curve) often occur in the spring season, from March to May. Yet this is not always the case, which can be seen from the year 2017, which started with a strong northern storm.
- The graph also shows the difference between subsequent years. For example, 2013 was a bad year with mostly southward transport, whereas 2015 was a relatively good year, with a lot of northward transport. Consequently, the shoreline position has also advanced during this year, even though no nourishment has taken place in this year.

- Figure 6.1 shows that the last five years there has been a net northward sediment transport. However, Figure 6.1 also shows that there has been just as much, or even more, retreat of the coastline, while one would expect a stronger coastline advance with northward transport. Apparently, southward direct sediment transport leads to more erosion than northward transport leads to sedimentation and recovery of this section. This can be addressed to the fact that with northward transport, not all sediment is accumulated at the hard-soft transition, but part of it is also transported further north. This sediment will be deposited partly seaward of the breakwater, and partly landward of the breakwater, on the cobble beach.
- This would mean that the sediment supply by northward transport cannot totally restore the sediment that is lost from the northern transects of the soft sea defence by southward storms. However, what can also be seen is that when fitting a linear curve through the variations in shoreline positions over the last five years, the shoreline has overall been quite stable including nourishments. If this trend would persevere during the coming years, this would mean that nourishing once every two years is enough to keep the coastline overall stable, be it with larger variations than desired.

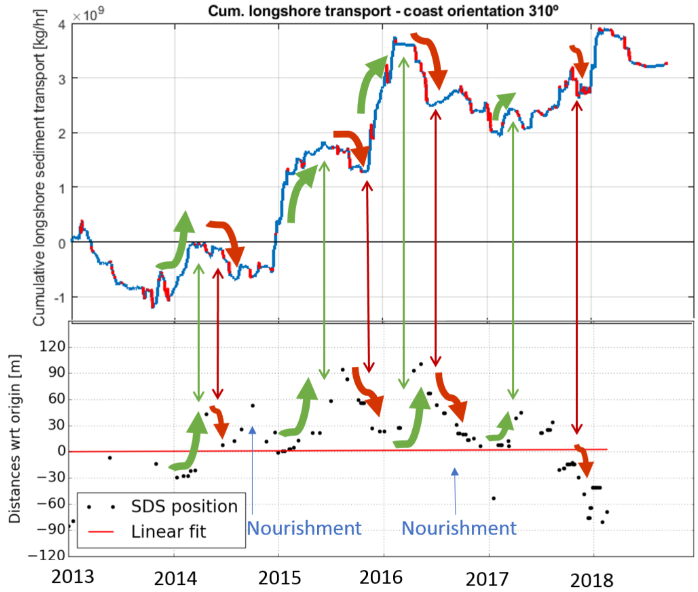

Figure 6.1: Potential longshore sediment transport for a coastline orientation of 310 °based on CERC formulation (upper graph) compared to coastline change at hard-soft transition based on ShorelineMonitor data (Luijendijk et al., 2018). The wave data used is from Europlatform. Green arrows show potential northward transport in the upper figure and accompanying coastline advance in the lower figure, whereas red arrows show potential southward transportin the upper figure and accompanying coastline retreat in the lower figure.

In order to find out whether there is a general trend in the occurrence of certain wave directions throughout the year, the magnitude and direction of the resulting energy flux (as was explained in Chapter 3) was now computed per month. The mean of all years (2013 - 2018) was computed for each month to find a trend, and the sample standard deviation was computed to quantify the amount of variation in the dataset. The sample standard deviation was computed as follows:

$$s = \sqrt{\frac{\sum_{i=1}^{N}(x_i - \overline{x})^2}{N-1}} \tag{6.1}$$

From Tables 6.1 and 6.2, the following can be concluded:

- The general trend in **magnitude** of the wave energy flux is that in the winter months November, December and January, the largest magnitudes for the wave energy flux are found. In the summer months June, July and August, the waves are less energetic. This agrees with the fact that energetic wave events often occur during the winter months, whereas calmer conditions prevail during the summer months.
- When looking at the **direction** of the wave energy flux in Table 6.2, the trend is less clear. In general, during the late winter months (December, January, February) the mean direction of the wave energy

flux is from west and west-northwest (WNW). These are conditions that induce northward sediment transport and recovery of the hard-soft transition. On the other hand, during the early spring months (March, April and May) the mean direction of the wave energy flux is from northwest (NW). These are conditions that induce southward transport and erosion of the hard-soft transition.

- The computed standard deviations in the last column show that there is quite a large deviation in the direction in the dataset. However, the month April, which contains relatively more Northern waves than other months (and which is therefore also causing the most erosion), has a relatively low standard deviation (of 15 °N). This implies that over the last five years, the most southward transport, and therefore also the most severe erosion around the hard-soft transition, occured in the month April.
- For a more reliable trend analysis, this analysis should be extended with data from more years (e.g. 1979 - present).

Table 6.1: Magnitude of total energy flux per month, computed with offshore data from Europlatform.

	2013 Magn. $m^{2.5}$	2014 Magn. $m^{2.5}$	2015 Magn. $m^{2.5}$	2016 Magn. $m^{2.5}$	2017 Magn. $m^{2.5}$	2018 Magn. $m^{2.5}$	Mean Magn. $m^{2.5}$	St. Dev.
January	6944	8921	25339	18375	14696	18776	15509	6826
February	7407	18260	4778	12135	6488	5591	9110	5173
March	7009	2759	10002	303	5951	3668	4949	3429
April	1629	3139	3696	6621	5031	3074	3865	1740
May	4113	5067	6790	6229	1924	4986	4852	1723
June	3187	2848	3440	3998	7796	554	3637	2358
July	918	4668	6389	4392	3514	260	3357	2347
August	1894	7950	2486	6273	4441	1810	4142	2544
September	8322	3238	6966	4510	9034		6414	2476
October	11851	9866	1998	5601	17204		9304	5837
November	12833	2491	25790	5671	16192		12595	9181
December	14264	21533	19850	4458	16248		15271	6691

Table 6.2: Direction of total energy flux per month, computed with offshore data from Europlatform.

	2013 Dir (°N)	2014 Dir (°N)	2015 Dir (°N)	2016 Dir (°N)	2017 Dir (°N)	2018 Dir (°N)	Mean	St. Dev.
January	248	251	256	273	322	259	268	28
February	329	234	279	251	262	312	278	37
March	22	275	280	275	250	6	305	55
April	338	327	294	328	330	316	322	15
May	307	248	242	347	340	343	305	48
June	273	344	260	322	243	328	295	42
July	278	337	278	242	265	330	288	37
August	262	265	267	247	253	266	260	8
September	303	344	313	248	263		294	39
October	269	276	350	337	284		303	37
November	300	247	259	321	308		287	32
December	270	268	235	270	291		267	20

1.2 How does the evolved coastal shape (cross-shore and longshore) influence its own morphological changes?

In cross-shore direction, the coastal profile as observed in 2017 contains less sediment on the shoreface and on the beach. Therefore, waves break higher in the profile. This has relative little effect on longshore sediment transport gradients over the entire active zone, but it does give more beach erosion. The rotated coastline over the northernmost 300 m of the hard-soft transition is a dynamic equilibrium profile which fluctuates between the rotated and straight situation. The rotated coastline is created by occurrence of north/northwestern storms that induce a coastline retreat over the northenmost transects. Under the influence of southwestern storms, this original 'straight' coastline is somewhat restored as the 'gap' created by the retreated coastline is filled up. The latter finding is clarified below.

Combining research question 1.1 and research question 1.2

By combining research question 1.1 and 1.2, it was found that the 'supply' of sediment by northward transport is deposited at different regions around the hard-soft transition, depending on different processes. This can be seen by combining the results found in Hypothesis 2 and 4:

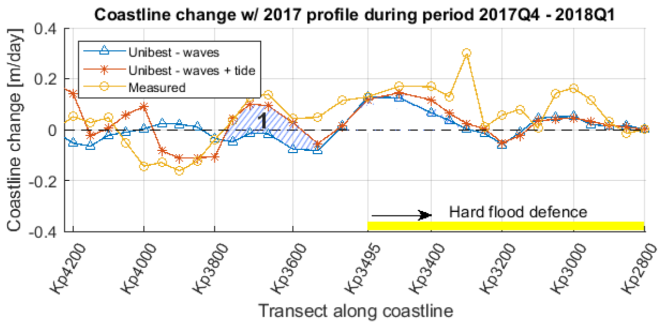

Figure 6.2: Sedimentation under influence of the tide

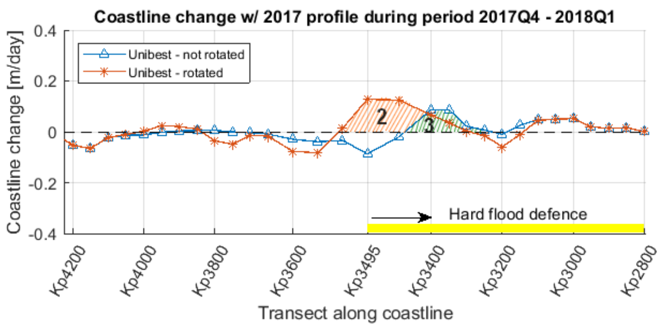

Figure 6.3: Deposition areas for rotated versus non-rotated case

Figure 6.4: Location of deposition areas in a 2D view.

The different areas of deposition, which are marked in Figure 6.4, are linked to different processes:

- 1. Under the influence of the **tide**, sediment is deposited in the area marked with '1'. This could be observed from the UNIBEST results when comparing a case with tide to a case without tide (Figure 6.2). The sediment deposition can be explained by the fact that the net northward tidal current velocities decrease between Kp3800 and Kpp3495, which allows part of the sediment to settle.
- 2. Deposition in area 2 is a result of the rotated coastline shape, leading to longshore transport gradients (see Figure 6.3). When the northernmost transects are rotated (like in Figure 6.4b), the rotated shape erodes sediment in area '1' (between Kp3600 and Kp3800), which is deposited in area '2' and partly in area '3'. The rotated coastline is thus rotated back/flattend out again.
- 3. Deposition in area '3' happens when the coastline is not rotated (see Figure 6.3): sediment transport rates decrease because the water depth increases here.
- 4. Finally, part of the supplied sediment will not settle in one of the three areas, and will be transported further north, which will probably lead to a net loss of sediment.

1.3 What is the relative contribution of wave reflection at the breakwater to the observed erosion around the hard-soft transition?

The effect of **short wave** reflection was investigated in SWAN, and the effect of **long wave** reflection was investigated in XBeach surfbeat. Concluding from the SWAN results, it was confirmed that short wave reflection indeed is very small near the hard-soft transition, because the water depth is shallow and therefore most short waves have been broken or dissipated. However, also further north, where short wave reflection was expected to be larger (and should be about 20% because this is what is imposed at the breakwater), the modelled reflection is a lot smaller in SWAN. This can have several causes related to the SWAN model, which were discussed in Chapter 5.

In XBeach, a preliminary investigation into the long wave reflections was done. The main findings were that the reflection coefficient found in earlier physical model tests is only representative for the middle section of the hard flood defence as it only includes high wave frequencies. Along the southern part of the hard soft flood defence, long waves play a larger role because of bound long wave shoaling and free long wave reflection. Therefore the earlier found reflection coefficient of 0.2 does not apply here. An initial assessment of the morphological effect of wave reflection was done by comparing a case with reflection to a case without reflection. The case without reflection was mimicked by locally increasing the friction at the breakwater in order to dissipate the reflected waves. This method showed changes in the sedimentation-erosion patterns by 10% of the original erosion- /sedimentation. The reflected long waves around the hard-soft transition affect the sedimentation-erosion patterns until quite far offshore (+/- 300 m from the breakwater/shore). For the wave condition imposed in this case, this leads to extra stirring up of sediment in front of the breakwater, which is in transported further south by the longshore transport. Generally, the results found suggest that the reflected waves stir up extra sediment in front of the breakwater, which is transported either southwards or northwards depending on the wave direction.

However, it has to be noted that the artificial damping of the reflection in this scenario is probably not a completely correct representation of the situation, because not all waves will be dissipated by the increased friction. Therefore recommendations on how the reflection should be tested according to the author are presented in Chapter 8.

1.4 Are tide and wave-tide interactions an important factor contributing to the morphological changes around the hard-soft transition?

Presence of the tide both stengthens the supply of sediment from south during northward transport, but also reinforces the erosion observed south of the hard-soft transition during southward transport. This is because of the absence of sediment in this transport. It is possible that the offshore directed tidal current at the hard-soft transition leads to a loss of sediment from the system, but this is something that could not be modelled with the used models and is therefore something that has to be looked into further.

Visualisation of the found processes influencing the morphological behaviour of Maasvlakte 2
Below, the findings from this research regarding the morphological behaviour of Maasvlakte 2 are summarized in four figures. Note that Figure 6.5a, b and c show processes that can be generally found at other hard-soft transitions as well. Figure 6.5d shows a process that is case-specific for Maasvlakte 2. For other hard-soft transitions the tide will play a role as well, but this very much depends on the prevailing tidal current patterns.

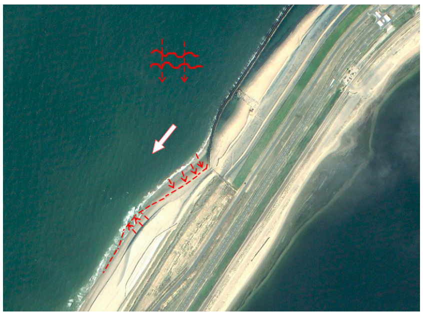

(a) Subquestion 1.1: erosion of the hard-soft transition under the influence of northwestern waves by longshore sediment transport gradients

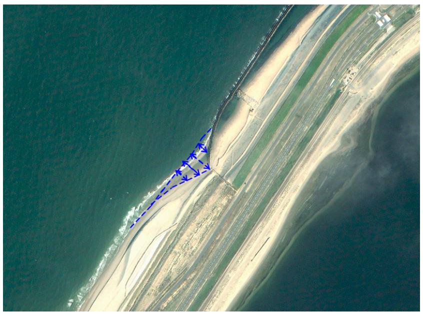

(b) Subquestion 1.2: the observed rotated coastal shape is a dynamic equilibrium profiles which is caused by the behaviour described in subquestion 1.1, and restores itself by southwestern waves.

(c) Subquestion 1.3: reflection around the hard-soft transition is caused by long waves which reaches until quite far offshore. Order of magnitude of influenced sedimentation-erosion is thought to be 10-15% of total sedimentation/erosion.

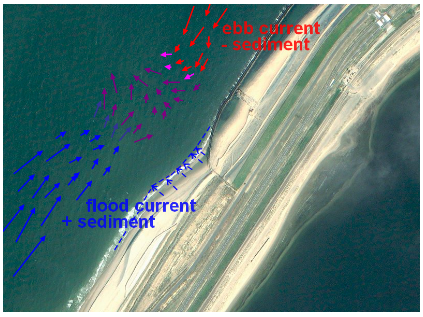

(d) Subquestion 1.4: net northward flood current along soft flood defence supplies extra sand to the hard-soft transition; net southward ebb current along hard flood defence picks up little sediment on its way and therefore contributes to the morphological behaviour little to not

Figure 6.5: Morphological behaviour of the hard-soft transition of MV2 visualised in four figures, each figure showing the found results of one subquestion.

6.2. Research question 2

"2. What is the morphological behaviour around hard-soft transitions in general?"

The morphological system behaviour of the hard-soft transition of Maasvlakte 2 is now understood for a great part. Now the question arises whether the underlying processes that define this morphological behaviour are very specific for Maasvlakte 2 or more generic for hard-soft transitions in general. If the latter is the case, the outcomes of this research can be more generally applied. The following general lessons can be taken from the outcomes of this study:

- A strong dynamic variability is usually present at the hard-soft transition, in the form of coastline retreat which gives a rotated coastline shape. This is also visible when looking at old satellite photographs of the old Hondsbossche- and Pettemer sea defence, see pictures in Appendix F. The timescale of this dynamic variability is heavily dependent on the prevailing wave climate. Also the degree of erosion and ability to recover itself naturally is dependent on the wave climate.
- Wave reflections on hard-soft transition are a complex phenomenon. The reflection of short waves will likely be larger at the deeper located part of the hard flood defence. Closer to the transition zone, where sediment from the soft flood defence is deposited, short wave reflection will be smaller, but bound long waves have more time to develop and therefore long wave reflection will play a larger role here. The reflection further depends on the wave climate (storm or swell climate, wind or long waves), on the slope and material properties (i.e. roughness) of the material and the degree of transmission through the hard flood defence. In general the largest reflection will take place for steep, smooth slopes (or even vertical walls) without wave transmission.
- In general the highest erosion will be observed in periods with oblique wave incidence where sediment is lost due to longshore sediment transport gradients. However, storm erosion in periods with more perpendicular wave incidence (typically a cross-shore sediment transport process) also indirectly contributes to this loss of sediment as it transports sediment from high in the coastal profile to lower in the coastal profile, where it can be transported by longshore transport.
- Concluding from the above statements, the morphological behaviour of a hard-soft transition is very case- and site-specific.

  In Figure 6.6, the morphological behaviour around a coastal hard-soft transition is divided into zones. In table 6.3 the processes occurring in each zone are summarised. These processes are based on the results of this research. The italic text is site-specific for MV2, whereas the regular text is generic for other hard-soft transitions. In Figure 6.6, the zones are applied to the MV2 case. However, the zones can be applied to any hard-soft transition, as can be seen in Figure 6.7 where the zones are applied to the old Hondsbossche- and Pettemer Zeewering (HPZ).

Figure 6.6: Visualisation of the morphological behaviour at the hard-soft transition of MV2

Figure 6.7: Visualisation of the general morphological behaviour of hard-soft transitions, here applied to the old Hondsbossche- and Pettemer Zeewering (HPZ).

Table 6.3: Explanation of the different zones in Figures 6.6 and 6.7

Zone	Hydrodynamic processes	Condition	Morphological response
1	*net dominant flood current (northward)*		-
	longshore sediment transports		-
2	*decelerating flood tidal currents*		sediment deposition
	negative sediment transport gradient from soft part to hard-soft transition due to increase in water depth	waves from direction of soft section	sediment deposition
	positive sediment transport gradient from hard part to soft part	waves from direction of hard section	erosion
	long wave reflection from zone 3	waves from direction of hard section	erosion/deposition
3	*dominant ebb tidal current (decelerating), unsaturated with sediment*		-
	increased reflection of long waves		erosion next to hard structure deposition offshore, *extra erosion of subtidal bar*
	reflection of short waves, depending on material properties and design of hard structure		scour hole next to hard structure
4	*dominant ebb tidal current (unsaturated with sediment)*		-
	short wave reflection		erosion next to hard structure, deposition further offshore

6.3. Research question 3

"3. How can the design and nourishment strategy of hard-soft transitions be improved?"

3.1 How can the design and nourishment strategy of the hard-soft transition of Maasvlakte 2 be optimised?

Design

First of all, it has to be noted that it is favourable that this coastal hard-soft transition is soft on the southern side and hard on the northern side. With the prevailing wave climate, this means that coastline retreat caused by erosion at the hard-soft transition can naturally restore itself to a certain extent as well. Moreover, to restrict the longshore transport gradients at the transition, the transition should be made as gradual as possible. This is the case for the design of the Maasvlakte 2 hard-soft transition. From model results it was shown that reflection is relatively small for the hard-soft transition of the Maasvlakte 2. This is because much sand has accumulated in front of the transition, but also because there is transmission of waves through the breakwater, thus decreasing the reflection coefficient. This is therefore also a well-chosen design aspect of the hard sea defence, reducing the negative effects of reflection that would be the case for a fully closed hard sea defence. Nevertheless, for future projects, some optimisations can be applied to improve the design of the hard-soft transition. This is discussed in research question 3.2.

Surveying and nourishment

The current approach for surveying and nourishing entails that a survey is done each year in Q2 (end of March/ beginning of April). Every two years, the soft flood defence is nourished, based on the required volume that follows from the Q2 survey. The nourishment operation is usually carried out in Q3, after the summer. When looking at research question 1.1 , this is a well-chosen timing: according to the trend that was observed, often waves from western directions occur in the period following after the nourishment operation, transporting the sand from southern transects further north and thereby feeding the hard-soft transition.

However, the moment of surveying is debatable. The surveys are carried out in Q2, but this is also the period with a lot of waves from northern directions, inducing southward transport and corresponding erosion. This means that if the required nourishment volumes for Q3 are based on surveys from Q2, it is very well possible that in between Q2 and Q3 the shore has significantly eroded further. Therefore the calculated nourishment volumes based on the Q2 will likely be insufficient by the time the nourishment is carried out. It is thus recommended to conduct the survey in Q3, at the end of the summer, and carry out the nourishment operations shortly after.

Moreover, the last five years the location of the nourishments (beach, shoreface or offshore) were based on the observed volumes and required volumes within these layers (beach, shoreface or offshore). For example, the last two years especially the beach eroded significantly, so this is where the next nourishment will take place. However, it is argued whether this is the best approach. As was found in literature (Roelvink and Reniers, 2009), shoreface nourishments provide beachface stability by protecting the beach from severe wave attack during storms. Beach nourishments, on the other hand, immediately disburden the beach, but are prone to severe beach erosion during storms. From the results presented in section 5.2 it could also be seen that with the 2017 profile, which contained less sediment on the shoreface as compared to the 2013 profile, the beach was clearly more vulnerable to wave attack because less waves are dissipated on the shoreface. Therefore, even though the beach might show a sediment deficit, it could be more effective to (also) nourish on the shoreface, instead of just on the beach itself.

3.2 What recommendations can be done for other hard-soft transitions?

In this study the most important factors influencing the morphological changes around the hard-soft transition of Maasvlakte 2 have been unravelled. Ideally, this would lead to a standard design guideline for future designs of hard-soft transitions, such that undesired effects and excessive maintenance can be prevented. However, it has again been confirmed that the morphological behaviour of a hard-soft transition is strongly influenced by external factors such as waves, wind and tide. Therefore the best way to start making a design of a hard-soft transition is by making an analysis of the wave climate and based on that determine how the transition will be designed. This is actually no different from any other coastal protection project, as the appropriate solution of a coastal erosion problem always starts with a clear understanding of the coastal processes that cause the problem. It is advised to look at least at these aspects:

- Wave climate analysis: year-round climate, wave energy flux per year and per month and expected potential sediment transports (e.g. based on a longshore transport formula such as CERC or Kamphuis)

- When it follows from this wave climate analysis that there is a large wave component coming from the direction of the hard flood defence (Figure 6.8a), it has to be taken into account that severe erosion at the hard-soft transition is expected, which will not naturally restore itself. In that case it is debatable whether it is even wise to make the transition at this location without too frequent maintenance. Other options can then be explored as well, such as extending the hard structure and making the transition at a more suitable location with more favourable wave conditions. Or, if the hard structure can be replaced by a soft solution, it can be wise to do this (just as was done for the HPZ). In this way the coast will again form one integral coastal system and negative effects of hard-transition will be prevented.

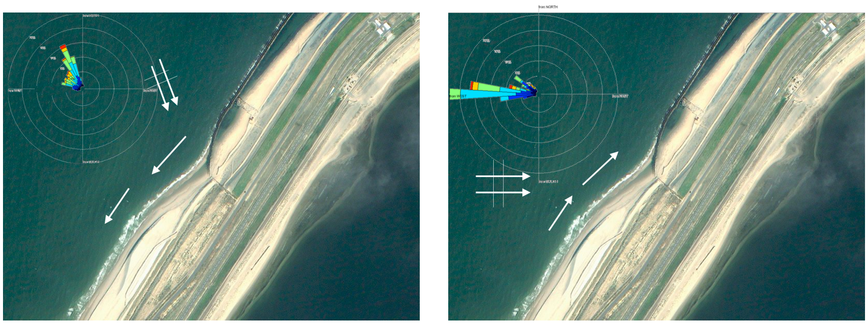

(a) Unfavourable wave climate (b) Favourable wave climate.

Figure 6.8: Examples of an unfavourable (a) vs favourable (b) wave climate. The wave roses presented are hypothetical wave climates.

When the consequences of a hard-soft transition seem acceptable or when it is unavoidable to make the transition structure, the following general recommendations are given:

- Take into account the dynamic variability of the hard-soft transition from the beginning. This can be done in terms of design (see design examples below), safety assessments or maintenance.

- If the area in which the project is situated has a more predictable wave climate (e.g. monsoon-type of forcing) , the nourishment scheme can be adjusted to this.

- In some areas, (frequent) nourishments may not be allowed if the area is located in a zone with a rich nearshore ecological value. If nourishment operations are restriced or even completely forbidden, a solution has to be found which is maintenance-free.

- Make the transition as gradual as possible and if possible, make sure the hard structure is designed such that wave reflection is small.

Furthermore, the following design ideas are suggested to reduce the frequency of nourishments:

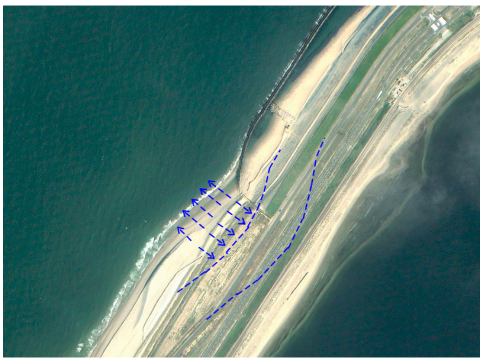

Figure 6.9: Visualisation of a solution which allows more dynamic variability

1. More room for dynamic variability around the hard-soft transition (soft solution) Since the hard-soft transition is a transition from one coastal system to another, it will always be a dynamic system. As we have seen in the data analysis (Chapter 3) this section shows more variability than the rest of the soft sea defence, and as we saw in Chapter 5 this can be addressed mainly to large longshore transport gradients, depending on the wave direction. Therefore, the system not only varies on a seasonal scale, but on a smaller time scale. As was shown in Chapter 5 , the dynamic variability does not only imply extra erosion, but also frequent periods of sedimentation by sediment supply from southwestern waves. So another approach could be to accept the fact that this section will be more dynamic than the rest of the system and give the system more room for this variability. This can be done by making the beach wider in landward direction, for example over a distance of 400 m over the northernmost part of the soft sea defence. In this way the required volume in the system can still be satisfied. For the case of the MV2, this is not a very attractive solution because the dune row, as well as the road behind it would have to be moved in landward direction. But for future designs, this extra room for dynamic variability could be implemented already in the design. However, this will only work if the hard-soft transition is favourably positioned regarding the wave climate, so that the system will also partly recover itself after periods of erosion.

2. Mega nourishment upstream of soft flood defence (soft solution) This solution can be applied if there is a natural longshore transport from upstream of the soft flood defence to the hard-soft transition (just as is the case for MV2) and accumulation of sand in front of the hard flood defence is not a problem. If the wave climate is such that frequent restoration of the retreated hard-soft transition is ensured by waves coming from the direction of the soft flood defence, but regular nourishments are required to ensure enough sediment availability in this transport, the nourishment lifetime could possibly be increased by creating a mega nourishment. The mega nourishment could be located at some distance from the hard-soft transution (see Figure 6.10), and will supply the hard-soft transition with sand for a longer period of time. For the case of MV2 this could possibly harm the navigation channel towards MV2, so it is safer to keep nourishing every two years.

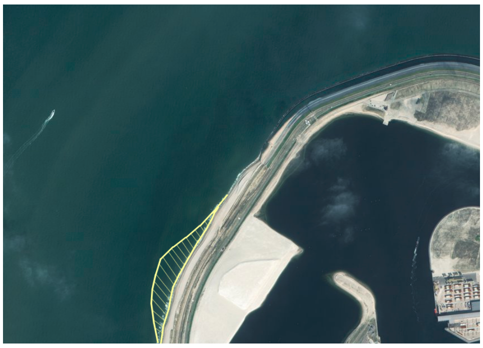

Figure 6.10: Visualisation of a mega nourishment created upstream of hard-soft transition to decrease nourishment frequency.

3. Hidden revetment (hard solution)
This solution can be applied at the beginning of the design stage, if one wants to be sure that safety of the dune is always ensured. For Maasvlakte 2, the underlying reason why a minimum volume of sand has to be contained within each layer and transect, is that the dune has to be protected. In order to still secure protection of the dune, even with a smaller volume of sand, a 'hidden sea defence' can be constructed in the dune, over, for example, the length of the transition zone (e.g. 400 m). Also for MV2 this idea has been suggested in earlier studies (Onderwater, 2016). However, it was reasoned that these hard structures could, next to a positive influence on the actual morphological system, also (negatively) influence the morphological system during design conditions. Therefore this design optimization has not been implemented for the MV2.

However, for future designs of hard-soft transitions this could be an attractive option if it is already implemented in earlier stages of the design process. That way verification of the design requirements can be taken into account from the very start. The stability of the dune flood defence is always secured, regardless of the volume of sand in front of it. When a design storm of 1/10 000 occurs and the hidden sea defence becomes exposed to waves, the hard structure might indeed cause negative side effects further downstream. It then becomes another hard-soft transition, so in fact the problem of the hard-soft transition is shifted downstream. Having said that, the chance that this 1/10 000 storm occurs is very small so probably the hidden sea defence will never be exposed, and if it does, the system can recover by southwestern waves, or a nourishment can be done. With his solution, the negative side effects of hard structures have to be taken into account, such as toe erosion. This solution can actually be found in many dune systems already, and is also applied at the hard-soft transition of Wangerooge, Germany (Figure 6.11).

(a) Situation with narrow beach

(b) Situation with widebeach

Figure 6.11: Photograph of a similar solution applied at the hard-soft transition at Wangerooge, Germany.

7 Conclusions

The coastal hard-soft transition of the Maasvlakte 2, which was completed in 2013, experienced highly variable and unpredictable erosion rates for which the current nourishment scheme proved to be insufficient. Therefore, an extensive data- and model study was conducted in order to unravel the most important factors contributing to the morphological behaviour of the system and their relative effect. The final aim was to be able to make recommendations for design and maintenance of this and potential other coastal hard-soft transitions, making use of the knowledge gained in this research.

Morphological behaviour of the hard-soft transition of Maasvlakte 2
The role of the following factors in the morphological behaviour of the hard-soft transition was investigated:

- Influence of longshore transport gradients by different wave directions
- Influence of the evolved coastal shape (bar and trough; rotated coastline over northernmost 300 m of soft flood defence
- Influence of wave reflection on the breakwater
- Influence of tide

For the case of Maasvlakte 2, it was found that the most severe erosion at the hard-soft transition is found during periods with strong longshore transports, which causes longshore transport gradients at the transition. Cross-shore processes such as storm erosion also indirectly contribute to this as it transport sediment from higher in the profile to lower in the profile, but at that time the sediment is not lost yet. This longshore sediment transport-induced erosion is found under the influence of north/northwestern waves because sediment transport rates increase quickly over the northernmost part of the soft flood defence, leading to erosion. On the other hand, southwestern waves can partly restore the retreated coastline because in that case the northward directed longshore transport rates decrease and lead to accumulation of sediment.

Regarding the influence of wave reflection, only some preliminary results were found. This was because the models at hand did not seem to capture the hydrodynamic processes related to wave reflection well. Using SWAN and UNIBEST, it was shown that as expected, short wave reflection mainly plays a role at the deeper located parts of the breakwater, and less near the hard-soft transition where water depths are shallower. However, the wave reflection in SWAN was very low compared to expectations and therefore probably underestimated the wave reflection. Using XBeach, some observations were done. Firstly, it was found that the reflection coefficient that was measured in earlier physical model tests (≈ 0.2) is only representative for a middle section of the breakwater, because this coefficient does not include long waves. Along the southern part of the hard soft flood defence, long waves play a larger role because of bound long wave shoaling and free long wave reflection (this was also confirmed by XBeach results). Therefore the earlier found reflection coefficient of 0.2 does not apply here. An initial assessment of the morphological effect of wave reflection was done by comparing a case with reflection to a case without reflection. This method showed changes in the sedimentation-erosion patterns by 10% of the original erosion- /sedimentation. The results found suggest that the reflected waves stir up extra sediment in front of the breakwater, which is transported either southwards or northwards depending on the wave direction. However, it has to be noted that the method for comparing the two scenarios is probably not a completely correct representation of the situation. Therefore it is recommended to further look into this with a more correct comparison of the two scenarios (with and without reflection).

As regards to the role of the tide, it was found that the dominant northward directed flood tidal current along the soft flood defence strengthens the supply of sediment from south during northward transport. On the other hand, the dominant southward directed ebb current along the hard flood defence hardly picks up any sediment and therefore it does not contribute to the morphological changes at the hard-soft transition.

Morphological behaviour of hard-soft transitions in general
The morphological behaviour of a hard-soft transition is very case- and site-specific. However, some observations in the morphological behaviour of Maasvlakte 2 are more generic and will therefore also be found at other hard-soft transitions:

- A strong dynamic variability is usually present at the hard-soft transition, in the form of coastline retreat which gives a rotated coastline shape. The timescale of this dynamic variability, and the degree of erosion and ability to recover itself are dependent on the prevailing wave climate. However, even though some hard-soft transitions can partly recover from the observed erosion, generally a structural erosion trend will be found at the hard-soft transition. Therefore nourishments are required.
- Wave reflections on hard-soft transitions are a complex phenomenon. The reflection of short waves will likely be larger at the deeper located part of the hard flood defence. Closer to the transition zone, where sediment from the soft flood defence is deposited, short wave reflection will be smaller, but bound long wave reflection will be larger. The reflection further depends on the wave climate, on the slope and roughness of the material and the degree of transmission through the hard flood defence.
- In general the highest erosion will be observed in periods with oblique wave incidence where sediment is lost due to longshore sediment transport gradients. However, storm erosion in periods with more perpendicular wave incidence (a cross-shore sediment transport process) also indirectly contributes to this loss of sediment.

Practical implications for maintenance of Maasvlakte 2
For Maasvlakte 2, the main recommendation is to base the required nourishment volumes that are executed in Q3 on Q3 surveys instead of Q2 surveys. This is because it was found that the period Q2-Q3 often includes many northwestern waves which will cause erosion of the hard-soft transition. Therefore the volumes based on the Q2 surveys will not be sufficient by the time the nourishment is carried out.

Practical implications for design and maintenance of hard-soft transitions in general
This study has again confirmed that the morphological behaviour of a hard-soft transition is strongly influenced by external factors such as waves, wind and tide. Therefore the best way to start making a design of a hard-soft transition is by making an analysis of the wave climate and based on that determine how the transition will be designed. It is advised to make a wave climate analysis including the year-round climate, wave energy flux per year and per month, and the expected potential sediment transports. Furthermore the following design aspects are always advised to decrease the erosion at the hard-soft transition:

- Take into account the dynamic variability of the hard-soft transition from the beginning. This can be done in terms of design (see design examples below), in terms of safety assessments or in terms of maintenance.
- Make the transition as gradual as possible.
- If possible, make sure the hard structure is designed such that wave reflection is small.

Depending on the desired situation and the wave climate, the following design optimisations are given for the soft part of the transition zone to decrease the nourishment frequency:

- More room for dynamic variability around the hard-soft transition ('managed retreat') by widening the beach in landward direction and allowing the coast to retreat more until the next nourishment.
- Mega nourishment upstream of soft flood defence, if there is natural longshore transport from upstream of the soft flood defence to the hard-soft transition.
- A hidden revetment over the transition length (e.g. 400 or 500 m) of the soft flood defence to secure protection of the dune even with a smaller volume of sand in front of it

8 Recommendations

This chapter discusses the recommendations following from the research. These recommendations are only related to further research; the design and nourishment recommendations can be found in Chapter 6 as they are embedded into the research questions.

- An important recommendation that follows from this research is related to modelling the wave reflection in the XBeach model. This is because the answers found in this research come with certain uncertainties, and another modelling approach is recommended to acquire more conclusive results.
  - The preliminary investigation has shown that around the hard-soft transition long wave reflection is large, and long waves make up 10-15% of the total wave height. Therefore the earlier found reflection coefficient of 0.2 that is representative for a cross-section along the middle part of the hard flood defence is not representative for the southern part. Further research is therefore needed to find the total reflection coefficient at a southern section of the hard flood defence.
  - The method with which the morphological effects of wave reflection has now been assessed (in XBeach) gives an initial impression of the sedimentation-erosion patterns under the influence of **long wave reflection** for certain wave conditions. However, this method will not eliminate all wave reflection and therefore a more suitable method should be chosen to compare the scenarios with and without reflection more correctly. Therefore the following method is recommended:
  - In order to entirely eliminate all reflection along the breakwater, an absorbing boundary should be imposed at the breakwater. This can be done by adjusting the XBeach source code. Considering the time and resources available within this research, this was not done and it was chosen to make an initial assessment using a workaround method.
  - It is recommended to make a local model with a finer grid (compared to the current model which has a minimum grid cell size of 10 by 10 m) for more accurate results. The boundary conditions can be obtained from the larger, coarser current model.
  - To include the effect of short wave reflection as well, XBeach should be run in nonhydrostatic mode. In the current model, running the nonhydrostatic mode gave large errors at the model boundaries which could not be fixed in the time available. Therefore it was chosen to use the surfbeat mode, which did produce the wave boundaries correctly. In order to make the nonhydrostatic model work to test this hypothesis, the errors at the boundary should be fixed first. It is not sure if this is possible with XBeach, since a possible cause is the fact that XBeach only has one layer in the vertical. If this is indeed the cause for the problem, a different model should be used which has more layers in the vertical (e.g. SWASH). However, this model does not have a morphological module, so a different model has to be used (or built in Matlab) to look into the morphological effects.
  - Moreover, different wave conditions should be tested to see under which conditions wave reflection is highest (presumably low wave conditions with low water levels), and to see if indeed the stirred up sediment is transported either south or north by different wave directions.

  - Furthermore, for a better representation the tide can be included in the XBeach model as well, as it is currently not included.

- The reflected short waves modelled in SWAN were significantly lower than was expected with the reflection coefficient of 0.2 imposed at the breakwater. Several causes for this were discussed in Chapter 5, and the following measures could be taken to improve the model and to check if this gives more realistic results:
  - To inspect the hydrodynamic processes in greater detail at the breakwater, the grid cell size could locally be reduced a bit further. However, as was described in Section 4.2.2, a limitation of the SWAN model is that it becomes unstable when the resolution is too fine. Therefore this has to be done with caution.
  - Possibly the amount of points used to define the obstacle was still too large and the results can be improved by reducing the amount of points.
  - An obstacle in SWAN might work better with a curvilinear grid, so this could be investigated.

- The role of the tide on the longshore sediment transports was investigated (using UNIBEST), but there are several other aspects that should still be looked into. For example, an offshore-drected tidal current is found at the hard-soft transition, where the dominant flood current from the soft flood defence and the dominant ebb current from the hard flood defence meet (Onderwater, 2016). Since this is not something that can be modelled in UNIBEST it has not been investigated if this has any (negative) effects on the morphological behaviour. For example, this offshore-directed tidal current could also be one of the reasons for a loss of sediment at the hard-soft transition.

- Furthermore, further research could be done to whether there is a difference in the longshore sediment transports and associated coastline changes (as presented in Figure 6.1) between storm conditions or normal conditions. The results show that also longer, calmer periods of waves from one direction cause these longshore transports, but the morphological system is likely to behave different in the case of a storm. During a storm, generally high water levels are observed, so that the active profile height of the profile is larger. Moreover, with very high water levels, the waves also enter the area behind the breakwater, and therefore the cobble beach (including the sand that is transported here) will likely also take part in the sediment transports.

- Moreover, this research has shown the morpodynamic behaviour of the hard-soft transition in a qualitative manner. However, it would be interesting to investigate in more detail which processes cause the net loss in sediment that is observed. This could be due to offshore directed tidal currents at the transition, due to transport of sand in front of the breakwater eventually ending up in the navigation channel, or due to the transport of sand into (and out of) the cobble beach behind the breakwater. This sand can partly also be transported back during northwestern storms if water levels are high enough so that waves also reach the cobble beach and can transport the sand back. The latter subject is currently being investigated by a fellow student and together with this research will form a more complete picture of the sediment budgets around the hard-soft transition.

- Next to the subject above (processes behind the sand transport into and out of the cobble beach behind the breakwater), some other areas and processes around the hard and soft flood defence of Maasvlakte 2, are of interest for research. These were not included in the scope of this research, as it was focused on the morphological behaviour of the soft part. The following subjects are currently being investigated as well: 1) the processes behind the sand transport into the cobble beach of the hard flood defence, 2) the longshore transport behaviour of the dynamic rock slope of the cobble beach and 3) the effect of the sand transport on the stability of the hard flood defence.

- Regarding research of hard-soft transitions in general the following recommendations are made:
  - For a more general research of hard-soft transitions, a database could be set up of different hard-soft transitions on sandy shorelines, and the observations could be compared to find similarities and differences. This, however, requires site-specific data (bathymetry data based on surveys, and tidal data) which is often hard to acquire for countries outisde the Netherlands or when it concerns a specific project.
  - The effectiveness of the design solutions that are proposed in this study can be tested using numerical models.

Bibliography

Battjes, J., Bakkenes, H., Jansen, T., and van Dongeren, A. (2004). Shoaling of subharmonic gravity waves. *Journal of Geophysical Research*, 109.

Battjes, J., Isaacson, M., and Quick, M. (1994). Shallow water wave modelling. *Proceedings of Waves-Physical and Numerical Modelling*, pages 1–24.

Bijker, E. (1971). Longshore transport computation. *J. Waterway. Harbour. Coast. Eng. Div.*, 97:687–701.

Bijker, E. (1976). *Some considerations about scales for coastal models with movable bed.* Phd thesis, TU Delft.

Boers, M. (2012). Technisch rapport duinwaterkeringen en hybride keringen. Technical report, Deltares.

Booij, N., Ris, R., and Holthuijsen, L. (1999). A third-generation wave model for coastal regions: 1. model description and validation. *Journal of Geophysical Research - Oceans*, 104:7649–7666.

Bosboom, J. and Stive, M. J. F. (2015). *Coastal Dynamics I - Lecture Notes CIE4305.* Delft Academic Press.

Boshek, M. (2009). Reflection and diffraction around breakwaters.

Bruun, P. (1954). Coastal erosion and the development of beach profiles. beach erosion board, u.s. army corps of engineers. *Technical Memo*, 44.

Caccioppoli, B. (2013). Riding the waves of change: A revised beach cycle for mixed sand and gravel beaches. Retrieved from https://oceanbites.org/riding-the-waves-of-change-a-revised-beach-cycle-for-mixed-sand-and-gravel-beaches/.

Dean, R. G. (1977). Equilibrium beach profiles: U.s. atlantic and gulf coast. *Ocean Engineering report*, 12.

Dean, R. G. (1990a). Coastal sediment processes, toward engineering solutions. *Proceedings of Speciality Conference on Coastal Sediments*, ASCE:New York.

Dean, R. G. (1990b). Equilibrium beach profiles: Characteristics and applications. *Journal of Coastal Research*, 7:53–84.

Deltares (2018). Technical specifications unibest-cl+. Retrieved from https://www.deltares.nl/en/software/unibest-cl/#technical-specifications.

den Bieman, J. (2016). Hydraulische belastingen 2017 voor duinwaterkeringen. Technical report, Deltares.

Folley, M. (2016). *Numerical Modelling of Wave Energy Converters*, chapter 11, pages 217–225. AP Academi Press.

Guza, R., Thornton, E., and Holman, R. (1984). Swash on steep and shallow beaches. *Coastal Engineering Proceedings*, 1.19:708–723.

Hillen, R. and Roelse, P. (1994). Dynamic preservation of the coastline in the netherlands. *Journal of Coastal Conservation*, 1(1):17–28.

Hofland, B. and van Gent, M. (2010). Maasvlakte 2: Harde zeewering, stenig duin + blokkendam. meetrapport van aanvullend 2d schaalmodelonderzoek scheldegoot proevenseries 1 t/m 10. Technical report, Deltares.

Institute, W. H. O. (2001). Beach and dune profiles: An educational tool for observing and comparing dynamic coastal environments. Retrieved from https://web.whoi.edu/seagrant/wp-content/uploads/sites/24/2015/01/WHOI-G-01-001-Sea-Grant-Beach-and-Dune-Pr.pdf.

Kamphuis, J. (1991). Alongshore sediment transport rate. *Journal of Waterway, Port, Coastal and Ocean Engineering*, 117 (6):624–641.

Komar, P. and Inman, D. (1970). Longshore sand transport on beaches. *Journal of Geophysical Research*, 75(30):5914–5927.

Kroon, A., Hoekstra, P., Houwman, K., and Ruessink, G. (1994). Morphological monitoring of a shoreface nourishment, nourtec experiment at terschelling, the netherlands. *Proceedings of ICCE 1994*.

Lodder, Q. and Sorensen, P. (2015). Comparing the morphological behaviour of 585 dutch-danish shoreface nourishments. *Coastal Management: Changing coast, changing climate, changing minds*.

Longuet-Higgins, M. and Stewart, R. (1962). Radiation stresses and mass transport in gravity waves, with application to 'surf beats'. *Journal of Fluid Mechanics*, 13.

Luijendijk, A., Hagenaars, G., Ranasinghe, R., Baart, F., Donchyts, G., and Aarninkhof, S. (2018). The state of the world's beaches. *Scientific Reports*, 8:Article number: 6641.

Mansard, E. and Funke, E. (1980). The measurement of incident and reflected spectra using a least squares method. *17th International Conference on Coastal Engineering*.

Onderwater, M. (2016). Optimalisatie van beheer en onderhoud rondom noordelijke beëiniding van zachte zeewering van maasvlakte 2. Technical report, Arcadis.

Onderwater, M. (2018a). Maasvlakte 2, noordelijke deel van zz en conus - uitwerking werkelijke standzekerheid t.b.v. aanpassing keuringsmethodiek. Technical report, Arcadis.

Onderwater, M. (2018b). Memo - effect van meer zand in het duin bij kp3.495 op de standzekerheid en onderhoudsfrequentie. Technical report, Arcadis.

Onderwater, M. and van der Baan, J. (2017). Memo - standzekerheid rondom overgang hz-zz, berekend met xbeach (2dh). Technical report, Arcadis.

Plant, N., Holman, R., Freilich, M., and Birkemeier, W. (1999). A simplemodel for interannual sandbar behavior. *Journal of Geophysical Research: Oceans*, 104:15755– 15776.

PUMA (2013). Beheer- en instandhouding buitencontour in de instelperiode. Technical report, PUMA.

Radermacher, M., de Schipper, M., Price, T., Huisman, B., Aarninkhof, S., and A.J.H.M., R. (2018). Behaviour of subtidal sandbars in response to nourishments. *Geomorphology*, 313:1–12.

Reniers, A., van Dongeren, A., Battjes, J., and Thornton, E. (2002). Linear modeling of infragravity waves during delilah. *Journal of Geophysical Research: Oceans*, 107.

Rijkswaterstaat (2017). Kustlijnkaarten 2018. Retrieved from http://publicaties.minienm.nl/documenten/kustlijnkaarten-seriebeschrijving.

Roelvink, D. and Reniers, A. (2009). A guide to modeling coastal morphology. *Advances in Coastal and Ocean Engineering*, 12:1133–1152.

Roelvink, D., Reniers, A., van Dongeren, A., van Thiel de Vries, J.and McCall, R., and Lescinski, J. (2009). Modelling storm impacts on beaches, dunes and barrier islands. *Elsevier Journal of Coastal Engineering*, 56:1133–1152.

Roelvink, D., van Dongeren, A., McCall, R., Hoonhout, B., van Rooijen, A., van Geer, P., de Vet, L., Nederhoff, K., and Quataert, E. (2015). *XBeach Technical Reference: Kingsday Release*.

Ruessink, B. and Kroon, A. (1994). The behaviour of a multiple bar system in the 635 nearshore zone of terschelling, the netherlands: 1965-1993. *Marine Geology*, 121:187–197.

Ruessink, B., Wijnberg, K., Holman, R., Kuriyama, Y., and van Enckevort, I. (2003). Intersite comparison of interannual nearshore bar behavior. *Journal of Geophysical Research: Oceans*, 108.

Shand, R. and Bailey, D. (1999). A review of net offshore bar migration with photographic illustrations from wanganui, new zealand. *Journal of Coastal Research*, 15:365–378.

Steetzel, H. (1995). Toetsing aansluitingsconstructies - advies formulering toetsingsregels voor de vormgeving van de aansluiting tussen de verschillende waterkeringsconstructies. Technical report, Waterloopkung Laboratorium.

Tatui, F., Vespremeanu-Stroe, A., and Ruessink, G. (2016). Alongshore variability of cross-shore bar behavior on a nontidal beach. *Earth Surface Processes and Landforms*, 41:2085 – 2097.

van de Graaff, J. (1984). Leidraad voor de beoordeling van de veiligheid van duinen als waterkering. Technical report, Rijkswaterstaat.

van Dongeren, A., Battjes, J., Janssen, T., van Noorloos, J., Steenhauer, K., Steenbergen, K., and Reniers, A. (2007). Shoaling and shoreline dissipation of low-frequency waves. *Journal of Geophysical Research*, 112.

van Duin, M., Wiersma, N., Walstra, D., van Rijn, L., and Stive, M. (2004). Nourishing the shoreface: observations and hindcasting of the egmond case, the netherlands. *Coastal Engineering*, 51:813 – 837.

van Gent, M. R. A. and van der Werf, I. (2010). Maasvlakte 2, harde zeewering, stenig duin + blokkendam. meetrapport van aanvullend 2d schaalmodelonderzoek deltagoot proevenseries 13 t/m 15. Technical report, Deltares.

van Santen, R., Steetzel, H., van Thiel de Vries, J., and van Dongeren A. (2012). Modelling storm impact on complex coastlines - westkapelle, the netherlands. *ICCE 2012: Proceedings of the 33rd International Conference on Coastal Engineering*.

van Verkeer en Waterstaat, M. (2007). Voorschrift toetsen op veiligheid primaire waterkeringen. Technical report, Ministerie van Verkeer en Waterstaat.

Vellinga, P. (1986). *Beach and dune erosion during storm surges*. Phd thesis, TU Delft.

Vijverberg, T. (2018). Samenvatting keuringen en ervaringen instelperiode: Volume morfologische schillen. Technical report, PUMA.

Walstra, D., Wesselman, D., van der Deijl, E., and Ruessink, B. (2016). On the intersite variability in inter-annual nearshore sandbar cycles. *Journal of Marine Science and Engineering*.

A

Research design

A.1. Choice of models

Empirical vs process-based models

First of all, a distinction is made between (semi-)empirical versus process-based models. Empirical models are based on observed associations between variables (empirical formulas). They are often based on equilibrium relationships and therefore require that an equilibrium state exists or is forced. Process-based models, on the other hand, are based on physical processes. Semi-empirical models are based on a combination of observed associations between variables and physical processes. Empirical models are well suitable for situations that are similar to the situations with which they have been fitted, whereas process-based models are more universally applicable, as physics do not change for different situations (H. Rijper, 2018). An example of a semi-empirical model is Unibest-CL+, and Xbeach is an example of a process-based model. Duros+ and D++ are based on empirical formulas and are therefore empirical models.

Coastal profile, coastline and area models

Traditionally, coastal morphology models were divided into three types of models (Roelvink and Reniers, 2009):

- Coastal profile models: focused on the cross-shore profile, and neglecting the longshore variations
- Coastline models: focused on the longshore transports, and assuming that the cross-shore profile retains its shape, even during coastline retreat or advance
- Coastal area models: which combines the above two models, and variations in both directions are resolved. This can be either a 2DH model (solving depth-averaged equations) or a 3D model (where variations in the vertical are resolved as well).

An overview of the different model types, the directions that are solved, their dimension and a few examples of models is given in table A.1 below.

Table A.1: Overview of model types. From: Roelvink and Reniers, 2009

Model type	Direction	Dimension	Example
Coastal profile	cross-shore	1D	Duros+, D++, DurosTA
Coastline	longshore	1D	Unibest-LT/CL, GENESIS, LITPACK, BEACHPLAN
Coastal area	cross-shore and longshore	2DH or 3D	Xbeach, Delft3D, MIKE21, TELEMAC ADCIRC, ROMS-SED, FINEL

The choice of the model was made with the help of a decision tree which can be found in Figure A.2 (Roelvink and Reniers, 2009). First, it has to be decided whether the focus will be on the cross-shore profile development or on the longshore transport and coastline changes. Next, the spatial and temporal scale can be determined based on Figure A.1 and a suitable model can be selected by using the decision tree in Figure A.2.

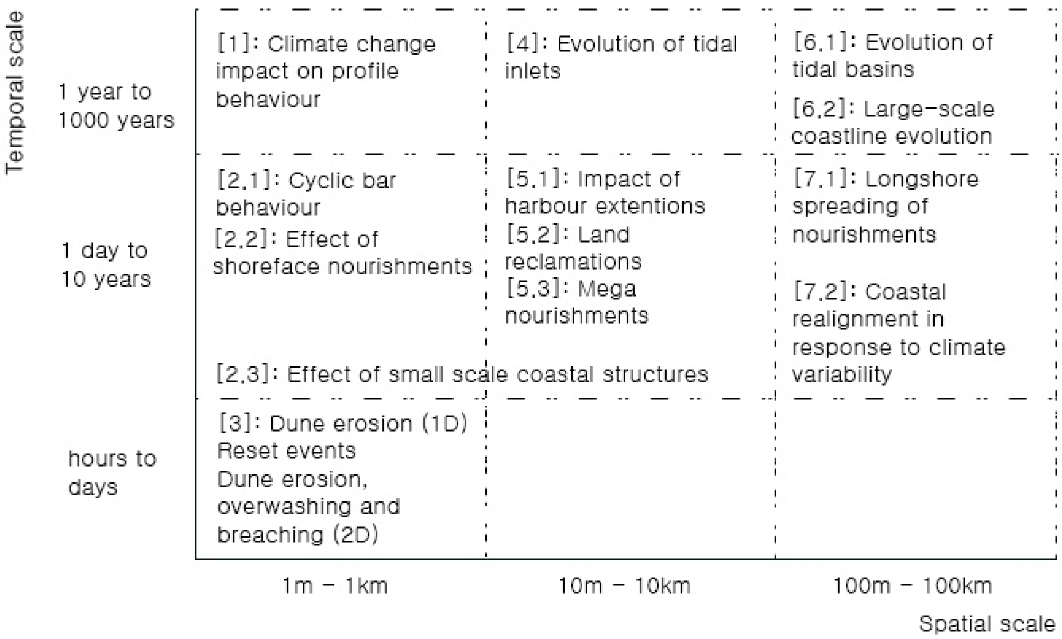

Figure A.1: Temporal scales for various engineering applications Source: Roelvink and Reniers, 2009

.

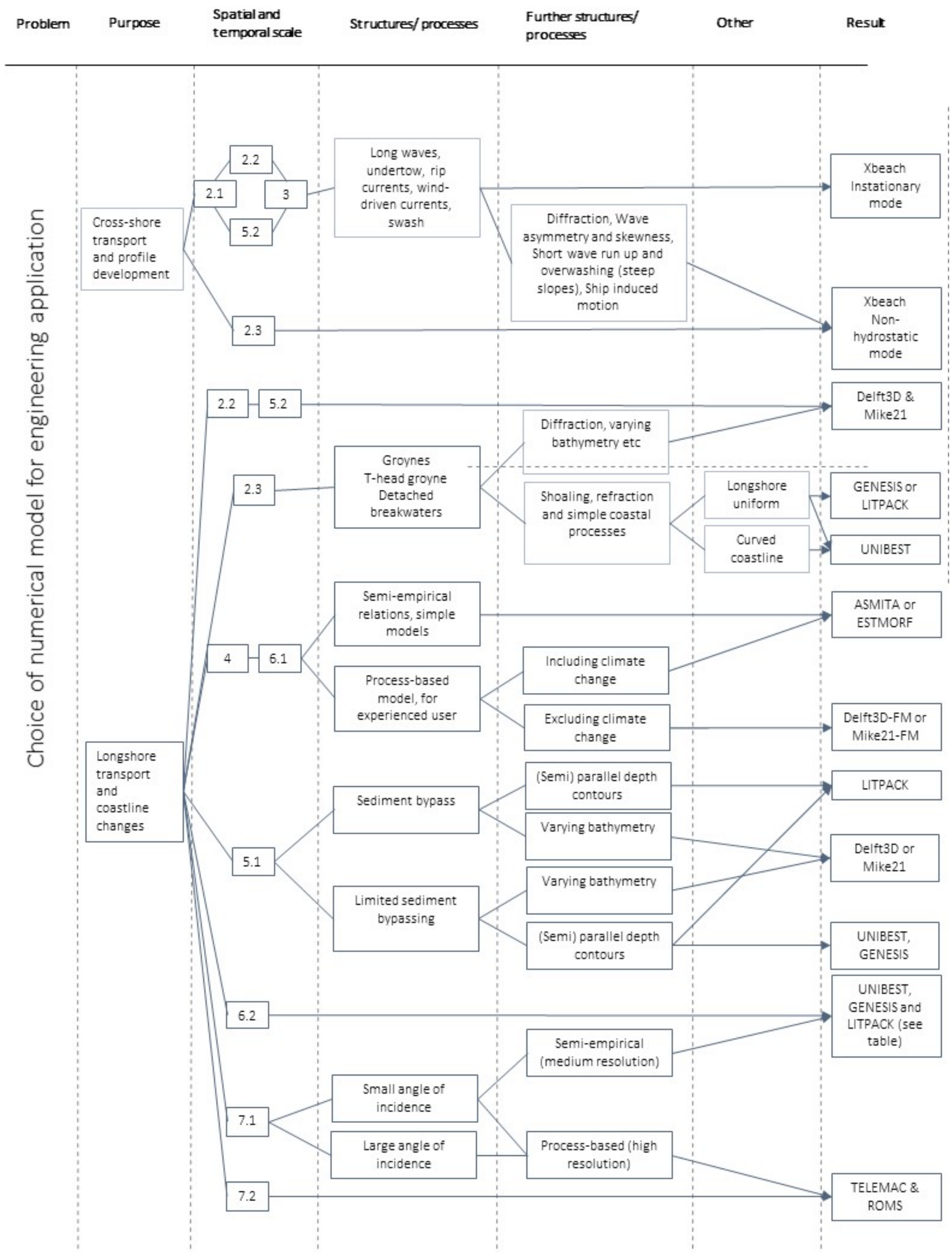

Figure A.2: Decision Tree for Cross-shore transport and profile development and Long-shore transport and coastline changes. Source: Roelvink and Reniers, 2009

As is explained in Section 1.2, both the cross-shore and longshore dynamics will be studied. From Figure A.1 we see that that we are interested in amongst others, cyclic bar behaviour (2.1), the effect of shoreface nourishments (2.2) (and the effect of small scale structures (2.3)). These applications correspond to a temporal scale of 1 day to 10 years and a spatial scale of 1 m to 1 km (which agrees indeed with the earlier defined temporal and spatial scale). From Figure A.2 it then follows that Xbeach is a suitable candidate for modelling the cross-shore transport and profile development. The instationary mode or non-hydrostatic mode has to be chosen. For the longshore transport an coastline changes, UNIBEST appears to be a good candidate, as it is more suitable for modelling with curved coastlines, according to the decision tree.

A.1.1. Duros+, D++ and DurosTA

Duros, D++ and DurosTA are all 1D cross-shore transport models for design storm conditions. DUROS+ and D++ calculate the post-storm cross-shore profile independent of time. The calculated profile is a function of the water level, significant wave height, peak period, and the fall velocity of the sediment. The difference between DUROS+ and D++ is that DUROS+ requires hydraulic boundary conditions on deep water, whereas D++ allows hydraulic boundary conditions at shallow water (Boers, 2012).

DurosTA differs from the other two in that it is a **time dependent**, process-based cross shore transport model for extreme conditions. It calculates the development of a cross-shore coastal profile during a storm.

A.2. Research material

1. Hydraulic Boundary Conditions

When choosing the boundary conditions, it is important to first determine whether the aim is to model **storm conditions** (used for example when assessing dune safety, or when designing a coastal structure) or to model **yearly averaged** conditions (used to look at the long-term morphological behaviour).

Hydraulic boundary conditions for dune flood defences are available in the report 'Hydraulic loads 2017 for dune flood defences' (den Bieman, 2016). These are design conditions, corresponding to a 1/10,000 storm, as used for the design of the flood defence, and for the morphological studies conducted by Arcadis (**?** (**?**), Onderwater and van der Baan (2017), Onderwater (2018a) and Onderwater (2018b)).

Because of the scope of this research, we are not interested in the design conditions, but in average conditions. Therefore we need measurements of (amongst others) wave heights and wave periods from a nearby buoy or station. The station 'Europlatform' is a suitable station, or the buoy 'Maasgeul' - see Figure A.3 (left figure). Rijkswaterstaat collects these data, which can be requested on their website. The right figure shows all available measurements in the Netherlands/in the North Sea, showing that, when a strategic location is chosen, it should be possible to find hydraulic boundary conditions for other hard-soft case studies as well.

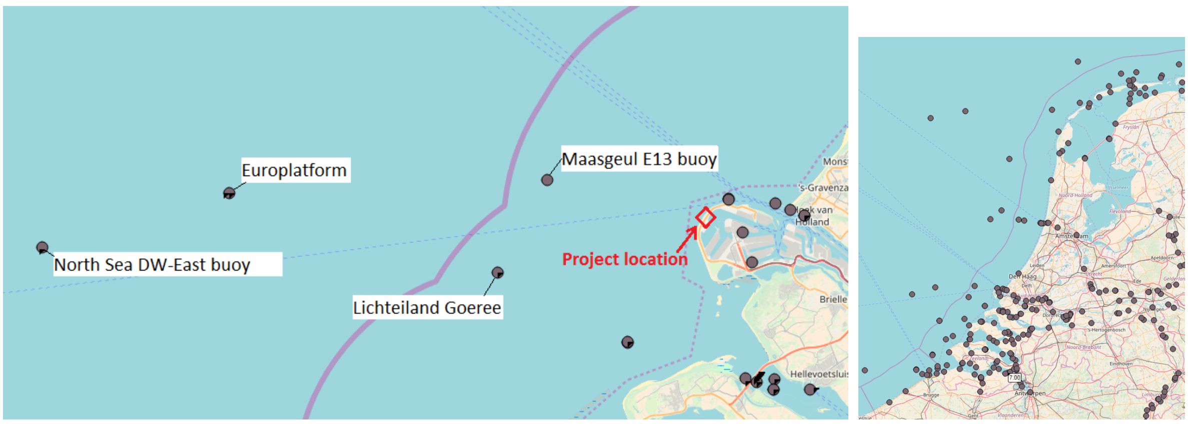

(a) Nearby buoy/station locations for MV2

(b) All locations in Dutch North Sea.

Figure A.3: Buoy locations providing measurements for hydraulic boundary conditions. Source: waterberichtgeving.rws.nl

2. Bathymetry and coastline data for MV2

The bathymetry and coastline data for the MV2 case study is available in xyz format. The underwater profile has been measured by multi-beam for the northern part of the soft flood defence. For the southern part, a single-beam is used. **3. Sediment characteristics**

The soft flood defence was initially designed with a grain size distribution with a D_{50} of 370 μm. After completion and assessment of the actual D_{50} found, a D_{50} of 330 μm. This has been corrected by adjusting the minimum layer volumes accordingly. Therefore, this D_{50} could be used for the calculations, as this is the actual average median grain size found along the flood defence. A smaller median grain size could be considered as well, as it appears from figure A.4 that in the northernmost transects (Kp4200 - Kp3495, which is the focus area of this study), smaller grain sizes were found.

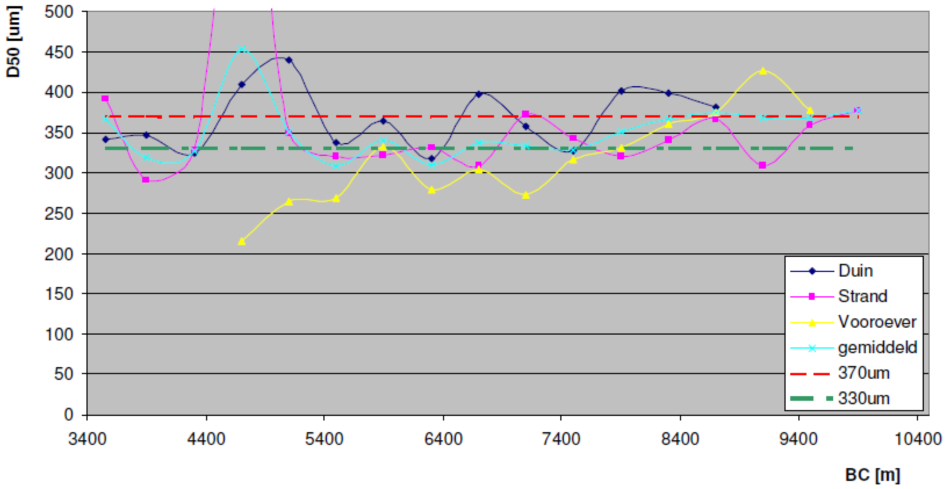

Figure A.4: D_{50} per layer volume, found along the soft flood defence

.

4. Bathymetry and coastline data for other hard-soft transitions
In the Netherlands, the coastline is measured every year along so-called JARKUS (Jaarlijke Kustlodingen) transects from 2008 to present. This is also done after the storm season has ended, in (or after) april. The JARKUS transects are distributed along the entire Dutch coastline, with a mutual spacing of 200 to 250 m. The data can be downloaded as xyz data in ASCII format, netCDF data or KML format for visualization in Google Earth. Moreover, all the data can be found and easily analysed with the software MorphAn, developed by Deltares. The data is initially divided into two types, each requiring a different way of measuring:

a) **Altitude measurements** for the dry coast (from approx. -1 to +5 m NAP). Before 1996 this was measured with a stereophotogrammetry plane, after 1996 it was done with laser altimetry. The laser altimetry measurements are carried out between 15 march to 15 april.

b) **Bathymetry measurements** for the underwater profile (approx. -8 to -20 m NAP) of the coast. These are obtained by single beam measurements at every transect, with mutual distance of 100 m.

JARKUS transects and according measurements are not available yet for the Maasvlakte 2, as it is not officially part of the Dutch coastline yet (it will be from 2023). The measurements assembled by Boskalis will probably be used as JARKUS transect measurements later on.

B

Literature study

B.1. Coastal profiles by Bruun, Dean and Vellinga

Bruun

Bruun (1954) was the first engineer to formulate an empirical relation for the dynamic equilibrium profile. He formulated an equation where the water depth is related to the offshore distance:

$$h = A(x')^m \tag{B.1}$$

In which:
m = exponent equal to m = $\frac{2}{3}$
h = water depth [m]

'A' is a shape factor which depends on the "stability characteristics of the bed material", with dimension $m^{1/3}$) (Bosboom and Stive, 2015).

Dean

Dean (1990b) supported Bruun's equation by showing that equation B.1 is consistent with uniform wave energy dissipation per unit volume ε within the breaking zone (Dean, 1990b). The wave energy dissipation per unit is given by:

$$\epsilon = \frac{1}{h}\frac{\delta}{\delta y}(EC_g) \tag{B.2}$$

with
E = wave energy density per unit sea area [J//m^2]
C_G = group velocity [m/s]
h = water depth [m]

And it can be shown from linear shallow water wave theory that A and D are related by:

$$A = \left[\frac{24\varepsilon D_{50}}{5\rho g^{3/2}\gamma^2}\right]^{2/3} \tag{B.3}$$

with
D_{50} = particle diameter [m]
γ = breaker parameter [-]

So, Dean supported Bruun's equilibrium profile definition, but found the shape factor A to be a function of the particle diameter D_{50}. The parameter A is seen to vary from 0.079 to 0.398 $m^{1/3}$ (Dean, 1977). Dean (1990a) later related equation B.3 to the fall velocity, w_s:

$$A = 0.067 {w_s}^{0.44} \tag{B.4}$$

where w_s is the fall velocity in cm/s.

Comparison with observed profiles along the Dutch coast show, however, that optimal values of A differ per location whereas the sediment size D_{50} is the same for each location. Apparently the use of equationB.1 is still limited, and the factor A appears to be dependent on more variables than the fall velocity (Bosboom and Stive, 2015).

The dynamic equilibrium profiles described by Bruun (1954) and Dean (1977) can be used as tools to predict the expected dynamic equilibrium profile, e.g. to design the slope of a new land reclamation or artificial beach. Therefore, for the design of the soft flood defence of the Maasvlakte 2, the design profile of the beach was also a Dean (1977) profile.

Vellinga

Later, Vellinga (1986) proposed a formulation for the 'erosion profile' or post-storm profile (see Figure 2.2a). Note that this is different from the dynamic equilibrium profiles defined by Bruun and Dean, as it describes the cross-shore profile after a storm, rather than a profile that is the mean of all dynamic oscillations. The shape of the Vellinga profile is described by:

$$h = A(x')^{0.78} \tag{B.5}$$

In which he describes the shape factor A as:

$$A = 0.39 {w_s}^{0.44} \tag{B.6}$$

with A in m/s. Note the difference between the shape factor defined by Vellinga and Dean's definition of the shape factor, namely $A = 0.5{w_s}^{0.44}$.

B.2. Calculation of critical profile

The minimum height, width and corresponding volume of the critical profile depend on the local significant wave height H_{m0} and peak wave period T_p. The crown height of the critical profile above chart datum (reken-peil) is derived with the following formula:

$$h_{gp} = 0.12 T_p H_{m0} \qquad (minimum 2.5m) \tag{B.7}$$

In which:
h_{gp} = crown height critical profile above chart datum [m]
T_p = peak period [s]
H_{m0} = significant wave height [m]

And the width of the critical profile or crown width b_{gp} is a fixed value: $b_{gp} = 3$.

By combining these two we can calculate the required volume of the critical profile:

$$A_{gp} = 1.5{h_{gp}}^2 + 3h_{gp} \qquad (minimum 16.875 m^3/m) \tag{B.8}$$

In which: A_{gp} : volume of critical profile per running meter coast $[m^3/m]$

B.3. Guidelines for safety assessment of transition structures

Step 1. Safety assessment of each separate component (hard structure, soft part)

Step 2. Determination of sediment volume transported to front of hard structure (A_{ont})
A_{ont} is the volume of sediment that is transported from the soft flood defence to the hard flood defence. This is because there is a demand of sediment in front of the hard structure, because the supply of material from the mainland or dune is (partly) cut off by the hard structure. In principle A_{ont} is calculated based on the difference between the coastal profile on both sides of the transition. The difference is calculated based on the 'profile difference' after the design storm. Because the cross-shore profiles might already differ before the storm, the following notation is used:

- A, B are the cross-shore profiles before the storm
- A', B' are the cross-shore profiles after the storm;
- D1 = A - B, is the profile difference before the storm;
- D2 = A' - B', is the profile difference after the storm.

Finally, the loss of sediment A_{ont} is the calculated with A_{ont} = D2 - D1.

Step 3. Extra coastline retreat T_e (simple approach)
The extra coastline retreat due to the sediment that is lost from the soft part to the hard structure is calculated as:

$$T_e = A_{ont}[\sqrt{h_a \cdot h_0} + h_0]^{-1} \tag{B.9}$$

In which:
h_A = height of the erosion zone [m]
h_0 = height of the erosion zone until the intersection point with the hard structure [m]

An example of the calculation and an indication h_A and h_0 are given in Figure B.1.

Step 4. Extra coastline retreat T_e (detailed approach)
In this detailed method, the course of T_e is estimated more accurately. This is done by using a lower- and upper limit to determine the course of T_e over the entire transition zone, divided into a number of zones. To use this method, expert help is advised. The method is graded with 'sufficient' if the coast over the entire transition zone can withstand the extra retreat T_e for both upper- and lower limit of A_{ont}.

Step 5: Advanced asessment transition structures
If with the detailed method no score can be awarded, further research needs to be carried out. This will lead to a final judgement: 'good, 'sufficient' or 'insuficcient'.

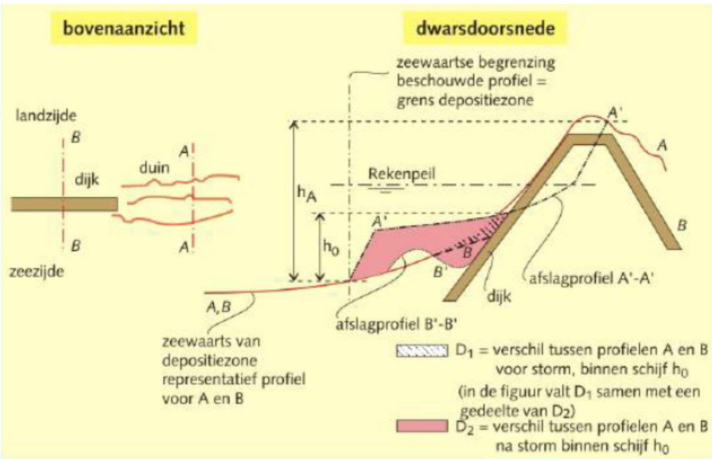

Figure B.1: Calculation example for assessment of transition structures. Source: Boers (2012)

.

B.4. Examples of hard-soft transition along the North Sea coast

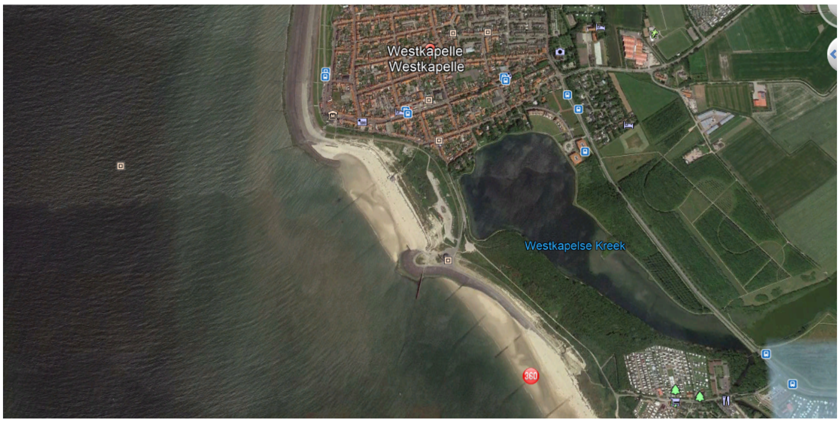

Figure B.2: Westkapelle, Zeeland

.

Figure B.3: Cocksdorp, Texel, Noord-Holland

.

Figure B.4: Cocksdorp, Texel, Noord-Holland

.

Figure B.5: West-Terschelling, Friesland

.

Figure B.6: Hollum, Ameland, Friesland

.

Figure B.7: Spiekeroog, Duitsland

.

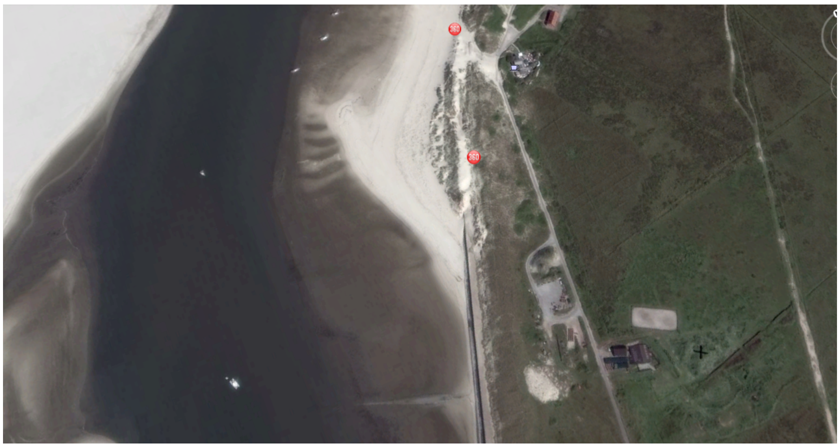

Figure B.8: Spiekeroog, Duitsland

.

Figure B.9: Wangerooge, Duitsland

.

Figure B.10: Wangerooge, Duitsland

.

Figure B.11: Wangerooge, Duitsland

.

B.5. Case study of a hard-soft transition: Westkapelle

van Santen et al. (2012) conducted a research to model such a coastline section with a 2DH model (XBeach) and compared it with model results of that area with a 1D model (DurosTA and XBeach 1D). As a 'test area' they choose the complex coastline section near Westkapelle. From their results they concluded that:

- For the parts in the domain with (almost) uniform nearshore bathymetry, the large-scale sedimentation- and erosion patterns were quite similar for the 1D and 2D models. See Figure B.14.
- For the complex parts (non-uniform and/or around transition structures), large differences were found in the erosion- sedimentation patterns, due to the alongshore processes that play a role here. See Figure B.13.

This test case showed that for complex coasts, using a 2DH storm impact model like XBeach is a good alternative for 1D models like DurosTA.

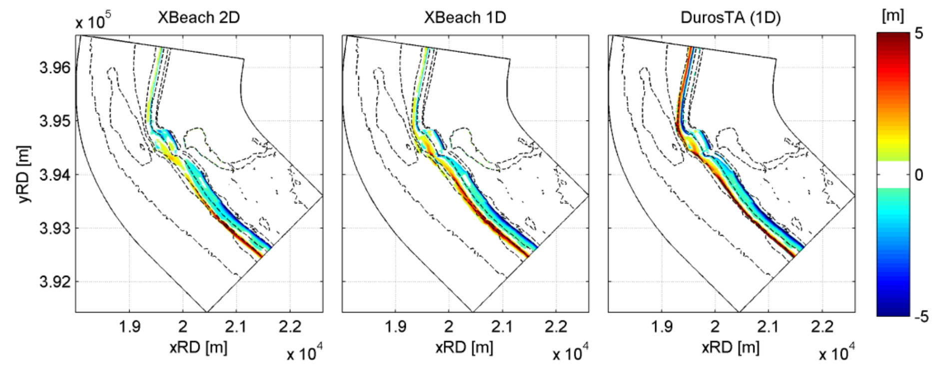

Figure B.12: Bed level changes, as result of 30h of simulation with normative storm conditions and westerly waves. A comparison is made between XBeach 2D, XBeach 1D and DurosTA. Reddish colours indicate deposition areas and bluish colours are associated with erosion patterns. Source: van Santen et al. (2012)

.

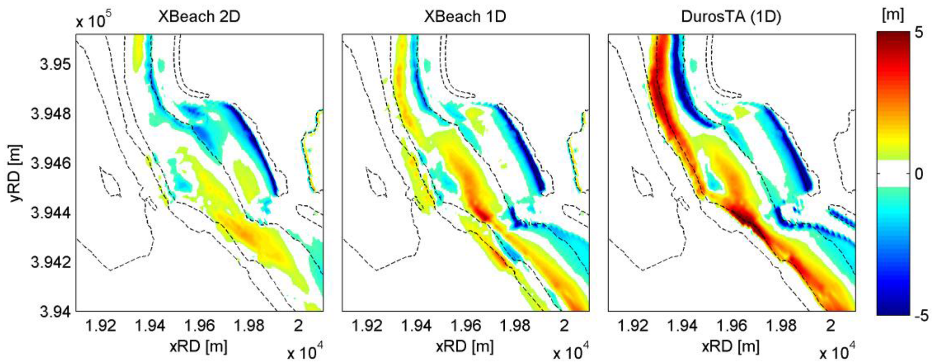

Figure B.13: Bed level changes in area-of-interest, as result of 30h of simulation with normative storm conditions and westerly waves. A comparison is made between XBeach 2D, XBeach 1D and DurosTA. Reddish colours indicate deposition areas and bluish colours are associated with erosion patterns. Source: van Santen et al., (2012)

B.6. Design of flood defence Maasvlakte 2

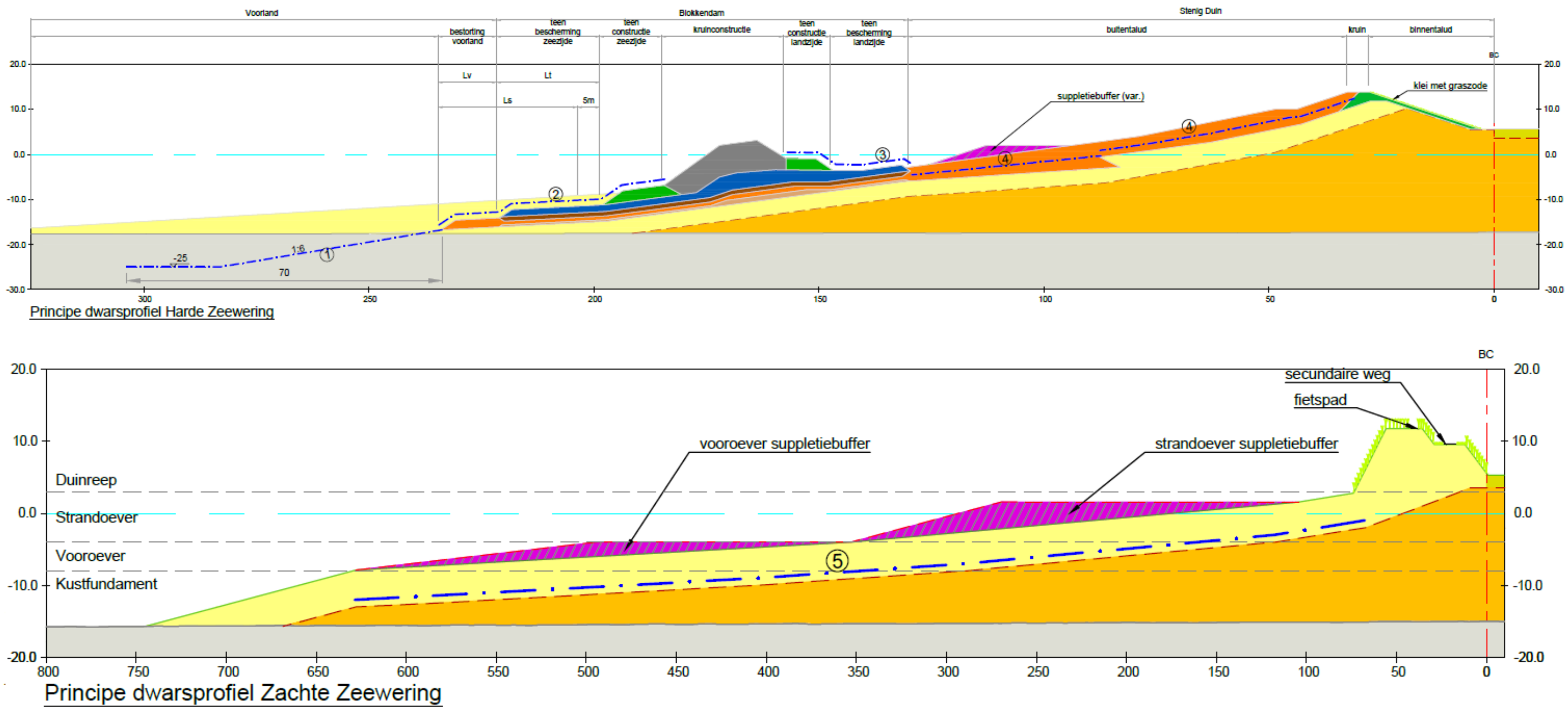

Figure B.14: Wangerooge, Duitsland

.

C

System Analyses

C.1. 2D plots

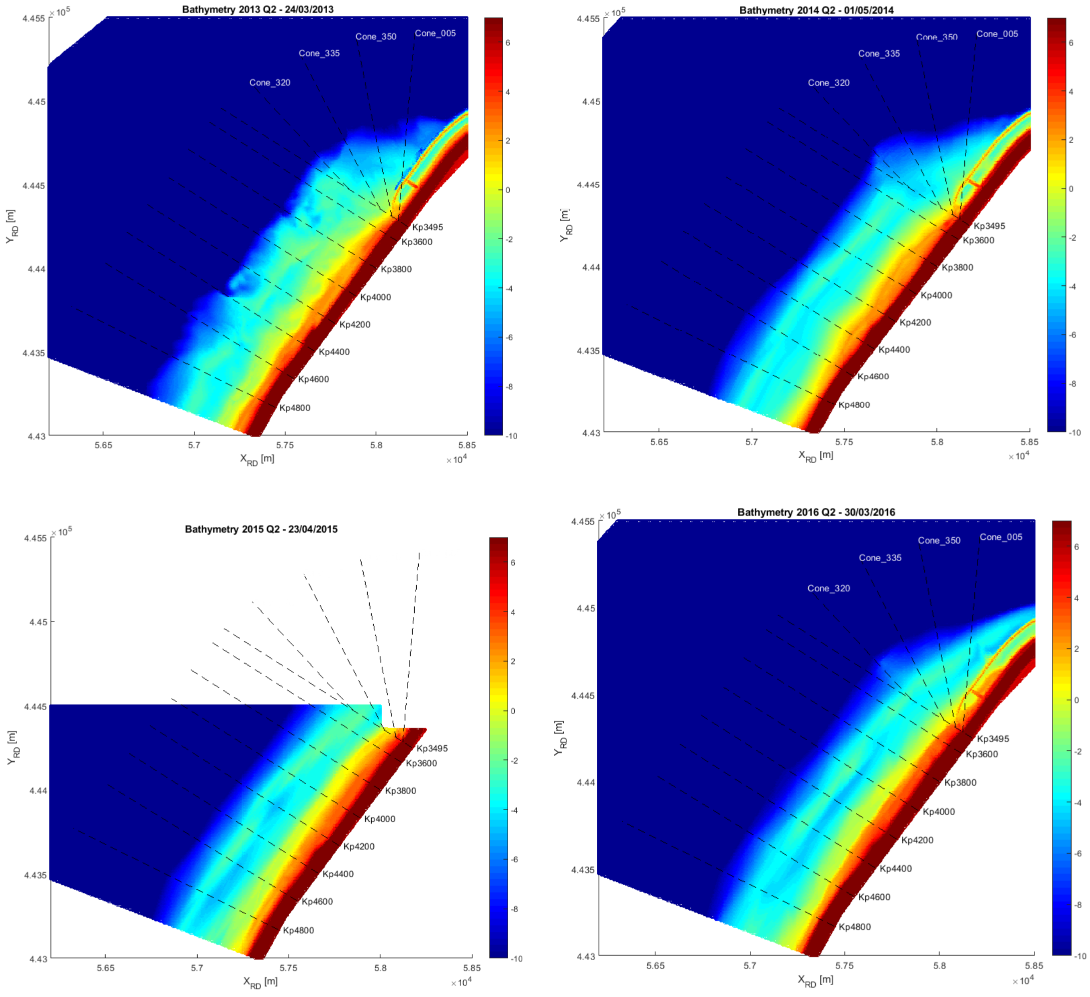

Figure C.1: 2D Scatter plots of 2013Q2, 2014Q2, 2015Q2 and 2016Q2.

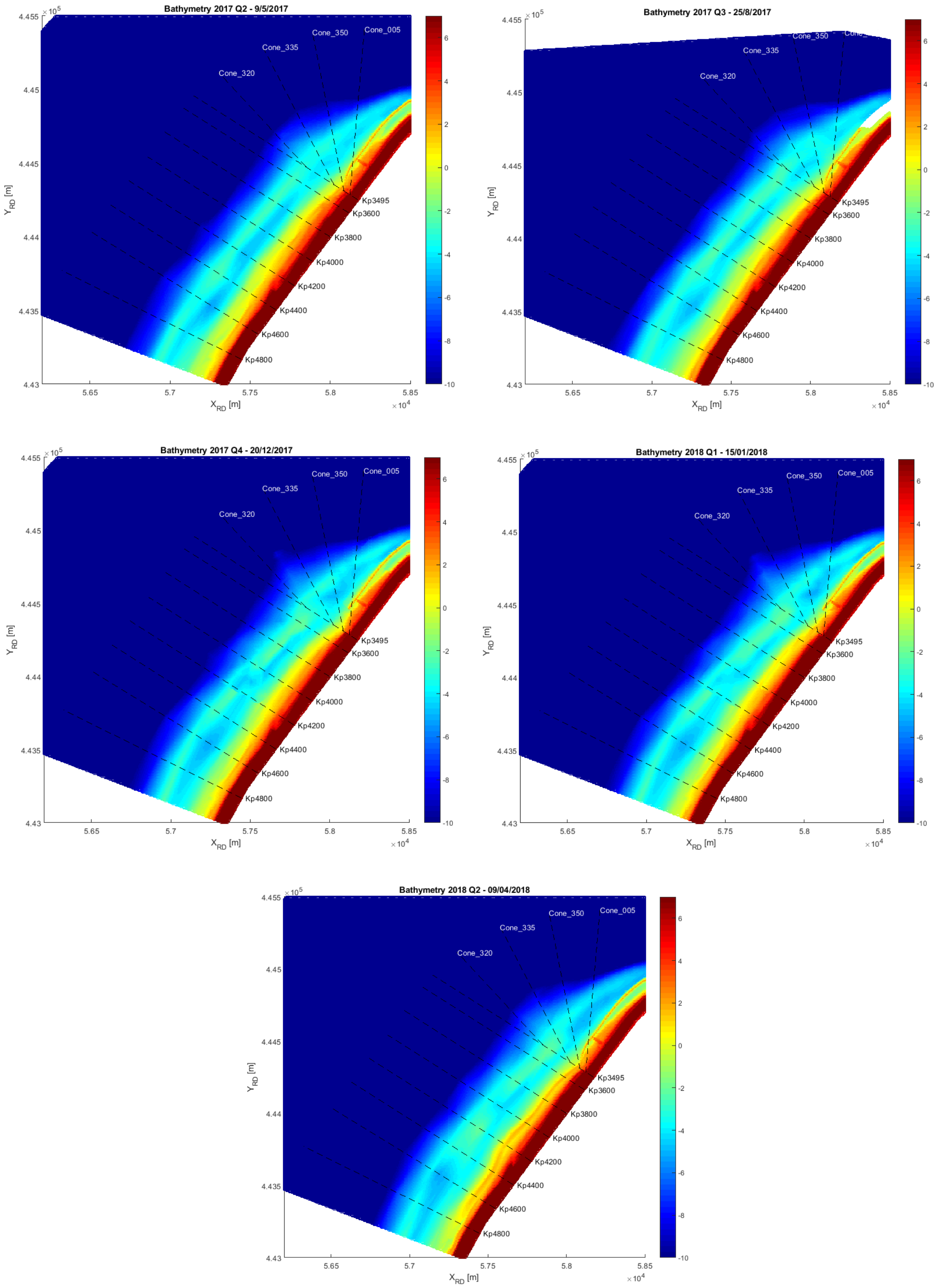

Figure C.2: 2D scatter plots of 2017Q2, 2017Q3, 2017Q4, 2018Q1, and 2018Q2.

C.2. Contour plots

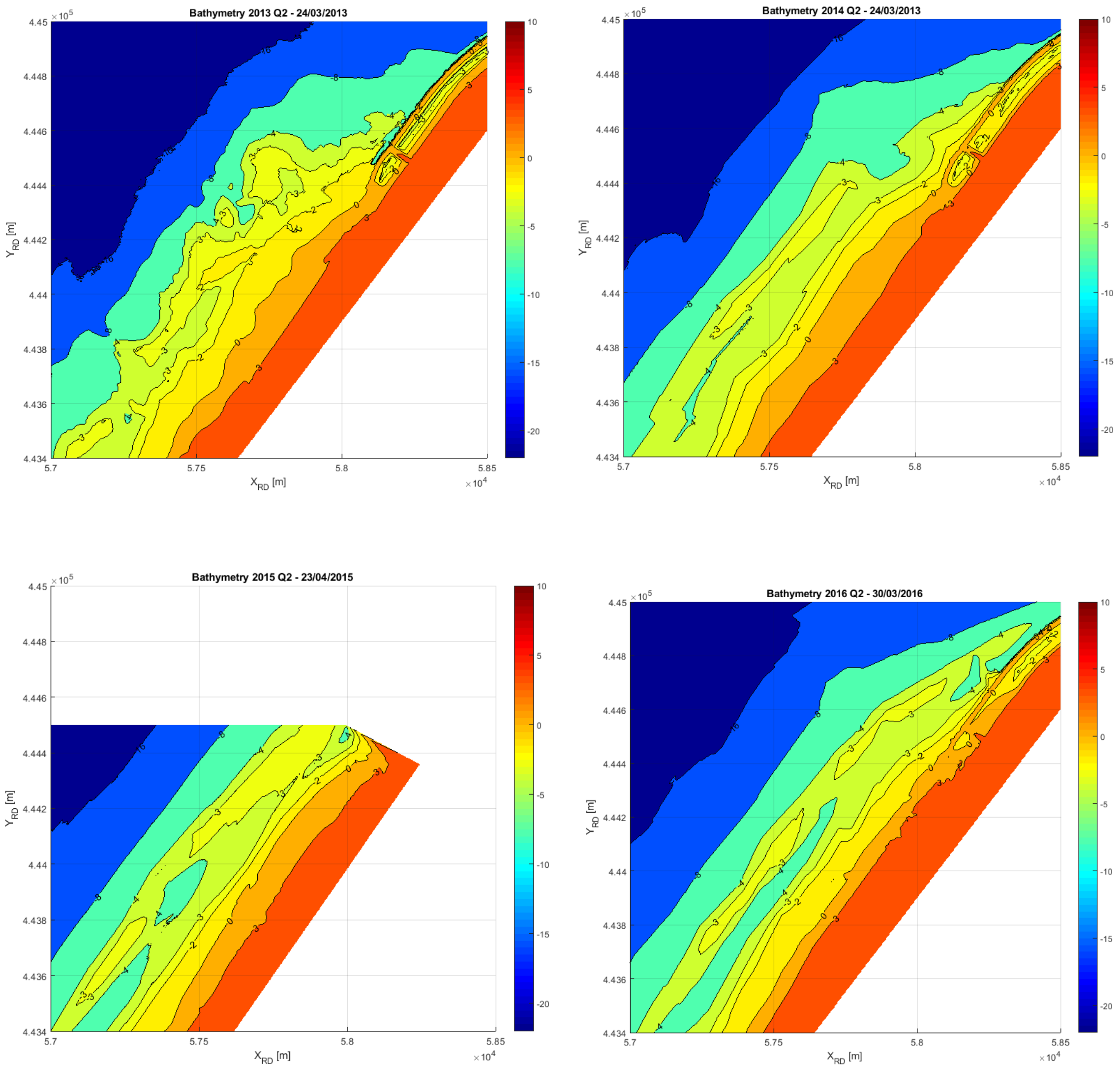

Figure C.3: Contour plots of bathymetry between 2013 and 2016.

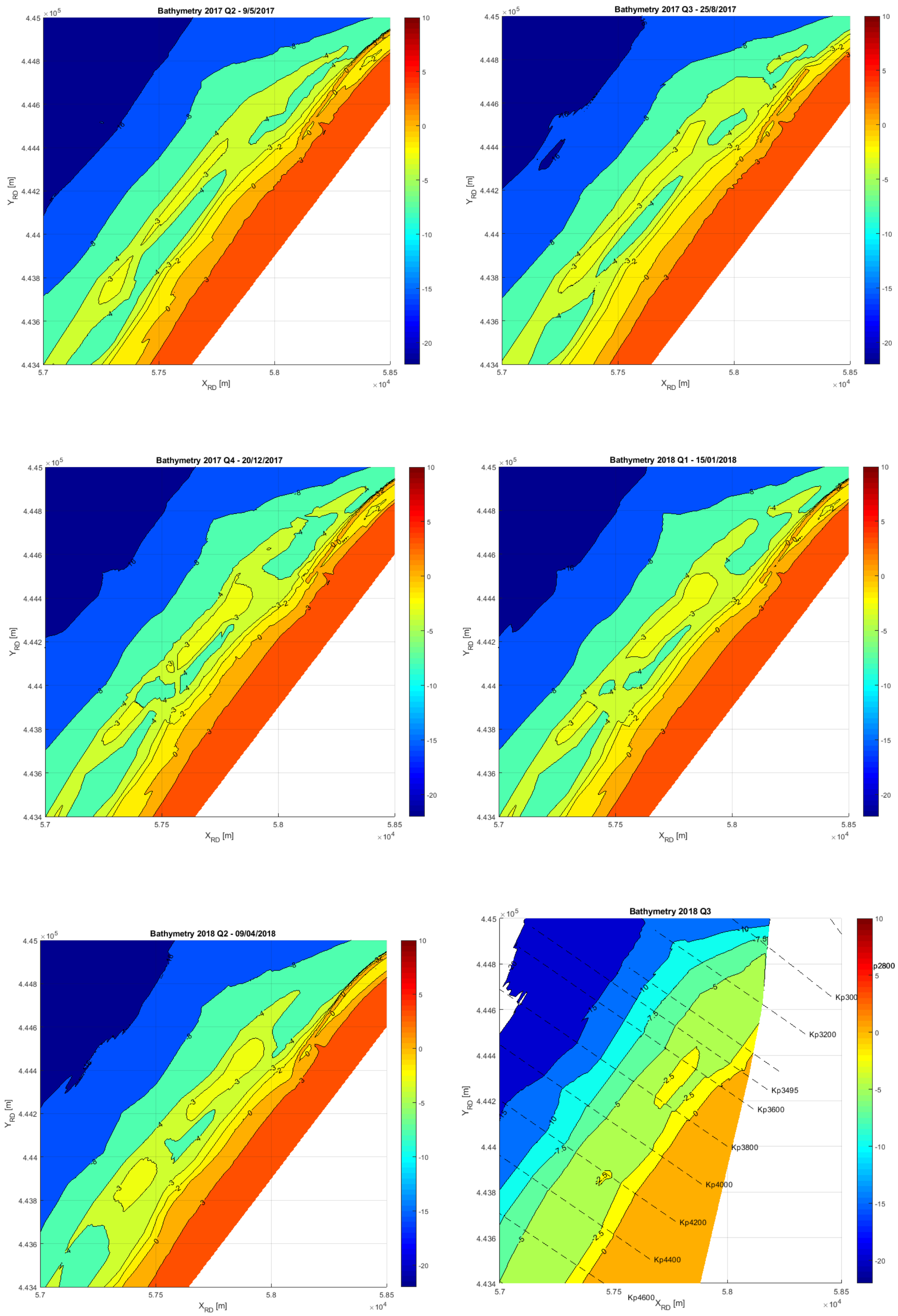

Figure C.4: Contour plots of bathymetry between 2013 and 2016.

C.3. Cross-sections

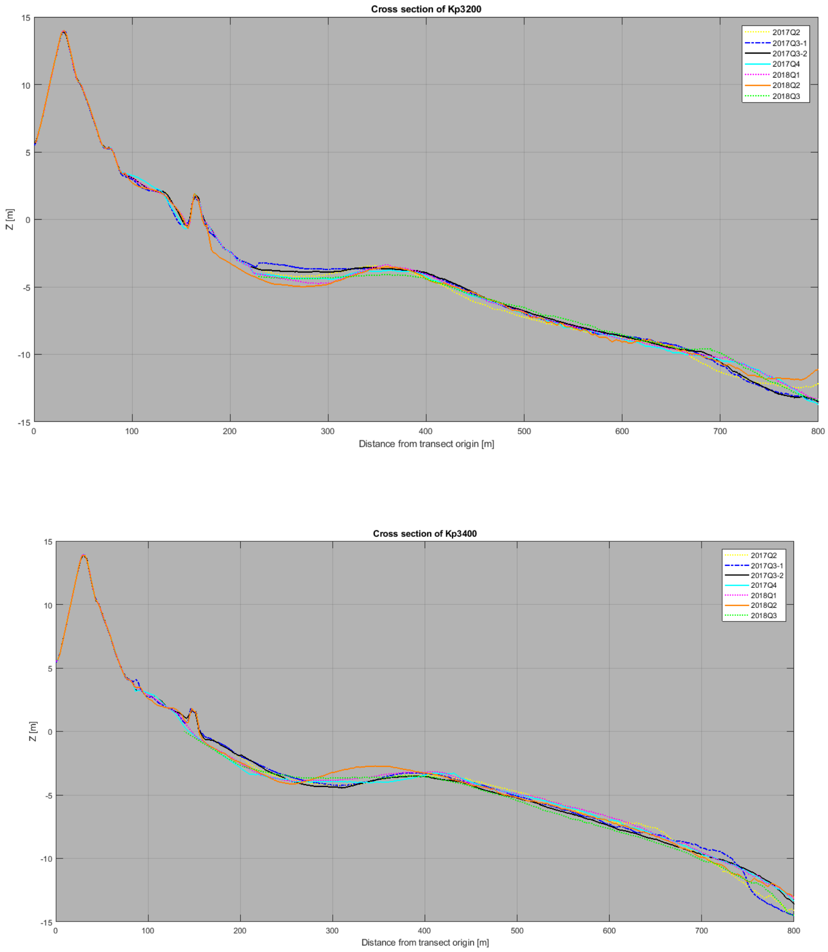

Figure C.5: Cross sections of transects Kp3200 and Kp3400 between 2017 and 2018.

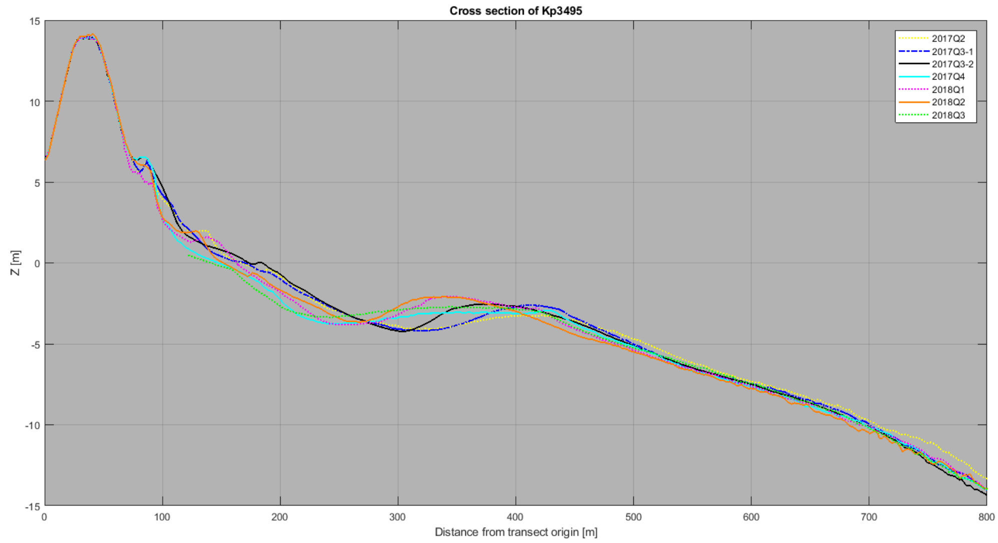

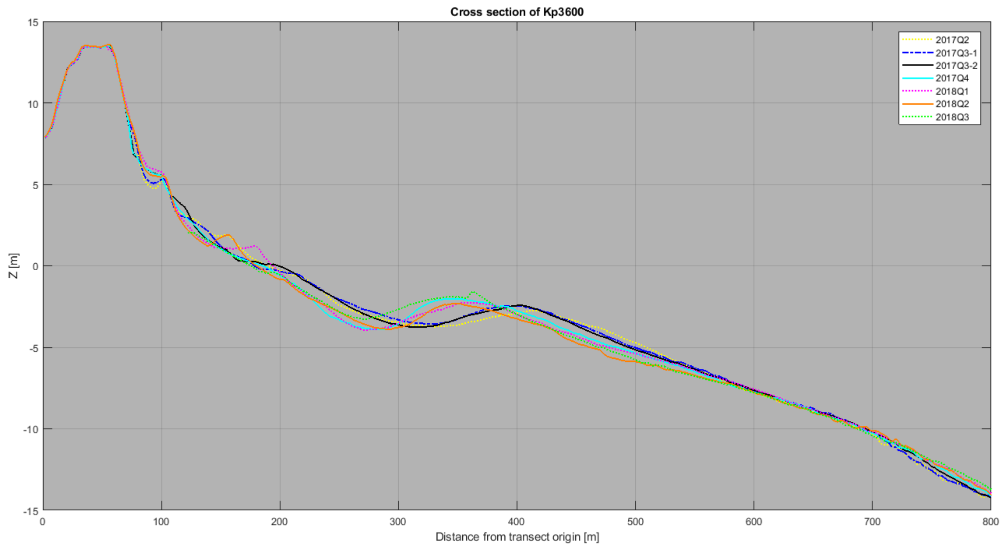

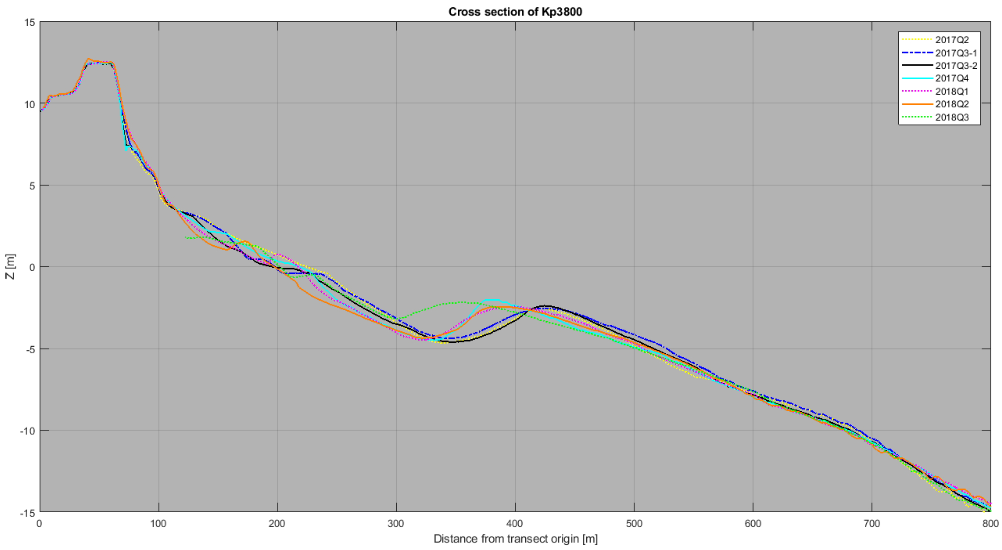

Figure C.6: Cross sections of transects Kp3495 to Kp3800 between 2017 and 2018.

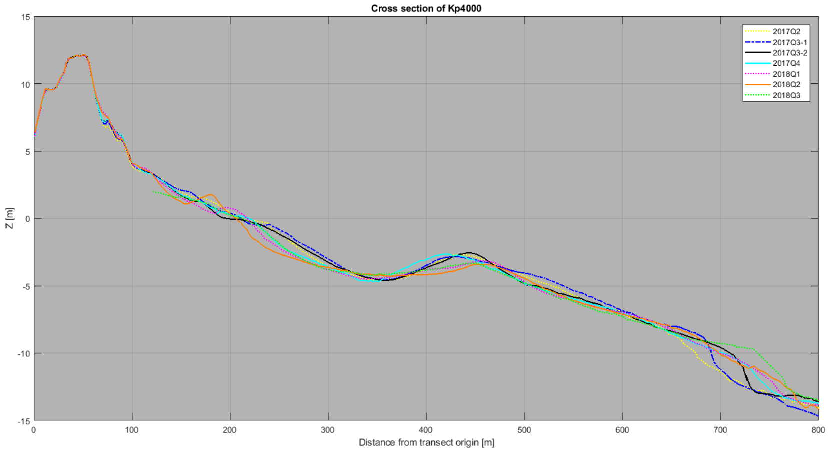

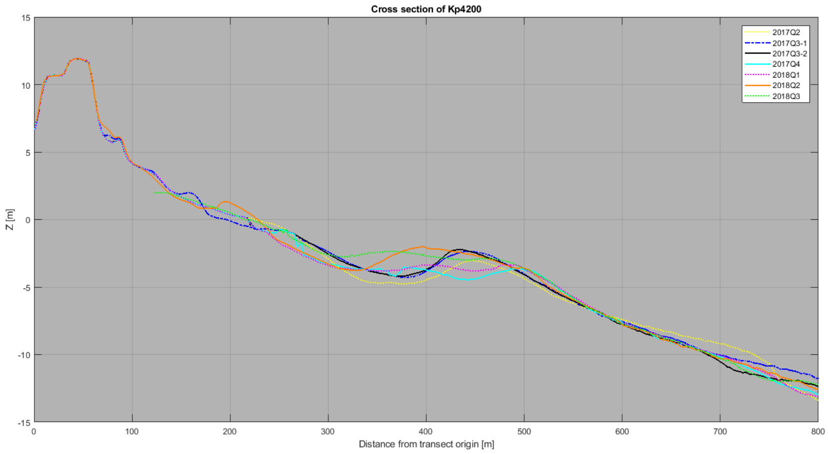

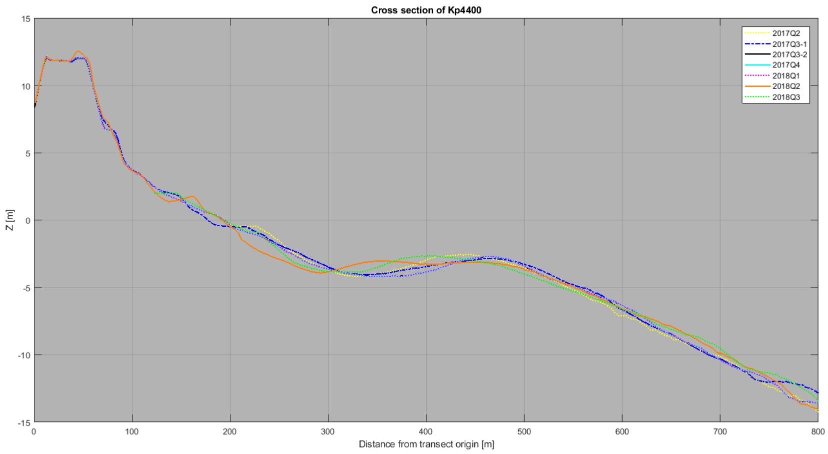

Figure C.7: Cross sections of transects Kp4000 to Kp4400 between 2017 and 2018.

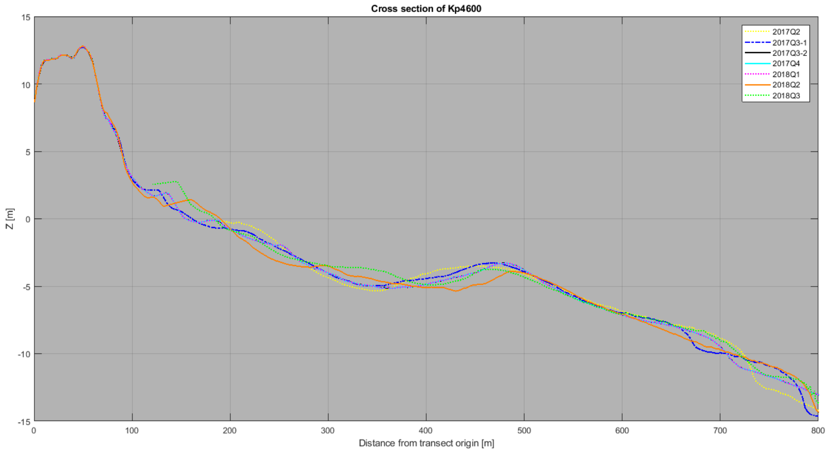

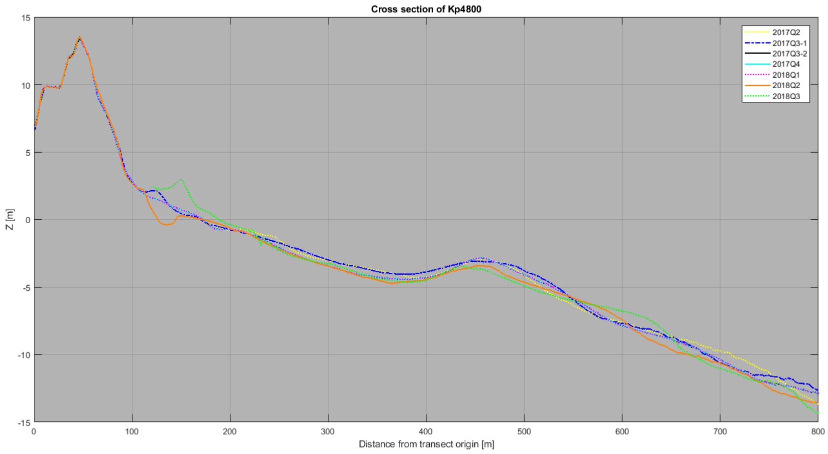

Figure C.8: Cross sections of transects Kp4600 and Kp4800 between 2017 and 2018.

C.4. Sedimentation erosion graphs

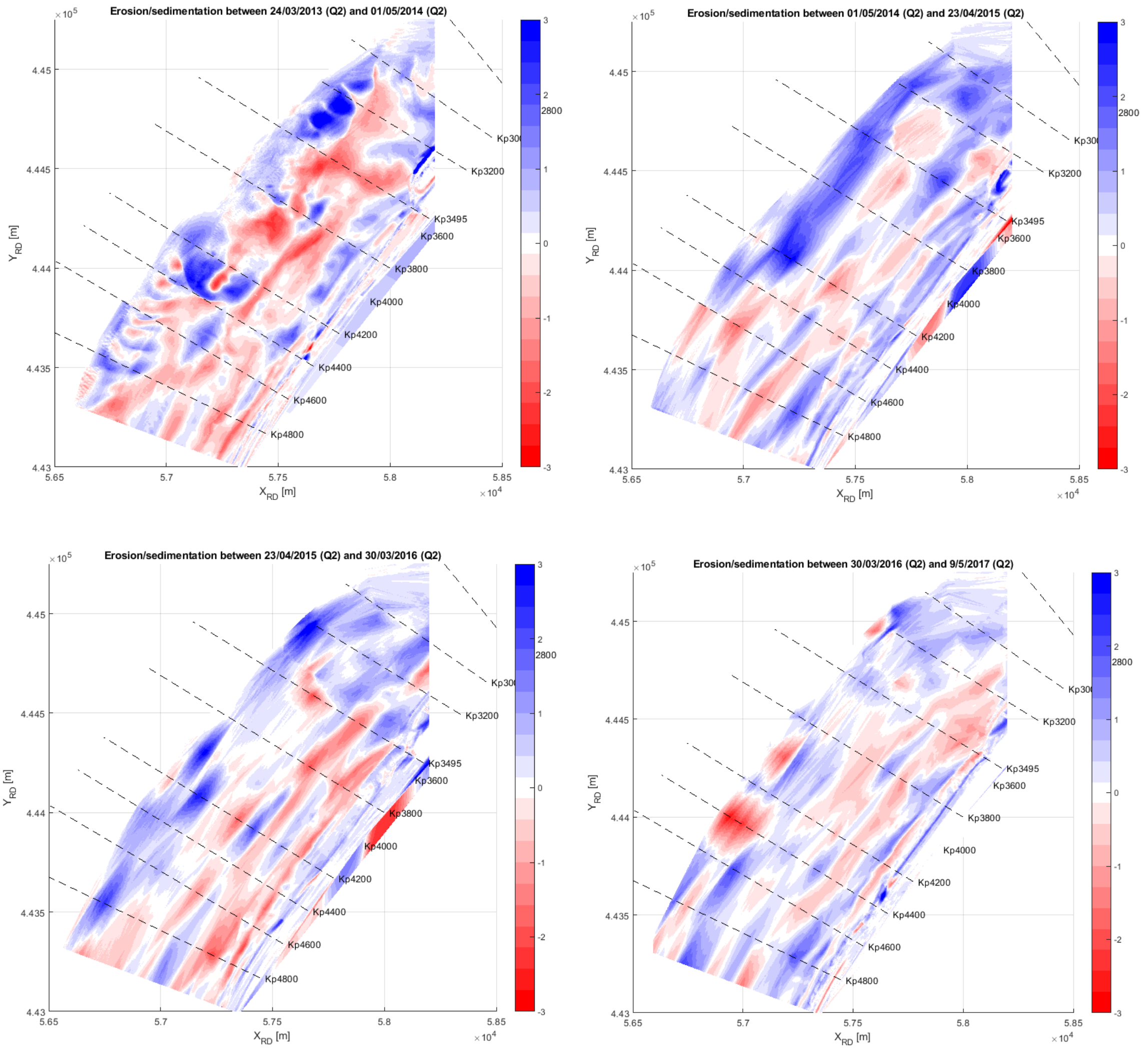

Figure C.9: Sedimentation-erosion between 2013 and 2017.

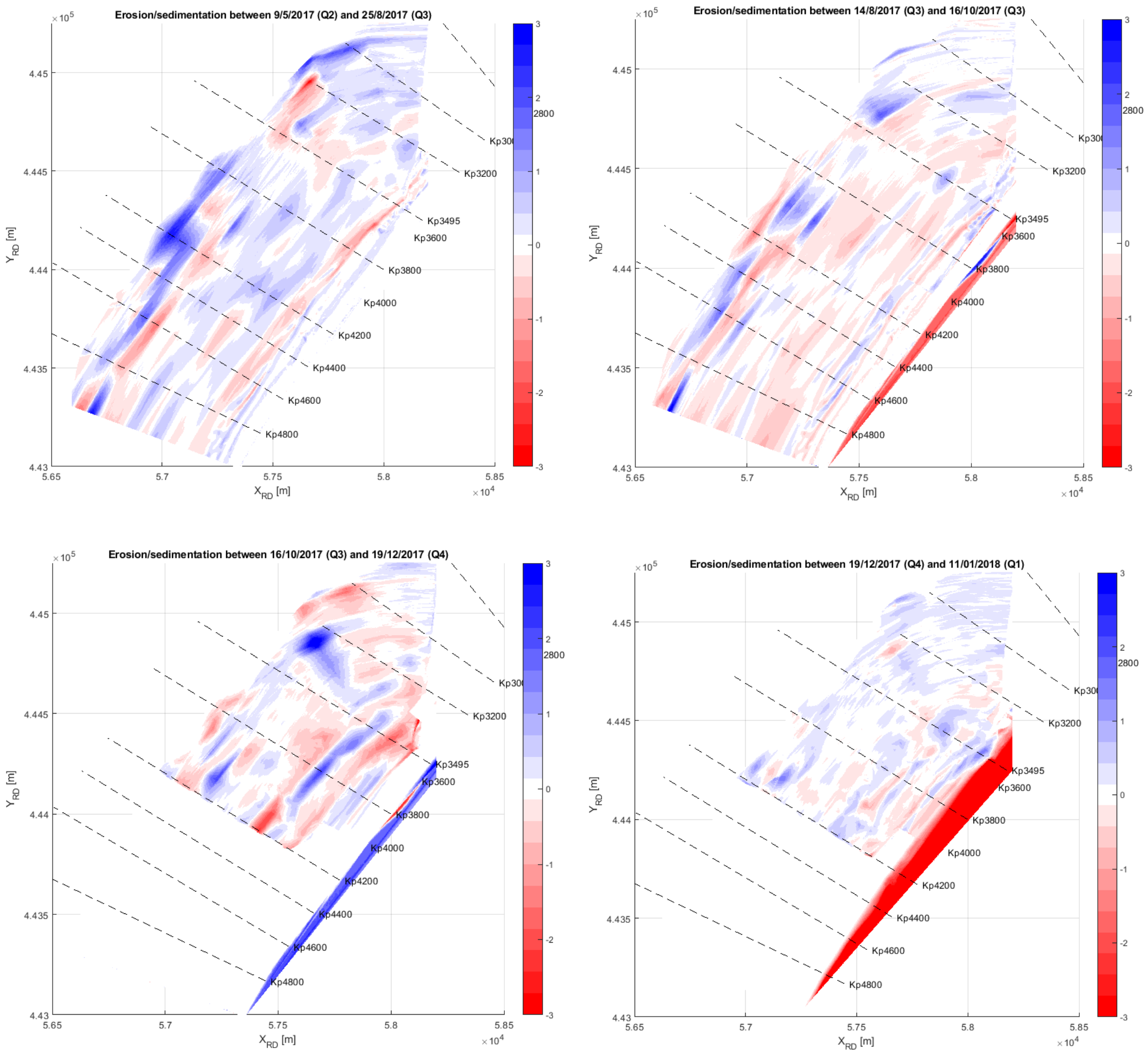

Figure C.10: Sedimentation and erosion between 2017 and 2018.

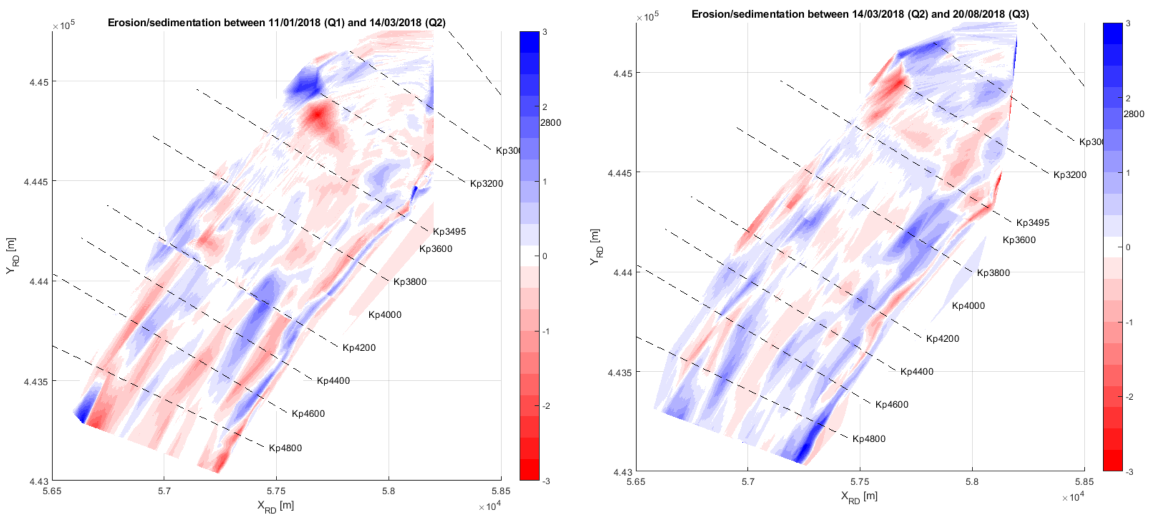

Figure C.11: Sedimentation and erosion between 2018Q1 and 2018Q3.

C.5. Wave energy flux

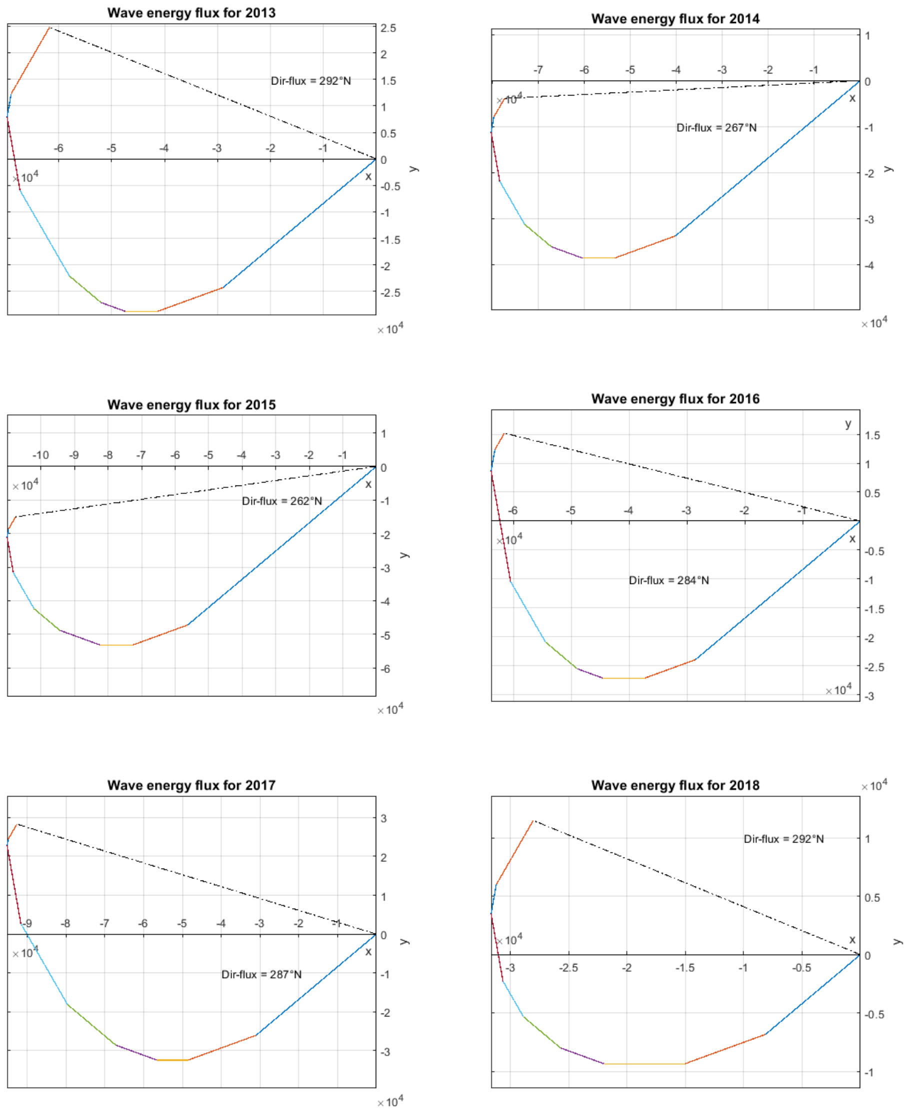

Figure C.12: Wave energy flux computation based on offshore data for years 2013 to 2018.

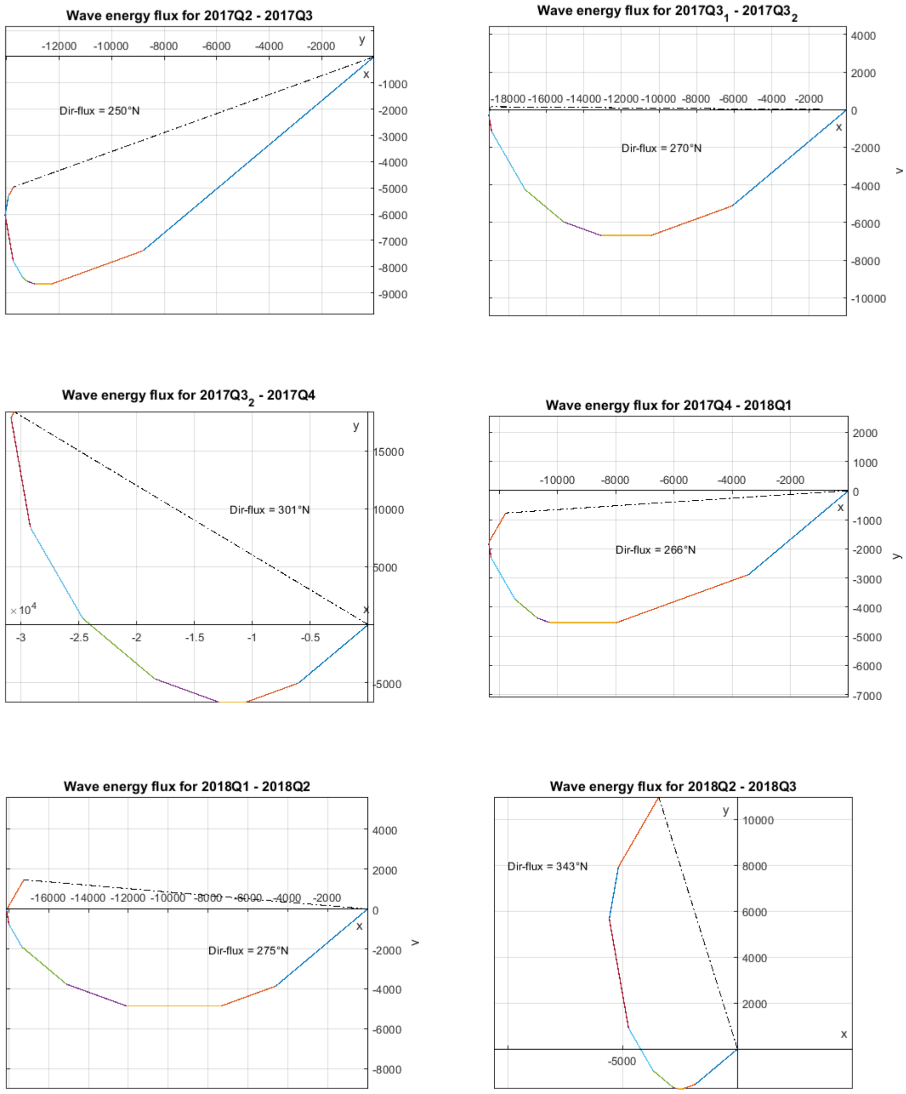

Figure C.13: Wave energy flux computation based on offshore data per period between 2017Q2 and 2018Q3.

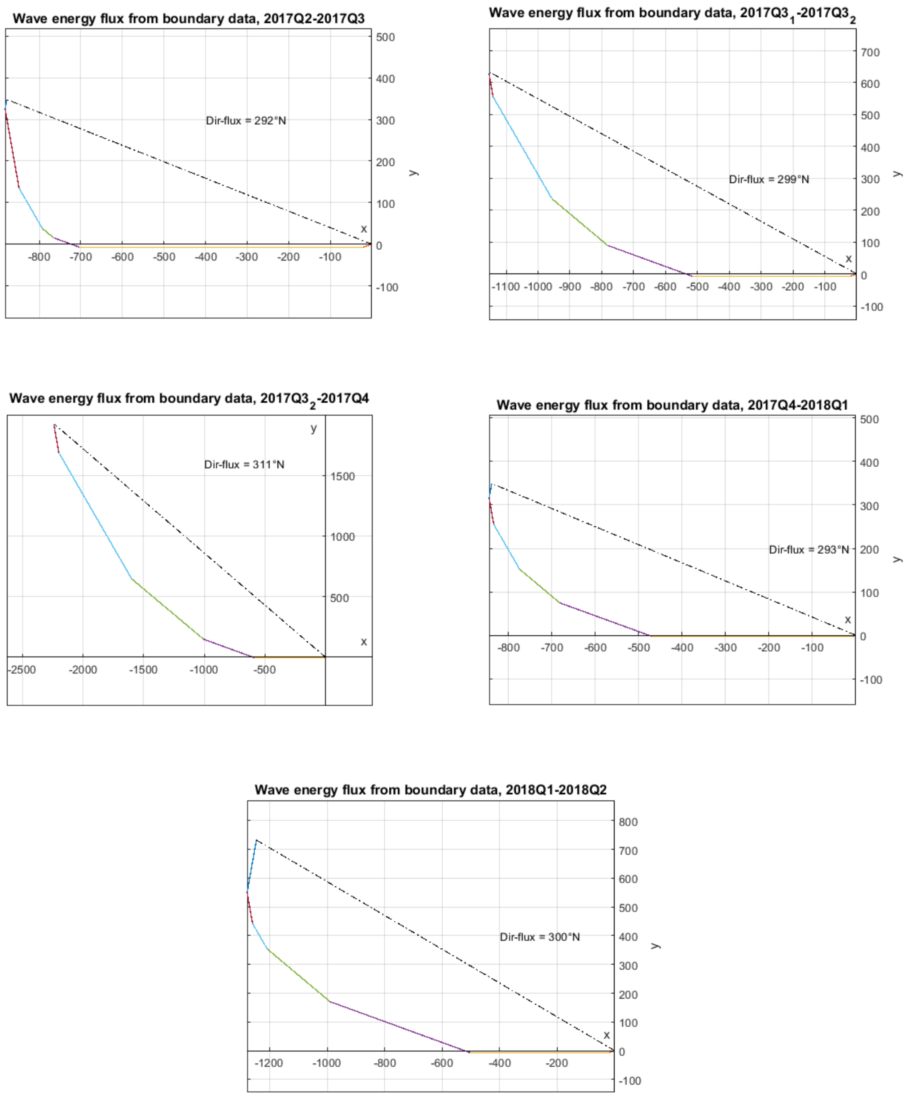

Figure C.14: Wave energy flux computation based on nearshore data per period between 2017Q2 and 2018Q3.

D

Methods and Tools

D.1. UNIBEST

D.1.1. Model Inputs - cross sections

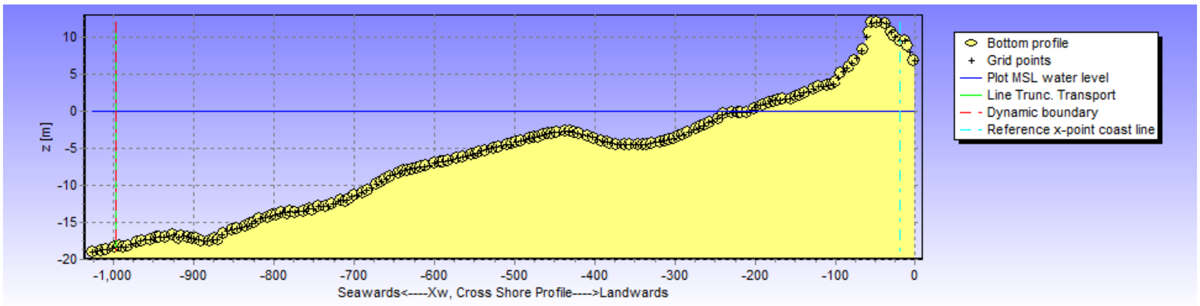

(a) Cross-shore profile of Kp4000, 2017 as implemented in UNIBEST

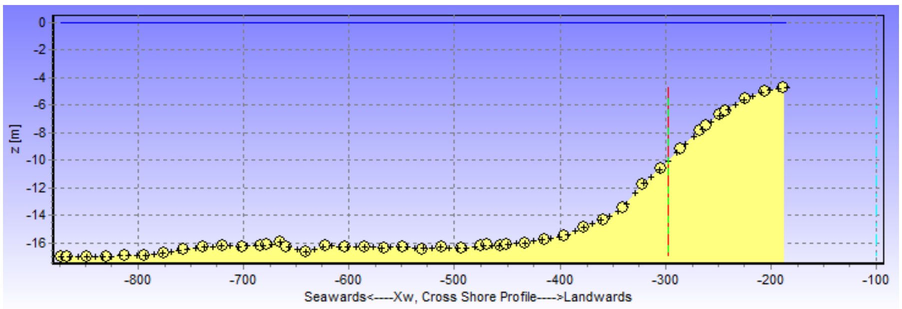

(b) Cross-shore profile of Kp2800, 2017, as implemented in UNIBEST. Note how the profile is cutoff at x = +/- -200 m, at a depth of 4 m, because this is where the breakwater starts and therefore sediment transport is obstructed.

Figure D.1: Two typical transects in UNIBEST (KP4000 and Kp2800

Table D.1: Tabular input of cross-shore profile Kp2800 in UNIBEST.

X [m]	Depth [m]
-187.638	4.7334
-206.057	4.9836
-224.476	5.5448
-242.895	6.3746
-248.461	6.6995
-261.315	7.4754
-266.881	7.8211
-285.3	9.1321
-303.719	10.5695
-322.138	11.7685
-340.557	13.4739
-358.977	14.3012
-377.396	14.8889
-395.815	15.4804
-414.234	15.709
-432.654	15.9776
-451.073	16.1356
-456.639	16.233
-469.492	16.1177
-475.058	16.2337
-493.477	16.3836
-511.896	16.2951
-530.316	16.4189
-548.735	16.2555
-567.154	16.3521
-585.573	16.2592
-603.992	16.3167
-622.412	16.1961
-640.831	16.6402
-659.25	16.2672
-664.816	15.9435
-677.669	16.1407
-683.235	16.1715
-701.654	16.251
-720.074	16.215
-738.493	16.2711
-756.912	16.496
-775.331	16.6936
-793.75	16.9426
-812.17	16.9243
-830.589	16.9625
-849.008	16.9905
-867.427	16.9721
-872.993	16.967

D.1.2. Model inputs - wave climate

In Table D.2, the imposed wave climate of the period 2017Q3-2-2017Q4 is presented.

Table D.2: Wave climate as imposed in UNIBEST for the period 2017Q3-2-2017Q4.

Scenario duration	64 days
Normalisation base	365 days

water level elevation [m]	Hsig [m]	Period [s]	Alfa [deg]	Duration [day]
0	0.5	3	5	0.166667
0	0.5	7	5	0.291667
0	1.25	7	5	0.166667
0	0.5	3	15	0.25
0	0.5	7	15	0.166667
0	0.5	3	25	0.041667
0	0.5	7	25	0.125
0	0.5	3	235	0.041667
0	0.5	7	235	0.041667
0	0.5	3	245	0.958333
0	0.5	7	245	0.041667
0	0.5	3	255	1.333333
0	0.5	7	255	0.625
0	0.5	3	265	2.458333
0	0.5	7	265	3.25
0	1.25	7	265	3.708333
0	1.75	7	265	0.375
0	0.5	3	275	1.5
0	0.5	7	275	1.958333
0	1.25	7	275	3.791667
0	1.75	7	275	1.333333
0	2.25	7	275	0.041667
0	0.5	3	285	1.125
0	0.5	7	285	0.666667
0	0.5	11	285	0.125
0	1.25	7	285	1.416667
0	1.75	7	285	1.041667
0	2.25	7	285	0.041667
0	0.5	3	295	0.875
0	0.5	7	295	0.5
0	0.5	11	295	0.041667
0	1.25	7	295	0.708333
0	1.75	7	295	1.625
0	2.25	7	295	0.375
0	0.5	3	305	0.208333
0	0.5	7	305	0.291667
0	0.5	11	305	0.083333
0	1.25	7	305	1.416667
0	1.75	7	305	1.958333

water level elevation [m]	Hsig [m]	Period [s]	Alfa [deg]	Duration [day]
0	0.5	11	315	0.041667
0	1.25	7	315	1.291667
0	1.75	7	315	0.875
0	1.75	15	315	0.125
0	2.25	7	315	0.916667
0	2.75	7	315	0.208333
0	2.75	11	315	0.041667
0	0.5	3	325	0.5
0	0.5	7	325	1
0	0.5	11	325	0.041667
0	1.25	7	325	2.5
0	1.75	7	325	2.041667
0	1.75	15	325	0.041667
0	2.25	7	325	0.666667
0	2.25	11	325	0.041667
0	2.75	7	325	0.125
0	0.5	3	335	0.375
0	0.5	7	335	2.208333
0	0.5	11	335	0.416667
0	1.25	7	335	3.583333
0	1.25	11	335	0.166667
0	1.75	7	335	3.041667
0	2.25	7	335	0.458333
0	2.25	11	335	0.208333
0	2.75	7	335	0.416667
0	2.75	11	335	0.125
0	3.3	11	335	0.041667
0	0.5	3	345	0.083333
0	0.5	7	345	1.583333
0	0.5	11	345	0.208333
0	1.25	7	345	2.041667
0	1.75	7	345	0.791667
0	2.25	7	345	0.041667
0	0.5	3	355	0.208333
0	0.5	7	355	0.208333
0	0.5	11	355	0.083333
0	1.25	7	355	0.125
0	1.75	7	355	0.25

D.1.3. Model inputs - Wave and transport parameters

Table D.3: Wave and transport parameters used in UNIBEST computations.

Transport formula	Bijker (1967,1971)
D50 [mum]	330
D90 [mum]	500
Sediment density [kg/m3̂]	2650
Seawater density [kg/m3̂]	1025
Porosity [-]	0.4
Bottom roughness [m]	0.05
Sediment fall velocity [m/s]	0.02
Criterion deep water, Hsig/h	0.07
Coefficient b deep water	2
Criterion shallow water, Hsig/h	0.6
Coefficient b shallow water	5
Coefficient for wave breaking (gamma) -	0.8
Coefficient for wave breaking (alfa)	1
Coefficient for bottom friction (f_w) [-]	0
Value of the bottom roughness (k_b) [m]	0.1

D.1.4. Model inputs - schematized tides for different transects

Table D.4: Schematized Tide for transect Kp2800

Kp2800			
DH	Vgety [m/s]	Ref. depth [m]	Perc. [%]
-0.7	-0.693	15	11.69
-0.945	-0.936	15	9.09
-0.865	-0.857	15	12.99
-0.83	-0.822	15	12.99
-0.575	-0.57	15	7.79
-0.11	-0.109	15	5.2
0.7	0.693	15	6.49
1.04	1.03	15	6.49
0.82	0.812	15	12.99
0.09	0.089	15	12.99

Table D.5: Schematized Tide for transect Kp3400

Kp3400			
DH	Vgety [m/s]	Ref. depth [m]	Perc. [%]
-0.54	-0.535	10	11.69
-0.785	-0.778	10	9.09
-0.705	-0.698	10	12.99
-0.67	-0.664	10	12.99
-0.415	-0.411	10	7.79
0.05	0.05	10	5.2
0.86	0.852	10	6.49
1.2	1.189	10	6.49
0.98	0.971	10	12.99
0.25	0.248	10	12.99

Table D.6: Schematized Tide for transect Kp4000

Kp4000			
DH	Vgety [m/s]	Ref. depth [m]	Perc. [%]
-0.34	-0.337	10	11.69
-0.585	-0.579	10	9.09
-0.505	-0.5	10	12.99
-0.47	-0.466	10	12.99
-0.215	-0.213	10	7.79
0.25	0.248	10	5.2
1.06	1.05	10	6.49
1.4	1.387	10	6.49
1.18	1.169	10	12.99
0.45	0.446	10	12.99

D.1.5. Calibration active profile height

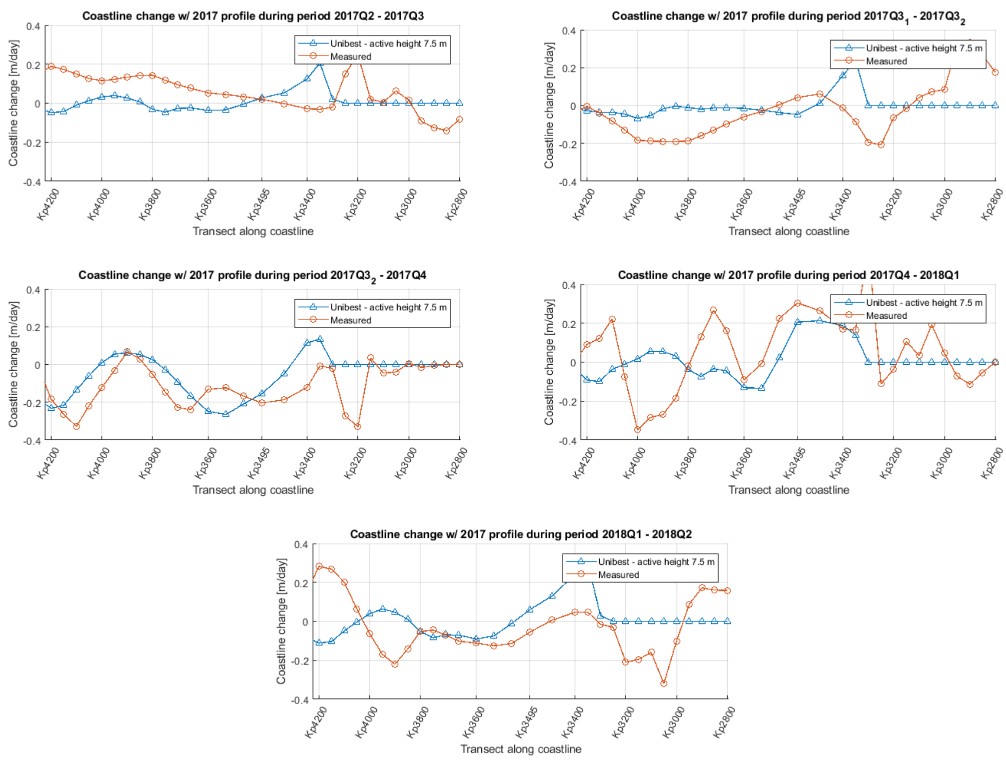

Figure D.2: UNIBEST results for an active profile height of 7.5 m.

D.1.6. Validation of reduced wave climate

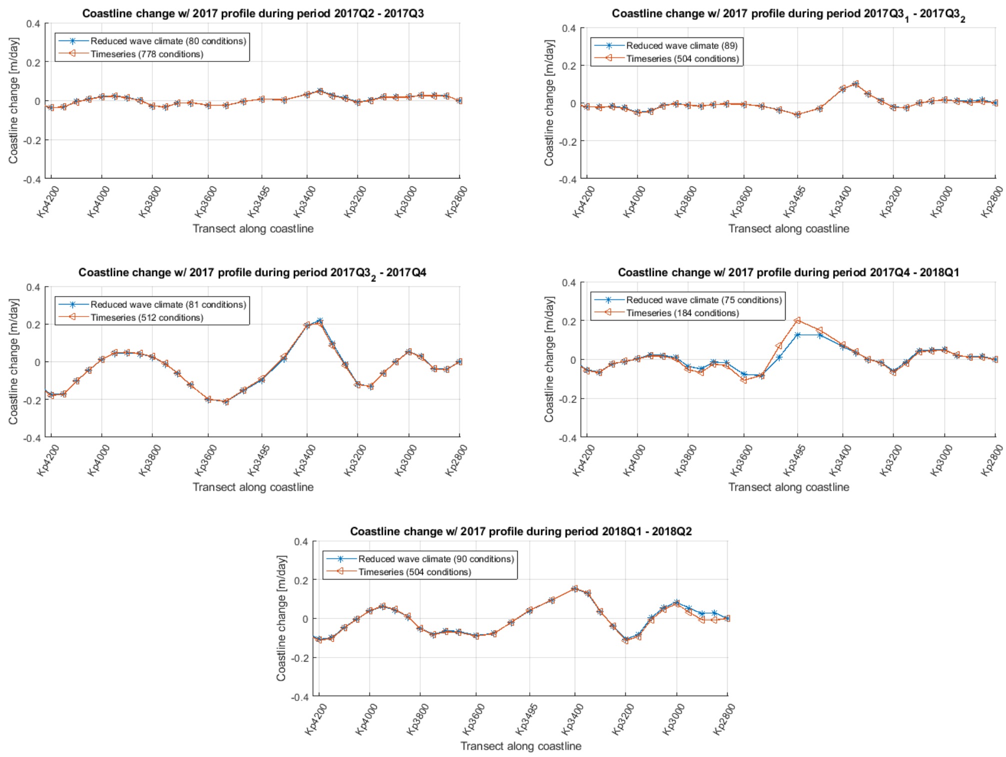

Figure D.3: Validation of reduced wave climate for UNIBEST with only wave input.

D.2. SWAN - nested grids

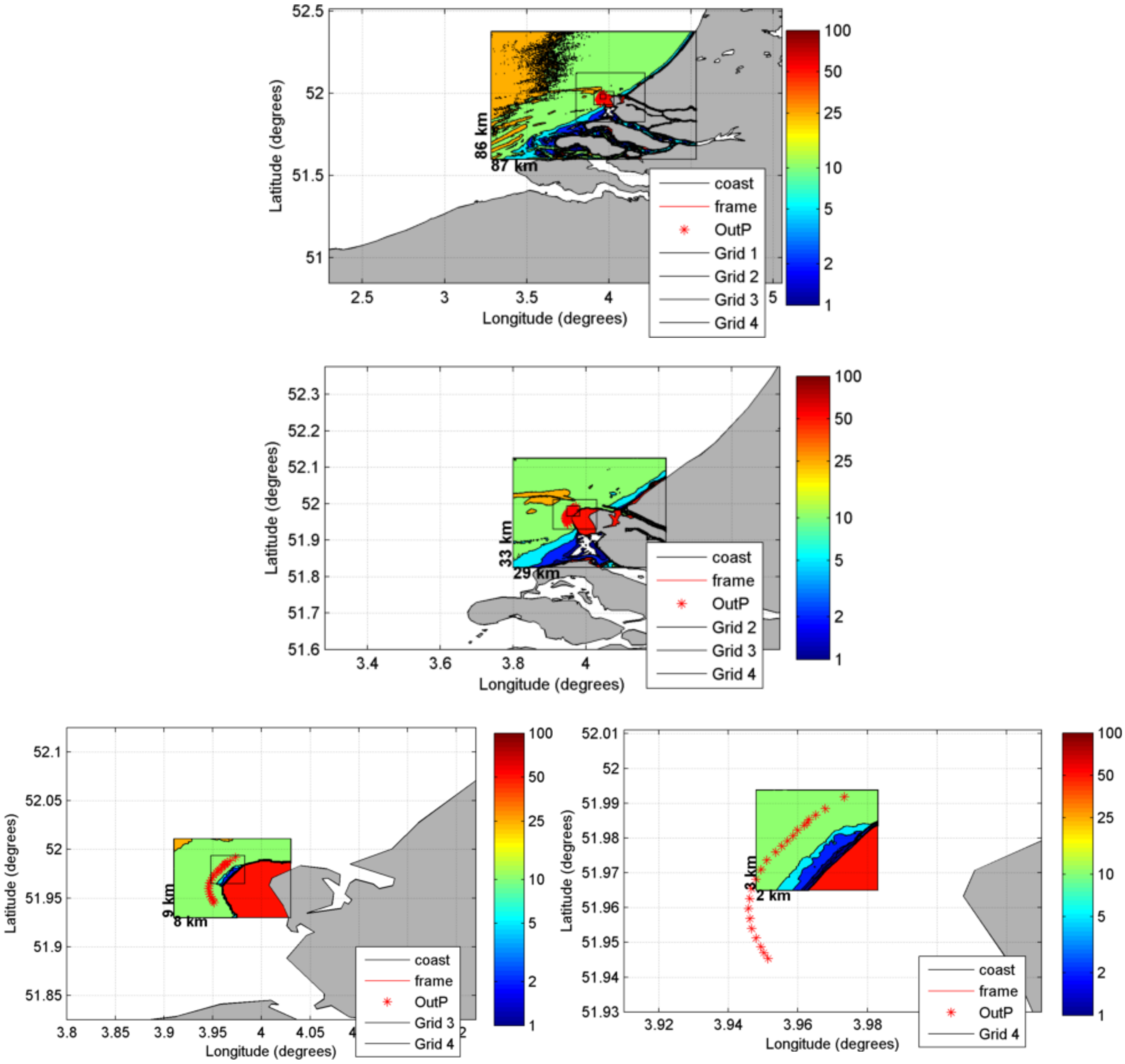

Figure D.4: Visualization of nested grids for the DIONE model.

D.3. SWAN master files for base case run without reflection

D.3.1. Input file base case run without reflection, grid A

```
$ *********************************************************************************************
$ *                              General model configuration                                  *
$ *********************************************************************************************
$ For documentation, go to:
$   http://swanmodel.sourceforge.net/
$
$ Project: MV2_ALAK
PROJ 'A' '0001'
SET LEVEL [LEV] CDCAP 0.002  HSRERR 0.15 NAUTICAL
MODE STATIONARY TWODIMENSIONAL
COORDINATES SPHERICAL
$ *********************************************************************************************
$ *                                    CGRID / BOTTOM                                         *
$ *********************************************************************************************
$               [xpc] [ypc]     [alpc] [xlenc] [ylenc]     [mxc] [myc]
CGRID REGULAR 3.283300 51.600000 0.000000 1.250000 0.775000 250 250 CIRCLE 36 &
flow=0.034500 fhigh=1.000000 msc=37
$     REGular [xpinp] [ypinp] [alpinp] [mxinp] [myinp] [dxinp] [dyinp]
INPGRID BOTTOM REGULAR 3.283300 51.600000 0.000000 250 250 0.005000 0.003100 EXC -999
READINP BOTTOM 1 'bottom\BIP2013_combined_a_99m_0m_closed.dep' 3 0 FREE
$ *********************************************************************************************
$ *                                         WIND                                              *
$ *********************************************************************************************
WIND [U10] [UDIR]
$ *********************************************************************************************
$ *                                       BOUNDARY                                            *
$ *********************************************************************************************
BOUND SHAPESPEC JONSWAP [GAMMA] PEAK DSPR DEGREES
BOUNDSPEC SIDE S CONSTANT PAR [HM0] [TP] [WDIR] [SPREAD]
BOUNDSPEC SIDE W CONSTANT PAR [HM0] [TP] [WDIR] [SPREAD]
BOUNDSPEC SIDE N CONSTANT PAR [HM0] [TP] [WDIR] [SPREAD]
BOUNDSPEC SIDE E CONSTANT PAR [HM0] [TP] [WDIR] [SPREAD]
NGRID 'B' 3.800000 51.825000 0.000000 0.420000 0.300000 350 400
NESTOUT 'B' 'bnest\B_[CASE_ID].bnd'
$ *********************************************************************************************
$ *                               COMPUTATIONAL PARAMETERS                                    *
$ *********************************************************************************************
$
GEN3 KOMen
$ DELTA=1 moves the dissipation focus towards high frequencies
WCAP KOM DELTA=1.0
PROP BSBT
OFF BNDCHK
FRICTION JONSWAP CONSTANT 0.038
BREaking CONstant 1.0 0.73
NUMERIC ACCUR 0.01 0.01 0.01 100.5 STAT 20
$ *********************************************************************************************
$ *                              POINT / FRAME / LINE definitions                             *
$ *********************************************************************************************
POINTS 'plist' FILE 'points\pointlist.txt'
$ *********************************************************************************************
$ *                                        OUTPUT                                             *
$ *********************************************************************************************
BLOCK 'COMPGRID' NOHEAD 'block\A01_[CASE_ID].mat' &
LAYOUT 3 XP YP DEPTH HS DIR PDIR WIND TPS TMM10 UBOT
```

```
TABLE 'plist' HEAD 'table\A01_[CASE_ID].tab' &
XP YP DEPTH WATLEV BOTLEV HS DIR PDIR TPS TMM10 TM02 WIND HSWELL UBOT
TEST 1 0 POINTS XY 3.973310 51.991780 &
3.967870 51.988400 &
3.958600 51.980620 &
PAR 'par\A01_[CASE_ID].par'[SPEC]
$ ********************************************************************************************
$ *                                          WRAP UP                                          *
$ ********************************************************************************************
INITIAL DEFAULT
COMPUTE
STOP
```

D.3.2. Input file base case run without reflection, grid B

```
$ ********************************************************************************************
$ *                            General model configuration                                    *
$ ********************************************************************************************
$ For documentation, go to:
$   http://swanmodel.sourceforge.net/
$
$ Project: MV2_ALAK
PROJ 'B' '0001'
SET LEVEL [LEV] CDCAP 0.002  HSRERR 0.15 NAUTICAL
MODE STATIONARY TWODIMENSIONAL
COORDINATES SPHERICAL
$ ********************************************************************************************
$ *                                   CGRID / BOTTOM                                          *
$ ********************************************************************************************
$               [xpc] [ypc]     [alpc] [xlenc] [ylenc]     [mxc] [myc]
CGRID REGULAR 3.800000 51.825000 0.000000 0.420000 0.300000 350 400 CIRCLE 36 flow=0.034500 &
fhigh=1.000000 msc=37
$     REGular [xpinp] [ypinp] [alpinp] [mxinp] [myinp] [dxinp] [dyinp]
INPGRID BOTTOM REGULAR 3.800000 51.825000 0.000000 350 400 0.001200 0.000750 EXC -999
READINP BOTTOM 1 'bottom\BIP2013_combined_B_99m_0m_closed.dep' 3 0 FREE
$ ********************************************************************************************
$ *                                        WIND                                               *
$ ********************************************************************************************
WIND [U10] [UDIR]
$ ********************************************************************************************
$ *                                      BOUNDARY                                             *
$ ********************************************************************************************
BOUNDNEST NEST 'bnest\B_[CASE_ID].bnd' CLOSED
NGRID 'C' 3.910000 51.930000 0.000000 0.120000 0.081000 400 450
NESTOUT 'C' 'bnest\C_[CASE_ID].bnd'
$ ********************************************************************************************
$ ********************************************************************************************
$ *                               COMPUTATIONAL PARAMETERS                                    *
$ ********************************************************************************************
$
GEN3 KOMen
$ DELTA=1 moves the dissipation focus towards high frequencies
WCAP KOM DELTA=1.0
PROP BSBT
OFF BNDCHK
FRICTION JONSWAP CONSTANT 0.038
BREaking CONstant 1.0 0.73
NUMERIC ACCUR 0.01 0.01 0.01 100.5 STAT 20
```

```
$ ***************************************************************************************
$ *                         POINT / FRAME / LINE definitions                            *
$ ***************************************************************************************
POINTS 'plist' FILE 'points\pointlist.txt'
$ ***************************************************************************************
$ *                                       OUTPUT                                        *
$ ***************************************************************************************
BLOCK 'COMPGRID' NOHEAD 'block\B01_[CASE_ID].mat' &
LAYOUT 3 XP YP DEPTH HS DIR PDIR WIND TPS TMM10 UBOT
TABLE 'plist' HEAD 'table\B01_[CASE_ID].tab' &
XP YP DEPTH WATLEV BOTLEV HS DIR PDIR TPS TMM10 TM02 WIND HSWELL UBOT
TEST 1 0 POINTS XY 3.973310 51.991780 &
3.967870 51.988400 &
3.958600 51.980620 &
PAR 'par\B01_[CASE_ID].par'[SPEC]
$ ***************************************************************************************
$ *                                      WRAP UP                                        *
$ ***************************************************************************************
INITIAL DEFAULT
COMPUTE
STOP
```

D.3.3. Input file base case run without reflection, grid C

```
$ ***************************************************************************************
$ *                         General model configuration                                 *
$ ***************************************************************************************
$ For documentation, go to:
$   http://swanmodel.sourceforge.net/
$
$ Project: MV2_ALAK
PROJ 'C' '0001'
SET LEVEL [LEV] CDCAP 0.002  HSRERR 0.15 NAUTICAL
MODE STATIONARY TWODIMENSIONAL
COORDINATES SPHERICAL
$ ***************************************************************************************
$ *                                  CGRID / BOTTOM                                     *
$ ***************************************************************************************
$               [xpc] [ypc]     [alpc] [xlenc] [ylenc]     [mxc] [myc]
CGRID REGULAR 3.910000 51.930000 0.000000 0.120000 0.081000 400 450 CIRCLE 36 flow=0.034500 &
fhigh=1.000000 msc=37
$     REGular [xpinp] [ypinp] [alpinp] [mxinp] [myinp] [dxinp] [dyinp]
INPGRID BOTTOM REGULAR 3.910000 51.930000 0.000000 400 450 0.000300 0.000180 EXC -999
READINP BOTTOM 1 'bottom\BIP2017_goed_C.dep' 3 0 FREE
$ ***************************************************************************************
$ *                                       WIND                                          *
$ ***************************************************************************************
WIND [U10] [UDIR]
$ ***************************************************************************************
$ *                                     BOUNDARY                                        *
$ ***************************************************************************************
BOUNDNEST NEST 'bnest\C_[CASE_ID].bnd' CLOSED
NGRID 'D' 3.948000 51.965000 0.000000 0.035000 0.028800 350 480
NESTOUT 'D' 'bnest\D_[CASE_ID].bnd'
$ ***************************************************************************************
$ ***************************************************************************************
$ *                              COMPUTATIONAL PARAMETERS                               *
$ ***************************************************************************************
```

```
$
GEN3 KOMen
$ DELTA=1 moves the dissipation focus towards high frequencies
WCAP KOM DELTA=1.0
PROP BSBT
OFF BNDCHK
FRICTION JONSWAP CONSTANT 0.038
BREaking CONstant 1.0 0.73
NUMERIC ACCUR 0.01 0.01 0.01 100.5 STAT 20
$ ***************************************************************************************
$ *                           POINT / FRAME / LINE definitions                          *
$ ***************************************************************************************
POINTS 'plist' FILE 'points\pointlist.txt'
$ ***************************************************************************************
$ *                                         OUTPUT                                      *
$ ***************************************************************************************
BLOCK 'COMPGRID' NOHEAD 'block\C01_[CASE_ID].mat' &
LAYOUT 3 XP YP DEPTH HS DIR PDIR WIND TPS TMM10 UBOT
TABLE 'plist' HEAD 'table\C01_[CASE_ID].tab' &
XP YP DEPTH WATLEV BOTLEV HS DIR PDIR TPS TMM10 TM02 WIND HSWELL UBOT
TEST 1 0 POINTS XY 3.973310 51.991780 &
3.967870 51.988400 &
3.958600 51.980620 &
PAR 'par\C01_[CASE_ID].par'[SPEC]
$ ***************************************************************************************
$ *                                        WRAP UP                                      *
$ ***************************************************************************************
INITIAL DEFAULT
COMPUTE
STOP
```

D.3.4. Input file base case run without reflection, grid C

```
$ ***************************************************************************************
$ *                           General model configuration                               *
$ ***************************************************************************************
$ For documentation, go to:
$   http://swanmodel.sourceforge.net/
$
$ Project: MV2_ALAK
PROJ 'D' '0001'
SET LEVEL [LEV] CDCAP 0.002  HSRERR 0.15 NAUTICAL
MODE STATIONARY TWODIMENSIONAL
COORDINATES SPHERICAL
$ ***************************************************************************************
$ *                                     CGRID / BOTTOM                                  *
$ ***************************************************************************************
$               [xpc] [ypc]     [alpc] [xlenc] [ylenc]     [mxc] [myc]
CGRID REGULAR 3.948000 51.965000 0.000000 0.035000 0.028800 350 480 CIRCLE 36 flow=0.034500 &
fhigh=1.000000 msc=37
$     REGular [xpinp] [ypinp] [alpinp] [mxinp] [myinp] [dxinp] [dyinp]
INPGRID BOTTOM REGULAR 3.948000 51.965000 0.000000 350 480 0.000100 0.000060 EXC -999
READINP BOTTOM 1 'bottom\BIP2017_goed_D.dep' 3 0 FREE
$ ***************************************************************************************
$ *                                          WIND                                       *
$ ***************************************************************************************
WIND [U10] [UDIR]
$ ***************************************************************************************
```

```
$ *                                    BOUNDARY                                      *
$ ************************************************************************************
BOUNDNEST NEST 'bnest\D_[CASE_ID].bnd' CLOSED
$ ************************************************************************************
$ *                              COMPUTATIONAL PARAMETERS                            *
$ ************************************************************************************
$
GEN3 KOMen
$ DELTA=1 moves the dissipation focus towards high frequencies
WCAP KOM DELTA=1.0
PROP BSBT
OFF BNDCHK
FRICTION JONSWAP CONSTANT 0.038
BREaking CONstant 1.0 0.73
NUMERIC ACCUR 0.01 0.01 0.01 100.5 STAT 20
$ ************************************************************************************
$ *                           POINT / FRAME / LINE definitions                       *
$ ************************************************************************************
POINTS 'plist' FILE 'points\pointlist.txt'
$ ************************************************************************************
$ *                                         OUTPUT                                   *
$ ************************************************************************************
BLOCK 'COMPGRID' NOHEAD 'block\D01_[CASE_ID].mat' &
LAYOUT 3 XP YP DEPTH HS DIR PDIR WIND TPS TMM10 UBOT
TABLE 'plist' HEAD 'table\D01_[CASE_ID].tab' &
XP YP DEPTH WATLEV BOTLEV HS DIR PDIR TPS TMM10 TM02 WIND HSWELL UBOT
TEST 1 0 POINTS XY 3.973310 51.991780 &
3.967870 51.988400 &
3.958600 51.980620 &
PAR 'par\D01_[CASE_ID].par'[SPEC]
$ ************************************************************************************
$ *                                        WRAP UP                                   *
$ ************************************************************************************
INITIAL DEFAULT
COMPUTE
STOP
```

D.4. SWAN master files for run with reflection coefficient = 0.2

D.4.1. Input file run with reflection coefficient = 0.2, grid A

```
$ ************************************************************************************
$ *                           General model configuration                            *
$ ************************************************************************************
$ For documentation, go to:
$   http://swanmodel.sourceforge.net/
$
$ Project: MV2_ALAK
PROJ 'A' '0001'
SET LEVEL [LEV] CDCAP 0.002  HSRERR 0.15 NAUTICAL
MODE STATIONARY TWODIMENSIONAL
COORDINATES SPHERICAL
$ ************************************************************************************
$ *                                   CGRID / BOTTOM                                 *
$ ************************************************************************************
$               [xpc] [ypc]     [alpc] [xlenc] [ylenc]     [mxc] [myc]
CGRID REGULAR 3.283300 51.600000 0.000000 1.250000 0.775000 250 250 CIRCLE 36 flow=0.034500 &
fhigh=1.000000 msc=37
$     REGular [xpinp] [ypinp] [alpinp] [mxinp] [myinp] [dxinp] [dyinp]
```

```
INPGRID BOTTOM REGULAR 3.283300 51.600000 0.000000 250 250 0.005000 0.003100 EXC -999
READINP BOTTOM 1 'bottom\BIP2013_combined_a_99m_0m_closed.dep' 3 0 FREE
$ ***********************************************************************************
$ *                                    WIND                                          *
$ ***********************************************************************************
WIND [U10] [UDIR]
$ ***********************************************************************************
$ *                                  BOUNDARY                                        *
$ ***********************************************************************************
BOUND SHAPESPEC JONSWAP [GAMMA] PEAK DSPR DEGREES
BOUNDSPEC SIDE S CONSTANT PAR [HM0] [TP] [WDIR] [SPREAD]
BOUNDSPEC SIDE W CONSTANT PAR [HM0] [TP] [WDIR] [SPREAD]
BOUNDSPEC SIDE N CONSTANT PAR [HM0] [TP] [WDIR] [SPREAD]
BOUNDSPEC SIDE E CONSTANT PAR [HM0] [TP] [WDIR] [SPREAD]
NGRID 'B' 3.800000 51.825000 0.000000 0.420000 0.300000 350 400
NESTOUT 'B' 'bnest\B_[CASE_ID].bnd'
$ ***********************************************************************************
$ *                                  OBSTACLES                                       *
$ ***********************************************************************************
$ DC5
OBST TRANSM 0 REFL 0.2 LINE 3.97649939812764 51.97889410537202 &
3.976493226422213 51.97914785432025 &
3.976569542908324 51.9794558632759 &
3.976672001865342 51.97979349027777 &
3.9770817686321 51.98042857500133 &
3.977379941086288 51.98074283872213 &
3.978154214154608 51.98142754656075 &
3.979052033606692 51.98236865389117 &
3.980187941330153 51.98325027378962 &
3.981761281786811 51.98424483685323 &
3.983879510855899 51.98515076031148 &
3.987946452444438 51.9862543348671 &
3.991760273070166 51.9871778358249 &
3.997121932564751 51.98820630951006 &
4.00039389962958 51.9888493807999 &
4.004709341892296 51.98919999174062 &
4.008869037443745 51.98908252587329 &
4.013605499782265 51.98818117068539 &
4.023442675555168 51.98570184351814 &
$ ***********************************************************************************
$ *                           COMPUTATIONAL PARAMETERS                               *
$ ***********************************************************************************
$
GEN3 KOMen
$ DELTA=1 moves the dissipation focus towards high frequencies
WCAP KOM DELTA=1.0
PROP BSBT
OFF BNDCHK
FRICTION JONSWAP CONSTANT 0.038
BREaking CONstant 1.0 0.73
NUMERIC ACCUR 0.01 0.01 0.01 100.5 STAT 20
$ ***********************************************************************************
$ *                         POINT / FRAME / LINE definitions                         *
$ ***********************************************************************************
POINTS 'plist' FILE 'points\pointlist.txt'
$ ***********************************************************************************
$ *                                    OUTPUT                                        *
```

```
$ ***********************************************************************************
BLOCK 'COMPGRID' NOHEAD 'block\A01_[CASE_ID].mat' &
LAYOUT 3 XP YP DEPTH HS DIR PDIR WIND TPS TMM10 UBOT
TABLE 'plist' HEAD 'table\A01_[CASE_ID].tab' &
XP YP DEPTH WATLEV BOTLEV HS DIR PDIR TPS TMM10 TM02 WIND HSWELL UBOT
TEST 1 0 POINTS XY 3.973310 51.991780 &
3.967870 51.988400 &
3.958600 51.980620 &
PAR 'par\A01_[CASE_ID].par'[SPEC]
$ ***********************************************************************************
$ *                                       WRAP UP                                    *
$ ***********************************************************************************
INITIAL DEFAULT
COMPUTE
STOP
```

D.4.2. Input file run with reflection coefficient = 0.2, grid B

```
$ ***********************************************************************************
$ *                          General model configuration                             *
$ ***********************************************************************************
$ For documentation, go to:
$   http://swanmodel.sourceforge.net/
$
$ Project: MV2_ALAK
PROJ 'B' '0001'
SET LEVEL [LEV] CDCAP 0.002  HSRERR 0.15 NAUTICAL
MODE STATIONARY TWODIMENSIONAL
COORDINATES SPHERICAL
$ ***********************************************************************************
$ *                                 CGRID / BOTTOM                                   *
$ ***********************************************************************************
$               [xpc] [ypc]     [alpc] [xlenc] [ylenc]     [mxc] [myc]
CGRID REGULAR 3.800000 51.825000 0.000000 0.420000 0.300000 350 400 CIRCLE 36 flow=0.034500 &
fhigh=1.000000 msc=37
$     REGular [xpinp] [ypinp] [alpinp] [mxinp] [myinp] [dxinp] [dyinp]
INPGRID BOTTOM REGULAR 3.800000 51.825000 0.000000 350 400 0.001200 0.000750 EXC -999
READINP BOTTOM 1 'bottom\BIP2013_combined_B_99m_0m_closed.dep' 3 0 FREE
$ ***********************************************************************************
$ *                                      WIND                                        *
$ ***********************************************************************************
WIND [U10] [UDIR]
$ ***********************************************************************************
$ *                                    BOUNDARY                                      *
$ ***********************************************************************************
BOUNDNEST NEST 'bnest\B_[CASE_ID].bnd' CLOSED
NGRID 'C' 3.910000 51.930000 0.000000 0.120000 0.081000 400 450
NESTOUT 'C' 'bnest\C_[CASE_ID].bnd'
$ ***********************************************************************************
$ *                                    OBSTACLES                                     *
$ ***********************************************************************************
$ DC5
OBST TRANSM 0 REFL 0.2 LINE 3.97649939812764 51.97889410537202 &
3.976493226422213 51.97914785432025 &
3.976569542908324 51.9794558632759 &
3.976672001865342 51.97979349027777 &
3.9770817686321 51.98042857500133 &
3.977379941086288 51.98074283872213 &
```

```
3.978154214154608 51.98142754656075 &
3.979052033606692 51.98236865389117 &
3.980187941330153 51.98325027378962 &
3.981761281786811 51.98424483685323 &
3.983879510855899 51.98515076031148 &
3.987946452444438 51.9862543348671 &
3.991760273070166 51.9871778358249 &
3.997121932564751 51.98820630951006 &
4.00039389962958 51.9888493807999 &
4.004709341892296 51.98919999174062 &
4.008869037443745 51.98908252587329 &
4.013605499782265 51.98818117068539 &
4.023442675555168 51.98570184351814 &
$ ******************************************************************************************
$ *                               COMPUTATIONAL PARAMETERS                                 *
$ ******************************************************************************************
$
GEN3 KOMen
$ DELTA=1 moves the dissipation focus towards high frequencies
WCAP KOM DELTA=1.0
PROP BSBT
OFF BNDCHK
FRICTION JONSWAP CONSTANT 0.038
BREaking CONstant 1.0 0.73
NUMERIC ACCUR 0.01 0.01 0.01 100.5 STAT 20
$ ******************************************************************************************
$ *                            POINT / FRAME / LINE definitions                            *
$ ******************************************************************************************
POINTS 'plist' FILE 'points\pointlist.txt'
$ ******************************************************************************************
$ *                                          OUTPUT                                        *
$ ******************************************************************************************
BLOCK 'COMPGRID' NOHEAD 'block\B01_[CASE_ID].mat' &
LAYOUT 3 XP YP DEPTH HS DIR PDIR WIND TPS TMM10 UBOT
TABLE 'plist' HEAD 'table\B01_[CASE_ID].tab' &
XP YP DEPTH WATLEV BOTLEV HS DIR PDIR TPS TMM10 TM02 WIND HSWELL UBOT
TEST 1 0 POINTS XY 3.973310 51.991780 &
3.967870 51.988400 &
3.958600 51.980620 &
PAR 'par\B01_[CASE_ID].par'[SPEC]
$ ******************************************************************************************
$ *                                         WRAP UP                                        *
$ ******************************************************************************************
INITIAL DEFAULT
COMPUTE
STOP
```

D.4.3. Input file run with reflection coefficient = 0.2, grid C

```
$ ******************************************************************************************
$ *                            General model configuration                                 *
$ ******************************************************************************************
$ For documentation, go to:
$   http://swanmodel.sourceforge.net/
$
$ Project: MV2_ALAK
PROJ 'C' '0001'
SET LEVEL [LEV] CDCAP 0.002  HSRERR 0.15 NAUTICAL
```

```
MODE STATIONARY TWODIMENSIONAL
COORDINATES SPHERICAL
$ ***************************************************************************************
$ *                                  CGRID / BOTTOM                                      *
$ ***************************************************************************************
$               [xpc] [ypc]     [alpc] [xlenc] [ylenc]     [mxc] [myc]
CGRID REGULAR 3.910000 51.930000 0.000000 0.120000 0.081000 400 450 CIRCLE 36 flow=0.034500 &
fhigh=1.000000 msc=37
$     REGular [xpinp] [ypinp] [alpinp] [mxinp] [myinp] [dxinp] [dyinp]
INPGRID BOTTOM REGULAR 3.910000 51.930000 0.000000 400 450 0.000300 0.000180 EXC -999
READINP BOTTOM 1 'bottom\BIP2017_goed_C_blokkendamweg.dep' 3 0 FREE
$ ***************************************************************************************
$ *                                       WIND                                           *
$ ***************************************************************************************
WIND [U10] [UDIR]
$ ***************************************************************************************
$ *                                     BOUNDARY                                         *
$ ***************************************************************************************
BOUNDNEST NEST 'bnest\C_[CASE_ID].bnd' CLOSED
NGRID 'D' 3.948000 51.965000 0.000000 0.035000 0.028800 350 480
NESTOUT 'D' 'bnest\D_[CASE_ID].bnd'
$ ***************************************************************************************
$ *                                     OBSTACLES                                        *
$ ***************************************************************************************
$ DC5
OBST TRANSM 0 REFL 0.2 LINE 3.97649939812764 51.97889410537202 &
3.976493226422213 51.97914785432025 &
3.976569542908324 51.9794558632759 &
3.976672001865342 51.97979349027777 &
3.9770817686321 51.98042857500133 &
3.977379941086288 51.98074283872213 &
3.978154214154608 51.98142754656075 &
3.979052033606692 51.98236865389117 &
3.980187941330153 51.98325027378962 &
3.981761281786811 51.98424483685323 &
3.983879510855899 51.98515076031148 &
3.987946452444438 51.9862543348671 &
3.991760273070166 51.9871778358249 &
3.997121932564751 51.98820630951006 &
4.00039389962958 51.9888493807999 &
4.004709341892296 51.98919999174062 &
4.008869037443745 51.98908252587329 &
4.013605499782265 51.98818117068539 &
4.023442675555168 51.98570184351814 &
$ ***************************************************************************************
$ *                            COMPUTATIONAL PARAMETERS                                  *
$ ***************************************************************************************
$
GEN3 KOMen
$ DELTA=1 moves the dissipation focus towards high frequencies
WCAP KOM DELTA=1.0
PROP BSBT
OFF BNDCHK
FRICTION JONSWAP CONSTANT 0.038
BREaking CONstant 1.0 0.73
NUMERIC ACCUR 0.01 0.01 0.01 100.5 STAT 20
$ ***************************************************************************************
```

```
$ *                          POINT / FRAME / LINE definitions                          *
$ **********************************************************************************
POINTS 'plist' FILE 'points\pointlist.txt'
$ **********************************************************************************
$ *                                        OUTPUT                                  *
$ **********************************************************************************
BLOCK 'COMPGRID' NOHEAD 'block\C01_[CASE_ID].mat' &
LAYOUT 3 XP YP DEPTH HS DIR PDIR WIND TPS TMM10 UBOT
TABLE 'plist' HEAD 'table\C01_[CASE_ID].tab' &
XP YP DEPTH WATLEV BOTLEV HS DIR PDIR TPS TMM10 TM02 WIND HSWELL UBOT
TEST 1 0 POINTS XY 3.973310 51.991780 &
3.967870 51.988400 &
3.958600 51.980620 &
PAR 'par\C01_[CASE_ID].par'[SPEC]
$ **********************************************************************************
$ *                                       WRAP UP                                  *
$ **********************************************************************************
INITIAL DEFAULT
COMPUTE
STOP
```

D.4.4. Input file run with reflection coefficient = 0.2, grid D

```
$ **********************************************************************************
$ *                          General model configuration                           *
$ **********************************************************************************
$ For documentation, go to:
$   http://swanmodel.sourceforge.net/
$
$ Project: MV2_ALAK
PROJ 'D' '0001'
SET LEVEL [LEV] CDCAP 0.002  HSRERR 0.15 NAUTICAL
MODE STATIONARY TWODIMENSIONAL
COORDINATES SPHERICAL
$ **********************************************************************************
$ *                                   CGRID / BOTTOM                               *
$ **********************************************************************************
$                [xpc] [ypc]     [alpc] [xlenc] [ylenc]     [mxc] [myc]
CGRID REGULAR 3.948000 51.965000 0.000000 0.035000 0.028800 350 480 CIRCLE 36 flow=0.034500 &
fhigh=1.000000 msc=37
$     REGular [xpinp] [ypinp] [alpinp] [mxinp] [myinp] [dxinp] [dyinp]
INPGRID BOTTOM REGULAR 3.948000 51.965000 0.000000 350 480 0.000100 0.000060 EXC -999
READINP BOTTOM 1 'bottom\BIP2017_goed_D_blokkendamweg.dep' 3 0 FREE
$ **********************************************************************************
$ *                                         WIND                                   *
$ **********************************************************************************
WIND [U10] [UDIR]
$ **********************************************************************************
$ *                                       BOUNDARY                                 *
$ **********************************************************************************
BOUNDNEST NEST 'bnest\D_[CASE_ID].bnd' CLOSED
$ **********************************************************************************
$ *                                       OBSTACLES                                *
$ **********************************************************************************
$ DC5
OBST TRANSM 0 REFL 0.2 LINE 3.97649939812764 51.97889410537202 &
3.976493226422213 51.97914785432025 &
3.976569542908324 51.9794558632759 &
```

```
3.976672001865342 51.97979349027777 &
3.9770817686321 51.98042857500133 &
3.977379941086288 51.98074283872213 &
3.978154214154608 51.98142754656075 &
3.979052033606692 51.98236865389117 &
3.980187941330153 51.98325027378962 &
3.981761281786811 51.98424483685323 &
3.983879510855899 51.98515076031148 &
3.987946452444438 51.9862543348671 &
3.991760273070166 51.9871778358249 &
3.997121932564751 51.98820630951006 &
4.00039389962958 51.9888493807999 &
4.004709341892296 51.98919999174062 &
4.008869037443745 51.98908252587329 &
4.013605499782265 51.98818117068539 &
4.023442675555168 51.98570184351814 &
$ *******************************************************************************************
$ *                              COMPUTATIONAL PARAMETERS                                  *
$ *******************************************************************************************
$
GEN3 KOMen
$ DELTA=1 moves the dissipation focus towards high frequencies
WCAP KOM DELTA=1.0
PROP BSBT
OFF BNDCHK
FRICTION JONSWAP CONSTANT 0.038
BREaking CONstant 1.0 0.73
NUMERIC ACCUR 0.01 0.01 0.01 100.5 STAT 20
$ *******************************************************************************************
$ *                           POINT / FRAME / LINE definitions                             *
$ *******************************************************************************************
POINTS 'plist' FILE 'points\pointlist.txt'
$ *******************************************************************************************
$ *                                         OUTPUT                                         *
$ *******************************************************************************************
BLOCK 'COMPGRID' NOHEAD 'block\D01_[CASE_ID].mat' &
LAYOUT 3 XP YP DEPTH HS DIR PDIR WIND TPS TMM10 UBOT
TABLE 'plist' HEAD 'table\D01_[CASE_ID].tab' &
XP YP DEPTH WATLEV BOTLEV HS DIR PDIR TPS TMM10 TM02 WIND HSWELL UBOT
TEST 1 0 POINTS XY 3.973310 51.991780 &
3.967870 51.988400 &
3.958600 51.980620 &
PAR 'par\D01_[CASE_ID].par'[SPEC]
$ *******************************************************************************************
$ *                                        WRAP UP                                         *
$ *******************************************************************************************
INITIAL DEFAULT
COMPUTE
STOP
```

D.5. Other SWAN input files

D.5.1. Output points

```
3.981296 51.985258
3.980198 51.984976
3.979159 51.984694
3.978059 51.984501
3.976414 51.984481
```

```
3.975253 51.984377
3.974094 51.984183
3.972921 51.983989
3.972187 51.983711
3.971101 51.983069
3.970044 51.982427
3.969875 51.982245
3.969549 51.981971
3.969266 51.981698
3.968608 51.980881
3.967056 51.979334
3.965605 51.977789
3.963285 51.976592
3.962175 51.974870
3.960097 51.973407
3.958332 51.971228
3.956888 51.969053
3.956017 51.966705
3.955320 51.964359
3.954694 51.962104
3.981625 51.984993
3.980524 51.984800
3.979529 51.984518
3.978547 51.984237
3.977479 51.983954
3.976672 51.983675
3.975645 51.983483
3.974824 51.983203
3.973942 51.983013
3.972221 51.982633
3.970827 51.982077
3.970774 51.981896
3.970567 51.981534
3.970416 51.981263
3.969833 51.980357
3.968280 51.978810
3.966315 51.977438
3.964850 51.975892
3.963150 51.974433
3.961187 51.972971
3.959816 51.970797
3.958444 51.968622
3.957305 51.966451
3.956428 51.964283
3.955729 51.962027
3.982073 51.984639
3.980911 51.984535
3.980017 51.984254
3.979080 51.983973
3.978113 51.983692
3.977365 51.983414
3.976561 51.983044
3.975798 51.982766
3.975079 51.982487
3.973682 51.982021
3.972345 51.981466
3.972162 51.981284
```

```
3.971938 51.981011
3.971568 51.980737
3.970793 51.979919
3.969267 51.978462
3.967362 51.977001
3.965912 51.975455
3.963929 51.974173
3.823702 51.955805
3.960802 51.970449
3.959323 51.968453
3.958152 51.966372
3.957322 51.964114
3.956838 51.961951
3.982135 51.984504
3.981463 51.984119
3.980776 51.983742
3.980104 51.983356
3.979534 51.982945
3.979049 51.982625
3.978493 51.982258
3.978039 51.981893
3.977791 51.981441
3.977001 51.980623
3.976090 51.979982
3.975702 51.979798
3.975388 51.979614
3.974972 51.979430
3.973859 51.978697
3.972144 51.977238
3.970414 51.975779
3.968623 51.974409
3.967220 51.972774
3.965816 51.971139
3.963976 51.969499
3.962433 51.967682
3.961579 51.965694
3.960417 51.963792
3.959843 51.961718
```

D.5.2. Wave conditions

```
# Number of cases
9
# Theta (degree) / Hm0 (m) / Tp (s) / Water level (m) / u10 (m/s) / u10d (degree)
227.000000 4.510000 8.330000 0.810000 2.000000 220.000000 3.300000 30.000000
263.000000 5.000000 9.090000 -0.750000 0.000000 280.000000 3.300000 30.000000
341.000000 4.030000 8.330000 -0.610000 1.500000 320.000000 3.300000 30.000000
295.000000 5.000000 8.330000 0.350000 1.400000 280.000000 3.300000 30.000000
341.000000 3.140000 10.000000 0.280000 1.300000 330.000000 3.300000 30.000000
47.000000 3.360000 7.140000 -0.720000 1.600000 70.000000 3.300000 30.000000
324.000000 4.600000 9.090000 -0.690000 1.800000 310.000000 3.300000 30.000000
357.000000 3.280000 7.690000 -0.730000 1.300000 10.000000 3.300000 30.000000
16.000000 2.610000 7.140000 -0.410000 1.200000 330.000000 3.300000 30.000000
```

D.6. XBeach input files

D.6.1. Input file run with reflection

```
%%%%%%%%%%%%%%%%%%%%%%%%%%%%%%%%%%%%%%%%%%%%%%%%%%%%%%%%%%%%%%%%%%%%%%%%%%%%%%%%
%%% XBeach parameter settings input file                                     %%%
%%%                                                                          %%%
%%% date:     14-Mar-2014 15:31:14                                           %%%
%%% function: xb_write_params                                                %%%
%%%%%%%%%%%%%%%%%%%%%%%%%%%%%%%%%%%%%%%%%%%%%%%%%%%%%%%%%%%%%%%%%%%%%%%%%%%%%%%%

%%% Bed composition parameters %%%%%%%%%%%%%%%%%%%%%%%%%%%%%%%%%%%%%%%%%%%%%%%%%

D50          = 0.000330
D90          = 0.000500

%%% Flow boundary condition parameters %%%%%%%%%%%%%%%%%%%%%%%%%%%%%%%%%%%%%%%%%

left         = neumann
right        = neumann
epsi         = -1

%%% General %%%%%%%%%%%%%%%%%%%%%%%%%%%%%%%%%%%%%%%%%%%%%%%%%%%%%%%%%%%%%%%%%%%%

gridform     = delft3d
xyfile       = mv2_nest_ref3_xb.grd

%%% Grid parameters %%%%%%%%%%%%%%%%%%%%%%%%%%%%%%%%%%%%%%%%%%%%%%%%%%%%%%%%%%%%

depfile      = present_170509_xb_kruin.dep
posdwn       = 1
alfa         = 0
xori         = 0
yori         = 0
thetamin     = 270
thetamax     = 390
dtheta       = 20
thetanaut    = 1

%%% Initial conditions %%%%%%%%%%%%%%%%%%%%%%%%%%%%%%%%%%%%%%%%%%%%%%%%%%%%%%%%%

zs0file      = storm_opgetreden_waterlevels.txt

%%% Model time %%%%%%%%%%%%%%%%%%%%%%%%%%%%%%%%%%%%%%%%%%%%%%%%%%%%%%%%%%%%%%%%%

tstop        = 154800

%%% Morphology parameters %%%%%%%%%%%%%%%%%%%%%%%%%%%%%%%%%%%%%%%%%%%%%%%%%%%%%%

morfac       = 10
morstart     = 7200
struct       = 1
ne_layer     = struct_smooth2.dat

%%% Tide boundary conditions %%%%%%%%%%%%%%%%%%%%%%%%%%%%%%%%%%%%%%%%%%%%%%%%%%%

tideloc      = 2
paulrevere   = 0
```

```
%%% Wave boundary condition parameters %%%%%%%%%%%%%%%%%%%%%%%%%%%%%%%%%%%%%%%%%

instat       = 41
lateralwave  = wavecrest

%%% Wave-current interaction parameters %%%%%%%%%%%%%%%%%%%%%%%%%%%%%%%%%%%%%%%%

wci          = 0

%%% Wave-spectrum boundary condition parameters %%%%%%%%%%%%%%%%%%%%%%%%%%%%%%%%

bcfile       = storm_opgetreden.txt
random       = 0

%%% Output variables %%%%%%%%%%%%%%%%%%%%%%%%%%%%%%%%%%%%%%%%%%%%%%%%%%%%%%%%%%%

outputformat = netcdf
tintm        = 3600
tintp        = 600
tintg        = 600
tstart       = 0

nglobalvar   = 8
zb
zs
H
thetamean
u
v
Sutot
Svtot

nmeanvar     = 7
zb
zs
H
u
v
Sutot
Svtot

npointvar    = 0

npoints      = 0
```

D.6.2. Input file run without reflection

```
%%%%%%%%%%%%%%%%%%%%%%%%%%%%%%%%%%%%%%%%%%%%%%%%%%%%%%%%%%%%%%%%%%%%%%%%%%%%%%%%
%%% XBeach parameter settings input file                                     %%%
%%%                                                                          %%%
%%% date:     14-Mar-2014 15:31:14                                           %%%
%%% function: xb_write_params                                                %%%
%%%%%%%%%%%%%%%%%%%%%%%%%%%%%%%%%%%%%%%%%%%%%%%%%%%%%%%%%%%%%%%%%%%%%%%%%%%%%%%%

%%% Bed composition parameters %%%%%%%%%%%%%%%%%%%%%%%%%%%%%%%%%%%%%%%%%%%%%%%%%

D50          = 0.000330
D90          = 0.000500
```

```
%%% Flow boundary condition parameters %%%%%%%%%%%%%%%%%%%%%%%%%%%%%%%%%%%%%%%%%

left         = neumann
right        = neumann
epsi         = -1

%%% General %%%%%%%%%%%%%%%%%%%%%%%%%%%%%%%%%%%%%%%%%%%%%%%%%%%%%%%%%%%%%%%%%%%%

gridform     = delft3d
xyfile       = mv2_nest_ref3_xb.grd

%%% Grid parameters %%%%%%%%%%%%%%%%%%%%%%%%%%%%%%%%%%%%%%%%%%%%%%%%%%%%%%%%%%%%

depfile      = present_170509_xb_kruin.dep
posdwn       = 1
alfa         = 0
xori         = 0
yori         = 0
thetamin     = 270
thetamax     = 390
dtheta       = 20
thetanaut    = 1

%%% Initial conditions %%%%%%%%%%%%%%%%%%%%%%%%%%%%%%%%%%%%%%%%%%%%%%%%%%%%%%%%%

zs0file      = storm_opgetreden_waterlevels.txt

%%% Model time %%%%%%%%%%%%%%%%%%%%%%%%%%%%%%%%%%%%%%%%%%%%%%%%%%%%%%%%%%%%%%%%%

tstop        = 154800

%%% Morphology parameters %%%%%%%%%%%%%%%%%%%%%%%%%%%%%%%%%%%%%%%%%%%%%%%%%%%%%%

morfac       = 10
morstart     = 7200
struct       = 1
ne_layer     = struct_smooth2.dat

%%% Bed friction parameters %%%%%%%%%%%%%%%%%%%%%%%%%%%%%%%%%%%%%%%%%%%%%%%%%%%

bedfriction = chezy
bedfricfile = bedfric_20.dep

%%% Tide boundary conditions %%%%%%%%%%%%%%%%%%%%%%%%%%%%%%%%%%%%%%%%%%%%%%%%%%%

tideloc      = 2
paulrevere   = 0

%%% Wave boundary condition parameters %%%%%%%%%%%%%%%%%%%%%%%%%%%%%%%%%%%%%%%%%

instat       = 41
lateralwave  = wavecrest

%%% Wave-current interaction parameters %%%%%%%%%%%%%%%%%%%%%%%%%%%%%%%%%%%%%%%%

wci          = 0
```

```
%%% Wave-spectrum boundary condition parameters %%%%%%%%%%%%%%%%%%%%%%%%%%%%%%%%

bcfile       = storm_opgetreden.txt
random       = 0

%%% Output variables %%%%%%%%%%%%%%%%%%%%%%%%%%%%%%%%%%%%%%%%%%%%%%%%%%%%%%%%%%%%

outputformat = netcdf
tintm        = 3600
tintp        = 600
tintg        = 600
tstart       = 0

nglobalvar   = 8
zb
zs
H
thetamean
u
v
Sutot
Svtot

nmeanvar     = 7
zb
zs
H
u
v
Sutot
Svtot

npointvar    = 0

npoints      = 0
```

D.6.3. Wave boundary condition file

```
1.81 6.69 332.3 3.3 20 3600 1
2.06 7.31 330.5 3.3 20 3600 1
2.13 7.68 330.7 3.3 20 3600 1
2.29 7.37 319.2 3.3 20 3600 1
2.5 8.25 324.5 3.3 20 3600 1
2.22 8.21 321.6 3.3 20 3600 1
2.19 8.2 315.5 3.3 20 3600 1
2.23 7.76 318.5 3.3 20 3600 1
1.98 6.85 314 3.3 20 3600 1
2.26 7.8 316.2 3.3 20 3600 1
2.12 7.31 315.4 3.3 20 3600 1
2.27 7.38 311.8 3.3 20 3600 1
2.2 8.2 309.1 3.3 20 3600 1
2.15 7.68 307.5 3.3 20 3600 1
1.81 6.68 302.8 3.3 20 3600 1
1.99 6.82 315.2 3.3 20 3600 1
2.47 7.88 320.6 3.3 20 3600 1
2.87 8.99 322.1 3.3 20 3600 1
2.83 8.43 322.7 3.3 20 3600 1
```

```
3.05 9.04 322.6 3.3 20 3600 1
3.11 9.86 323.9 3.3 20 3600 1
3.49 11 325.8 3.3 20 3600 1
3.36 10.99 324.5 3.3 20 3600 1
3.35 9.9 328.5 3.3 20 3600 1
3.06 9.86 328.7 3.3 20 3600 1
3.08 9.86 328.9 3.3 20 3600 1
2.57 7.96 330.7 3.3 20 3600 1
2.42 7.87 328.4 3.3 20 3600 1
2.63 8.97 331.8 3.3 20 3600 1
2.39 8.94 330 3.3 20 3600 1
2.24 8.94 335.5 3.3 20 3600 1
2.22 8.94 331.8 3.3 20 3600 1
1.63 6.21 326.1 3.3 20 3600 1
1.77 6.64 325.7 3.3 20 3600 1
2.13 8.93 327.3 3.3 20 3600 1
2.32 10.93 326.2 3.3 20 3600 1
2.36 8.94 326.6 3.3 20 3600 1
2.31 7.82 330.2 3.3 20 3600 1
2 6.89 335 3.3 20 3600 1
2.14 8.2 329.1 3.3 20 3600 1
2.04 8.19 336.4 3.3 20 3600 1
1.9 7.61 333.3 3.3 20 3600 1
2.04 8.2 336.5 3.3 20 3600 1
1.78 7.23 335.9 3.3 20 3600 1
1.79 6.76 333.1 3.3 20 3600 1
```

D.6.4. Wave levels boundary condition file

```
0 0.09 0.09
3600 0.78 0.78
7200 1.05 1.05
10800 0.93 0.93
14400 0.7 0.7
18000 0.17 0.17
21600 -0.4 -0.4
25200 -0.58 -0.58
28800 -0.47 -0.47
32400 -0.53 -0.53
36000 -0.58 -0.58
39600 -0.43 -0.43
43200 -0.02 -0.02
46800 0.85 0.85
50400 1.41 1.41
54000 1.28 1.28
57600 1.12 1.12
61200 0.72 0.72
64800 0.14 0.14
68400 -0.27 -0.27
72000 -0.26 -0.26
75600 -0.32 -0.32
79200 -0.4 -0.4
82800 -0.36 -0.36
86400 -0.28 -0.28
90000 0.2 0.2
93600 1 1
97200 1.11 1.11
100800 0.95 0.95
```

```
104400 0.62 0.62
108000 0 0
111600 -0.57 -0.57
115200 -0.59 -0.59
118800 -0.45 -0.45
122400 -0.54 -0.54
126000 -0.53 -0.53
129600 -0.39 -0.39
133200 0.07 0.07
136800 1.11 1.11
140400 1.48 1.48
144000 1.24 1.24
147600 1.03 1.03
151200 0.56 0.56
154800 -0.05 -0.05
```

D.6.5. Implementation of non-erodible layer in XBeach.

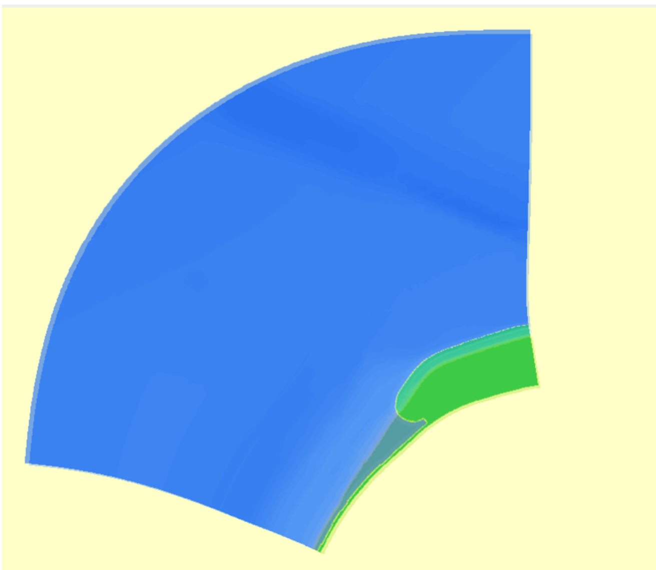

Figure D.5: Visualisation of non-erodible layer in XBeach model (green layer)

.

D.6.6. Implementation of locally increased friction coefficient

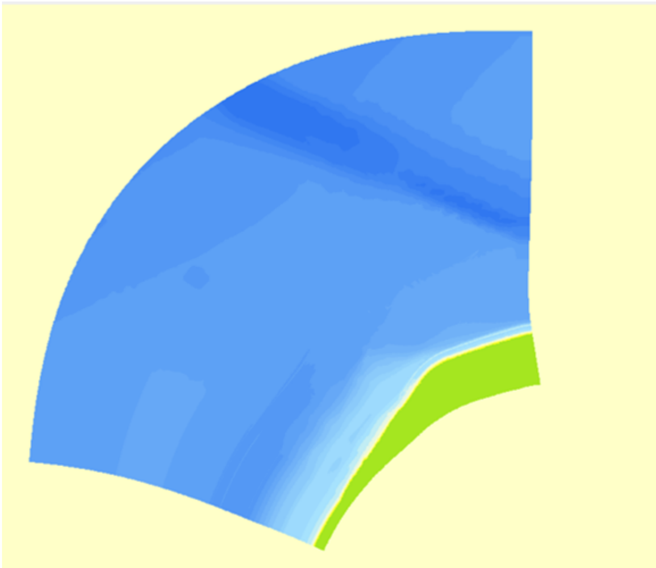

(a) XBeach depfile

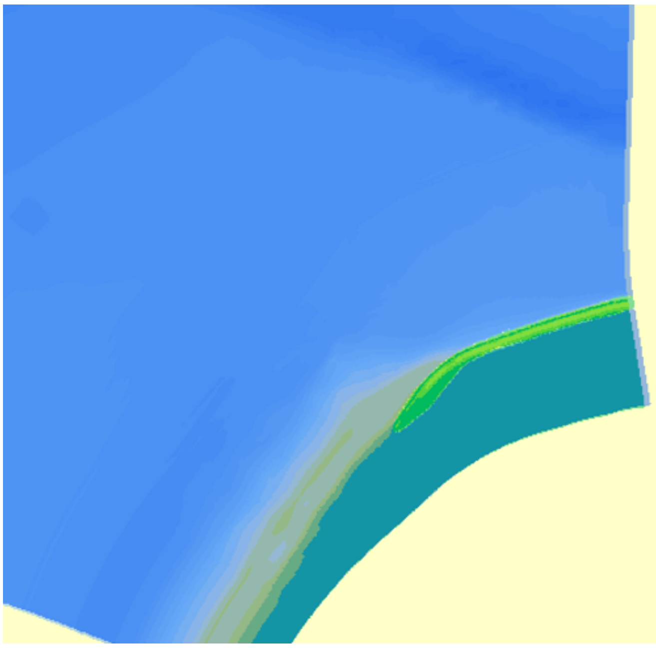

(b) XBeach depfile with Chezy layer on top of it (green colour)

Figure D.6: Visualisation of locally increased friction in the XBeach model

D.7. Tidal current patterns from Delft3D

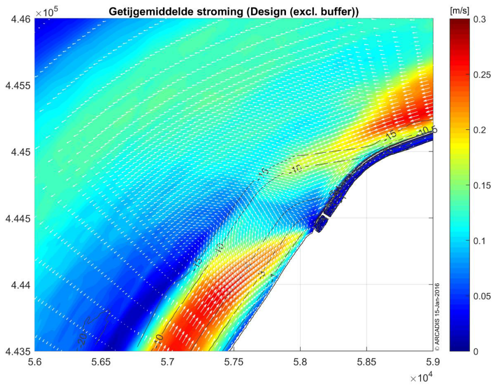

(a) Tide-averaged current pattern

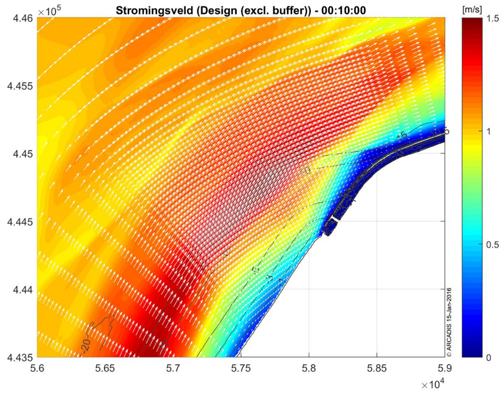

(b) Current pattern during flood, showing maximum flood velocities

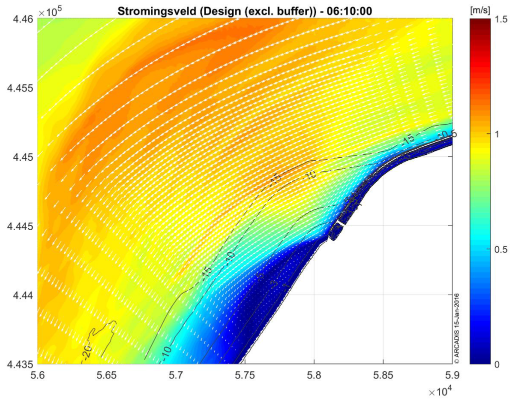

(c) Current pattern during ebb, showing maximum ebb velocities

Figure D.7: Tidal current patterns in Delft3D, as presented in (Onderwater, 2016)

D.8. Overview of simulations

Table D.7: Add caption

	Tool	Period	Characteristic	Hypothesis (1, 2, 3, 4) or goal					
Simulation				Validation	Boundary conditions generation	1	2	3	4
1	UNIBEST	1, 2, 3, 4, 5	wave forcing only	X		X			
2	UNIBEST	1, 2, 3, 4, 5	wave and tide forcing			X			X
3	UNIBEST	1, 2, 3, 4, 5	2017 bottom profile				X		
4	UNIBEST	1, 2, 3, 4, 5	2013 bottom profile				X		
5	UNIBEST	1, 2, 3, 4, 5	northern transects				X		
6	UNIBEST	1, 2, 3, 4, 5	not rotated				X		
7	UNIBEST	9 conditions	waves without reflection					X	
8	UNIBEST	9 conditions	waves with reflection = 0.2					X	
9	SWAN	2017Q2-2018Q2	2017 bathymetry		X				
10	SWAN	9 conditions	2017 bathymetry				X		
11	SWAN	9 conditions	2013 bathymetry				X		
12	SWAN	9 conditions	Design bathymetry				X		
13	SWAN	9 conditions	2017 bathy, Refl. coeff = 0.2					X	
14	SWAN	9 conditions	2017 bathy, Refl. coeff = 0.5					X	
15	Xbeach	NW storm	Base case (with reflection)					X	
16	XBeach	NW storm	Without reflection					X	
17	XBeach	4	With reflection	X					
18	XBeach	3	With reflection	X					

E

Results

E.1. Hypothesis 2

E.1.1. SWAN results - bathymetry design, 2013 and 2017

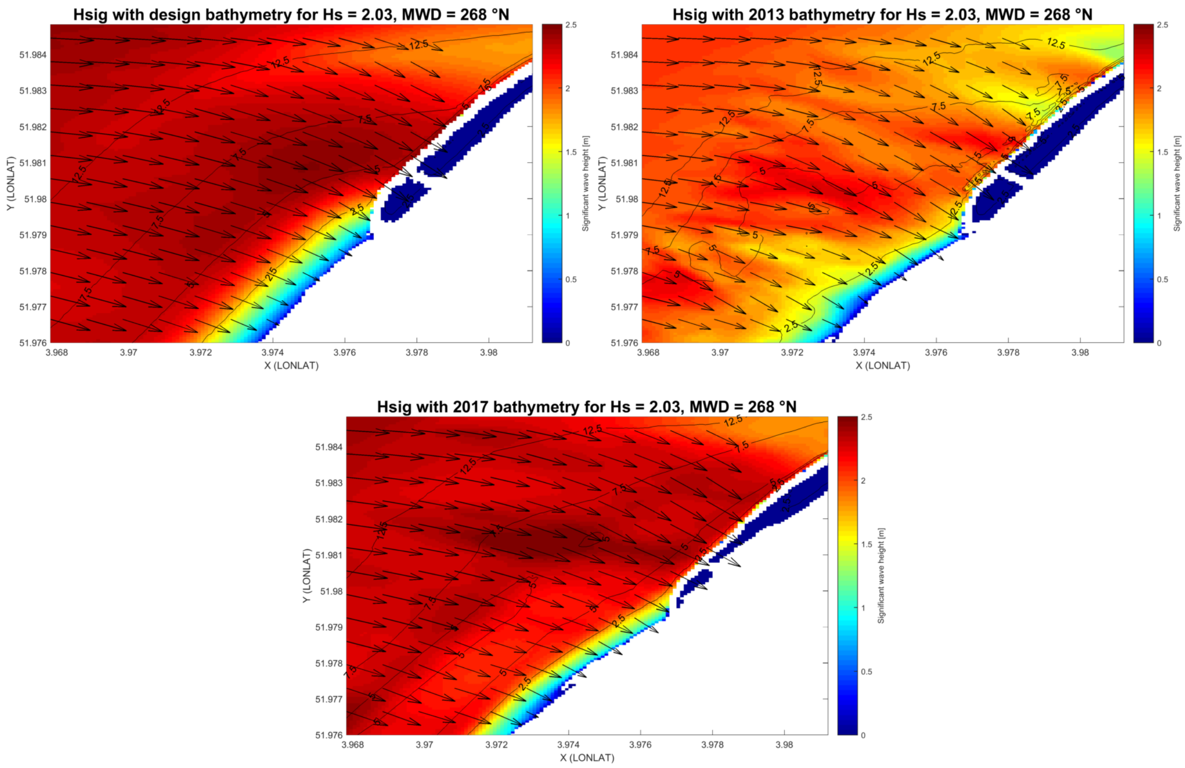

Figure E.1: Wave transformation for condition 1: H_s = 4.51, MWD = 227 °N at Europlatform.

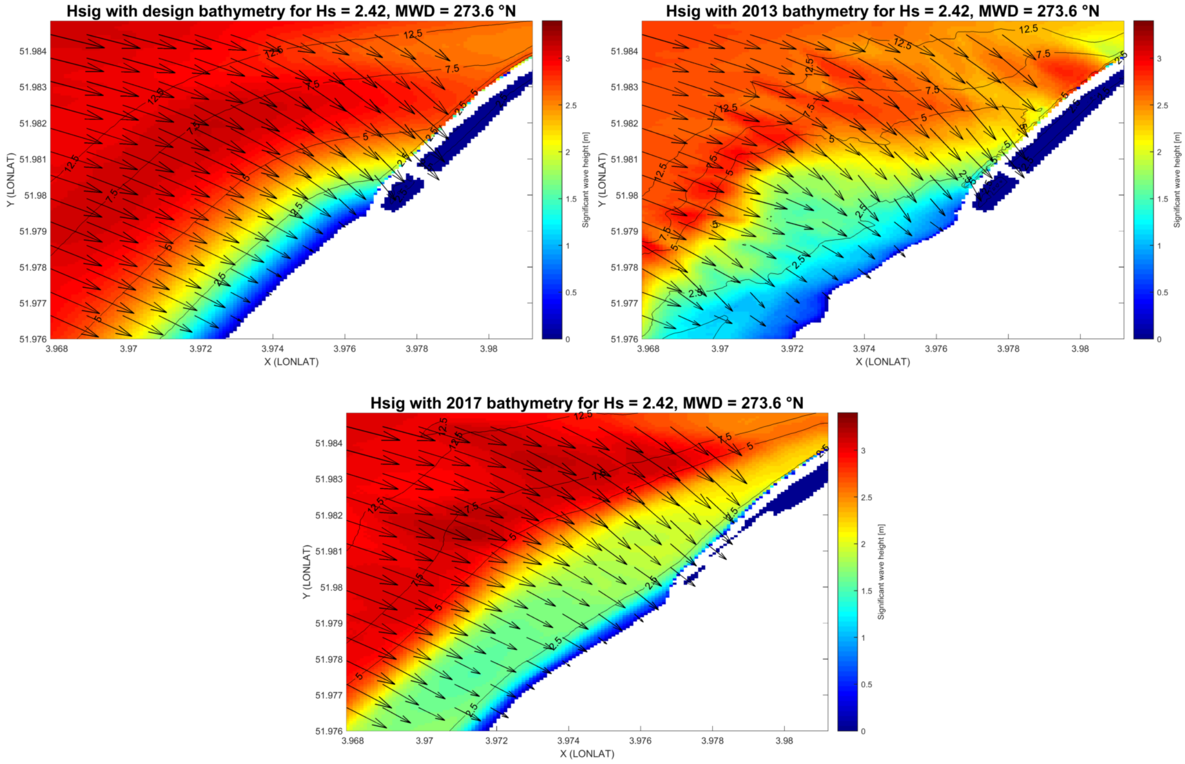

Figure E.2: Wave transformation for condition 2: $H_s = 5$, MWD = 263 °N at Europlatform.

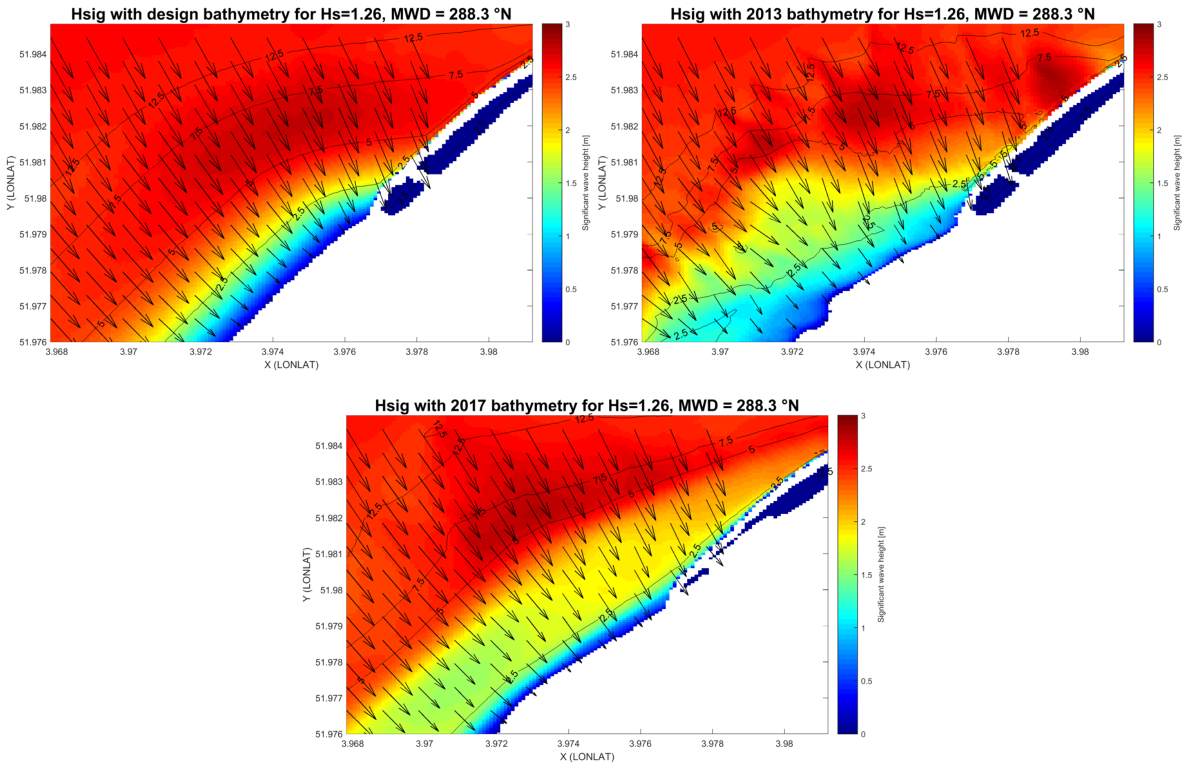

Figure E.3: Wave transformation for condition 3: $H_s = 4.03$, MWD = 341 °N at Europlatform.

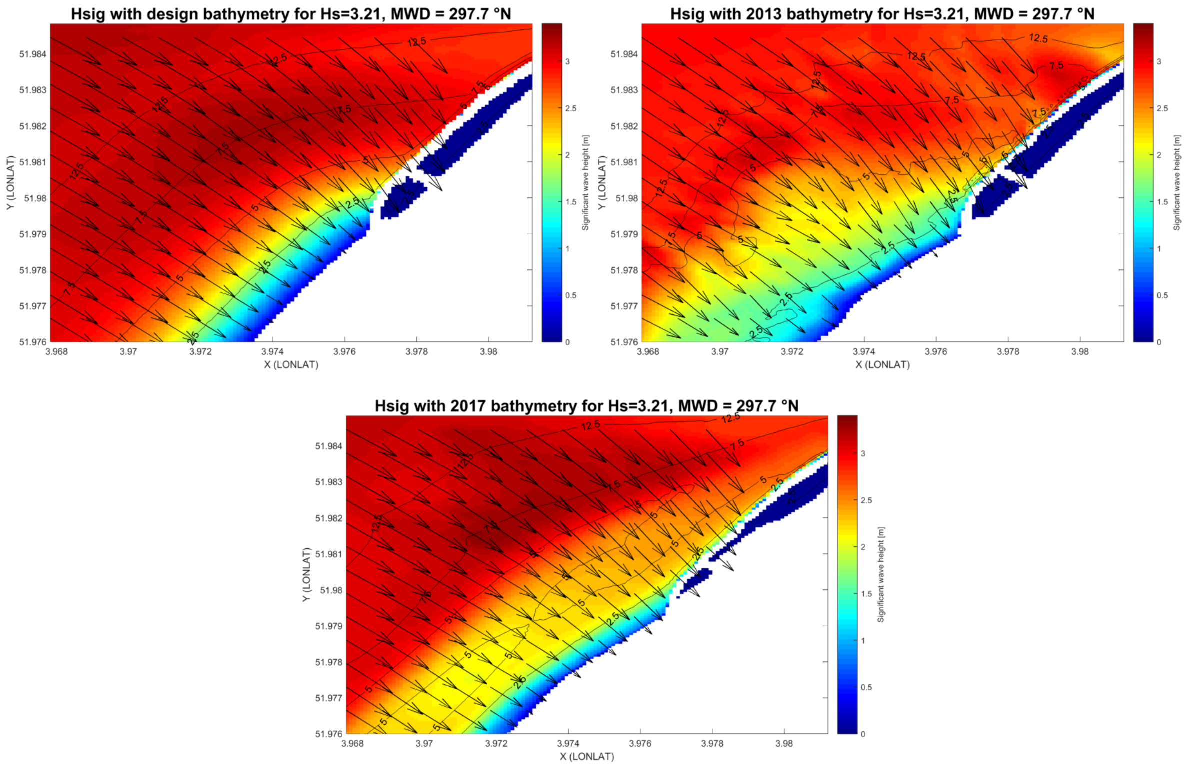

Figure E.4: Wave transformation for condition 4: H_s = 5, MWD = 295 °N at Europlatform.

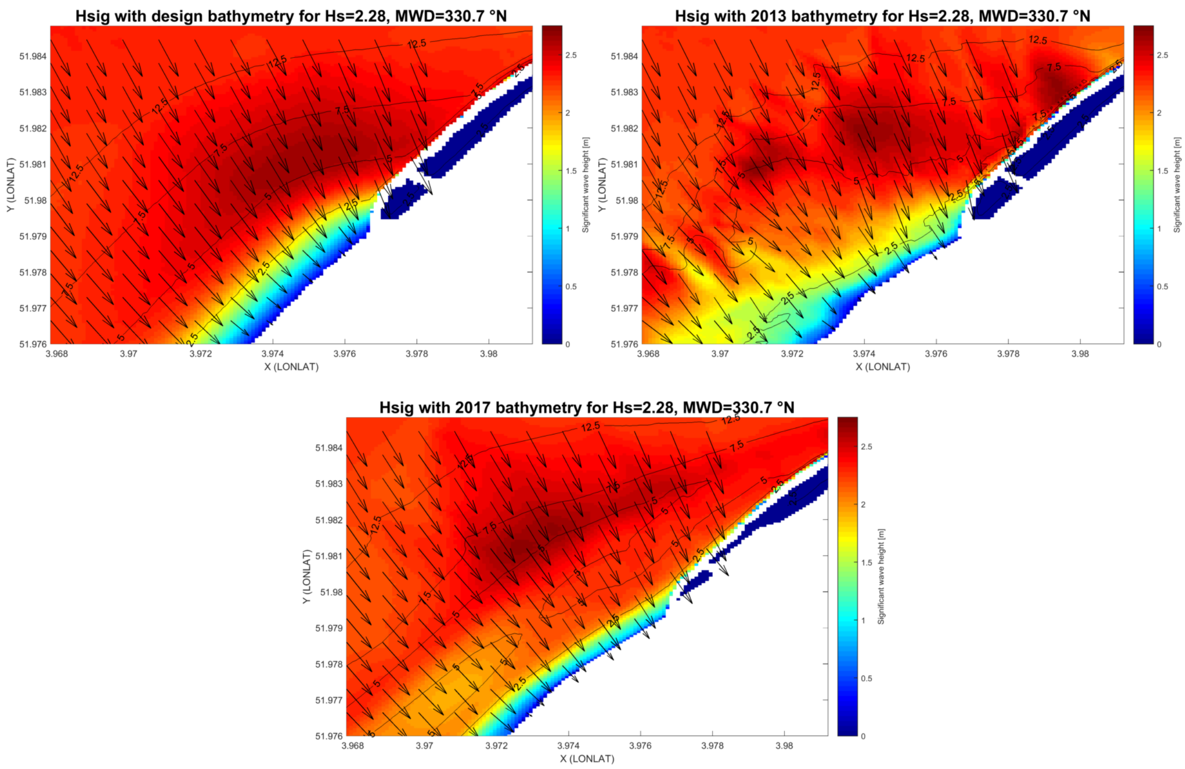

Figure E.5: Wave transformation for condition 5: H_s = 3.14, MWD = 341 °N at Europlatform

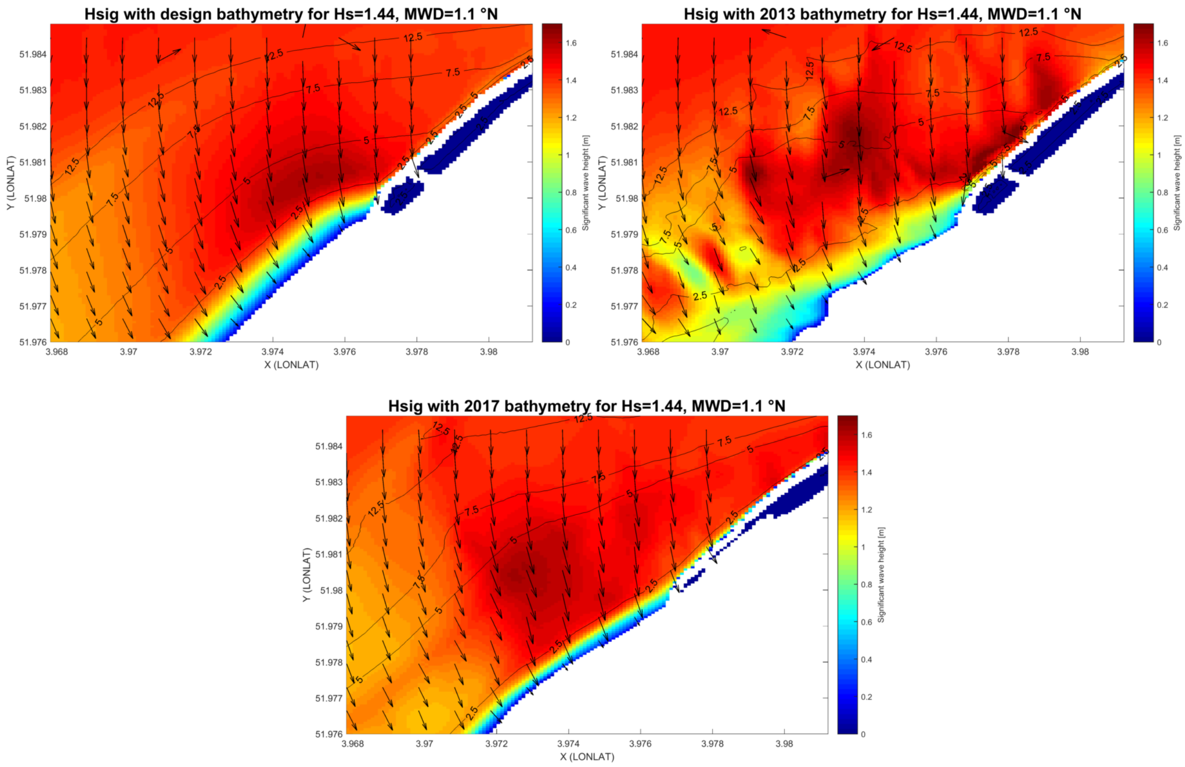

Figure E.6: Wave transformation for condition 6: H_s = 3.36, MWD = 47 °N at Europlatform.

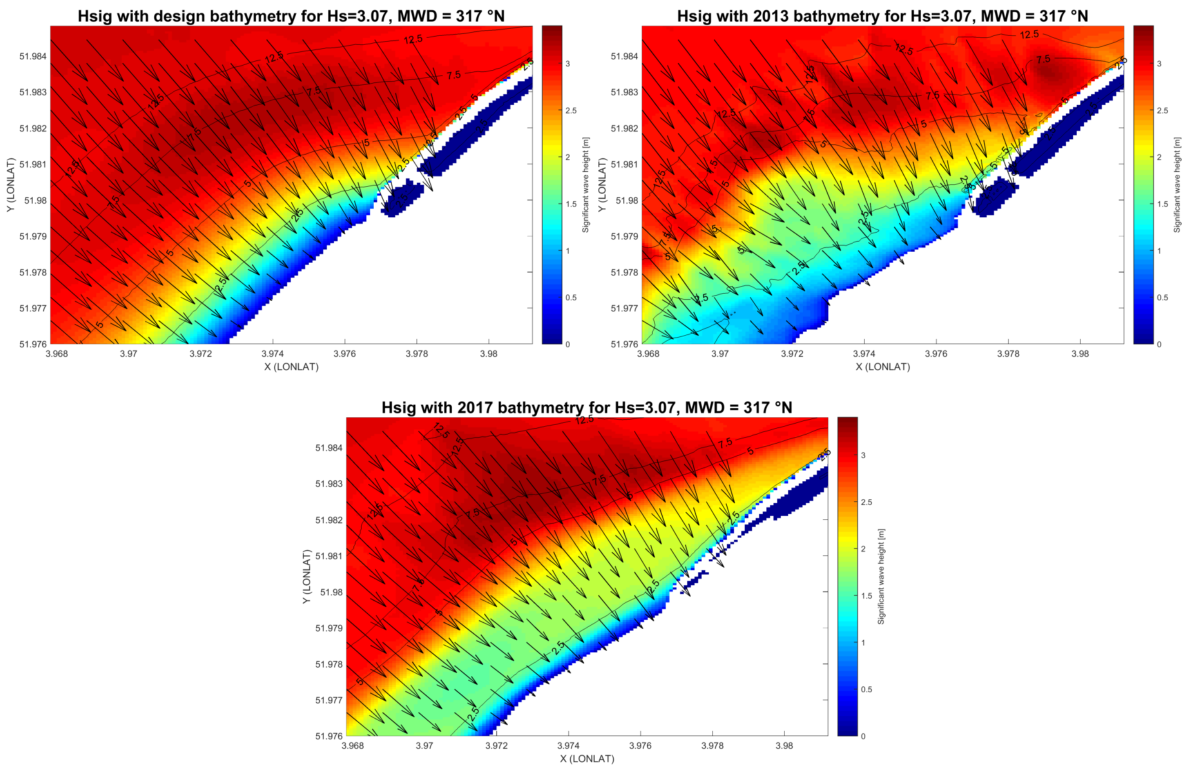

Figure E.7: Wave transformation for condition 7: H_s = 4.5, MWD = 324 °N

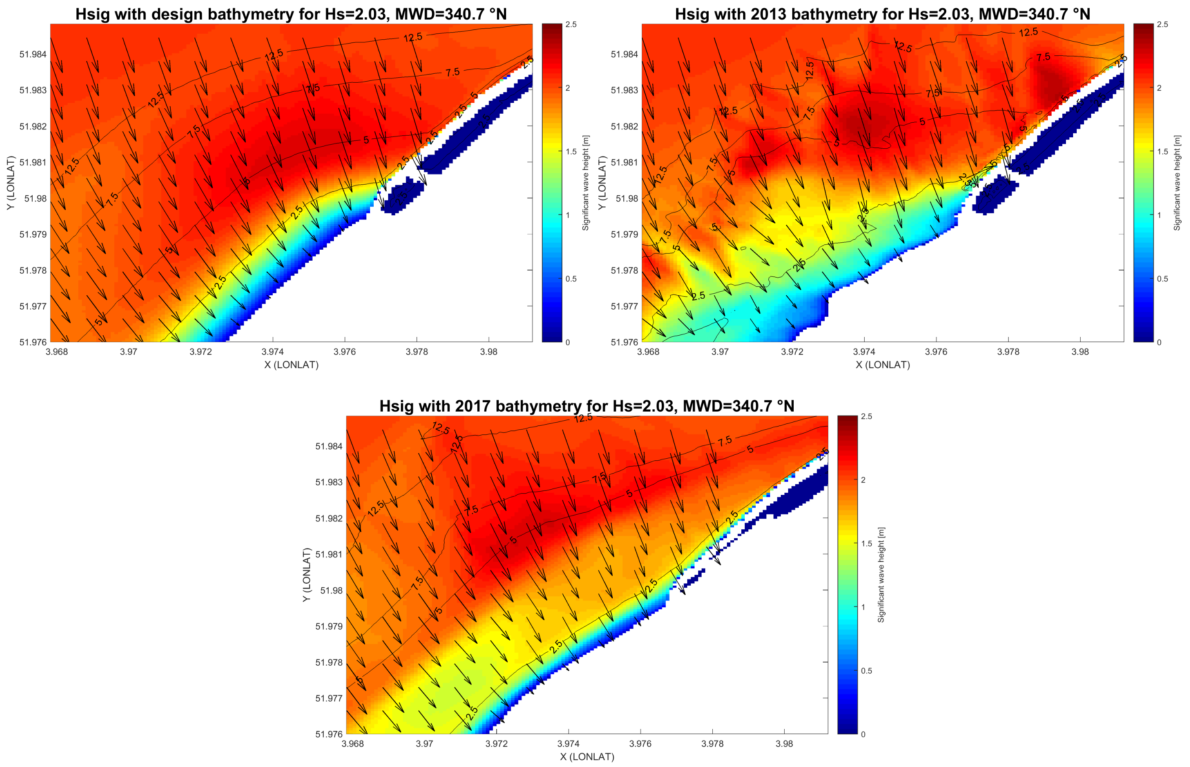

Figure E.8: Wave transformation for condition 8: H_s = 3.28, MWD = 357 °N at Europlatform.

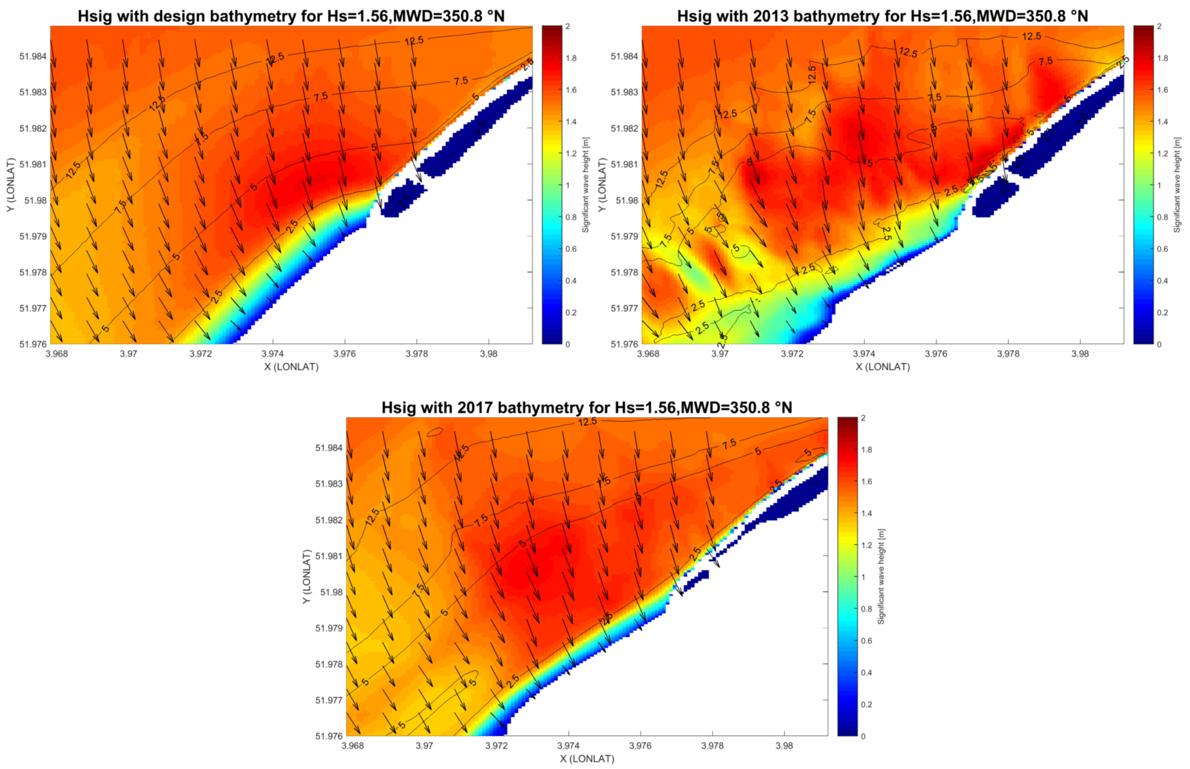

Figure E.9: Wave transformation for condition 9: H_s = 2.61, MWD = 16 °N at Europlatform.

E.2. Hypothesis 3: reflection

E.2.1. SWAN 2D results: close up

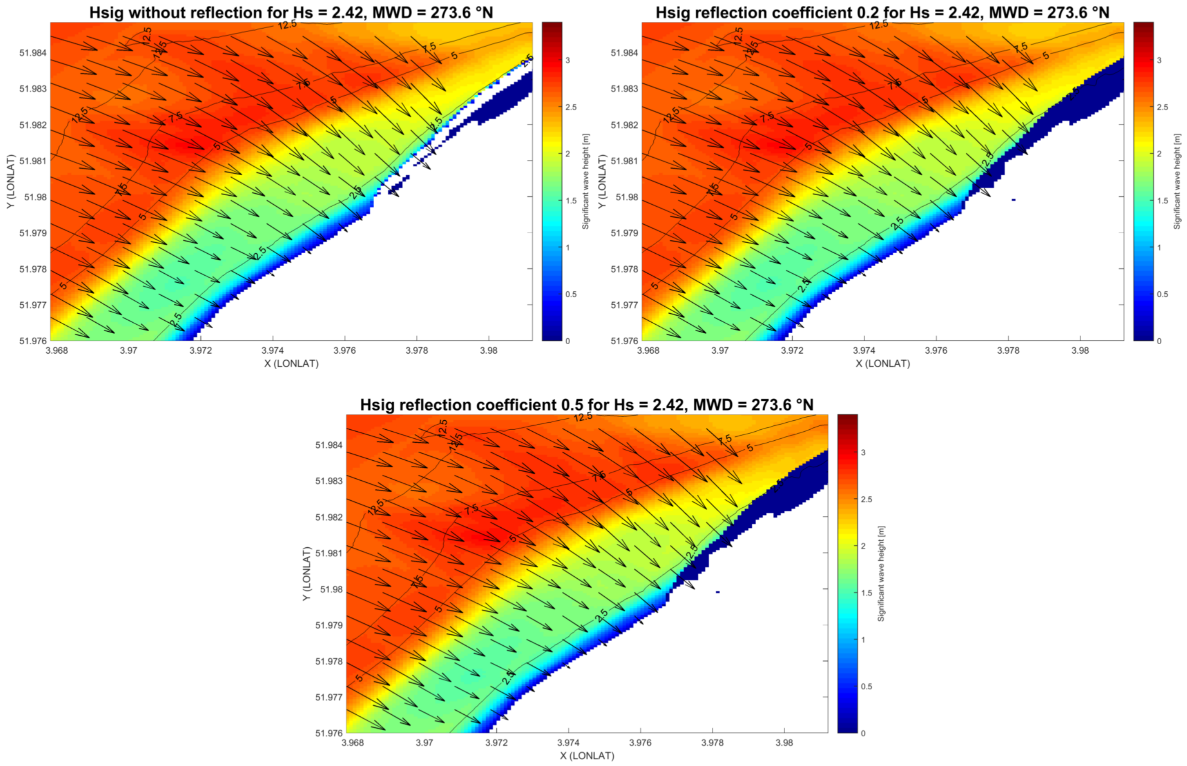

Figure E.10: Wave transformation for condition 2: H_s = 5, MWD = 263 °N at Europlatform.

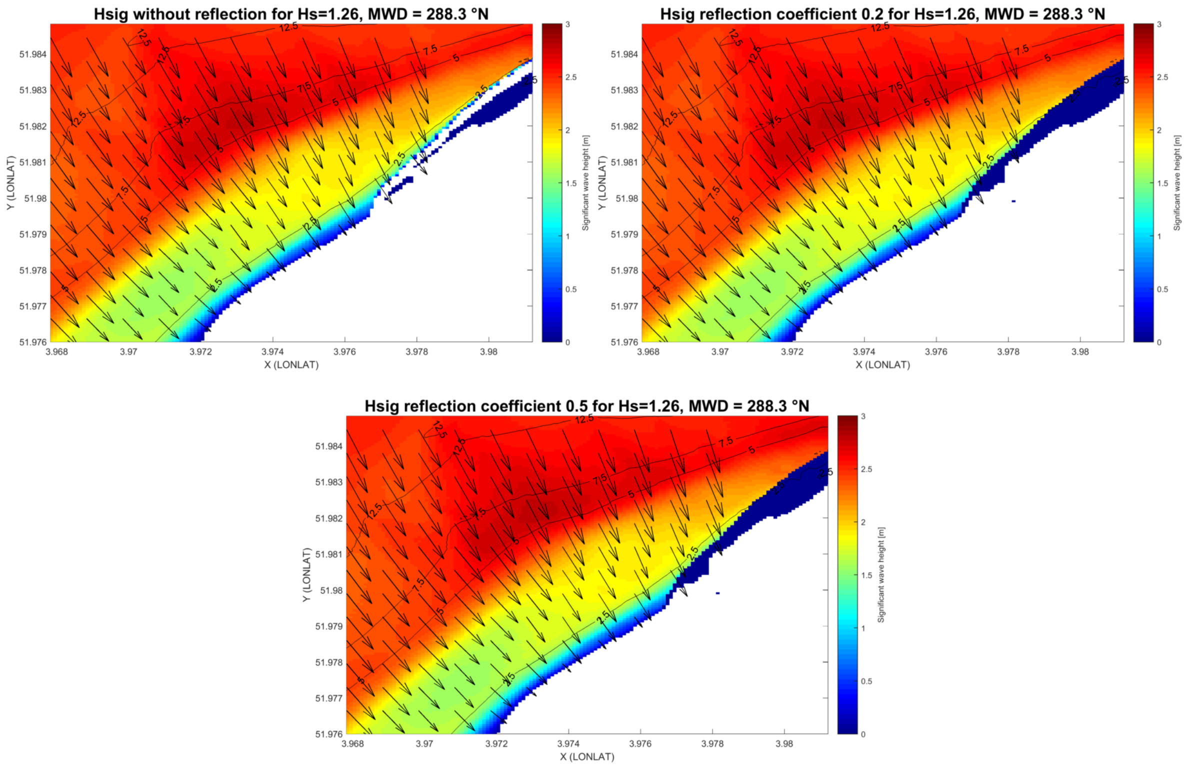

Figure E.11: Wave transformation for condition 3: H_s = 4.03, MWD = 341 °N at Europlatform.

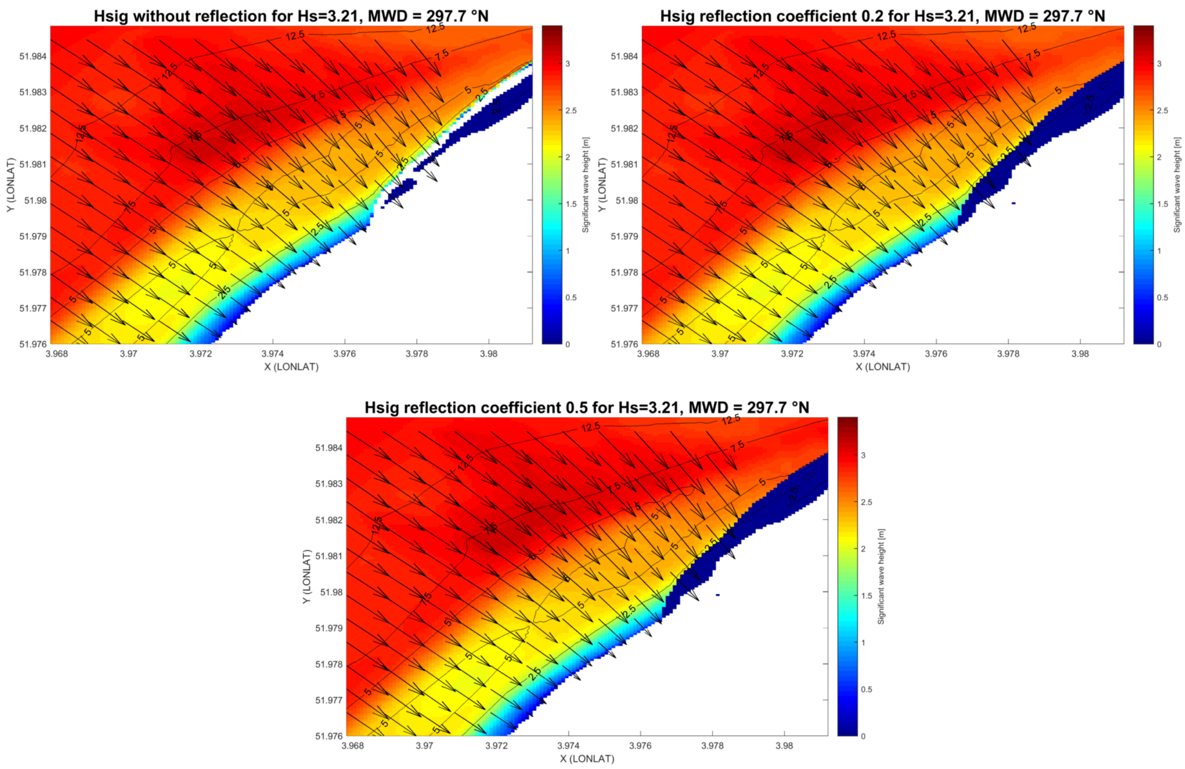

Figure E.12: Wave transformation for condition 4: H_s = 5, MWD = 295 °N at Europlatform.

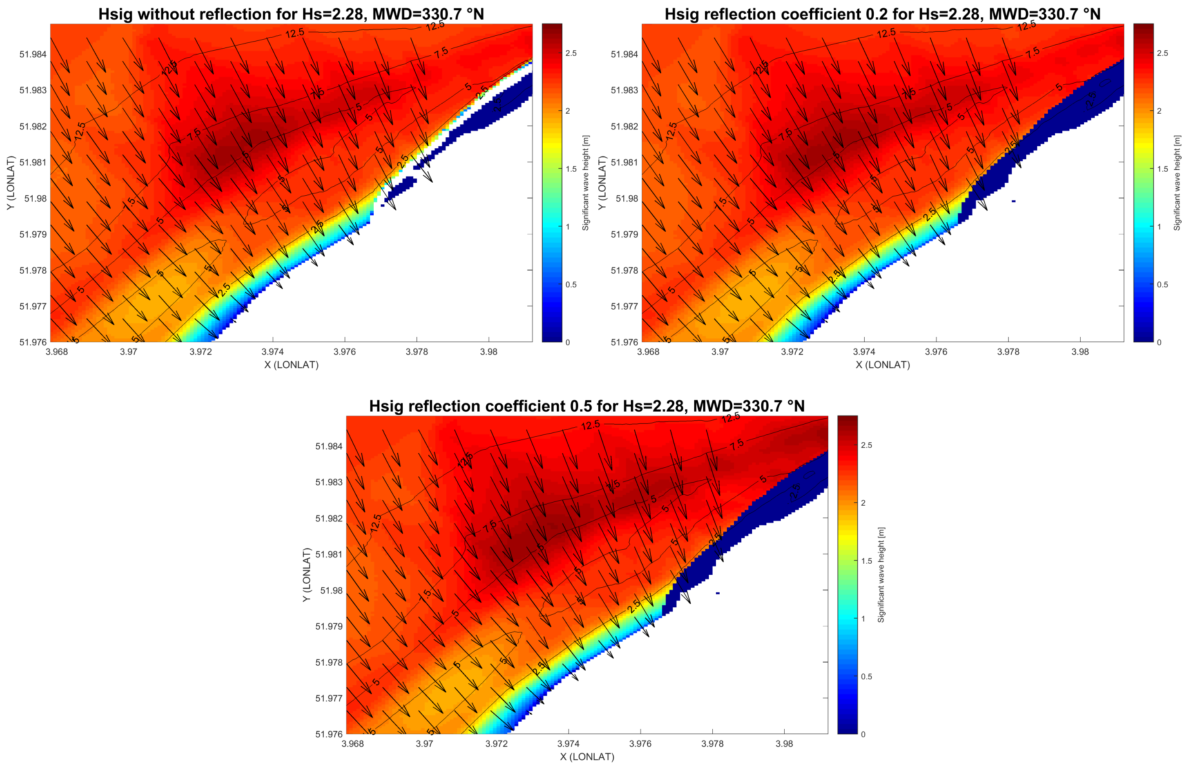

Figure E.13: Wave transformation for condition 5: H_s = 3.14, MWD = 341 °N at Europlatform

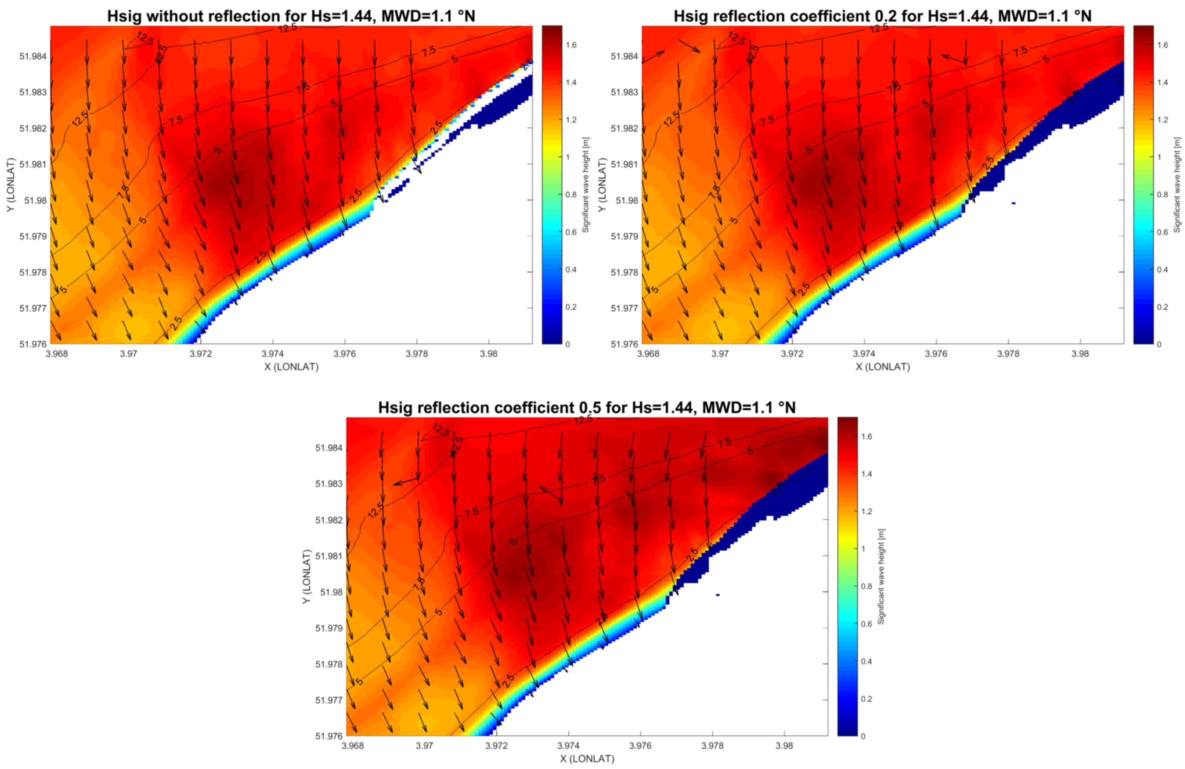

Figure E.14: Wave transformation for condition 6: H_s = 3.36, MWD = 47 °N at Europlatform.

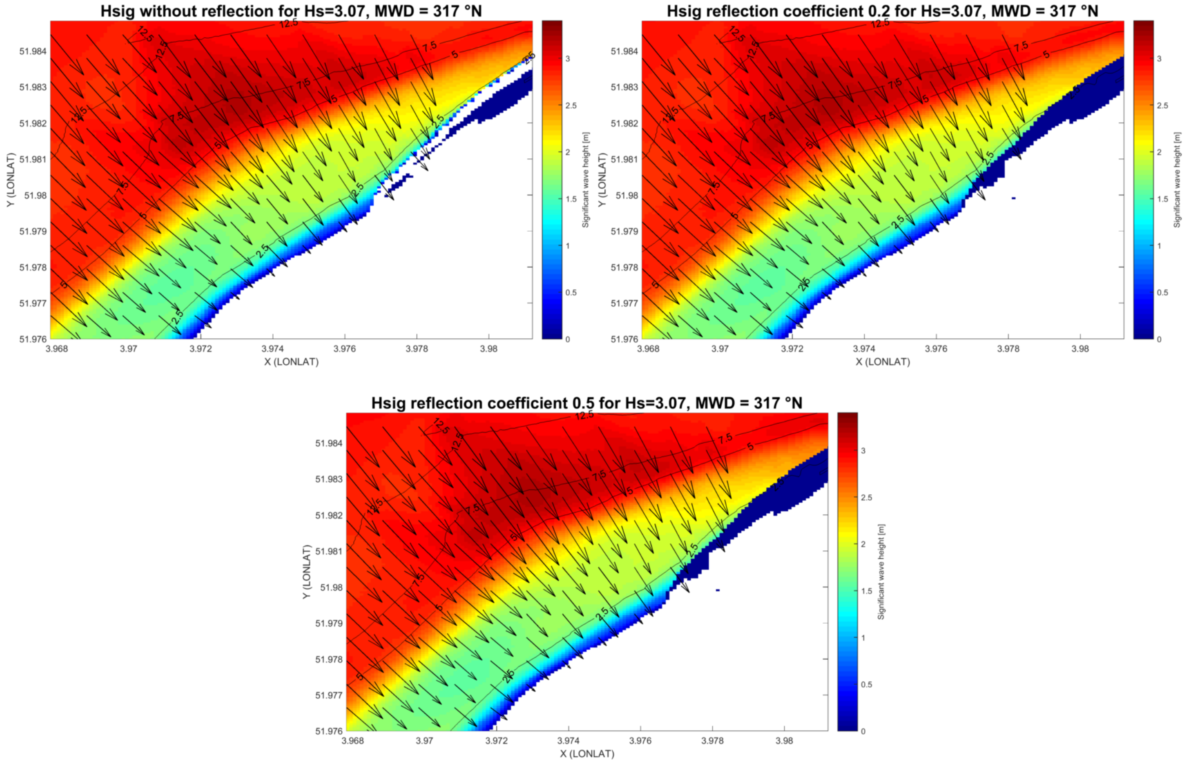

Figure E.15: Wave transformation for condition 7: $H_s = 4.5$, MWD = 324 °N

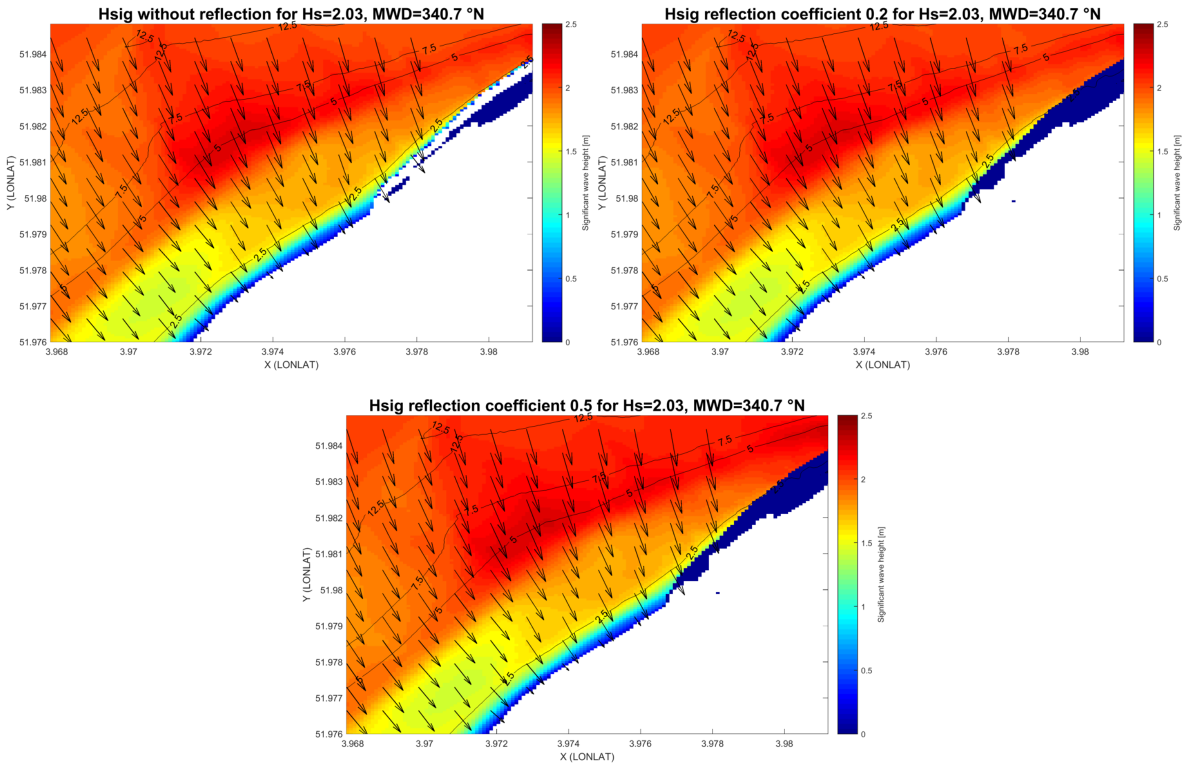

Figure E.16: Wave transformation for condition 8: $H_s = 3.28$, MWD = 357 °N at Europlatform.

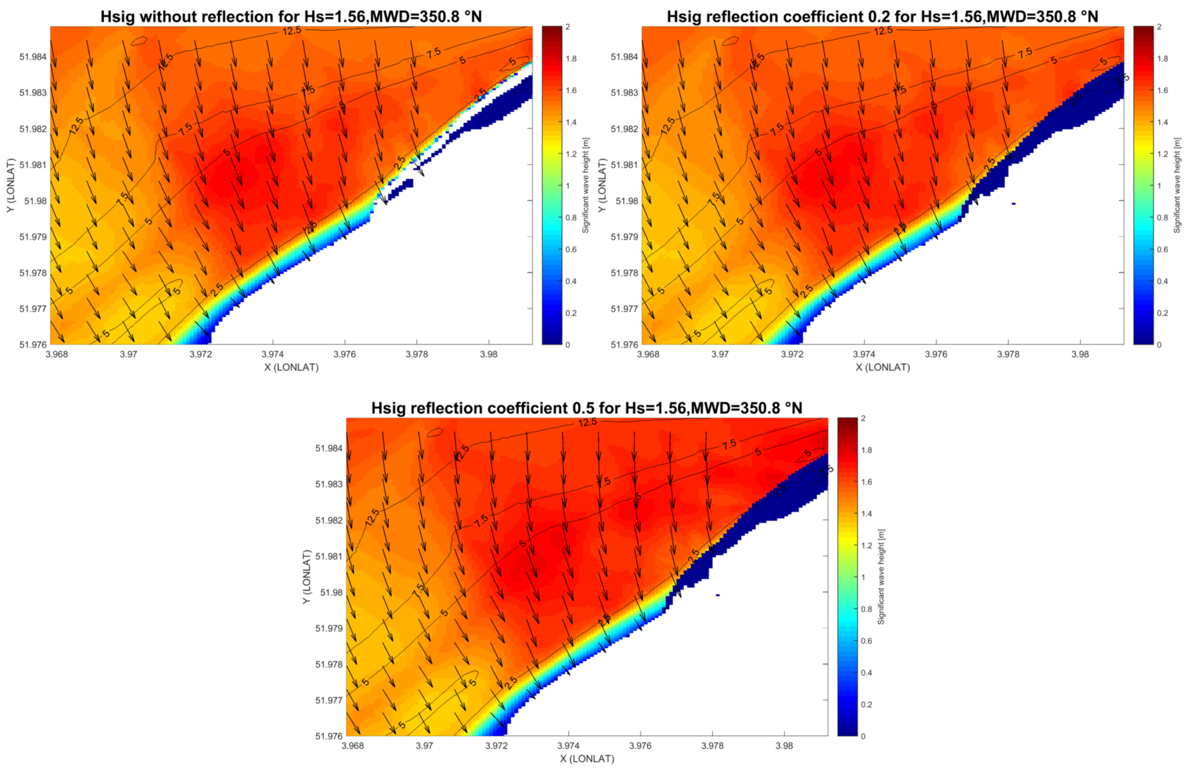

Figure E.17: Wave transformation for condition 9: H_s = 2.61, MWD = 16 °N at Europlatform.

F

Discussion

F.1. Satellite photographs of Hondsbossche- and Pettemer seadefence showing dynamic variability

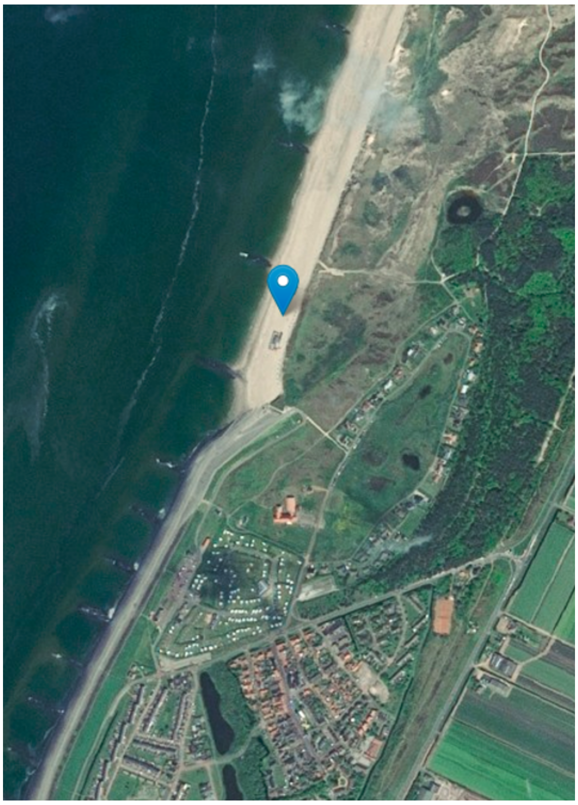

(a) Satellite photograph of HPZ, May 2014.

(b) Satellite photograph of HPZ, June 2014.

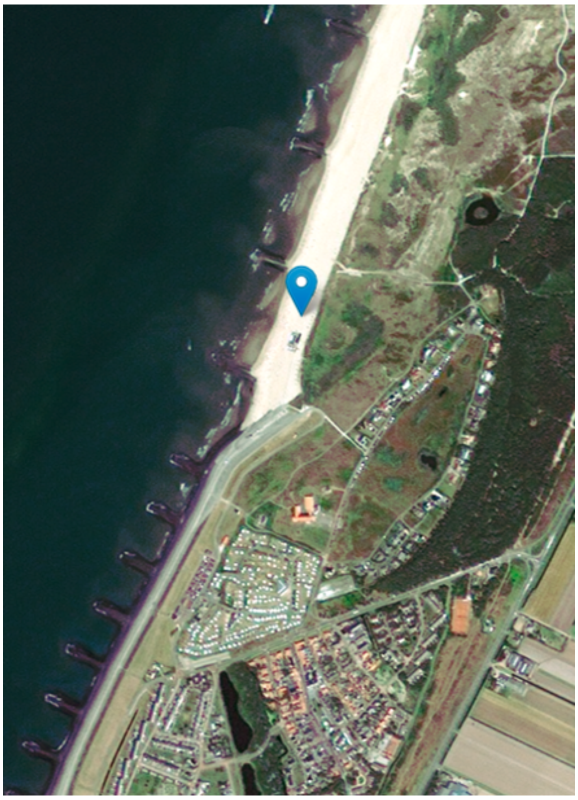

(c) Satellite photograph of HPZ, July 2014.

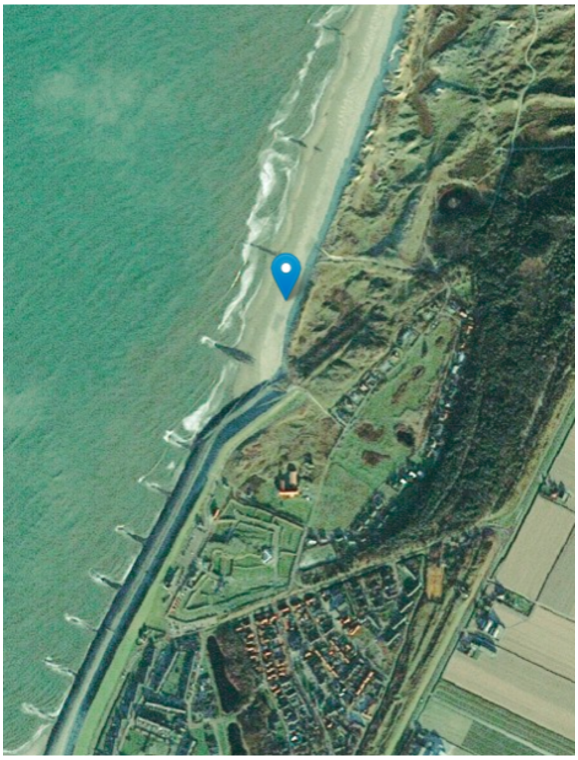

(d) Satellite photograph of HPZ, December 2014.

Figure F.1: Satellite photographs of HPZ, showing the dynamic variability around the hard-soft transition.